TOJSAT
The Online Journal of Scince and Technology

ISSN 2146-7390

The Online Journal of Science and Technology

Volume 3 Issue 4
October 2013

www.tojsat.net
October 2013

Published in TURKEY

Contact Address:

Prof. Dr. Aytekin İŞMAN- TOJSAT, Editor in Chief Sakarya-Turkey

Message from the Editor-in-Chief

I am happy to announce that TOJSAT is the rapidly growing journal in the field of sciences with the support and qualified studies of international researchers all around the world. It is great pleasure for me to present current volume and issue of TOJSAT, October 2013 to the academic agenda. I would like to thank Editor and his delegation for the process of the publications. Further to this, I would like to thank authors who shared their valuable research papers to the academic world through TOJSAT. Upon the developments of the journal, it is significant to ensure quality by pointing out interdisciplinary papers, methodologies and context to be part of the journal scope. In this respect, we are pleased to get qualified research papers to share in the academic world for the next issues of TOJSAT.

Prof. Dr. Aytekin İŞMAN

Editor-in-Chief of TOJSAT

Message from the Editor

Dear Readers,

Today, we have reached to the end of third volume of our journal. Almost three years past from the journals' first issue published on-line. Our goal is to rewiev and accept all kinds of research paper, rewiev articles, etc. fort the journal from scientific World such as "Different treatment trains for rainwater purification for human consumption in México City", A New Laminate Composite System: Metallic-Intermetallic Laminate Material, The Effect of Antioxidant Proteins due to Salt Stress and Wounding in Vicia Faba against Bean Yellow Mosaic Virus, Role of construction industry wastes on the properties of mortars" in this issue of journal.

I will thank to the readers all around the World for supports by sending their valuable scientific works to publish in the journal.

Prof. Dr. M. Şahin DÜNDAR

Editor, TOJSAT

Table of Contents

A Model for Measuring Institutionalization Level of SMEs

Özer UYGUN[1], Tuba CANVAR KAHVECI[1], Harun TAŞKIN[1], Beytullah PRİŞTİNE[2]

[1]Department of Industrial Engineering,Sakarya University,Esentepe Campus,Serdivan,Turkey
[2]Department of Industrial Engineering,Sakarya University,Esentepe Campus,Serdivan,Turkey
e-mail: ouygun@sakarya.edu.tr

Abstract: Institutionalization help an organization to gain legitimacy, increase resources and maintain survival. In other words, institutionalization is realized by developing appropriate and meaningful behaviors with the environment to gain legitimacy and conformity and transferring them to next generations. It is a crucial issue especially for small and medium sized enterprises (SMEs) to adopt themselves according to the changes in the environment, and sustain competitive. In this study, fuzzy hybrid multi-criteria decision making approach is used in order to measure institutionalization level of SMEs. For achieving this, first of all, criteria that indicate the institutionalization level of SMEs are determined. Then cause and effect interaction among main criteria is determined by fuzzy DEMATEL method. According to the inter influence derived from fuzzy DEMATEL, fuzzy analytic network process (ANP) is implemented in order to obtain the weights of the criteria. Expert opinions and group decision making approach are utilized during both fuzzy DEMATEL and fuzzy ANP methods. After acquiring the weights, several SMEs are evaluated according to the criteria predefined and VIKOR method is implemented for measuring the level of institutionalization of the SMEs.

Keywords: Institutionalization, multi-criteria decision making, Fuzzy DEMATEL, Fuzzy ANP, VIKOR

Introduction

The organizations are not stable; they change with the time in common with their environment. While some of the organizations manage to survive during this period, some of them cannot survive because of not being institutionalized. The main reasons of not being able to survive are the resistance to the change in the organization environment, innovation and improvement, not having strategic thinking and successful knowledge management system. The basic result of the institutionalization is to make the organizations more surviving and consistent. So the institutionalization has come up due to the modern society

Institutionalization is the administration of the enterprise within a set objectives and targets as well as principles and values. These values are comprised of vision, mission, principles and values. The set objectives, principles and values are combining every employee including the managers within a corporation (Kahveci, 2007). Institutionalization is also defined as processes which include creation of a formal structure, emergence of informal norms, development of impersonal/objective procedures, administrative rituals, ideologies, legalization, and focus on legitimization (Alpay et al., 2008).

Institutionalization processes include creation of a formal structure, emergence of informal norms, development of impersonal/objective procedures, administrative rituals, ideologies, legalization, and focus on legitimization. Institutional theory therefore traces the “emergence of distinctive forms, processes, strategies, outlooks, and competences” (Selznick, 1996) from patterns of organizational interaction and adaptation in response to internal and external environments.

Attempts to measure institutionalization at the firm level are rare (Alpay et al, 2008). One of the main objectives of this study is to measure institutionalization level of an organization. The assessment of institutionalization process is based on multiple criteria. Therefore, multi-criteria decision making techniques are used in this study. The process also requires more than one expert opinion. That is why group decision making approach is applied in the measurement model.

Literature Review

Institutionalization

The institutionalization is defined in different ways the literature. The institutional is generally defined by expressing the characteristics of the institutionalized organizations. If the organization is institutionalized, its activities must be performed systematically according to the particular rules. According to these view, the institutionalization is becoming a system. The institutionalized organizations have the common and eligible organizational culture. The professionalism is the other character of the institutionalized organizations (Kahveci, 2007). The organizational culture must be structured based on the strategic management activities and supported by the information systems to gain the expected results of the institutionalization process.

Actually, the institutionalization is an organizational theory which explains the interaction between the organizations and the environment they operate in. It is mainly concerned with the reasons of the changes within the organizations that occur due to pressures by the institutional environment which mainly consists of the governments and some professional organizations. This theory accepts that organizations can not just act rationally to follow their interests. They also have to take the expectations of the institutional environment into consideration. So the decisions maker of the organizations must to consider these expectations and pressures for their decisions.

Institutionalization is the organizational progress in common with the environmental change, and obtaining the standards. In this definition, three following subject are remarkable; (1) The institutionalized organizations changes along with the environmental change; (2) They learn this change; (3) They develop the new standards according to the new circumstance.

The researcher who firstly mentions this theory is Selznick and he notices that organizations adapt and *develop values specific to organization* to adapt to environment thus become legal and reach stability. Zucker considers institutionalization as a tool which provides social stability. According to him, institutionalization is realized by *developing appropriate and meaningful behaviors with the environment* to gain legitimacy and conformity and transferring them to next generations. Meyer and Rowan mentioned that the purpose of institutionalization is to gain legitimacy, increase resources and maintain survival of organizations. They argue that the institutionalization occurs by *developing shared values with the environment.* From another point of view, DiMaggio and Powell posit that institutionalization occurs by *imitating other successful competitors* as a means of adaptation to environment. According to Friedland and Alford, organizations institutionalize in order to affect cognitive and normative pressures *by trying to manipulate the environment* (Apaydın, 2009).

The common idea the researchers mentioned above is that, institutionalization is a process which influences every aspect of organizations, e.g. strategies, structure, decisions, activities, behaviors and performance. As it has a wide and deep impact on organizations, it deserves further researches (Apaydın and Coşkun, 2008).

Ironically, however, the institutional approach has yet to become institutionalized here is very little consensus on the definition of key concepts, measures or methods within this theoretic tradition. Also there has been little attention given to conceptualizing and specifying the processes of institutionalization. In the other words, the process-based approach to institutionalization has not been followed in most organizational analyses. Instead, institutionalization is almost always treated as a qualitative state: structures are institutionalized, or they are not. The institutionalization theory cannot provide the sufficient and concrete suggestions the way of the institutionalization. Consequently, important questions of the determinants of variations in levels of institutionalization, and of how such variation might affect the degree of similarity among sets of organizations, have been largely neglected. There is the need to develop more direct measures and better documentation of claims of the institutionalization of structures, since outcomes associated with a given structure are likely to depend on the stage or level of institutionalization. Also, attempts to measure institutionalization at the firm level are rare (Alpay et al, 2008).

Multi-Criteria Decision Making

Many traditional multi-criteria decision making (MCDM) methods are based on the additive concept along with the independence assumption (Zeleny, 1982). Several previously proposed MCDM methods are very useful but they have generally considered only for independent effects during selection or evaluation of criteria. DEMATEL method and its fuzzy version take into account that any factor of MCDM may affect other factors or may be affected by others.

Wu (2008) stated that knowledge management (KM) strategy selection is a kind of multiple criteria decision-making problem, which requires considering a large number of complex factors as multiple evaluation criteria. He proposed an effective solution based on a combined ANP and DEMATEL approach to help organizations evaluating and selecting KM strategies. Several multi-criteria decision making methods can be implemented in a combined manner. DEMATEL method is very suitable to be combined with ANP as can be seen in Yang and Tzeng (2011), Lee et al (2011) and Wu (2008). Some examples about combination of DEMATEL, ANP and VIKOR techniques can be found in Ho et al. (2011), and Liou and Chuang (2010). DEMATEL, ANP and TOPSIS combinations can be seen in Lin et al. (2010) and combination of three models in fuzzy environment can be seen in Büyüközkan and Çifçi (2012). There are some other combined methods also. In this paper DEMATEL, fuzzy ANP and VIKOR methods are implemented for assessing institutionalization level of organizations.

Readiness Assessment Model for Institutionalization

As there is not common key concepts about the institutionalization process, the components of this process are defined in the different ways too. According to Korkmaz, the basic components of the institutionalization are defined as knowledge, foresight, rationalism, consistency, constancy, reliability, adaptability, flexibility and maintainability. So, the institutionalization is making these components dominant over the organizations to institutionalize the organizations (Korkmaz, 2003). In the other study, the components of the institutionalization are stated as simplicity, diversification, flexibility and autonomy. These components can be used to determine the institutionalization level of the organizations (Karpuzoğlu, 2004). The dimensions of institutionalization are formalization, professionalism, cultural strength, consistency and accountability. Essentially, all of them are either the results of the institutionalization process or the characteristics of the institutionalized organizations. However, the way of institutionalization and measuring the level of institutionalization were not mentioned in the literature.

The simplicity of the job and maintaining it as simplicity cause the Simplicity component of the institutional. The simplicity of the job only can be done by applying the process management approach. On the other hand, when the enterprise handles the competition primarily, focuses on the market and human resources, and concentrates in the main goals, it achieves the Diversification in its structure and operations.

The other component of the institutionalization is the Flexibility which is the adaptability of the enterprise to its environment, can be done by networking, continuous revolution for continuance in the market, monitoring the basic cycles, establishing the systems such as production planning, strategic planning and investment planning.

Finally, the strategic view, the mission union, the managing with the reality and determining the priorities are composing the corporate identity and also provide the Autonomy. The other determinative of the autonomy is certainly capital structure.

When the enterprise is evaluated from the simplicity of their job, the processes should be the focus of this evaluation. The enterprise can gain the diversification on account of its product, human resources and technological resources in the environment. The flexibility is exactly the conformity to the environment. The autonomy of the enterprise is based on the strategy of the enterprise. Consequently, the enterprise should implement strategic management, process management, technology management, human resource management, product management, knowledge management and consider its environment. As a result the evaluation criteria used in institutionalization assessment model are summarized in Table 1.

Table 1. Main and sub-criteria of the institutionalization assessment model

Main Criteria	Sub-criteria
C1: Strategic Management	C11: Strategic Analysis
	C12: Strategy Definition and Planning
	C13: Strategic Performance Evaluation
C2: Process Management	C21: Process Identification and Monitoring
	C22: Process Improvement and Innovation
	C23: Process Implementation
C3: Technology Management	C31: Technology Planning
	C32: Research and Development, Innovation Management
	C33: Marketing and Commercialization of Technology
C4: Product Management	C41: Product Planning& Product Data Management
	C42: Product Specifications
	C43: Product Innovation
C5: Knowledge Management	C51: Enterprise Knowledge Definition and Storage
	C52: Usage of Knowledge and Knowledge Technology
	C53: Knowledge Culture and Performance of Knowledge Management
C6: Human Resource Management	C61: Human Resource Planning, Selection and Orientation
	C62: Personnel Development and Performance Evaluation
	C63: Participation of management, labour relations and organizational structure
C7: Enterprise Environment	C71: Suppliers
	C72: Market and Competitors
	C73: Customers

Technical Background

Fuzzy DEMATEL Method

The DEMATEL method was developed by Gabus and Fontela (1972). It analyzes the influential status and strength between the factors and converts them into an explicit structural mode of a system (Lin and Wu, 2008). Lin and Wu (2004, 2008) developed a fuzzy DEMATEL method to gather group ideas and analyze the cause and effect relationship of complex problems in fuzzy environments. The procedure of the fuzzy DEMATEL method implemented in this study is explained below:

Step 1: Identify the decision goal and set up a committee. During the group decision making process, decision goal is decided first, and subsequently a committee is set up for gathering group knowledge for problem solving.

Step 2: Develop the evaluation criteria and design the fuzzy linguistic scale. For evaluation, sets of criteria are established. Since evaluation criteria have the nature of causal relationship and usually comprise several complicated aspects, and to deal with the ambiguities of human assessments, the fuzzy linguistic scale is used in the group decision making. The different degrees of influence are expressed with five linguistic terms as {No, Low, Medium, High, Very high} and their corresponding positive triangular fuzzy numbers are shown in Table 2 and see Fig. 1.

Table 2. The correspondence of linguistic terms and linguistic values

Linguistic terms	Linguistic values
No Influence (N)	(0, 0, 0.25)
Low Influence (L)	(0, 0.25, 0.50)
Medium Influence (M)	(0.25, 0.50, 0.75)
High Influence (H)	(0.50, 0.75, 1.00)
Very High Influence (VH)	(0.75, 1.00, 1.00)

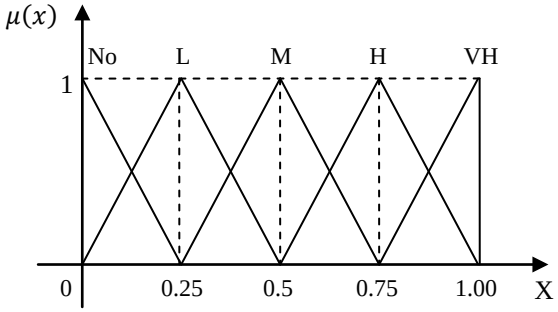

Fig. 1. Triangular fuzzy numbers for linguistic variables.

Step 3: Acquire and average the assessments of decision makers. In this step, a group of *p* expert is asked to acquire sets of pair-wise comparisons of the criteria $C = \{C_i | i = 1,2, \dots, n\}$ by linguistic terms in order to measure the relationship between criteria. So, *p* fuzzy matrices $\tilde{Z}^1, \tilde{Z}^2, \dots, \tilde{Z}^p$ were obtained, each corresponding to an expert. Then, the average fuzzy matrix $\tilde{Z}$ is calculated as below and is called the initial direct-relation fuzzy matrix.

$$\tilde{Z} = \frac{\tilde{Z}^1 \oplus \tilde{Z}^2 \oplus \dots \oplus \tilde{Z}^p}{p} \quad (1)$$

The initial direct-relation fuzzy matrix $\tilde{Z}$ is shown as following

$$\tilde{Z} = \begin{bmatrix} 0 & \tilde{z}_{12} & \cdots & \tilde{z}_{1n} \\ \tilde{z}_{21} & 0 & \cdots & \tilde{z}_{2n} \\ \vdots & \vdots & \ddots & \vdots \\ \tilde{z}_{n1} & \tilde{z}_{n2} & \cdots & 0 \end{bmatrix}$$

where $\tilde{z}_{ij} = (\ell_{ij}, m_{ij}, u_{ij})$ are triangular fuzzy numbers. $\tilde{z}_{ii}$ (i = *1, 2, …, n*) is shown as zero but whenever is necessary it will be regarded as triangular fuzzy number (0, 0, 0).

Step 4: Acquire the normalized direct-relation fuzzy matrix. By normalizing the initial direct-relation fuzzy matrix, normalized direct-relation fuzzy matrix $\tilde{X}$ is obtained by using

$$\tilde{X} = \begin{bmatrix} \tilde{x}_{11} & \tilde{x}_{12} & \cdots & \tilde{x}_{1n} \\ \tilde{x}_{21} & \tilde{x}_{22} & \cdots & \tilde{x}_{2n} \\ \vdots & \vdots & \ddots & \vdots \\ \tilde{x}_{n1} & \tilde{x}_{n2} & \cdots & \tilde{x}_{nn} \end{bmatrix}$$

where

$$\tilde{x}_{ij} = \frac{\tilde{z}_{ij}}{r} = \left(\frac{\ell_{ij}}{r}, \frac{m_{ij}}{r}, \frac{u_{ij}}{r}\right) \quad (2)$$

and

$$r = \max_{1 \le i \le n} \left(\sum_{j=1}^{n} u_{ij}\right) \quad (3)$$

It is assumed at least one *i* such that $\sum_{j=1}^{n} u_{ij} < r$ and this assumption is well satisfied in practical cases.

Step 5: Acquire the total-relation fuzzy matrix. Let $\tilde{x}_{ij} = (\ell'_{ij}, m'_{ij}, u'_{ij})$ and define three crisp matrices, whose elements are extracted from $\tilde{X}$, as follows:

$$X_\ell = \begin{bmatrix} 0 & \ell'_{12} & \cdots & \ell'_{1n} \\ \ell'_{21} & 0 & \cdots & \ell'_{2n} \\ \vdots & \vdots & \ddots & \vdots \\ \ell'_{n1} & \ell'_{n2} & \cdots & 0 \end{bmatrix} \quad X_m = \begin{bmatrix} 0 & m'_{12} & \cdots & m'_{1n} \\ m'_{21} & 0 & \cdots & m'_{2n} \\ \vdots & \vdots & \ddots & \vdots \\ m'_{n1} & m'_{n2} & \cdots & 0 \end{bmatrix} \quad X_u = \begin{bmatrix} 0 & u'_{12} & \cdots & u'_{1n} \\ u'_{21} & 0 & \cdots & u'_{2n} \\ \vdots & \vdots & \ddots & \vdots \\ u'_{n1} & u'_{n2} & \cdots & 0 \end{bmatrix}$$

As in the crisp DEMATEL, total-relation fuzzy matrix $\tilde{T}$ is defined as $\tilde{T} = \lim_{k\to\infty}(\tilde{X} + \tilde{X}^2 + \cdots + \tilde{X}^k)$ and is shown as:

$$\tilde{T} = \begin{bmatrix} \tilde{t}_{11} & \tilde{t}_{12} & \cdots & \tilde{t}_{1n} \\ \tilde{t}_{21} & \tilde{t}_{22} & \cdots & \tilde{t}_{2n} \\ \vdots & \vdots & \ddots & \vdots \\ \tilde{t}_{n1} & \tilde{t}_{n2} & \cdots & \tilde{t}_{nn} \end{bmatrix} \quad \text{where } \tilde{t}_{ij} = (\ell''_{ij}, m''_{ij}, u''_{ij}) \quad \text{and}$$

$$[\ell''_{ij}] = X_\ell \times (I - X_\ell)^{-1} \tag{4}$$

$$[m''_{ij}] = X_m \times (I - X_m)^{-1} \tag{5}$$

$$[u''_{ij}] = X_u \times (I - X_u)^{-1} \tag{6}$$

Step 6: Obtaining $(\widetilde{D}_i + \tilde{R}_i)^{def}$ *and* $(\widetilde{D}_i - \tilde{R}_i)^{def}$ *values*. Each $\tilde{t}_{ij} = (\ell''_{ij}, m''_{ij}, u''_{ij})$ triangular fuzzy numbers of total-relation fuzzy matrix $\tilde{T}$ is defuzzified and $\tilde{T}^{def}$ matrix is obtained as defined below:

$$\tilde{T}^{def} = \begin{bmatrix} \tilde{t}_{11}{}^{def} & \tilde{t}_{12}{}^{def} & \cdots & \tilde{t}_{1n}{}^{def} \\ \tilde{t}_{21}{}^{def} & \tilde{t}_{22}{}^{def} & \cdots & \tilde{t}_{2n}{}^{def} \\ \vdots & \vdots & \ddots & \vdots \\ \tilde{t}_{n1}{}^{def} & \tilde{t}_{n2}{}^{def} & \cdots & \tilde{t}_{nn}{}^{def} \end{bmatrix} \quad \text{where } \tilde{t}_{ij}{}^{def} = (\ell''_{ij}, m''_{ij}, u''_{ij})^{def}$$

Then, $\widetilde{D}_i{}^{def}$, $\tilde{R}_i{}^{def}$, $(\widetilde{D}_i{}^{def} + \tilde{R}_i{}^{def})$ and $(\widetilde{D}_i{}^{def} - \tilde{R}_i{}^{def})$ values are calculated as in crisp DEMATEL method where $\widetilde{D}_i{}^{def}$ and $\tilde{R}_i{}^{def}$ are the sum of rows and columns of matrix $\tilde{T}^{def}$, respectively.

In this study CFSC (Converting Fuzzy data into Crisp Scores) defuzzification method proposed by Opricovic and Tzeng (2003) is used for calculating defuzzified total-relation matrix $\tilde{T}^{def}$.

CFCS Defuzzification Method

There are several defuzzification methods. The most commonly used defuzzification method is the Centroid (Center of gravity) method (Yagler and Filev, 1994), but this does not distinguish between two fuzzy numbers which have the same crisp value in spite of different shapes. Therefore CFCS defuzzification method is used since it can give a better crisp value than the Centroid method.

CFCS method is generated by Opricovic and Tzeng (2003) for multi-criteria decision making which can distinguish two symmetrical triangular fuzzy numbers with the same mean, whereas the Centroid method does not distinguish between two such fuzzy numbers. CFCS method can also be applied when some values are crisp, $\ell = m = u$.

Let $\tilde{f}_{ij} = (\ell_{ij}, m_{ij}, u_{ij})$, *j=1, 2,…, J* be triangular fuzzy numbers, where *J* is the number of alternatives. The crisp value of *i*-th criterion could be determined by the following four step CFCS algorithm:

1. Normalization:

$R = \max_j u_{ij}$, $L = \min_j \ell_{ij}$ and $\Delta = R - L$

Compute for each alternatives

$$x_{\ell j} = (\ell_{ij} - L)/\Delta \text{ , } x_{mj} = (m_{ij} - L)/\Delta \text{ , } x_{uj} = (\mathrm{u}_{ij} - L)/\Delta \quad (7)$$

2. Compute left score (ls) and right score (rs) normalized values:

$$x_j^{ls} = x_{mj}/(1 + x_{mj} - x_{\ell j}) \text{ and } x_j^{rs} = x_{uj}/(1 + x_{uj} - x_{mj}) \quad (8)$$

3. Compute total normalized crisp value:

$$x_j^{crisp} = \left[x_j^{ls} \times \left(1 - x_j^{ls}\right) + x_j^{rs} \times x_j^{rs}\right]/\left[1 - x_j^{ls} + x_j^{rs}\right] \quad (9)$$

4. Compute crisp values for $\tilde{f}_{ij}$:

$$\tilde{f}_{ij}^{\ crisp} = L + x_j^{crisp} \times \Delta \quad (10)$$

Fuzzy ANP Method

Analytic network process (ANP) is the general form of analytic hierarchy process (AHP) and was proposed by Saaty (1996) to overcome the problem of interrelation among criteria or factors. Through a supermatrix, whose entries are themselves matrices of column priorities, the ANP synthesizes the outcome of dependence and feedback within and between clusters of elements (Yang and Chang, 2012). The initial supermatrix must be transformed to a matrix in which each of its columns sums to unity. For this reason, this matrix must be normalized by the cluster's weight to get the column sums to unity. Hence, the weighted supermatrix is obtained (Saaty and Vargas, 1998). The supermatrix representation is given in Fig. 2.

$$W = \begin{array}{c} \\ C_1 \\ \\ \\ C_2 \\ \\ \vdots \\ \\ C_m \\ \\ \end{array} \begin{array}{c} \begin{array}{cccccccccc} C_1 & & & C_2 & & \cdots & & C_m & & \\ e_{11} & \cdots & e_{1n_1} & e_{21} & \cdots & e_{2n_2} & \cdots & e_{m1} & \cdots & e_{mn_m} \end{array} \\ \begin{pmatrix} W_{11} & & & W_{12} & & \cdots & & W_{1m} \\ & & & & & & & & & \\ W_{21} & & & W_{22} & & \cdots & & W_{2m} \\ & & & & & & & & & \\ \vdots & & & \vdots & & \ddots & & \vdots \\ & & & & & & & & & \\ W_{m1} & & & W_{m2} & & \cdots & & W_{mm} \end{pmatrix} \end{array}$$

Fig. 2. The supermatrix representation

ANP equipped with fuzzy set theory helps in overcoming the impreciseness or vagueness in the preferences. Fuzzy set theory is more advantages than traditional set theory when describing set concepts in human language. The Fuzzy ANP (FANP) method can easily accommodate the interrelationships existing among the functional

activities (Mohanty et al., 2005). Table 3 gives the fuzzy linguistic terms and corresponding triangular fuzzy numbers (TFNs) which are used for pairwise comparisons. The pairwise comparisons are implemented according to Fuzzy ANP method within each cluster or main criteria, and according to dependency relationships which are obtained from DEMATEL in order to generate relative importance weights.

Table 3. The Linguistic variables and triangular fuzzy numbers for importance

Linguistic variables	Fuzzy number	Triangular fuzzy number	Triangular fuzzy reciprocal number
Equally Important (EI)	$\tilde{1}$	(1, 1, 1)	(1, 1, 1)
Weekly Important (WI)	$\tilde{3}$	(1, 3, 5)	(1/5, 1/3, 1)
Strongly Important (SI)	$\tilde{5}$	(3, 5, 7)	(1/7, 1/5, 1/3)
Very Important (VI)	$\tilde{7}$	(5, 7, 9)	(1/9, 1/7, 1/5)
Absolutely Important (AI)	$\tilde{9}$	(7, 9, 9)	(1/9, 1/9, 1/7)

There are many fuzzy AHP methods for calculating weights to be used in supermatrix of ANP. These methods were proposed by various authors in the literature (Buckley, 1985; Chang, 1992, 1996; Cheng, 1997; Deng, 1999; Leung & Cao, 2000; Mikhailov, 2004; Van Laarhoven & Pedrycz, 1983). These methods are systematic approaches to the alternative selection and justification problem by using the concepts of fuzzy set theory and hierarchical structure analysis (Yüksel and Dağdeviren, 2010). In this study, Chang's (1996) extent analysis method is employed. The extent analysis method is described below.

Let $X = \{x_1, x_2, \dots, x_n\}$ be an object set, and $G = \{g_1, g_2, \dots, g_m\}$ be a goal set. According to the method, each object is taken and extent analysis for each goal, g_i, is performed, respectively. Therefore, m extent analysis values for each object can be obtained with the following signs:

$$M_{g_i}^1, M_{g_i}^2, \dots, M_{g_i}^m, \quad i = 1, 2, \dots, n$$

where all the $M_{g_i}^j (j = 1, 2, \dots, m)$ are triangular fuzzy numbers (TFNs).

The steps of the extent analysis method are given below:

Step 1: The value of fuzzy synthetic extent with respect to the *i*th object is defined as

$$S_i = \sum_j^m M_{g_i}^j \otimes \left[\sum_{i=1}^n \sum_{j=1}^m M_{g_i}^j\right]^{-1} \quad (11)$$

To obtain $\sum_j^m M_{g_i}^j$, perform the fuzzy addition operation of m extent analysis values for a particular matrix such that

$$\sum_j^m M_{g_i}^j = \left(\sum_{j=1}^m l_j, \sum_{j=1}^m m_j, \sum_{j=1}^m u_j\right), \quad (12)$$

and to obtain $\left[\sum_{i=1}^n \sum_{j=1}^m M_{g_i}^j\right]^{-1}$, perform the fuzzy addition operation of $M_{g_i}^j (j = 1, 2, \dots, m)$values such that

$$\sum_{i=1}^n \sum_{j=1}^m M_{g_i}^j = \left(\sum_{i=1}^n l_i, \sum_{i=1}^n m_i, \sum_{i=1}^n u_i\right) \quad (13)$$

and then compute the inverse of the vector in Eq. (9) such that

$$\left[\sum_{i=1}^n \sum_{j=1}^m M_{g_i}^j\right]^{-1} = \left(\frac{1}{\sum_{i=1}^n l_i}, \frac{1}{\sum_{i=1}^n m_i}, \frac{1}{\sum_{i=1}^n u_i}\right) \quad (14)$$

Step 2: The degree of possibility of $M_2 = (l_2, m_2, u_2) \geq M_1 = (l_1, m_1, u_1)$ is defined as

$$V(M_2 \geq M_1) = sup\left[min\left(\mu_{M_1}(x), \mu_{M_2}(y)\right)\right]$$

and can be equivalently expressed as follows:

$$V(M_2 \geq M_1) = hgt(M_1 \cap M_2) = \mu_{M_2}(d) = \begin{cases} 1, & \text{if } m_2 \geq m_1, \\ 0, & \text{if } l_1 \geq u_2, \\ \frac{l_1 - u_2}{(m_2 - u_2) - (m_1 - l_1)}, & \text{otherwise,} \end{cases} \quad (15)$$

where d is the ordinate of the highest intersection point d between μ_{M_1} and μ_{M_2} (see Fig. 3). Both values of $V(M_1 \geq M_2)$ and $V(M_2 \geq M_1)$ are required in order to compare M_1 and M_2.

Step 3: The degree possibility for a convex fuzzy number to be greater than k convex fuzzy numbers $M_i (i = 1, 2, \ldots, k)$ can be defined by

$$V(M \geq M_1, M_2, \ldots, M_k) = V[(M \geq M_1) \text{ and } (M \geq M_2) \text{ and } \ldots \text{and } (M \geq M_k)]$$

$$= \min V(M \geq M_i), \quad i = 1, 2, \ldots, k. \quad (16)$$

Assume that

$$d'(A_i) = \min V(S_i \geq S_k) \quad \text{for } k = 1, 2, \ldots, n; k \neq i. \quad (17)$$

Then the weight vector is given by

$$W' = \left(d'(A_1), d'(A_2), \ldots, d'(A_n)\right)^T, \quad (18)$$

where $A_i (i = 1, 2, \ldots, n)$ are n elements.

Step 4: Via the normalization, the normalized weight vectors are

$$W = \left(d(A_1), d(A_2), \ldots, d(A_n)\right)^T, \quad (19)$$

where W is a nonfuzzy number.

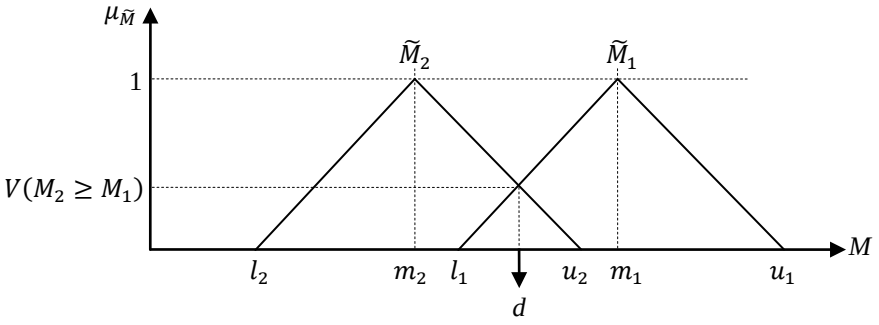

Fig. 3. The intersection between M_1 and M_2

VIKOR Method

VIKOR was developed by Opricovic (1998) and Opricovic and Tzeng (2002) with the Serbian name: VlseKriterijumska Optimizacija I Kompromisno Resenje, means multi-criteria optimization and compromise solution. The VIKOR method was developed for multicriteria optimization of complex systems and this method focuses on ranking and selecting from a set of alternatives, and determines compromise solutions for a problem with conflicting criteria, which can help the decision makers to reach a final decision. Development of the VIKOR method started with the following form of Lp-metric:

$$L_i^p = \{[\sum_{j=1}^n w_j \, (|f_j^* - f_{ij}|) \, / \, (f_j^* - f_j^-)]^p\}^{1/p} \quad (20)$$

where $1 \leq p \leq \infty$; alternatives i = 1, 2, …, m; w_j is derived from fuzzy ANP.

In the VIKOR method $L_i^{p=1}$ (as S_i) and $L_i^{p=\infty}$ (as R_i) are used to formulate ranking measure. The solution obtained by S_i is with a maximum group utility ("majority" rule), and the solution obtained by $\min R_i$ is with a minimum individual regret of the "opponent".

The main steps of the algorithm are taken from Sanayei et al.'s (2010) study:

Step 1: Obtain an aspired or tolerable level. Calculate the best f_j^* values (aspired level) and the worst f_j^- values (tolerable value) for all criterion *j = 1, 2, …, n*. Suppose the *jth* function denotes benefits:

$$f_j^* = max_i \, f_{ij}$$

$$f_j^- = min_i \, f_{ij}$$

or these values can be set by decision makers.

Step 2: Calculate mean of group utility and maximal regret. S_i is the synthesized gap for all criteria and R_i is the maximal gap in *i* criterion for prior improvement.

$$S_i = \sum_{j=1}^n w_j \, (|f_j^* - f_{ij}|) \, / \, (f_j^* - f_j^-) \quad (21)$$

$$R_i = \max_j (|f_j^* - f_{ij}|) \, / \, (f_j^* - f_j^-) \quad (22)$$

Step 3: Calculate the index value.

$$Q_i = v \frac{(S_i - S^*)}{(S^- - S^*)} + (1 - v) \frac{(R_i - R^*)}{(R^- - R^*)} \quad (23)$$

where

$$S^* = min_i \, S_i, \, S^- = max_i \, S_i, \, R^* = min_i \, R_i, \, R^- = max_i \, R_i$$

and *v* is introduced as the weight for the strategy of maximum group utility, whereas (1 – *v*) is the weight of the individual regret.

Step 4: Rank or improve the alternatives for a compromise solution. Order them decreasingly by the value of S_i, R_i and Q_i. Propose the alternative $A^{(1)}$as a compromise solution which is arranged by the measure $\min Q_i$ when the two conditions are satisfied:

C1. Acceptable advantage:

$Q(A^{(2)}) - Q(A^{(1)}) \geq 1/(m-1)$

where m is the number of alternatives and $A^{(2)}$ is the second position in the alternatives ranked by Q_i.

C2. Acceptable stability in decision making: Alternative $A^{(1)}$ must also be the best ranked by S_i or/and R_i.

If one of the conditions is not satisfied, then a set of compromise solutions is proposed, which consist of:

- Alternatives $A^{(1)}$ and $A^{(2)}$ if only the condition C2 is not satisfied,

or

- Alternatives $A^{(1)}$, $A^{(2)}$, . . ., $A^{(M)}$ if the condition C1 is not satisfied. $A^{(M)}$ is determined by the relation Q($A^{(M)}$) - Q($A^{(M)}$) < DQ for maximum M (the positions of these alternatives are close).

Implementation and Discussion

The case study is implemented in Sakarya, Turkey. First, interactions among the main criteria are derived asking expert opinions and using fuzzy DEMATEL approach. Then fuzzy ANP method is implemented according to the expert opinions in order to calculate the local weights of the sub-criteria. After determining the weights, five SMEs are investigated and graded according to each sub-criterion. As a result, each SME is scored between 0 and 100 implementing TOPSIS method.

The evaluation of one of the experts in terms of the effect between the criteria is given in Table 4. The corresponding triangular fuzzy numbers for the linguistic terms of the expert are given in Tablo 5. The linguistic terms and corresponding fuzzy numbers which were used during fuzzy DEMATEL approach were given in Table 2. Similarly, all of the evaluations from the rest of the experts are obtained and then averages of related triangular fuzzy numbers are calculated using Eq. (1). The average values are given in Table 6. The normalized direct-relation fuzzy matrix is obtained using Eqs. (2 and 3) and the result is shown in Table 7. After calculating the normalized direct-relation fuzzy matrix, the total-relation fuzzy matrix is obtained using Eqs. (4, 5, and 6). The total-relation fuzzy matrix is shown in Table 8.

Table 4. Linguistic evaluation of an expert in terms of effect among the criteria

	C1	C2	C3	C4	C5	C6	C7
C1	N	M	H	H	VH	VH	M
C2	M	N	L	M	M	M	M
C3	H	L	N	H	M	M	M
C4	H	H	M	N	L	L	L
C5	VH	H	H	H	N	M	H
C6	H	L	M	L	M	N	M
C7	VH	L	M	H	M	M	N

Table 5. Corresponding triangular fuzzy number for linguistic evaluation

	C1			C2			C3			C4			C5			C6			C7		
C1	0.00	0.00	0.00	0.25	0.50	0.75	0.50	0.75	1.00	0.50	0.75	1.00	0.75	1.00	1.00	0.75	1.00	1.00	0.25	0.50	0.75
C2	0.25	0.50	0.75	0.00	0.00	0.00	0.00	0.25	0.50	0.25	0.50	0.75	0.25	0.50	0.75	0.25	0.50	0.75	0.25	0.50	0.75
C3	0.50	0.75	1.00	0.00	0.25	0.50	0.00	0.00	0.00	0.50	0.75	1.00	0.25	0.50	0.75	0.25	0.50	0.75	0.25	0.50	0.75
C4	0.50	0.75	1.00	0.50	0.75	1.00	0.25	0.50	0.75	0.00	0.00	0.00	0.00	0.25	0.50	0.00	0.25	0.50	0.00	0.25	0.50
C5	0.75	1.00	1.00	0.50	0.75	1.00	0.50	0.75	1.00	0.50	0.75	1.00	0.00	0.00	0.00	0.25	0.50	0.75	0.50	0.75	1.00
C6	0.50	0.75	1.00	0.00	0.25	0.50	0.25	0.50	0.75	0.00	0.25	0.50	0.25	0.50	0.75	0.00	0.00	0.00	0.25	0.50	0.75
C7	0.75	1.00	1.00	0.00	0.25	0.50	0.25	0.50	0.75	0.50	0.75	1.00	0.25	0.50	0.75	0.25	0.50	0.75	0.00	0.00	0.00

Tablo 6. The initial direct-relation fuzzy matrix

	C1			C2			C3			C4			C5			C6			C7		
C1	0.000	0.000	0.000	0.542	0.792	0.917	0.417	0.667	0.875	0.375	0.625	0.833	0.625	0.875	1.000	0.583	0.833	0.958	0.250	0.500	0.750
C2	0.500	0.750	0.917	0.000	0.000	0.000	0.333	0.583	0.833	0.333	0.583	0.833	0.417	0.667	0.875	0.208	0.458	0.708	0.167	0.417	0.667
C3	0.417	0.667	0.917	0.417	0.667	0.875	0.000	0.000	0.000	0.583	0.833	0.958	0.417	0.667	0.875	0.375	0.625	0.833	0.250	0.500	0.750
C4	0.458	0.708	0.875	0.458	0.708	0.917	0.417	0.667	0.875	0.000	0.000	0.000	0.292	0.542	0.792	0.333	0.583	0.792	0.333	0.583	0.792
C5	0.667	0.917	1.000	0.458	0.708	0.917	0.458	0.708	0.917	0.458	0.708	0.958	0.000	0.000	0.000	0.458	0.708	0.917	0.542	0.792	1.000
C6	0.542	0.792	1.000	0.250	0.500	0.750	0.333	0.583	0.792	0.250	0.500	0.708	0.417	0.667	0.875	0.000	0.000	0.000	0.250	0.500	0.750
C7	0.583	0.833	0.958	0.042	0.292	0.542	0.250	0.500	0.750	0.500	0.750	0.958	0.292	0.542	0.792	0.292	0.542	0.792	0.000	0.000	0.000

Tablo 7. The normalized direct-relation fuzzy matrix

	C1			C2			C3			C4			C5			C6			C7		
C1	0.000	0.000	0.000	0.095	0.139	0.161	0.073	0.117	0.153	0.066	0.109	0.146	0.109	0.153	0.175	0.102	0.146	0.168	0.044	0.088	0.131
C2	0.088	0.131	0.161	0.000	0.000	0.000	0.058	0.102	0.146	0.058	0.102	0.146	0.073	0.117	0.153	0.036	0.080	0.124	0.029	0.073	0.117
C3	0.073	0.117	0.161	0.073	0.117	0.153	0.000	0.000	0.000	0.102	0.146	0.168	0.073	0.117	0.153	0.066	0.109	0.146	0.044	0.088	0.131
C4	0.080	0.124	0.153	0.080	0.124	0.161	0.073	0.117	0.153	0.000	0.000	0.000	0.051	0.095	0.139	0.058	0.102	0.139	0.058	0.102	0.139
C5	0.117	0.161	0.175	0.080	0.124	0.161	0.080	0.124	0.161	0.080	0.124	0.168	0.000	0.000	0.000	0.080	0.124	0.161	0.095	0.139	0.175
C6	0.095	0.139	0.175	0.044	0.088	0.131	0.058	0.102	0.139	0.044	0.088	0.124	0.073	0.117	0.153	0.000	0.000	0.000	0.044	0.088	0.131
C7	0.102	0.146	0.168	0.007	0.051	0.095	0.044	0.088	0.131	0.088	0.131	0.168	0.051	0.095	0.139	0.051	0.095	0.139	0.000	0.000	0.000

Tablo 8. The total-relation fuzzy matrix

	C1			C2			C3			C4			C5			C6			C7		
C1	0.071	0.280	1.285	0.139	0.352	1.282	0.120	0.334	1.297	0.117	0.341	1.330	0.157	0.378	1.348	0.146	0.361	1.301	0.084	0.286	1.212
C2	0.132	0.347	1.319	0.040	0.192	1.051	0.093	0.283	1.198	0.096	0.294	1.233	0.111	0.307	1.234	0.075	0.268	1.174	0.060	0.238	1.112
C3	0.130	0.364	1.396	0.115	0.318	1.252	0.046	0.213	1.140	0.143	0.354	1.321	0.118	0.331	1.306	0.108	0.314	1.260	0.079	0.271	1.188
C4	0.132	0.359	1.353	0.117	0.315	1.224	0.110	0.308	1.239	0.047	0.216	1.142	0.096	0.304	1.260	0.098	0.299	1.221	0.089	0.274	1.162
C5	0.182	0.433	1.509	0.130	0.350	1.347	0.129	0.351	1.370	0.135	0.366	1.416	0.062	0.256	1.268	0.132	0.355	1.362	0.132	0.337	1.308
C6	0.140	0.358	1.339	0.082	0.275	1.175	0.094	0.287	1.200	0.085	0.286	1.224	0.112	0.312	1.243	0.041	0.198	1.072	0.074	0.254	1.130
C7	0.144	0.359	1.315	0.048	0.241	1.130	0.080	0.271	1.177	0.122	0.317	1.240	0.090	0.289	1.213	0.089	0.281	1.177	0.031	0.170	0.998

The fuzzy values in total-relation fuzzy matrix is defuzzified by CFCS method using Eqs. (7-10). Then $(\widetilde{D}_i^{\,def} + \tilde{R}_i^{\,def})$ and $(\widetilde{D}_i^{\,def} - \tilde{R}_i^{\,def})$ values are calculated and shown in Table 9. The threshold value is determined as 0.48 according to the expert opinions. The values above the threshold are represented in bold in the table which gives the cause and effect relationship among the criteria. By using the dataset $(\widetilde{D}_i^{\,def} + \tilde{R}_i^{\,def})$ and $(\widetilde{D}_i^{\,def} - \tilde{R}_i^{\,def})$ given in Table 9, the causal diagram could be plotted as in Fig 3. The impact relation map indicating cause and effect relationship among main criteria can be illustrated as in Fig. 4, based on the information given in Table 9.

Table 9. Defuzzified total-relation matrix

	C1	C2	C3	C4	C5	C6	C7	$\widetilde{D}_i^{\,def}$	$\widetilde{D}_i^{\,def} + \tilde{R}_i^{\,def}$	$\widetilde{D}_i^{\,def} - \tilde{R}_i^{\,def}$
C1	0.45	**0.50**	**0.49**	**0.50**	**0.53**	**0.51**	0.44	3.42	7.03	-0.20
C2	0.50	0.34	0.44	0.45	0.46	0.42	0.39	3.00	6.10	-0.11
C3	**0.53**	0.47	0.37	**0.51**	**0.49**	0.47	0.42	3.26	6.40	0.13
C4	**0.52**	0.46	0.46	0.37	0.46	0.45	0.42	3.15	6.43	-0.12
C5	**0.59**	**0.51**	**0.51**	**0.53**	0.43	**0.52**	**0.50**	3.59	6.86	0.31
C6	**0.52**	0.43	0.44	0.44	0.47	0.35	0.40	3.04	6.18	-0.11
C7	**0.51**	0.39	0.42	0.47	0.44	0.43	0.31	2.98	5.86	0.10
$\tilde{R}_i^{\,def}$	3.61	3.10	3.13	3.28	3.27	3.15	2.88			

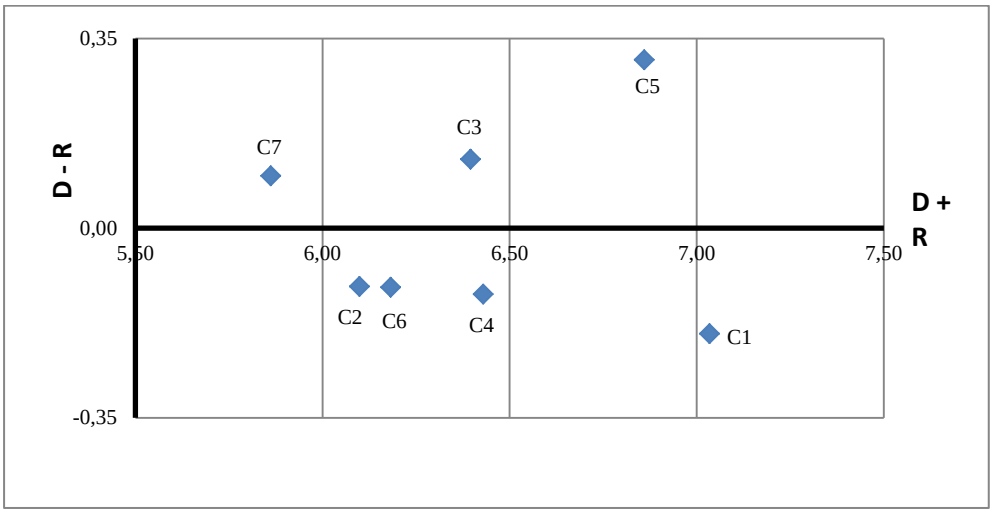

Fig. 3. The influence diagram of the main criteria

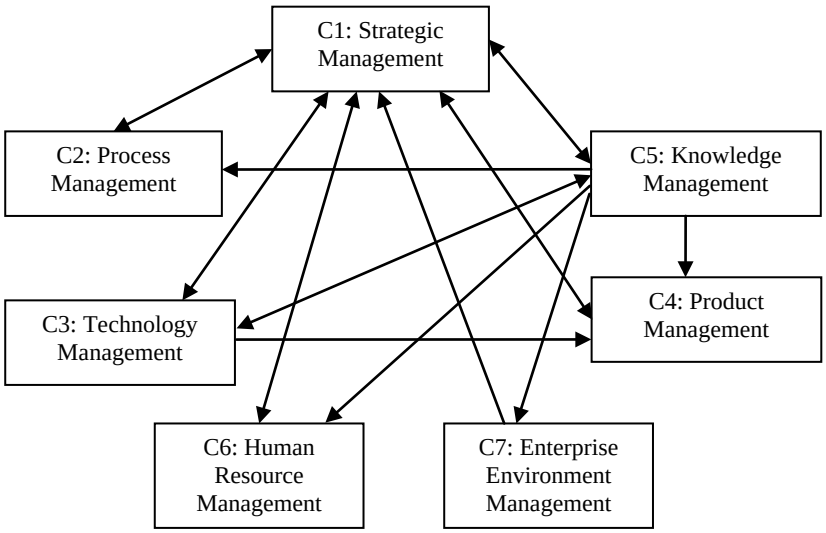

Fig. 4. The impact relation map for main criteria

According to the cause and effect relationship extracted from the fuzzy DEMATEL method, the weights of the sub-criteria are calculated following fuzzy ANP approach in order to form the supermatrix. For example, since "C1: Strategic Management" effects "C2: Process Management", the fuzzy evaluation of importance of sub-criteria of C2 (C21, C22 and C23) in terms of C11 is given in Table 10. Then geometric average is taken after obtaining evaluations of the rest of the experts in order to calculate the local weights using Eqs. (11-19). The result is shown in Table 11.

The rest of the local weights are calculated in the same way based on the interaction derived from the fuzzy DEMATEL. The supermatrix is formed for the sub-criteria and the local weights calculated are placed into the matrix accordingly. The unweighted supermatrix is presented in Table 12. Then, unweighted supermatrix is normalized to transform it the weighted supermatrix in which each of its columns sums to 1. The power of the weighted supermatrix is taken until the values of each column are stabilized and equal. These calculations are implemented using MATLAB software and the limit supermatrix is obtained which is given in Table 13. Any column of the matrix shows the weights of corresponding sub-criteria.

Tablo 10. Pairwise comparison matrix of an expert terms of C11: Strategic Analysis

Linguistic variables				Fuzzy numbers									
	C21	C22	C23		C21			C22			C23		
C21	EI	SI	VI	C21	1.00	1.00	1.00	3.00	5.00	7.00	5.00	7.00	9.00
C22		EI	WI	C22	0.14	0.20	0.33	1.00	1.00	1.00	1.00	3.00	5.00
C23			EI	C23	0.11	0.14	0.20	0.20	0.33	1.00	1.00	1.00	1.00

Tablo 11. Geometric average of all the expert evaluations, and the weights

	C21			C22			C23			Wi
C21	1.00	1.00	1.00	3.87	5.92	7.94	5.92	7.94	9.00	**0.95**
C22	0.12	0.17	0.26	1.00	1.00	1.00	1.00	3.00	5.00	**0.05**
C23	0.11	0.13	0.17	0.20	0.33	1.00	1.00	1.00	1.00	**0.00**

Tablo 12. Unweighted supermatrix

	C11	C12	C13	C21	C22	C23	C31	C32	C33	C41	C42	C43	C51	C52	C53	C61	C62	C63	C71	C72	C73
C11	0	0	0	0.36	0.32	0.23	0.00	0.00	0.25	0.35	0.77	0.37	0.84	0.36	0.05	0.36	0.35	0.36	0.00	0.19	0.08
C12	0	0	0	0.32	0.34	0.00	0.73	0.79	0.48	0.52	0.12	0.44	0.08	0.43	0.45	0.32	0.28	0.32	0.52	0.62	0.45
C13	0	0	0	0.32	0.33	0.77	0.27	0.21	0.26	0.13	0.11	0.20	0.08	0.21	0.50	0.32	0.37	0.32	0.48	0.18	0.47
C21	0.95	0.32	0.00	0	0	0	0	0	0	0	0	0	0.68	0.37	0.02	0	0	0	0	0	0
C22	0.05	0.42	0.60	0	0	0	0	0	0	0	0	0	0.00	0.52	0.49	0	0	0	0	0	0
C23	0.00	0.26	0.40	0	0	0	0	0	0	0	0	0	0.32	0.10	0.49	0	0	0	0	0	0
C31	0.53	0.35	0.28	0	0	0	0	0	0	0	0	0	0.50	0.12	0.53	0	0	0	0	0	0
C32	0.47	0.58	0.23	0	0	0	0	0	0	0	0	0	0.45	0.77	0.31	0	0	0	0	0	0
C33	0.00	0.07	0.49	0	0	0	0	0	0	0	0	0	0.05	0.11	0.16	0	0	0	0	0	0
C41	0.52	0.39	0.38	0	0	0	0.00	0.00	0.03	0	0	0	0.58	0.45	0.33	0	0	0	0	0	0
C42	0.11	0.26	0.05	0	0	0	0.10	0.00	0.36	0	0	0	0.21	0.00	0.33	0	0	0	0	0	0
C43	0.37	0.35	0.57	0	0	0	0.90	1.00	0.62	0	0	0	0.21	0.55	0.33	0	0	0	0	0	0
C51	0.43	0.39	0.43	0	0	0	0.00	0.00	0.00	0	0	0	0	0	0	0	0	0	0	0	0
C52	0.20	0.00	0.21	0	0	0	0.95	1.00	0.49	0	0	0	0	0	0	0	0	0	0	0	0
C53	0.38	0.61	0.36	0	0	0	0.05	0.00	0.51	0	0	0	0	0	0	0	0	0	0	0	0
C61	0.63	0.77	0.35	0	0	0	0	0	0	0	0	0	0.46	0.33	0.34	0	0	0	0	0	0
C62	0.00	0.12	0.37	0	0	0	0	0	0	0	0	0	0.09	0.35	0.14	0	0	0	0	0	0
C63	0.37	0.11	0.28	0	0	0	0	0	0	0	0	0	0.45	0.32	0.51	0	0	0	0	0	0
C71	0	0	0	0	0	0	0	0	0	0	0	0	0.61	0.33	0.36	0	0	0	0	0	0
C72	0	0	0	0	0	0	0	0	0	0	0	0	0.39	0.33	0.28	0	0	0	0	0	0
C73	0	0	0	0	0	0	0	0	0	0	0	0	0.00	0.33	0.36	0	0	0	0	0	0

Tablo 13. Limit supermatrix

	C11	C12	C13	C21	C22	C23	C31	C32	C33	C41	C42	C43	C51	C52	C53	C61	C62	C63	C71	C72	C73
C11	0.138	0.138	0.138	0.138	0.138	0.138	0.138	0.138	0.138	0.138	0.138	0.138	0.138	0.138	0.138	0.138	0.138	0.138	0.138	0.138	0.138
C12	0.158	0.158	0.158	0.158	0.158	0.158	0.158	0.158	0.158	0.158	0.158	0.158	0.158	0.158	0.158	0.158	0.158	0.158	0.158	0.158	0.158
C13	0.121	0.121	0.121	0.121	0.121	0.121	0.121	0.121	0.121	0.121	0.121	0.121	0.121	0.121	0.121	0.121	0.121	0.121	0.121	0.121	0.121
C21	0.043	0.043	0.043	0.043	0.043	0.043	0.043	0.043	0.043	0.043	0.043	0.043	0.043	0.043	0.043	0.043	0.043	0.043	0.043	0.043	0.043
C22	0.036	0.036	0.036	0.036	0.036	0.036	0.036	0.036	0.036	0.036	0.036	0.036	0.036	0.036	0.036	0.036	0.036	0.036	0.036	0.036	0.036
C23	0.024	0.024	0.024	0.024	0.024	0.024	0.024	0.024	0.024	0.024	0.024	0.024	0.024	0.024	0.024	0.024	0.024	0.024	0.024	0.024	0.024
C31	0.040	0.040	0.040	0.040	0.040	0.040	0.040	0.040	0.040	0.040	0.040	0.040	0.040	0.040	0.040	0.040	0.040	0.040	0.040	0.040	0.040
C32	0.047	0.047	0.047	0.047	0.047	0.047	0.047	0.047	0.047	0.047	0.047	0.047	0.047	0.047	0.047	0.047	0.047	0.047	0.047	0.047	0.047
C33	0.016	0.016	0.016	0.016	0.016	0.016	0.016	0.016	0.016	0.016	0.016	0.016	0.016	0.016	0.016	0.016	0.016	0.016	0.016	0.016	0.016
C41	0.045	0.045	0.045	0.045	0.045	0.045	0.045	0.045	0.045	0.045	0.045	0.045	0.045	0.045	0.045	0.045	0.045	0.045	0.045	0.045	0.045

C42	0.019	0.019	0.019	0.019	0.019	0.019	0.019	0.019	0.019	0.019	0.019	0.019	0.019	0.019	0.019	0.019	0.019	0.019	0.019	0.019	0.019	0.019
C43	0.073	0.073	0.073	0.073	0.073	0.073	0.073	0.073	0.073	0.073	0.073	0.073	0.073	0.073	0.073	0.073	0.073	0.073	0.073	0.073	0.073	0.073
C51	0.035	0.035	0.035	0.035	0.035	0.035	0.035	0.035	0.035	0.035	0.035	0.035	0.035	0.035	0.035	0.035	0.035	0.035	0.035	0.035	0.035	0.035
C52	0.041	0.041	0.041	0.041	0.041	0.041	0.041	0.041	0.041	0.041	0.041	0.041	0.041	0.041	0.041	0.041	0.041	0.041	0.041	0.041	0.041	0.041
C53	0.042	0.042	0.042	0.042	0.042	0.042	0.042	0.042	0.042	0.042	0.042	0.042	0.042	0.042	0.042	0.042	0.042	0.042	0.042	0.042	0.042	0.042
C61	0.057	0.057	0.057	0.057	0.057	0.057	0.057	0.057	0.057	0.057	0.057	0.057	0.057	0.057	0.057	0.057	0.057	0.057	0.057	0.057	0.057	0.057
C62	0.017	0.017	0.017	0.017	0.017	0.017	0.017	0.017	0.017	0.017	0.017	0.017	0.017	0.017	0.017	0.017	0.017	0.017	0.017	0.017	0.017	0.017
C63	0.029	0.029	0.029	0.029	0.029	0.029	0.029	0.029	0.029	0.029	0.029	0.029	0.029	0.029	0.029	0.029	0.029	0.029	0.029	0.029	0.029	0.029
C71	0.008	0.008	0.008	0.008	0.008	0.008	0.008	0.008	0.008	0.008	0.008	0.008	0.008	0.008	0.008	0.008	0.008	0.008	0.008	0.008	0.008	0.008
C72	0.007	0.007	0.007	0.007	0.007	0.007	0.007	0.007	0.007	0.007	0.007	0.007	0.007	0.007	0.007	0.007	0.007	0.007	0.007	0.007	0.007	0.007
C73	0.005	0.005	0.005	0.005	0.005	0.005	0.005	0.005	0.005	0.005	0.005	0.005	0.005	0.005	0.005	0.005	0.005	0.005	0.005	0.005	0.005	0.005

After calculating the weights of the criteria, it is time to implement VIKOR method, which is going to score institutionalization level of the SMEs investigated. Five SMEs are investigated in Sakarya region and assigned a score between 0-100 to each SME for each criterion. The scores are given in Table 14. f_j^* is taken as 100 since it is the maximum score of each criterion and f_j^- is take as 0 since it is the minimum score of each criterion.

VIKOR method is implemented by using Eq. (21-23) in order to obtain S_i, R_i and Q_i values. Table 15 shows the results ranked by S_i, R_i and Q_i. It is found out that, firm D is the best institutionalized one among the alternatives. The rest of the SMEs are ranked as A, C, E and B.

Tablo 14. Evaluation of the firms in terms of the sub-criteria

	A	B	C	D	E	f_j^*	f_j^-
C11	75.0	87.5	87.5	87.5	100.0	100	0
C12	81.3	0.0	68.8	75.0	75.0	100	0
C13	75.0	80.0	75.0	90.0	65.0	100	0
C21	63.4	60.3	75.9	65.6	41.5	100	0
C22	56.3	68.8	81.3	68.8	56.3	100	0
C23	100.0	100.0	100.0	75.0	75.0	100	0
C31	75.0	62.5	85.0	80.0	62.5	100	0
C32	81.3	47.5	70.0	92.5	56.3	100	0
C33	50.0	87.5	50.0	100.0	75.0	100	0
C41	82.5	67.5	82.5	85.0	62.5	100	0
C42	87.5	89.3	78.6	87.5	75.0	100	0
C43	75.0	65.0	55.0	95.0	75.0	100	0
C51	88.5	55.8	94.2	65.4	59.6	100	0
C52	81.3	87.5	96.9	68.8	50.0	100	0
C53	75.0	59.4	78.1	68.8	50.0	100	0
C61	81.8	79.5	95.5	63.6	54.5	100	0
C62	75.0	53.9	86.8	57.9	57.9	100	0
C63	75.0	51.6	95.3	68.8	67.2	100	0
C71	75.0	58.3	95.8	66.7	70.8	100	0
C72	100.0	37.5	100.0	68.8	68.8	100	0
C73	90.0	77.5	95.0	85.0	72.5	100	0

Tablo 15. Ranking the SMEs

S_i	Rank by S_i	R_i	Rank by R_i	Q_i	Rank by Q_i
0,205	D	0,034	A	0,021	D
0,206	C	0,039	D	0,059	A
0,227	A	0,042	E	0,062	C
0,312	E	0,049	C	0,319	E
0,391	B	0,158	B	1,000	B

Conclusion

One of the main objectives of this study is to measure institutionalization level of small and medium sized enterprises (SMEs). The assessment of institutionalization process is based on multiple criteria. Therefore, multi-criteria decision making techniques are implemented. The process also requires more than one expert opinion. That is why group decision making approach is applied in the measurement model.

In this study, fuzzy hybrid multi-criteria decision making approach is used in order to measure institutionalization readiness of SMEs. For achieving this, first of all, criteria and sub-criteria that indicate the institutionalization readiness level of SMEs are determined. Then, interactions among main criteria are derived by using fuzzy DEMATEL approach. According to the influence of each criterion over other criteria, the weights of the sub-criteria are calculated obtaining experts' opinion, and by using fuzzy ANP method. Several SMEs are evaluated in terms of the criteria predefined and VIKOR method is implemented for measuring the institutionalization level of the SMEs. The proposed approach can be applied for other multi-criteria decision making problems.

References

Alpay G., Bodur, M., Yılmaz, C., Çetinkaya, S., Arıkan, L., (2008). Performance implications of institutionalization process in family-owned businesses: Evidence from an emerging economy. Journal of World Business, 43, 435-448.

Apaydın, F., (2009). Kurumsal teori ve işletmelerin kurumsallaşması. C.Ü. İktisadi ve İdari Bilimler Dergisi, 10.

Apaydın, F., Coşkun, A. (2008). Organizational Institutionalization and Corporate Performance Results: A Study on Small and Medium Size Enterprises in Turkey, In: Proceeding of 1st International Conference on Management and Economics, Tirane, Albania.

Buckley, J.J. (1985). Fuzzy hierarchical analysis. Fuzzy Sets and Systems, 17, 233-247.

Büyüközkan, G., & Çifçi, G. (2012). A. novel hybrid MCDM approach based on fuzzy DEMATEL, fuzzy ANP and fuzzy TOPSIS to evaluate green suppliers. Expert Systems with Applications 39, 3000-3011

Chang, D.Y. (1992). Extent analysis and synthetic decision, optimization techniques and applications (Vol. 352). Singapore: World Scientific.

Chang, D.Y. (1996). Applications of the extent analysis method on fuzzy AHP. European Journal of Operational Research, 95, 649-655.

Cheng, C.H. (1997). Evaluating naval tactical missile systems by fuzzy AHP based on the grade value of membership function. European Journal of Operational Research, 96, 343-350.

Deng, H. (1999). Multicriteria analysis with fuzzy pairwise comparison. International Journal of Approximate Reasoning, 21, 215-231.

Ho, W.-R.J., Tsai, C.-L., Tzeng, G.-H., Fang, S.-K., (2011). Combined DEMATEL technique with a novel MCDM model for exploring portfolio selection based on CAPM. Expert Systems with Applications, 38, 16–25.

Kahveci, T.C., (2007). İmalat işletmelerinde kurumsallaşma ve kurumsal modelleme, PhD thesis, Sakarya University.

Karpuzoğlu, E. (2004). Büyüyen ve Gelişen Aile Şirketlerinde Kurumsallaşma. Hayat Yayınları.

Korkmaz, M., (2003). Kurumsallaşma nedir ve niçin gereklidir?. Dünya Gazetesi.

Lee, W.-S., Huang, A.Y., Chang, Y.Y., Cheng, C.M., (2011). Analysis of decision making factors for equity investment by DEMATEL and Analytic Network Process. Expert Systems with Applications, 38, 8375–8383.

Leung, L.C., Cao, D. (2000). On consistency and ranking of alternatives in fuzzy AHP. European Journal of Operational Research, 124, 102-113.

Lin, Chi-Jen, Wu, Wei-Wen (2008). A causal analytical method for group decision making under fuzzy environment. Expert Systems with Applications, 34, 205-213.

Lin, Chi-Jen, Wu, Wei-Wen (2004). A fuzzy extension of the DEMATEL method for group decision making. European Journal of Operational Research, 156, 445-455.

Lin, C.-L., Hsieh, M.-S., Tzeng, G.-H., (2010). Evaluating vehicle telematics system by using a novel MCDM techniques with dependence and feedback. Expert Systems with Applications, 37, 6723–6736.

Liou, J.J.H, Chuang, Y.T., (2010). Developing a hybrid multi-criteria model for selection of outsourcing providers. Expert Systems with Applications, 37, 3755–3761.

Mikhailov, L. (2004). A fuzzy approach to deriving priorities from interval pairwise comparison judgments. European Journal of Operational Research, 159, 687-704.

Mohanty, R.P., Agarwal, R., Choudhury, A.K., Tiwari, M.K., 2005. A fuzzy ANP based approach to R&D project selection: A case study. International Journal of Production Research, 43(24), 5199–5216.

Opricovic, S., (1998). Multicriteria optimization of civil engineering systems (in Serbian, Visekriterijumska optimizacija sistema u gradjevinarstvu). Faculty of Civil Engineering, Belgrade.

Opricovic, S., Tzeng, G.H. (2002). Multicriteria planning of post-earthquake sustainable reconstruction. Computer-Aided Civil and Infrastructure Engineering, 17, 211–220.

Opricovic, S., Tzeng, G.H. (2003). Defuzzification within a multicriteria decision model, International Journal of Uncertainty. Fuzziness and Knowledge-Based Systems, 11(5), 635-652.

Saaty, T.L. (1996). Decision Making with Dependence and Feedback: Analytic Network Process, RWS Publications, Pittsburgh.

Saaty, T.L., Vargas, L.G., (1998). Diagnosis with dependent symptoms: Bayes theorem and the analytic network process. Operations Research, 46(4), 491–502.

Sanayei, A., Mousavi, S.F., Yazdankhah, A., (2010). Group decision making process for supplier selection with VIKOR under fuzzy environment. Expert Systems with Applications, 37, 24–30.

Selznick, P., (1996). Institutionalism old and new. Administrative Science Quarterly, 41, 270-277.

Yager, R.R., Filev, D.P. (1994). Essentials of fuzzy modeling and control. New York: John Wiley & Sons.

Yüksel, İ., Dağdeviren, M. (2010). Using the fuzzy analytic network process (ANP) for Balanced Scorecard (BSC): A case study for a manufacturing firmExpert Systems with Applications, 37, 1270-1278.

Van Laarhoven, P.J.M., Pedrycz, W. (1983). A fuzzy extension of Saaty's priority theory. Fuzzy Sets and Systems, 11, 229-241.

Wu, Wei-Wen (2008). Choosing knowledge management strategies by using a combined ANP and DEMATEL approach. Expert Systems with Applications 35, 828–835.

Yang, H.W., Chang, K.F., (2012). Combining means-end chain and fuzzy ANP to explore customers' decision process in selecting bundles. International Journal of Information Management, 32, 381– 395.

Yang, J. L., Tzeng, G.-H., (2011). An integrated MCDM technique combined with DEMATEL for a novel cluster-weighted with ANP method. Expert Systems with Applications 38, 1417–1424

Zeleny, M. (1982). Multiple Criteria Decision Making, Mc-Graw-Hill, New York.

A New Laminate Composite System: Metallic-Intermetallic Laminate Material

[1]Tuba Yener, [1]Zeynep Öztekin, [1]İbrahim Altınsoy, [2]Gözde F.Çelebi Efe, [1]Sakin Zeytin

[1]Sakarya University, Engineering Faculty, Department of Metallurgy and Materials Engineering, Serdivan/Sakarya-Turkey
[2]Sakarya University, Karasu Vacotional High School, Department of Machinery and Metal Technologies, Karasu/Sakarya-Turkey

e-mail:tcerezci@sakarya.edu.tr

Abstract: Metallic-intermetallic laminate (MIL) composites consisting of alternating layers of Ta, Al and the intermetallic Al_3Ta have been fabricated by reactive foil sintering in open atmospheric furnace. In this study, tantalum and aluminum foils with initial thicknesses of 250 µm were used. Sintering process has carried at 850-900 and 950 ºC for 5 and 7.5 hours under 2 MPa pressure. The aluminium foil was consumed by forming a tantalum aluminide intermetallic compound. Thus, the final microstructure consists of alternating layers of intermetallic compound and unreacted Ta metal. Microstructural characterizations of produced composites have conducted by using scaning electron microscope. Hardness values of test samples have also measured by vickers indentation method.

Key Words: Intermetallic, tantalum aluminide, laminate composite, sintering

Introduction

It is well known that the widespread engineering application of ceramics and other highly brittle materials, e.g. intermetallic compounds, is severely limited by their low toughness. A number of toughening strategies have been proposed to improve the critical stress intensity required for crack propagation. One of the most effective toughening techniques is to introduce a ductile phase, which remains intact and bridges the crack faces in the wake of a growing crack. Under such a circumstance, the crack tip is shielded by the closure traction imposed by the plastic deformation of ductile ligaments. In particular, when layered ductile phases are incorporated, laminate composites can be formed, which enhance the toughness (Oktay, 2010, p.1043-1050, Peng, 2004, p.243-248).
Metallic-intermetallic composites can be designed for structural use to optimize the unique properties and benefits of the constituent components, resulting in materials that have the high strength and stiffness of the intermetallic phase and the high toughness of the metal. Pro intermetallics have been reinforced with particles, rods, or layers of ductile metals in efforts to increase toughness. Ductile phase reinforcement of brittle materials utilizes crack-laminate interactions to generate a zone of bridging ligaments that restrict crack opening and growth by generating closure tractions in the crack wake and utilize the work of plastic deformation in the ductile metal phase to increase fracture resistance of the composite (David, 2005).

Laminate composites are being intensively studied for a number of potential applications: electronic devices, structural components, armor, etc. Ceramic–ceramic, metal–ceramic, metal–metal, metal–ceramic–intermetallic and metal–intermetallic systems have shown desirable properties (Tiezheng, 2004, p.10-26). In particular, the Ti–Al_3Ti system has a great potential for structural applications because of its low density and excellent specific mechanical properties (Rohatgi, 2003, p.2933-2957, Price, 2011, p.1334-1346)

Titanium–titanium tri-aluminide (Ti–Al_3Ti) metallic–intermetallic laminate (MIL) composites have been produced from elemental titanium and aluminum foils by a novel one-step process utilizing a controlled reaction at elevated temperature and pressure. Of the various possible aluminides in the Ti–Al system, the formation of

the intermetallic Al_3Ti is thermodynamically and kinetically favored over the formation of other aluminides when reacting Al directly with Ti. This preferential formation of Al_3Ti is fortuitous as its Young's modulus (216 GPa) and oxidation resistance are higher, and the density (3.3 g/cm^3) lower than that of the other titanium aluminides such as Ti_3Al and TiAl **(**(Rohatgi, 2003, p.2933-2957, Zeytin, 2008).

Intermetallic compounds based upon aluminides of several transition metals such as iron, nickel, titanium, cobalt, niobium, and tantalum have been recognized as potential candidates for the high-temperature structural applications. Among various aluminides of transition metals, the compounds in the Ta–Al system have been of great interest for their excellent mechanical properties and high degree of structural complexity. The Ta–Al phase diagram depicted in Fig. 1 shows the existence of four aluminides, including Ta_2Al, TaAl, $TaAl_2$, and $TaAl_3$. (Yeh, 2010, p.153-158).

They are stable, refractory and reflective, and have been proposed as mirror coatings for use in the IR. Melting point of 1400°C and the density is 7.02 g/cm³. Because of this aspects, tantalum aluminides are can be used in high temperature applications (http://en.wikipedia.org/,2012)

Tantalum-aluminum system is one of the most well known in terms of the formation of intermetallic phase. This system is also in the priority among in laminate composite systems. The objective of the present research is to synthesize tantalum-tantalum aluminide metallic-intermetallic composites and its microstructural characterization.

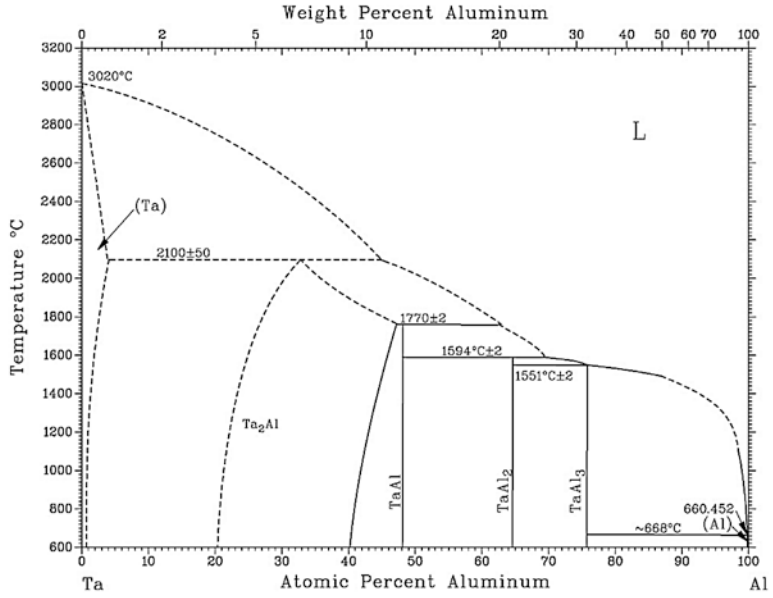

Figure 1: Ta-Al phase diagram (Yeh, 2010, p.153-158)

Materials and Method

The MIL process consists of stacking commercial purity aluminum and tantalum aluminide foils in alternating layers. The foils were provided from Alfa Aesar Company and their properties are shown in the table 1.

Table 1: Properties of foils used in experiments

Foil	Thickness, μm	Purity, %
Ta	250	99,5
Al	250	99,0

The foil dimensions were initially selected to completely consume the aluminum in forming the intermetallic compound with alternating layers of partially unreacted Ta metal. The dimensions of the processed samples are in the shape of platelets as 10mm×10mm. Samples were cleaned with alcohol and dried before stacking process. In each stack was consisting of 4 tantalum and 3 aluminum foil as in shown Fig.2a. An initial pressure of 2.0 MPa is applied at room temperature to ensure good contact between foils (Fig.2b). Sintering process is applied in an open air, electrical resistance furnace at 850-900-950 ºC for 5 and 7.5 hours for each temperature.

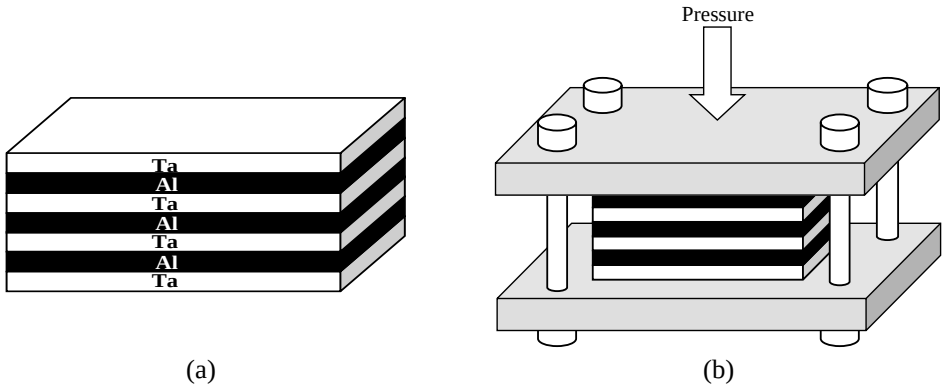

Figure 2:(a) Tantalum-Aluminum stack, (b) Schematic diagram of the synthesis apparatus. Image is not to scale and does not show the load frame (İpek, 2008, p.1262-1268)

Samples were ground and polished using standard metallographic techniques. Microstructure analyses of composites were performed with a JEOL JSM-5600 model scanning electron microscope (SEM). The presence of phases formed within the sintered samples was determined by Energy Dispersive Spectroscopy (EDS). Microhardness of composites were determined using a Leica WMHT-Mod model Vickers hardness instrument under an applied load of 300 g for intermetallic zone, and 100 g for metallic zone.

Results and Discussion

The typical microstructures of the MIL composites are shown in Fig.3-5. The presence of different regions indicates that different phases in the composites. In relatively low magnification (Fig.3.a) it is shown that foils are stacked properly. Furthermore, the laminated composites are well-bonded. There is a symmetric change from a light colored phase to another. Following the light colored phase there is a grey colored formation, subsequently, darker grey colored phase and in the center line a black colored phase. The light colored layers consist of unreacted Ta, which are separated by the apparently darker Al_3Ta-layers, as was identified by quantitative EDS analysis (Fig. 6). In metallic-intermetallic composites, interaction initially occurs at the interface then progress along the center of aluminum foil as well as along tantalum foil. But this progress reaction along tantalum is slower than that of in aluminum. As tantalum and aluminum react with each other, the impurities in aluminum or interface of Ta-Al, shifts in the front of the reaction. If the reaction ended before aluminum consuming these impurities deposited in aluminum, otherwise in centerline of the intermetallic. Because of this it is understood that the centerline is a problematic zone. As evidence in laminate composites centerline is one of the preferred zones for the formation of cracks.

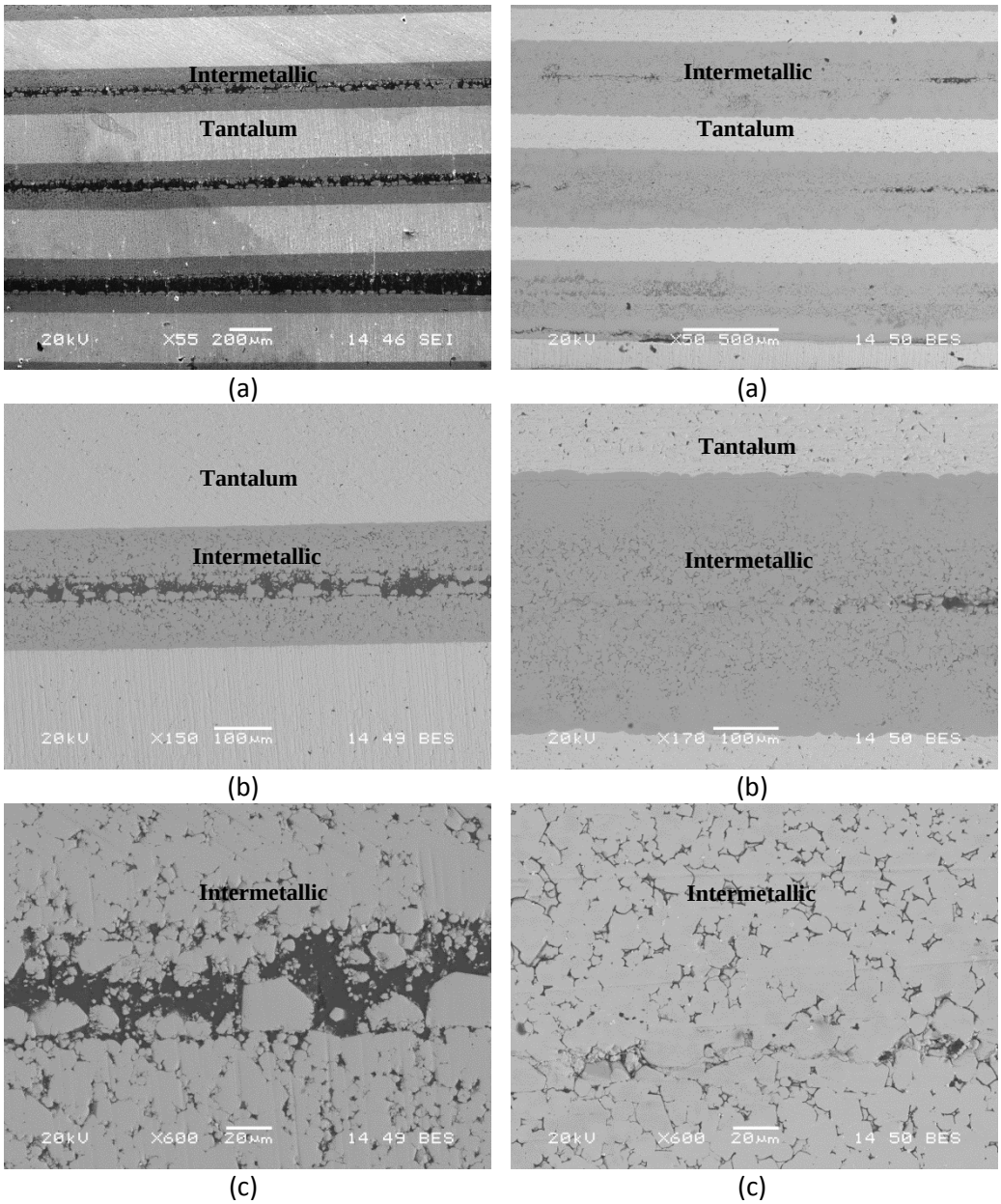

Figure 3:SEM micrographs of Ta-Al metallic–intermetallic composites in the left sintered at 850 °C,5 h (a)55X, (b)150X, (c)600X, in the right sintered at 850 °C ,7.5 h (a)50X ,(b)170X, (c)600X

It is clearly seen in metallic intermetallic Ta-Al composites sintered at 850 °C for 5 hours, the middle grey-black zone essentially formed by various phases such as residual aluminum, $TaAl_3$. As the sintering time increases from 5 hours to 7.5 hours, residual aluminum layer at the intermetallic centerline decreases. Moreover sintering process is better at relatively high temperature and time.

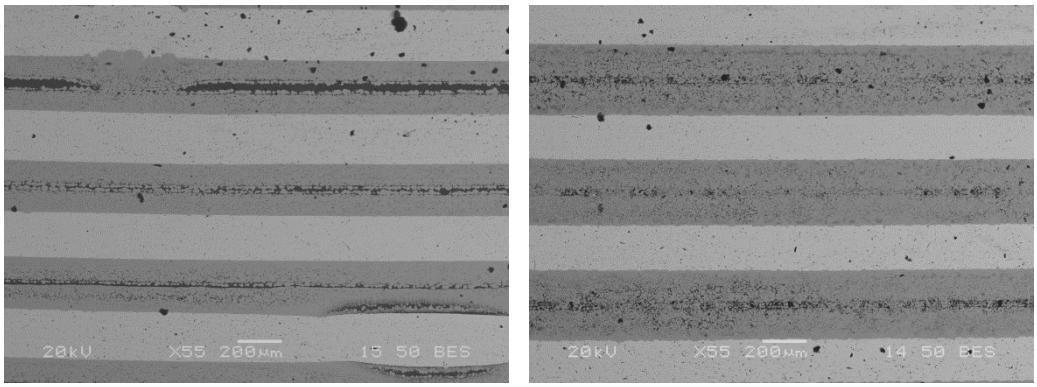

(a) (b)

Figure 4: SEM micrographs of Ta-$TaAl_3$ metallic–intermetallic composites 900 °C,(a) 5 h-55X, (b) 7.5 h-55X

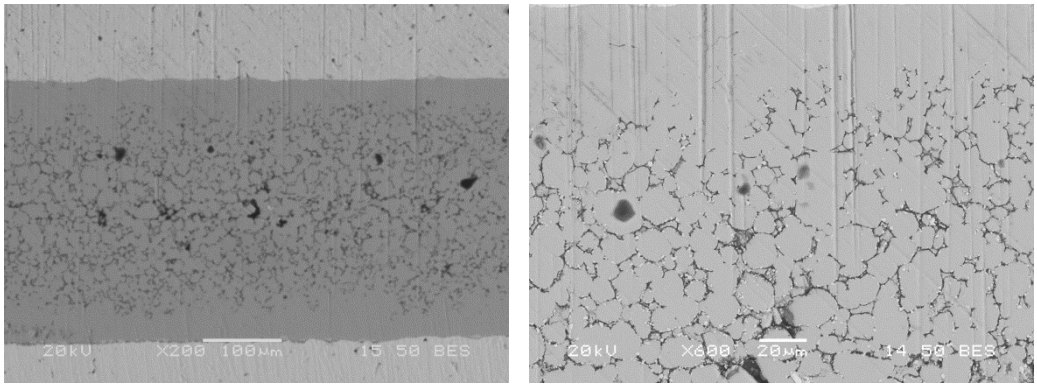

(a) (b)

Figure 5: SEM micrographs of Ta-$TaAl_3$ metallic–intermetallic composites 950 °C, 5 hour, (a)200X, (b)600X

From SEM micrographs for 850-900 and 950°C (Fig:3-5) it is seen that interface of metallic tantalum and tantalum-aluminum intermetallic is quite smooth. To form Ta-Al intermetallic, reaction between tantalum and aluminum initiate with nucleation in a number of different regions. These nucleuses grow and merge with each other. A whole aluminide layer form in this way. Stable metallic-intermetalic structure occurs when suitable temperature and time conditions are provided.

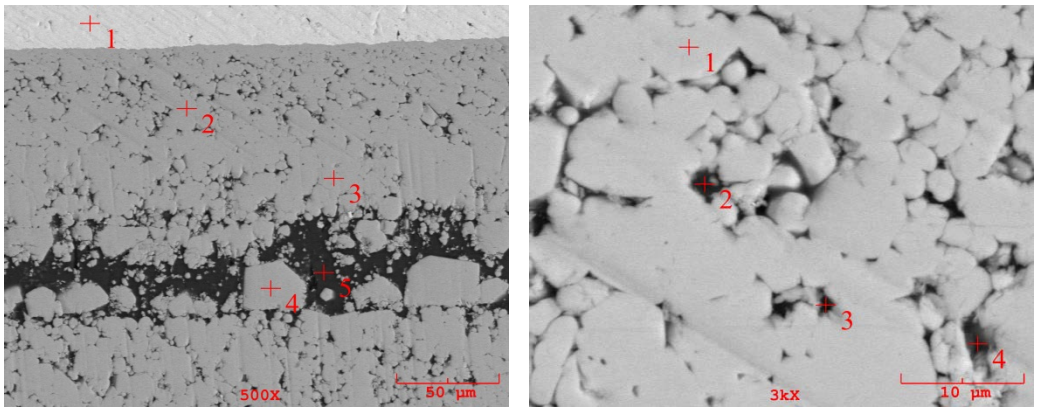

%Wt.	1	2	3	4	5
Ta	100	16.991	14.567	17.078	0.512
Al	0	83.991	85.433	82.922	99.488

(a)

%Wt	1	2	3	4
Ta	14.991	3.289	6.173	24.857
Al	85.009	96.711	93.827	75.143

(b)

Figure 6: SEM-EDS analysis of Ta-Al metallic-intermetallic composite sintered at 850ºC for 5 h.(a) 500X, (b) 3000X.

As in shown in Fig 6.a, spot 1 is located in the unreacted Ta layer and spots 2, 3 and 4 in the Al_3Ta layer with different positions. Some dark particles, identified as residual Al are also observed in the Al_3Ta layers. Furthermore, the laminated composites are well-bonded and remain some residual porosity in the final microstructure due to the relatively low temperature and time. Also in this EDS analyses show that, formation of intermetallic hasn't completed yet.

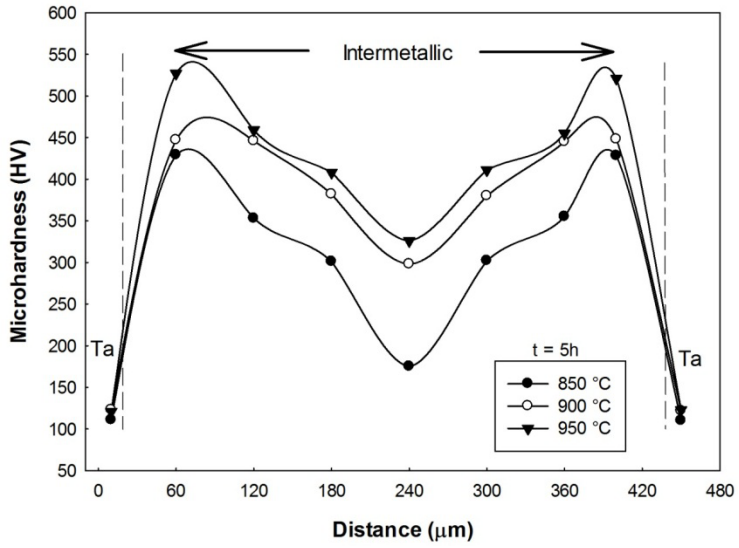

Figure 7: Hardness graphic of Ta-Al metallic-intermetallic composites sintered at 850, 900, 950 ºC, 5 hours.

The ceramic-like aluminide phases (Al_3Ti or Ni_3Al) give high hardness and stiffness to the composite, while the unreacted Ti or Ni provides the necessary high strength, toughness and ductility for the system to concurrently be flexible. The multi-layered structure of the composite allows for variations in the layer thickness and phase volume fractions of the Al and Ti or Ni components simply through the selection of initial thickness, which consequently allows for the optimization of mechanical and thermal management properties for practical application (Peng, 2005, 309-318).

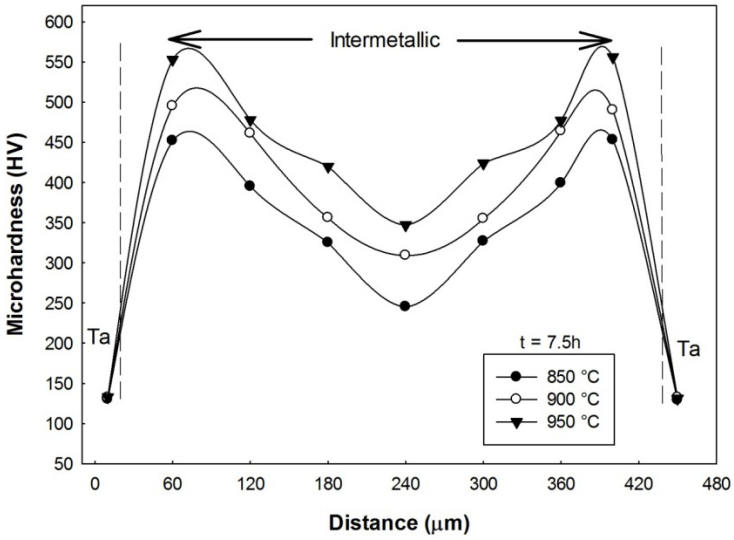

Figure 8: Hardness graphic of Ta-Al metallic-intermetallic composites sintered at 850, 900, 950 ºC, 7,5 hours.

The microhardness profile measured for several layers of the composite is shown in Fig.7, 8. As known, hardness value of metallic tantalum and its intermetallic structure is quite different. The average microhardness values for tantalum, aluminum and $TaAl_3$ are 120, 475 and 45 HV, respectively. While the hardness of the intermetallic layer is highest at the border $TaAl_3$-Ta, it gradually decreases toward the border $TaAl_3$-Al.These results are in good agreement with the literature. In addition, relatively high temperature and time is also very effective on sintering metallic-intermetallic laminate composite. As time and temperature increase, the hardness values raise because of bonding in the interface improved and residual aluminum started the consuming.

Conclusions

The conclusions of this research can be summarized as follows:

- By controlling the duration of the reactive foil sintering process, composites can be fabricated in which a tailored amount of residual aluminum remains at the intermetallic centerline. The result is a well-bonded composite with a high degree of microstructural control.
- Ta–Al_3Ta metal–intermetallic laminate (MIL) composites have been successfully synthesized by reactive foil sintering technique in open air at 850-900 and 950 ºC for 5 and 7.5 hours under 2 MPa pressure. The laminated structure is well-bonded, nearly fully dense.
- Microstructural characterization by, SEM and EDS indicates that Al_3Ta is the only intermetallic phase. Tantalum aluminide phase occurs due to the thermodynamics of the reaction between Ta and Al. The existence of liquid Al phase plays important roles in the nucleation and growth of Al_3Ta particles and the eventual formation of continuous alternative Al_3Ta intermetallic layers.
- The mechanic properties of hardness of the fabricated laminated composites were examined. Whereas the hardness of metallic aluminum and tantalum respectively is about 45, 120 HV, hardness of intermetallic zone is approximately 450-500 HV. The results showed that as time and temperature increase, the hardness values raise because of bonding in the interface improved and residual aluminum started the consuming.

Acknowledgements

The authors thank to experts Fuat Kayis for performing XRD and SEM-EDS studies and special appreciation are extended to technician Ersan Demir of Sakarya University for assisting with experimental studies.

References

Bataev, I.A. Bataev, A.A. Mali, V.I., Pavliukova, D.V., (2012) *Structural and mechanical properties of metallic–intermetallic laminate composites produced by explosive welding and annealing* (pp: 225–234), Materials and Design

İpek, M., Üstel, F., Zeytin S., (2008), *Fracture Behaviour of Ti-Al_3Ti Metallic-Intermetallic Laminate (MIL) Composites*, (p.1262-1268), Pamukkale University , Denizli.

Oktay, S, Yıldırım, H, Yener, T., İpek, M ., Zeytin S., Bindal, C. (2010), *Intermetallics Formation in Nickel Aluminum Laminate System*, (pp:1043-1050), Pamukkale University, Denizli

Peng, L.M. Wang, J.H., Li, H., Zhao, J.H., He, L.H, (2004) *Synthesis and microstructural characterization of Ti–Al3Ti metal–intermetallic laminate (MIL) composites*, (pp:243–248) Scripta Materialia

Peng, L.M., Li, H. Wang, J.H., (2005) *Processing and mechanical behavior of laminated titanium–titanium tri-aluminide (Ti–Al3Ti) composites*, (pp:309–318), Materials Science and Engineering

Price, R.D., Jiang, F., Kulin, R.M., Vecchio, K.S., (2011), *Effects of ductile phase volume fraction on the mechanical properties of Ti–Al3Ti metal-intermetallic laminate (MIL) composites*, (pp:3134-3146), Materials Science and Engineering

Rohatgi, A., Harach, D.J., Vecchio, K.S., Harvey, K.P., (2003) *Resistance-curve and fracture behavior of Ti–Al3Ti metallic–intermetallic laminate (MIL) composites*, (pp:2933–2957), Acta Materialia

Tiezheng Li, F. Grignon, D.J. Benson, K.S. Vecchio, E.A. Olevsky, Fengchun Jiang, A. Rohatgi, R.B. Schwarz, M.A. Meyers , (2004), *Modeling the elastic properties and damage evolution in Ti–Al3Ti metal intermetallic laminate (MIL) composites*, (pp:10–26), Materials Science and Engineering

Yeh, C.L., Wang, H.J., (2010) *Formation of Ta–Al intermetallics by combustion synthesis involving Al-based thermite reactions*, (pp:153–158), Journal of Alloys and Compounds

Zeytin S., Üstel, F., İpek, M., Kazdal, Zeytin, H., (2008), *Production of Ti–Al3Ti metal intermetallic laminate (MIL) composites*, Project Number:104M184, Tubitak Project

http://en.wikipedia.org/2012

Application of a continuous FB MSZ type crystallizer with jet pump driven by compressed air for recovery of phosphate(V) ions from mineral fertilizer industry wastewater

Agata Mazienczuk[1], Nina Hutnik[1], Krzysztof Piotrowski[2], Anna Kozik[1], Andrzej Matynia[1]

[1] Faculty of Chemistry, Wroclaw University of Technology, Wroclaw, Poland, e–mail: anna.kozik@pwr.wroc.pl
[2] Department of Chemical & Process Engineering, Silesian University of Technology, Gliwice, Poland
e–mail: krzysztof.piotrowski@polsl.pl

Abstract: New original construction of continuous FB MSZ (*Fluidized Bed with Mixed Suspension Zone*) crystallizer with internal circulation of suspension driven by jet pump fed with compressed air was used for continuous reaction crystallization of struvite $MgNH_4PO_4 \cdot 6H_2O$ from phosphorus fertilizers industry wastewater by magnesium and ammonium ions addition. This wastewater of pH < 4 contained 0.445 mass % of phosphate(V) ions and impurities: aluminium, calcium, copper, iron, potassium, magnesium, titanium, zinc, fluosilicate, fluoride and sulphate(VI) ions. Tests were carried out in 298 K, in stoichiometric conditions and at 20% excess of magnesium ions. Crystals of mean size. 27 – 43 μm were produced. Struvite crystals of the largest sizes and acceptable homogeneity were produced at 20% excess of magnesium ions, at pH 9 and elongated mean residence time of suspension 3600 s. Corresponding crystal linear growth rate was $8.52 \cdot 10^{-9}$ m/s according to SIG MSMPR (*Size Independent Growth, Mixed Suspension Mixed Product Removal*) kinetic model. Concentration of phosphate(V) ions decreased from 0.445 mass % in a feed to $9.3 \cdot 10^{-4}$ mass % in a postprocessed mother solution. In a product, besides main crystalline component – struvite, also all impurities from wastewater appeared in a form of hydroxides, phosphates(V) and other salts.

Key words: Struvite, FB MSZ crystallizer, industrial wastewater, continuous reaction crystallization, product quality, kinetics, phosphorus recycling.

Introduction

In most DTM (*Draft Tube Magma*) type crystallizers internal circulation of suspension is an effect of stirrer or pump action (Mullin, 1993). These can be, however, alternatively replaced by liquid jet pump devices (Synowiec, 2008). In typical constructions of liquid jet pump crystallizers (Matynia, 1997) driving agent is a possible fines-free mother solution collected from the crystallizer overflow and then redirected through the external circulation pump back into the feeding nozzle of a jet pump device. It is possible, however, to replace the circulating mother solution with the air (Matynia, 2009). Compressed air (or other gaseous medium) provided into feeding nozzle of a jet pump device becomes under these conditions working medium driving the internal circulation and mixing of suspension in the apparatus working volume. Troublesome in operating and control elements like crystallizer overflow and external circulation loop with the pump become thus unnecessary.

Laboratory research stand with a continuous FB MSZ (*Fluidized Bed with Mixed Suspension Zone*) type crystallizer were designed and constructed. This stand is especially destined for the tests concerning effectiveness, kinetics and optimisation of continuous reaction crystallization processes of struvite ($MgNH_4PO_4 \cdot 6H_2O$, MAP) from diluted aqueous solutions, wastewaters, liquid manure, etc. containing phosphate(V) ions (Parsons, 2001; Doyle, 2002). Chemical recovery of phosphates(V) from various waste solutions can be numbered among phosphorus recycling (Le Corre, 2009), and resulting products – sparingly soluble crystalline calcium or magnesium salts – can be practically utilized as a mineral fertilizer (de–Bashan, 2004).

The FB MSZ type crystallizer of working volume V_w 1.2 dm^3 with jet pump fed with compressed air was used. Feeding nozzle of a jet pump was installed inside mixing chamber where compressed air flow was directed downward. In a space between the jet pump mixing chamber and crystallizer body pseudofluidal layer of struvite crystals

self-established. The crystallizer was used for struvite continuous reaction crystallization process using real wastewater from phosphorus mineral fertilizers industry (leachate from phosphogypsum slag heap in Z. Ch. POLICE S.A., Poland, containing 0.445 mass % of PO_4^{3-}). It was continuously provided with feed solution (wastewater and reagents premixed) of the assumed molar ratio $[PO_4^{3-}]_{RM} : [Mg^{2+}]_{RM} : [NH_4^{+}]_{RM}$ as 1 : 1 : 1 or 1 : 1.2 : 1. Process ran in a constant temperature 298 K. Influence of pH (8.5 – 10) and mean residence time of suspension in a crystallizer τ (900 – 3600 s) on the product crystals quality was identified. Fundamental process kinetic parameter values were estimated from the product crystal size distributions. The most simplified model of mass crystallization process kinetics in a continuous MSMPR (*Mixed Suspension, Mixed Product Removal*) crystallizer – SIG (*Size Independent Growth*) – was used for the calculations. Characteristics of crystalline products and kinetic calculation results are presented and discussed below.

Materials and Method

Scheme of the research stand is presented in Figure 1a. The FB MSZ crystallizer with jet pump driven by compressed air was cylindrical tank of diameter D 90 mm and total height H_t 330 mm, made with *Plexiglas.*

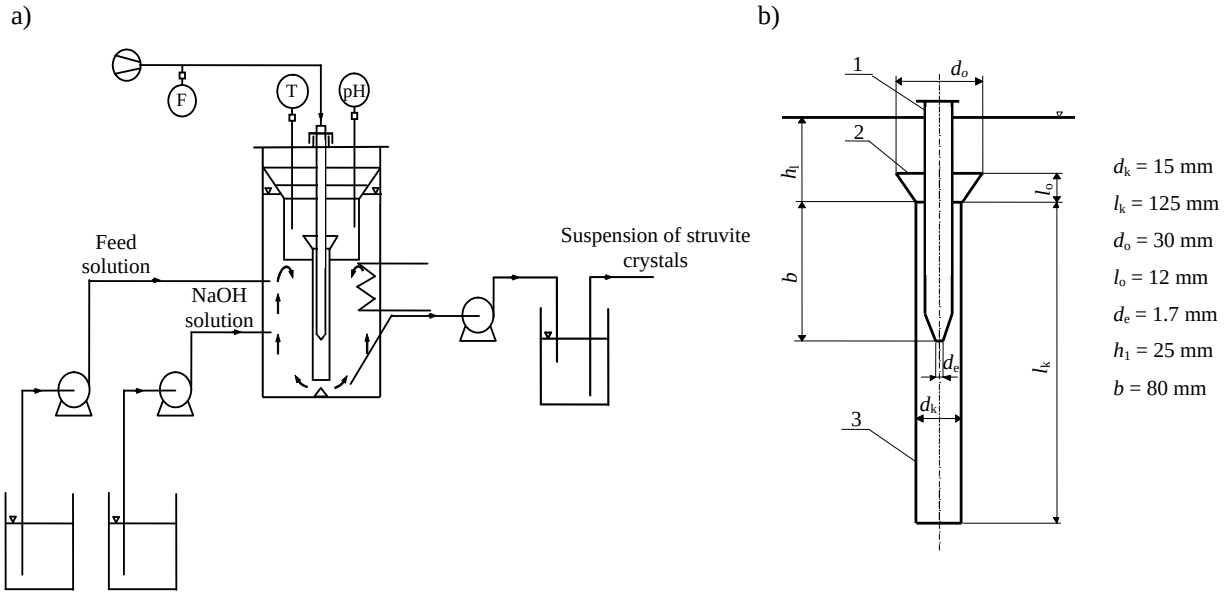

Figure 1: Scheme of laboratory stand with a continuous FB MSZ crystallizer with a gas–liquid jet pump: working volume of crystallizer V_w 1.2 dm^3, crystallizer's geometrical parameters: D 90 mm, H_t 330 mm, H_w 220 mm (a). Jet pump element in a FB MSZ crystallizer: 1 – feeding nozzle; 2 – confusor; 3 – mixing chamber (b).

Inside the crystallizer body gas-liquid jet pump was installed, presented schematically in Figure 1b. Feeding nozzle of a jet pump was provided with experimentally adjusted, minimal volumetric stream of the compressed air, q_{ve} 0.43 dm^3/s, indispensable only to keep all solid particles in a permanent movement. Resulting intensity of suspension circulation was thus also minimal. Geometrical proportions within a jet pump system are presented in Figure 1b. Owing to relatively small unit power of a feeding gaseous stream, relatively large struvite crystal density (ρ 1710 kg/m^3) and specific flow hydraulic conditions, the phenomenon of crystal suspension sucking into the mixing chamber space is not observed in a crystallizer. In such defined process conditions the pseudofluidal layer of crystals forms in a space between mixing chamber and crystallizer body.

The raw materials in a continuous struvite reaction crystallization process were: crystalline magnesium chloride hexahydrate $MgCl_2 \cdot 6H_2O$ and crystalline ammonium chloride NH_4Cl (p.a., POCh, Gliwice, Poland), as well as wastewater from phosphorus mineral fertilizers industry (Z.Ch. POLICE S.A., Poland) of pH 3.8 and detailed

composition presented in Table 1. The reagents (wastewater, $MgCl_2 \cdot 6H_2O$ and NH_4Cl) were first introduced into the mixer, in which the struvite precipitation reaction substrates dosed in a crystalline form dissolved. Mass stream values of these reagents resulted from the assumed molar ratio $[PO_4^{3-}]_{RM} : [Mg^{2+}]_{RM} : [NH_4^{+}]_{RM}$, assumed mean residence time τ of suspension in a crystallizer working volume and from working volume V_w of the crystallizer used. Clear solution of blended and totally dissolved reagents, of pH 3.6 (stoichiometric proportions of the reagents) or 3.5 (20% excess of magnesium ions), was introduced via pump into the crystallizer working volume. Crystallizer was also provided with aqueous solution of NaOH of concentration 5 mass %, responsible for stabilization of the required pH in struvite continuous reaction crystallization environment. Inlet places of reagents and alkalizing solution, as well as crystalline product suspension removal port are marked in Figure 1a. Temperature and inflow/outflow streams were strictly controlled and adjusted by computer system (BioScadaLab program).

Table 1: Chemical composition of phosphorus mineral fertilizers industry wastewater.

Component	Concentration, mass %
PO_4^{3-}	0.445
Al	$6.4 \cdot 10^{-4}$
Ca	0.044
Cu	$0.25 \cdot 10^{-4}$
Fe	$8.9 \cdot 10^{-4}$
K	$4.6 \cdot 10^{-3}$
Mg	0.0306
Si	$5.1 \cdot 10^{-3}$
Ti	$0.2 \cdot 10^{-4}$
Zn	$2.2 \cdot 10^{-4}$
F^-	$4.2 \cdot 10^{-3}$
SO_4^{2-}	0.0703

The research tests ran in temperature 298 ±0.2 K assuming pH 8.5, 9 or 10 (±0.1) and mean residence time of suspension in a crystallizer τ 900, 1800 or 3600 s (±20 s). The reagent concentrations in a feed solution were: $[PO_4^{3-}]_{RM}$ = 0.445 mass %, $[Mg^{2+}]_{RM}$ = 0.114 mass % and $[NH_4^{+}]_{RM}$ = 0.0844 mass % securing their molar ratio 1 : 1 : 1 or 0.445, 0.137 and 0.0844 for 20% excess of magnesium ions, appropriately. After stabilisation in a crystallizer the predetermined parameter values, process in a steady state ran through 5τ. After this time there were determined using standard analytical methods: concentration of solid phase in a crystal product suspension (M_T), chemical composition of mother solution and solid phase (among others: atomic absorption spectrometer iCE 3000, spectrophotometer UV–VIS Evolution 300), struvite crystal size distribution (solid particle analyser Beckman Coulter LS 13 320) and their habit (computer analysis of scanning electron microscope JEOL JSM 5800LV images). Accuracy of measurement data concerning continuous struvite reaction crystallization process in the described laboratory plant was estimated to be ca. 10%.

Kinetic parameter values of the process were estimated based on the population density distributions $n(L)$ of the product crystals (Mullin, 1993). The most simplified kinetic model valid for continuous MSMPR crystallizer, SIG kinetic model (Randolph and Larson, 1988), was assumed for the calculations. Equation of crystal population density distribution resulting from the assumed SIG kinetic model is in a form of Eq. (1):

$$n(L) = n_0 \exp\left(-\frac{L}{G\tau}\right) \tag{1}$$

from which for $L = 0$ one can determine the nuclei population density n_0 value and, from the slope in $\ln n - L$ coordinate system, linear crystal growth rate G for the known mean residence time τ of suspension in a crystallizer. Nucleation rate B can be calculated from Eq. (2):

$$B = n_0 G \quad (2)$$

Results and Discussion

From FB MSZ crystallizer properly shaped product crystals were removed. Statistical parameter values of size distribution of these crystals are presented in Table 2. From the table it results (tests No. 1, 2 and 3 in Table 2), that increase in pH of mother solution in a crystallizer from 8.5 to 10 resulted in decrease of crystal mean size L_m from 37.2 to 26.7 μm (by ca. 28%). The CV coefficient increased from 90.1 up to 99.3%. Crystal products manufactured under pH 10 characterised thus by not only smaller particle sizes, but also their higher variability. With the pH value increase nuclei population density also increases (see Table 4), what produces shifts in characteristic sizes of struvite crystals: L_m, L_{50} and L_d towards smaller values. Elongation of mean residence time of suspension in a crystallizer caused, however, increase in mean sizes of product crystals, by ca. 18%. Struvite crystals reached mean size L_m 41.8 μm for mean residence time τ 3600 s and pH 9. With the mean residence time elongation average supersaturation in solution decreased, producing as a result decrease of both kinetic components of the process: nucleation rate of solid phase and their linear growth rate values (see Table 4).

Table 2: Influence of selected technological parameters of continuous struvite reaction crystallization process from phosphorus mineral fertilizers industry wastewater in FB MSZ crystallizer on the product quality. Process temperature: 298 K.

No.	Process parameters		Suspension in crystallizer			Crystal characteristic				
	pH	τ	M_T	$[PO_4^{3-}]_{solution}$	$[PO_4^{3-}]_{crystals}$	L_m	L_{50}	L_d	CV	L_a/L_b
	–	s	kg crystals/m^3	mg/kg	mass %	μm	μm	μm	%	–
Molar proportions of reagent ions in a feed: $[PO_4^{3-}]_{RM} : [Mg^{2+}]_{RM} : [NH_4^+]_{RM} = 1 : 1 : 1$										
1	8.5	900	10.9	63.0	39.2	37.2	25.3	29.6	90.1	5.2
2	9	900	11.0	45.0	39.3	35.5	24.6	28.9	92.6	5.0
3	10	900	11.0	37.6	40.2	26.7	22.6	24.5	99.3	4.7
4	9	1800	11.1	31.8	40.1	41.7	30.3	36.1	92.6	5.1
5	9	3600	11.2	22.0	42.0	41.8	31.1	36.8	90.9	5.2
Molar proportions of reagent ions in a feed: $[PO_4^{3-}]_{RM} : [Mg^{2+}]_{RM} : [NH_4^+]_{RM} = 1 : 1.2 : 1$										
6	9	900	11.3	18.6	39.2	37.9	26.6	30.1	93.9	5.2
7	9	3600	11.4	9.3	42.1	43.2	33.3	37.2	92.1	5.3

$L_m = \Sigma x_i L_i$, where: x_i – mass fraction of crystals of mean fraction size L_i; L_{50} – median crystal size for 50 mass % cumulative undersize fraction; L_d – crystal mode size; $CV = 100(L_{84} - L_{16})/(2L_{50})$, where: L_{84}, L_{16}, L_{50} – crystal sizes corresponding to 84, 16 and 50 mass % cumulative undersize fractions.

Longer residence time of crystal population in supersaturated solution caused, however, that their sizes increased significantly. In solution of lower average supersaturation crystals grew slower, however more stable. Longer contact time of crystal phase with supersaturated mother solution influenced also struvite final crystal size distribution advantageously. Homogeneity within product crystal population increased slightly. The CV value decreased from 92.6 to 90.9%, in spite of increase in intensity of co-running processes of attrition and breakage of crystals with the elongation of their residence time in a mixed and circulated suspension.

Excess of magnesium ions in relation to phosphate(V) and ammonium ions concentrations in a crystallizer feed resulted in increase in mean size L_m of product crystals: from 35.5 to 37.9 μm (pH 9, τ 900 s), as well as from 41.8 to 43.2 μm (pH 9, τ 3600 s) (tests No. 2 and 6, 5 and 7 in Table 2, respectively). Crystal population homogeneity decreased slightly since the CV values increased from 92.6 to 93.9% and from 90.9 to 92.1%, respectively. In pure aqueous solutions of phosphate(V) ions excess of magnesium ions influences final sizes of struvite crystals

disadvantageously (Kozik, 2012). Presence of impurities in a process system (Table 1) resulted, however, that final result of continuous struvite reaction crystallization process was more advantageous (Table 2). Some of ionic impurities inhibit struvite nucleation, other can catalyse nuclei or crystals growth, while some other can significantly affect their shape and habit (Hutnik, 2011; Hutnik, 2012).

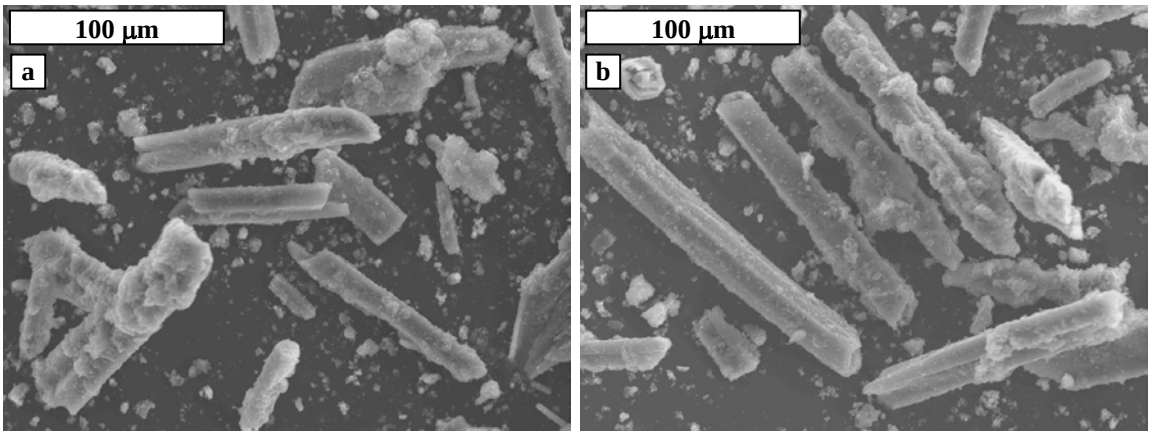

Figure 2: Scanning electron microscope images of struvite crystals produced from phosphorus mineral fertilizers industry wastewater in a continuous FB MSZ type crystallizer. Process parameters: $[PO_4^{3-}]_{RM} : [Mg^{2+}]_{RM} : [NH_4^{+}]_{RM}$ = 1 : 1 : 1 in a feed, pH 9, τ 900 s (a) and $[PO_4^{3-}]_{RM} : [Mg^{2+}]_{RM} : [NH_4^{+}]_{RM}$ = 1 : 1.2 : 1 in a feed, pH 9, τ 3600 s (b). Magnification: 500×.

In Figure 2 there are presented the scanning electron microscope images of exemplary product crystals. Diverse sizes of struvite crystals are clearly observable. Also other solid particles, co-precipitated from a complex wastewater system in the process conditions, are visible. The most often they form agglomerates on the struvite parent crystals surfaces. Struvite crystals are just stuck the co-precipitated hydroxides of metal impurities, hydroxyapatite and other salts around. Excess of magnesium ions favoured not only production of struvite crystals of larger sizes (Figure 2b), but also efficiency of phosphate(V) ions removal from wastewater. Concentration of phosphate(V) ions in a postprocessed mother solution $[PO_4^{3-}]_{solution}$ decreased from 45.0 to 18.6 mg/kg (pH 9, τ 900 s) and from 22.0 to 9.3 mg/kg (pH 9, τ 3600 s) (see Table 2). The best-formed struvite crystals were produced at low pH value (8.5 – 9), elongated mean residence time τ (3600 s) and at 20% excess of magnesium ions in a feed solution. In the process conditions tested, crystal length L_a to their width L_b ratio varied from 4.7 to 5.3 (Table 2). The L_a/L_b simplex values were calculated from planimetric measurements covering 50 crystals randomly selected from three different scanning electron microscope images of the same product sample. Based on microscope images analysis one can conclude, that struvite crystals surface was taken up by solid particles of impurity hydroxides and salts co-precipitated with struvite, what produced generation of significant tensions in parent struvite crystals structures. In result numerous crystal fractures and cracks, irregular surfaces, deformed edges, presence of characteristic tubular and trough-shaped crystals, etc. are observed (Figure 2). Product crystals habit distinctly deviated from the classical shape of struvite crystals produced from pure solutions of phosphates(V) (L_a/L_b ca. 6) or manufactured in the presence of single impurities (Hutnik, 2011; Hutnik, 2012). One can assume, that struvite crystal sizes and shapes are the resulting net effect of impurities presence in the investigated wastewater system and parameters of struvite continuous reaction crystallization process. From the microscope images it also results, that agglomeration within the struvite crystals was not significant, while attrition and breakage of crystal phase during their mixing and circulation in a crystallizer can be regarded moderate. Generally it speaks advantageously about process conditions established in a crystallizer working volume for struvite nucleation and its crystals growth. Original construction of FB MSZ crystallizer (lack of moving/rotating parts and elements), its work mode (formation of pseudofluidal crystal layer) and relatively low concentration of solid phase in suspension (M_T ca. 11 kg of struvite/m^3 of suspension) did not contribute to excessive attrition and breakage within crystal phase. Considering, however, all components of a complex process of continuous struvite reaction crystallization process in a FB MSZ crystallizer one can conclude, that main factor influencing the process course is solution supersaturation, very strongly dependent (assuming constant: feed solution composition,

process temperature and mixing/circulation intensity) on process environment's pH and mean residence time of suspension in a crystallizer working volume.

Table 3: Chemical compositions of solid phase and mother solution after filtration of crystal suspension removed from continuous FB MSZ crystallizer (see Table 2).

Component	Concentration in mother solution mg/kg	Concentration in solid phase* mass %
PO_4^{3-}	9.3 – 63.0**	39.2 – 42.1**
Mg^{2+}	30 – 240	9 – 10
NH_4^+	75 – 115	6.5 – 7.0
Al	0.1 – 0.3	$(4.8 – 5.5)\cdot10^{-2}$
Ca	< 50	2.5 – 4.0
Cu	0.02 – 0.10	$(0.6 – 1.3)\cdot10^{-4}$
Fe	0.03 – 0.07	0.10 – 0.20
K	25 – 39	0.12 – 0.22
Si	25 – 42	$(8.6 – 9.7)\cdot10^{-2}$
Ti	< 0.2	$< 2\cdot10^{-5}$
Zn	< 0.5	$(1.6 – 1.9)\cdot10^{-2}$
F^-	2 – 24	0.35 – 0.48
SO_4^{2-}	400 – 560	1.5 – 1.8

* after drying, without water washing of crystals on a filter
** see Table 2

In Table 3 there are presented the components concentration ranges identified in the postprocessed mother solution and in solid phase (without water washing of crystals on a filter and after their drying) removed from FB MSZ crystallizer (see Table 2). Crystalline product, as it results from Table 3, besides main component $MgNH_4PO_4\cdot6H_2O$, contained also all impurities present in wastewater, among others: phosphates(V) and metal hydroxides, fluosilicates, fluorides and sulphates. From these data analysis it results, that at magnesium ions excess practically total precipitation of aluminium, calcium, copper, iron and zinc ions is observed (compare these ions concentrations in raw wastewater (Table 1) and in postprocessed mother solution (Table 3)). One can also notice, that phosphate(V) ions concentration in a postprocessed mother solution varied from 63.0 (pH 8.5, τ 900 s) to 22.0 mg/kg (pH 9, τ 3600 s) (tests No 1 – 5 in Table 2). These concentration values decreased systematically with the pH raise and with elongation of mean residence time τ of struvite crystals suspension in a crystallizer. From the comparison it results, that phosphate(V) ions concentration decreased even 3-time. It is attributed to struvite solubility decrease with the increase in pH of reactive mixture or longer contact time of crystals with the supersaturated solution in a crystallizer (more thorough discharge of the generated supersaturation). The $[PO_4^{3-}]_{solution}$ values can be regarded small, thus efficiency of phosphate(V) ions removal from feed solution (above 98%) as a fully satisfactory.

Excess of magnesium ions with relation to concentration of phosphate(V) and ammonium ions influenced the process yield advantageously. Concentration of phosphate(V) ions in a postprocessed mother solution was ca. 2-time smaller than in stoichiometric conditions (see tests No 6 and 7 in Table 2).

In Figure 3 there are presented the exemplary experimental population density distributions of crystals produced at pH 9 and 10 for mean residence time of suspension in a crystallizer 900 s (stoichiometric conditions) and at pH 9, τ 3600 s (20% excess of magnesium ions). From these distribution courses, presented in $\ln n – L$ coordinate system it results, that for particles of sizes $L > 70$ μm (pH 8.5 and 9) or $L > 30$ μm (pH 10) these dependencies can be, with satisfactory precision, approximated with linear function. From Eq. (1) one can calculate linear crystals growth rate G value, and from Eq. (2) their nucleation rate B.

Table 4: Nucleation rate B and crystal linear growth rate G values estimated for continuous struvite reaction crystallization process in a FB MSZ crystallizer. Kinetic parameters calculated with SIG MSMPR model. Process conditions – see Table 2.

No. (see Table 2 for details)	Process kinetic parameter values (SIG MSMPR model) $n(L)$*)	R^2 (for linear segment)	n_0 1/(m m^3)	G m/s	B 1/(s m^3)
Molar proportions of reagent ions in a feed: $[PO_4^{3-}]_{RM} : [Mg^{2+}]_{RM} : [NH_4^+]_{RM} = 1 : 1 : 1$					
1	$n = 7.783\cdot10^{14}\exp(-4.098\cdot10^4 L)$	0.983	$7.8\cdot10^{14}$	$2.71\cdot10^{-8}$	$2.1\cdot10^{7}$
2	$n = 1.011\cdot10^{15}\exp(-4.360\cdot10^4 L)$	0.993	$1.0\cdot10^{15}$	$2.55\cdot10^{-8}$	$2.6\cdot10^{7}$
3	$n = 1.264\cdot10^{16}\exp(-7.501\cdot10^4 L)$	0.995	$1.3\cdot10^{16}$	$1.48\cdot10^{-8}$	$1.9\cdot10^{8}$
4	$n = 4.075\cdot10^{14}\exp(-3.453\cdot10^4 L)$	0.989	$4.1\cdot10^{14}$	$1.61\cdot10^{-8}$	$6.6\cdot10^{6}$
5	$n = 4.014\cdot10^{14}\exp(-3.444\cdot10^4 L)$	0.987	$4.0\cdot10^{14}$	$8.06\cdot10^{-9}$	$3.2\cdot10^{6}$
Molar proportions of reagent ions in a feed: $[PO_4^{3-}]_{RM} : [Mg^{2+}]_{RM} : [NH_4^+]_{RM} = 1 : 1.2 : 1$					
6	$n = 6.682\cdot10^{14}\exp(-4.134\cdot10^4 L)$	0.987	$6.7\cdot10^{14}$	$2.69\cdot10^{-8}$	$1.8\cdot10^{7}$
7	$n = 3.610\cdot10^{14}\exp(-3.261\cdot10^4 L)$	0.991	$3.6\cdot10^{14}$	$8.52\cdot10^{-9}$	$3.1\cdot10^{6}$

*) for $L > 70$ μm (pH 8.5 and 9), $L > 30$ μm (pH 10)

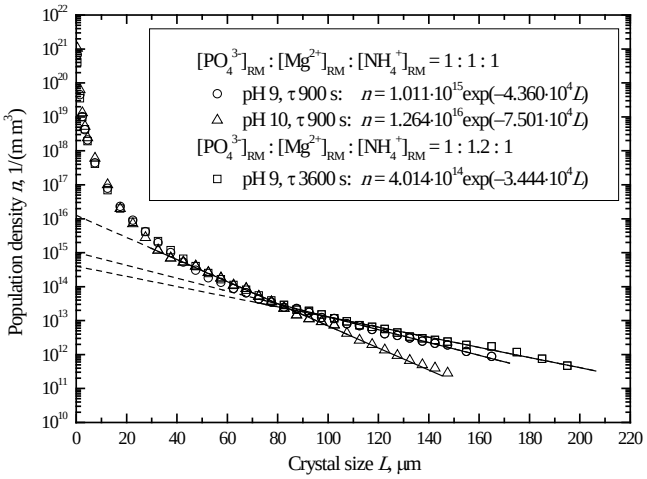

Figure 3: Exemplary population density distributions of crystals produced in a FB MSZ type crystallizer fed with a phosphorus mineral fertilizers industry wastewater assuming stoichiometric ratio between the main reagents and at 20% excess of magnesium ions. The points – experimental data, solid lines – values calculated with Eq. (1) (see Table 4) for crystals of sizes $L > 70$ μm (pH 8.5 and 9) and $L > 30$ μm (pH 10), dashed lines – linear extrapolations of SIG model to $L = 0$.

Determined parameters of population density distribution function $n(L)$ (Eq. (1)) for struvite product crystals and calculated on this basis G and B values are presented in Table 4. Nonlinearity in population density distribution courses for the crystals of size L smaller than 30 or 70 μm (in a $\ln n - L$ coordinate system, Figure 3) points on more complex process kinetics than it results from the assumed "linear" SIG MSMPR model. Thus the presented kinetic parameter values of the investigated process should be regarded only as the estimated ones. It especially concerns nucleation rate value B calculated with Eq. (2), with the use of strongly devaluated values of nuclei population density

n_0 ($n(L)$ for $L = 0$). As it results from Figure 3, the differences between n_0 values predicted by extrapolation with linear SIG MSMPR kinetic model and real population density values for the smallest crystals are in the order of 10^5. Calculated values of nucleation rate B are thus useful only for relative, conventional comparison of the investigated process parameter effects on its course and final results.

Analyzing the kinetic data presented in Table 4, one can notice regular decrease of struvite crystal linear growth rate G with the increase in process environment pH and with elongation of mean residence time of suspension in a crystallizer. Generally higher crystal growth rate values are observed for the shortest mean residence times in apparatus, what is in accordance with the observations concerning classical continuous mass crystallization processes. Exemplary, increase in pH of process environment in a crystallizer from 8.5 to 10 for τ 900 s results in decrease of linear growth rate of struvite crystals from $2.71 \cdot 10^{-8}$ to $1.48 \cdot 10^{-8}$ m/s. It is large decrement of G value (by ca. 45%). It is additionally accompanied by significant increase in nuclei population density n_0 value, thus nucleation rate B (from $2.1 \cdot 10^7$ to $1.9 \cdot 10^8$ 1/(s m^3)). In result final crystal mean size L_m decreased (37.2 → 26.7 μm). Elongation of mean residence time of suspension in a crystallizer limited struvite nucleation rate B (from $2.6 \cdot 10^7$ to $3.2 \cdot 10^6$ 1/(s m^3) for τ 900 → 3600 s, pH 9). Linear crystal growth rate also decreased (G $2.55 \cdot 10^{-8}$ → $8.06 \cdot 10^{-9}$ m/s), however longer contact time with supersaturated mother solution caused, as it was mentioned earlier, increase in mean struvite crystal size.

Excess of magnesium ions in a feed mixture caused advantageous changes in kinetic parameters of struvite continuous reaction crystallization process: decrease of nucleation rate and increase in linear crystal growth rate (compare: No. 2 and 6, as well as No. 5 and 7 in Table 4). Net effect of all partial interactions within the analysed process turned out to be advantageous for manufacturing the product crystals of larger sizes.

Conclusions

The research tests of struvite continuous reaction crystallization from phosphorus mineral fertilizers industry wastewater in a FB MSZ type crystallizer with internal circulation of suspension driven by jet pump fed with compressed air were carried out. Test results can be regarded satisfactory and advantageous. The FB MSZ crystallizer worked stable in a continuous work mode. Its original construction (absence of moving or rotating elements) and its work mode (formation of pseudofluidal crystals layer) did not arrange excessive attrition and breakage effects within the crystal phase. It was concluded, that the product crystals homogeneity was significantly influenced by technological process parameters (pH, mean residence time of suspension in a crystallizer, excess of magnesium ions in relation to phosphate(V) and ammonium ions in a feed), as well as intrinsic chemical composition of wastewater.

From FB MSZ crystallizer properly shaped struvite crystals of mean size L_m from ca. 27 to ca. 43 μm were removed. It was experimentally proved, that increase in pH value (from 8.5 to 10) caused decrease of mean crystal size (by ca. 28%, L_m 37.2 → 26.7 μm, τ 900 s). Contrary, elongation of mean residence time of suspension in a crystallizer from 900 to 3600 s produced significant increase in this size (by ca. 18%, L_m 41.8 μm at pH 9 and τ 3600 s). Products of low size homogeneity (CV ~ 90 – 100%) were removed from the crystallizer. It is a net effect of a complex influence of pH and mean residence time of suspension, as well as crystals attrition and breakage on supersaturation level in mother solution.

For the process kinetic parameters estimation the simplest kinetic model developed for ideal MSMPR crystallizer was applied. It was concluded, that linear crystal growth rate values of struvite varied within the $8.06 \cdot 10^{-9}$ – $2.71 \cdot 10^{-8}$ m/s range, while nucleation rate within the $3.2 \cdot 10^6$ – $1.9 \cdot 10^8$ 1/(sm^3) range. With the elongation of mean residence time of suspension both kinetic parameter values decreased. With the pH rise nucleation rate increased while simultaneously linear growth rate decreased. Reduction of both kinetic parameter, B and G, values with the elongation of mean residence time was correlated with increase in mean size L_m of product crystals. Lower values of linear growth rate are thus compensated with excess by longer contact time of crystals with supersaturated mother solution. Simultaneously decreasing nucleation rate values also advantageously affected the process of crystal phase growth and self-establishing in these conditions size distribution of the product suspension.

Excess of magnesium ions in a process system definitely advantageously influenced the struvite continuous reaction crystallization process yield. Concentration of phosphate(V) ions decreased from 0.445 mass % in a feed to $9.3 \cdot 10^{-4}$ mass % in a postprocessed mother solution, what can be regarded as a very good result of their removal process from inlet solution. It was accompanied by rise of mean size of product crystals (L_m up to 43.2 μm), crystal linear growth rate (G up to $8.52 \cdot 10^{-9}$ m/s) and nucleation rate decrease (B to $3.1 \cdot 10^6$ 1/(sm^3)).

In crystal product, besides main component – struvite, all impurities originally present in wastewater appeared in a form of hydroxides, phosphates(V) and other salts. Aluminium, copper, iron and zinc ions practically totally co-precipitated with struvite. Direct application of such crystalline mixture in agriculture is limited, however part of these impurities can be regarded as the soil enriching components (nutrients).

Acknowledgements

The work was financed by Ministry of Science and Higher Education of Poland in 2009 – 2012 under research project NN209 1174 37.

References

de–Bashan, L.E. & Bashan, Y. (2004). *Recent advances in removing phosphorus from wastewater and its future use as fertilizer*. Wat. Res. 38, 4222–4246.

Corre, K.S. Le, Valsami–Jones, E., Hobbs, P. & Parsons, S.A. (2009). *Phosphorus recovery from wastewater by struvite crystallization: A review*. Crit. Rev. Environ. Sci. Technol. 39, 433–477.

Doyle, J. & Parsons, S.A. (2002). *Struvite formation, control and recovery*. Wat. Res. 36, 3925–3940.

Hutnik, N., Piotrowski, K., Gluzinska, J. & Matynia, A. (2011). *Effect of selected inorganic impurities present in real phosphate(V) solutions on the quality of struvite crystals produced in continuous reaction crystallization process*. Progr. Environ. Sci. Technol. 3, 559–566.

Hutnik, N., Wierzbowska, B. & Matynia, A. (2012). *Effect of inorganic impurities on quality of struvite in continuous reaction crystallization at the excess of magnesium ions*. Przem. Chem. 91, 762–766 (in Polish).

Kozik, A., Matynia, A. & Piotrowski, K. (2012). *Recovery o struvite from diluted aqueous solutions of phosphate(V) ions in the presence of magnesium ions excess*. In: J. Markoš (Ed.): Proceedings of the 39th International Conference of Slovak Society of Chemical Engineering, Tatranskě Matliare, Slovakia, 742–749.

Matynia, A. (1997). *Crystallizers with a jet pump*. Inż. Ap. Chem. 36(6), 9–14 (in Polish).

Matynia, A., Piotrowski, K., Ciesielski, T. & Liszka, R. (2009). *New constructions of crystallizer with a compressed air driven jet–pump in the phosphorus recycling technology*. Przem. Chem. 88, 505–508 (in Polish).

Mullin, J.W. (1993). *Crystallization*. Oxford: Butterworth–Heinemann.

Parsons, S.A. (2001). *Recent scientific and technical developments: Struvite precipitation*. CEEP Scope Newslett. 41, 15–22.

Randolph, A.D. & Larson, M.A. (1988). *Theory of particulate processes: Analysis and techniques of continuous crystallization*. New York: Academia Press.

Synowiec, P. (2008). *Industrial crystallization from solution*. Warszawa: WNT (in Polish).

Characterization of cork lightweight material used in building thermal insulation

[1]Nassima Sotehi and [2]Abla Chaker

[1]Skikda University 20 Aout 1955, Algeria
[2]Energy Physics Laboratory, Mentouri University, Constantine, Algeria

e-mail: sotehis@gmail.com

Abstract: An experimental study was carried out in order to determine the thermal properties of new materials used in building insulation .We are particularly interested in cork lightweight concrete. In this work, the thermal conductivity of the tested samples is determined in terms of moisture, density and fibers dosage. The thermal conductivity is measured in the similar conditions as those of utilisation. The thermal resistance is obtained by calculation. The obtained results allow us to specify the optimal use conditions of the tested materials.

Key words: Thermal properties, thermal conductivity, thermal resistance, insulation material, cork, boxes method.

Introduction

For the buildings thermal design, two criteria are necessary; the first one is the user's comfort and second one is the energy efficiency. To achieve these objectives, we lead to reflect in particular on the materials choice used for building shielding, which has to prevent heat loss to the outside. This explains the recent development of new building materials, among these materials the lightweight concretes. They can play a role as an insulator, while maintaining adequate levels of performance. The thermal conductivity and the resistance are the most important thermophysical features for the thermal insulation material choice.

This work is a contribution to the experimental study of cork lightweight concrete thermal behaviour. This material is intended to be used for roof insulation and other building components (Kabbazi & al., 2003). Regarding the experimental measurements, in steady regime for the thermal conductivity, we have used the Boxes method.

Studied Materials

We have chosen to make mixtures with an identical matrix and different dosages of cork aggregates, by replacing a portion volume of cement paste with cork aggregates. Then we stopped when the volume occupied by the cork became so important that it became difficult for the mixer to mix everything. The amount of cork aggregates inserted is a mass fraction of the cement mass. The fiber dosages (L/B) studied are: 0, 2, 4, and 6 %. The used matrix consists of Portland cement (CPJ45, CMII), sand (0/4), and water. Table 1 lists the various mixtures studied.

Table 1: Studied compositions.

Cement (Kg) 450	450			
Sand (0/4) (Kg)	1350			
Water (l)	225			
E/C	0.5			
Cork mass (Kg)	0	9	18	27
Designation	B	BL2	BL4	BL6

Thermal Conductivity Measurements

Several methods are used for measuring the materials thermal conductivity: the guarded hot box method (Fournol, 1955), the guarded hot plate method (Tye, 1969), boxes method (Azizi, & al., 1989 ; Boukhattem & al., 2007; Chaker & Hamida, 2010), the method of radial flow (Crausse, 1983), among them we chose the boxes method, this last method was developed in the Thermal and Solar Studies Laboratory, Claude Bernard University in France ((Azizi, & al., 1989). It's of substantial precision, because the relative error of the measurement is evaluated to 5 %. This method made the object of several publications (Boukhattem, Kourchi & Bendou, 2007). It uses parallelepiped samples with sizes of (27 cm×27 cm) and thickness varies from 2 to 7 cm. The thermal conductivity measurements are based upon steady the heat conduction. The sample is set between two atmospheres (see Figure1).

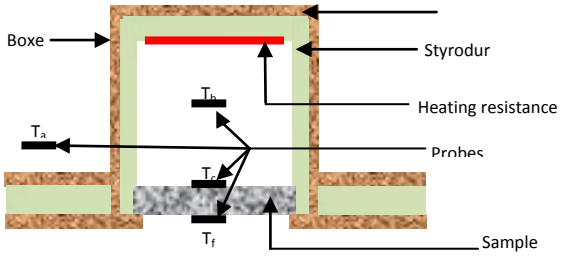

Figure 1: Box measurements

Their temperature corresponds to real cases. As surroundings are at the same temperature as upper boxes, the power q supplied by the electrical resistance goes through the sample and the thermal conductivity is given by the following formula (Menguy & al., 1986):

$$\lambda = \frac{e}{S\Delta T}(q + C\Delta T') \quad (1)$$

with:

λ: is the thermal conductivity in w m^{-1} K^{-1}, e: is the sample thickness in m, S: is the sample area in m^2, C: is the depredation thermal coefficient in W K^{-1}, q: is the unidirectional heat flow in W m^{-2}, ΔT: is the temperature variation between cold and heated sample faces in °C and ΔT': is the temperature variation between external and internal environments in °C.

The thermal resistance value R_{th} in m^2 K W^{-1} is expressed as:

$$R_{th} = \frac{e}{\lambda} \quad (2)$$

Results and Discussion

The apparent thermal conductivity measurements of the studied materials were carried out in the dry state, in the saturated state, and in the different moisture degrees. The levels of successive moisture contents were obtained by first saturating the samples tested, then the desaturated by drying in a ventilated oven. We noted that this technique allows to obtain a distribution as uniform as possible from the water within samples (Horton & al., 1982)

Moisture Influence

The obtained results of measuring the thermal conductivity as function of the water content are summarized in Figure 2.

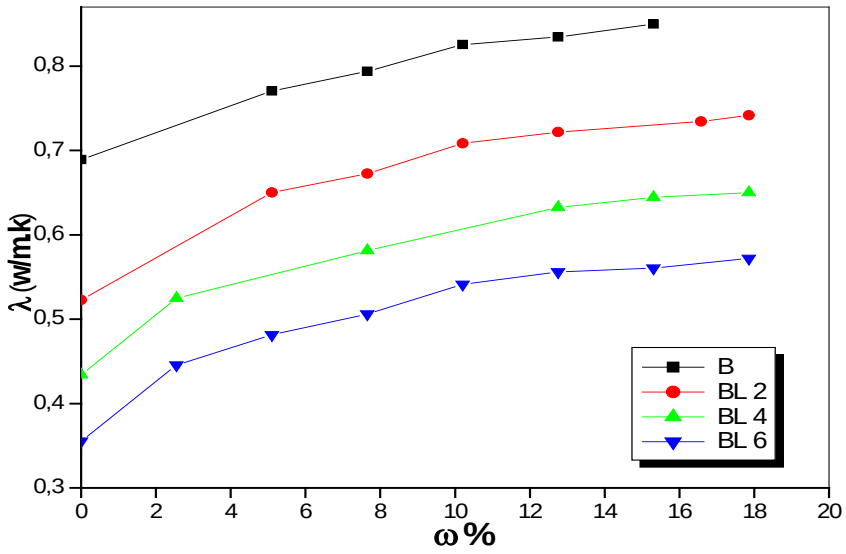

Figure 2: Thermal conductivity in terms of water content of cork lightweight concrete

As can be seen in Fig. 2, the thermal conductivity is an increasing function of the water content. This is explained by the fact that the materials under study are porous, the thermal conductivity depends only on that of the solid matrix and that of air about 0.26 W m^{-1} K^{-1} at 20 ° C, the latter is much lower than that of the water (about 0.60 W m^{-1} K^{-1} at 20 ° C), which partially replaces the air in the pores during the wetting, and thermal conductivity will depend on that of the water. Thus a water high concentration increases the thermal conductivity. This result has been observed on the other materials such as mortar based cement (Chaker & Hamida, 2010), brick hollow of earth stabilized with cement (Meukam & al., 2003) and cellular concrete (Laurent & Guerre-Chaley, 1995).
The evolution of the thermal resistance versus the water content is represented in Figure 3.

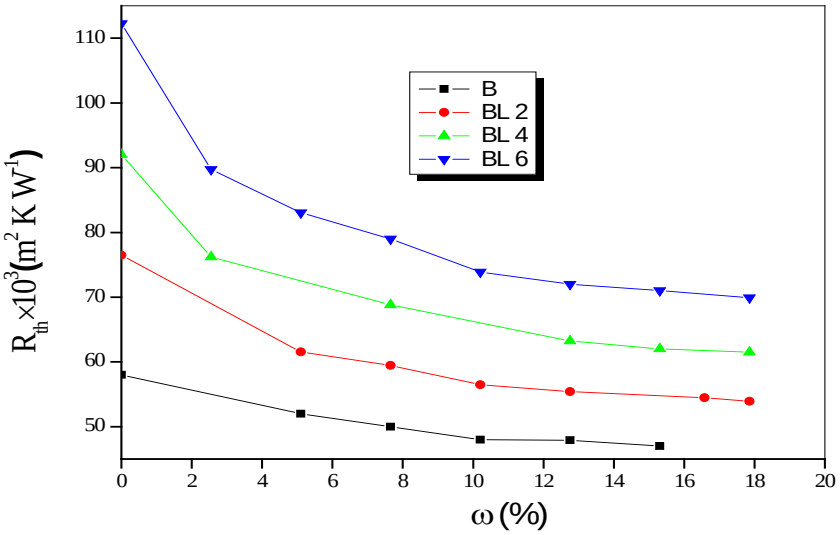

Figure 3: Thermal resistance in terms of water content of cork lightweight concrete

This figure shows a sharp decrease of thermal resistance with the water content, though the thermal conductivity increases slightly (see the Fig. 2). We can see that the thermal conductivity increasing and the thermal resistance decreasing are equal. Comparing the materials taking into account their thermal resistance, we announce that the cork lightweight concrete with L/B = 6 % in the dry state is more resistant to heat flow.

Density Effect

All the results from any action relating to the thermal conductivity evolution as function of the materials mass density are presented in Table 2 and plotted in Figure 4.

Table 2: The thermal conductivity of the studied samples in dry and saturated state.

Designation		B	BL2	BL4	BL6
ρ(Kg .m^{-3})		2168	2015	1862	1735
λ (W m^{-1} .K^{-1})	Dry state	0.689	0.523	0.434	0.355
	Saturated state	0.850	0.741	0.650	0.572

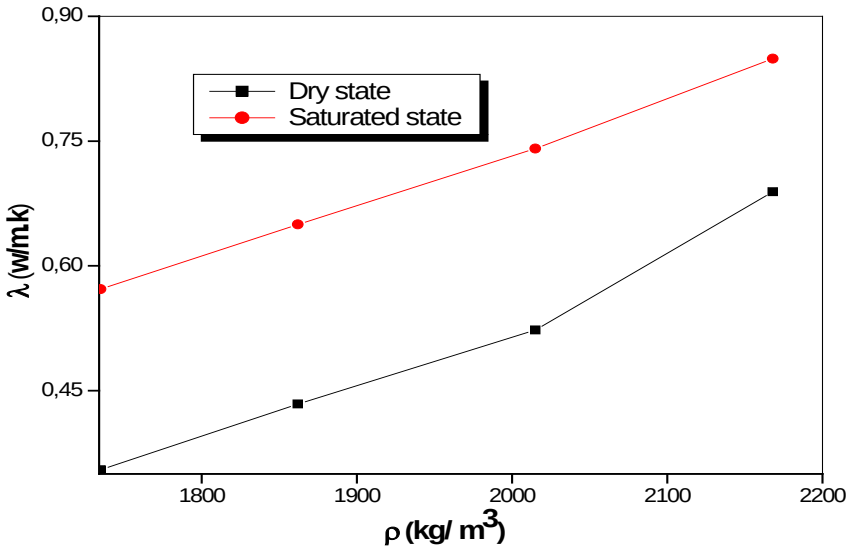

Figure 4: Thermal conductivity in terms of density in dry and saturated state

These results show that the concretes studied thermal conductivity increase linearly with the mass density. Indeed, the increasing densification of the material clogs the pores and removes the air inside, which its thermal conductivity is lower than that of the solid matrix.

The thermal resistance variation of cork lightweight concrete samples versus the density is represented in Figure 5. If we take a wall of about 4 cm thickness, the thermal resistance decreases from 112×10^{-3} m^2 K/ W at the dry state to 70×10^{-3} m^2 K/ W at the saturated state, this leads to say that the more the wall is dense, the more it is heat-resistant.

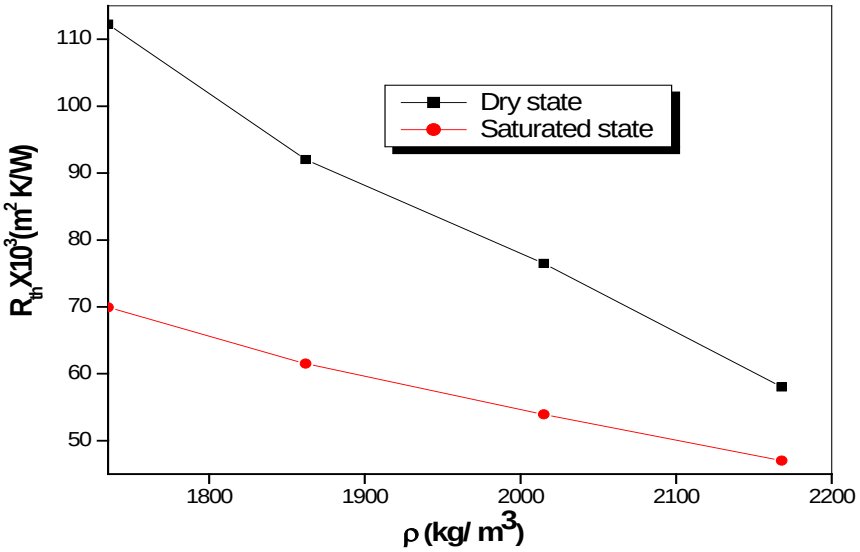

Figure 5: Thermal resistance terms of density in dry and saturated state

Cork Dosage Effect

The evolutions of the thermal conductivity and thermal resistance of lightweight concrete with the cork aggregates dosage have been shown in Figure.6.

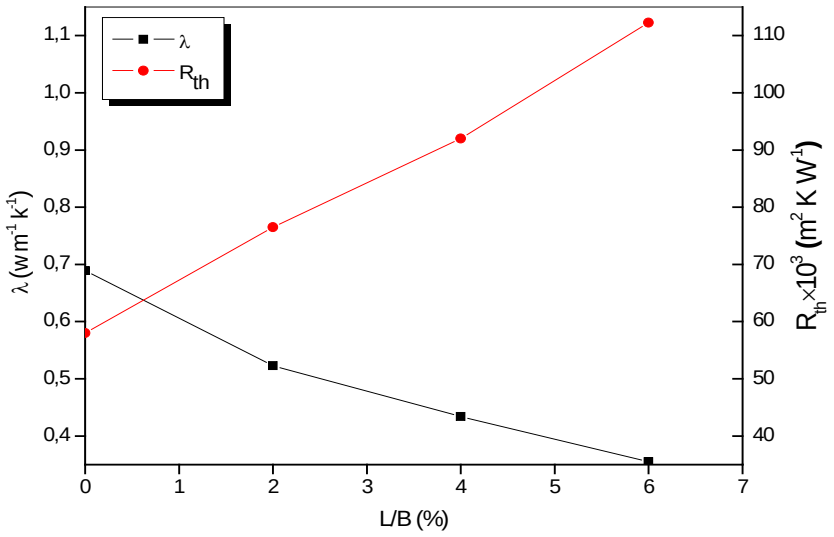

Figure 6: Variation of the thermal conductivity and thermal resistance in terms of cork aggregates dosage L / B.

From this figure, we found that the thermal resistance increases with the dosage increasing, but the thermal conductivity evolutions are in the opposite direction; this is explained by the fact that the cork aggregates thermal conductivity is very small compared to that of cement. So, the dosage increasing of these aggregates in concrete makes it more thermally insulated.

Conclusions

The results of measuring the thermal conductivity and resistance of cork lightweight concrete obtained using the boxes method it's in line (are in good agreement) with those presented by (Elbakkouri, 2004).
We have found that, the moisture influence on the thermal insulation materials is negative, the more the material is wet again its thermal conductivity is high, and thermal resistance is low.

We have also found that, the materials investigated thermal proprieties are strongly influenced by the density. The thermal conductivity increases and the thermal resistance decreases gradually as the material is dense.
The addition of cork granules in the initial material improves the thermal performance.

References

Kabbazi, A., Lahrahar, N., Termina, O. (2003). Etude Expérimentale Hygrothermique d'un Nouveau Matériau Isolant à Base de Granulats de Liège. *Phys. Chem. News*, (pp. 22- 25).

Fournol, A. (1955). La Chambre Thermique de la Station Expérimentale de Champs-sur-Marne, *Cahiers du CSTB*, n°216.

Tye, R. P. (1969). Thermal Conductivity. *Academic Press London and New-York*.

Azizi, S. & al. (1989). Conductivité Thermique des Milieux Poreux non Saturés Analyse Théorique et Expérience. *Heigh Temperatures – Heigh Pressures*, (pp . 383- 389).

Boukhattem, L., Mir, R., Kourchi, M., Bendou, A. (2007). Caractérisation Thermophysique du Mortier a Base du Ciment et de Sable. *Revue Internationale d'Héliotechnique Energie- Environnement, 36*, (pp. 03-12).

Chaker, A., Hamida, M.L. (2010). Etude de l'Effet des Ajouts Pailles et Sciure de Bois sur les Caractéristiques Thermophysiques du Matériau Plâtre. *Seventh International Conference on Material Sciences*, Lebanon.

Crausse, P. (1983). Etude Fondamentale des Transferts Couplés de Chaleur et d'Humidité en Milieux Poreux non Saturé. *Thèse de Doctorat*.

Menguy, G., Laurent, M.,Société Weber Broutin , Moutarda, A., Leveau, J. (1986). Cellule de Mesure des Caractéristiques Thermophysiques des Matériaux E1700. *Bulletin technique: Deltalab*.

Horton, R., Wierenga, P.J., Nielsen, D.R. (1982). A Rapid Technique for Obtaining Uniform Water Content Distributions in Unsaturated Soil Columns. *Soil science*, (pp. 397-399).

Meukam, P., Noumowe, A., Jannot, Y., Duval, R. (2003). Caractérisation Thermophysique et Mécanique des Briques de Terre Stabilisées en Vue de l'Isolation Thermique de Bâtiment. *Materials and Structures*, (pp. 453-460).

Laurent, J. P., Guerre-Chaley, C. (1995). Influence de la Teneur en eau et de la Température sur la Conductivité Thermique du Béton Cellulaire Autoclave. *Materials and Structures*, (pp. 464-472).

El bakkouri, A. (2004). Caractérisation Hygroscopique, Thermophysique et Mécanique des Matériaux Allégés : Cas du Béton Allégés avec du Liège ou avec des Grignions d'Olive. *Thèse de Doctorat*.

Conceptual Modeling of Performance Indicators of Higher Education Institutions

Tuba Canvar Kahveci, Harun Taşkın, Merve Cengiz Toklu

Department of Industrial Engineering,Sakarya University, Serdivan,Turkey

e-mail: tcanvar@sakarya.edu.tr

Abstract: Measuring and analyzing any type of organization are carried out by different actors in the organization. The performance indicators of performance management system increase according to products or services of the organization. Also these indicators should be defined for all levels of the organization. Finally, all of these characteristics make the performance evaluation process more complex for organizations. In order to manage this complexity, the process should be modeled at the beginning. The aim of this study is providing the conceptual performance model for higher education institutions to manage this complexity easily and evaluate the higher education institutions from all aspects. The proposed model is also exemplified by using Sakarya University case study.

Key words: Performance, modeling, higher education.

Introduction

All enterprises exist for the achievement of one or more goals and these goals vary depending on the type of organization. The main goal of a manufacturing company can be the realization of maximal profit while the goal of a non-profit organization can be to effectively provide its services. The measuring of performance and results of the enterprise shows the success of the management. Therefore, measuring and evaluating organizational performance plays an important role in turning organizational goals to reality, and the notions of a goal and a performance indicator are essential.

Today organizations need to define and make explicit company-specific performance indicators by using a systematic approach. That's why, it is necessary to formalize the concept of a performance indicator together with its characteristics, relationships to other performance indicators and relations to other formalized concepts such as goals, processes and roles. This study presents a framework of performance evaluation model of higher education institutions by modeling performance indicators and the relationships between them. The contribution of the study can be summarized in the following points:

i. clarification the required knowledge for performance measuring of higher education institutions by formalizing the concept of a performance indicators,
ii. formalization of the relationships between performance indicators,
iii. integration of the concepts of a performance indicator of higher education institutions,
iv. providing a basis model for application of information technology in a performance measuring system.

Performance Measurement Systems and Performance Indicators

Performance Measurement (PM) is defined as getting timely information about the operations have to be monitored and measured constantly for heading of company's success (Kanji, 2007). Although the immediate role of any performance measurement system is to check progress towards the established goals, such system fulfills several other purposes in the organization such as decision support, diagnosis, performance evaluation and

monitoring effect of strategic plans (Tehhumen et.al, 2002). By implementing PM, an enterprise can have following capabilities (Kanji, 2007);

- ability to identify major improvement opportunities,
- ability to achieve goal congruence and organizational alignment,
- ability to enhance accountability,
- ability to drive future resource allocation decisions
- ability to communicate to each individual how he/she can contribute to the overall strategy and thus to encourage and reinforce certain behaviors and attitude.

A performance measurement system is a set of performance indicators (PIs) to quantify actions. These PIs are the building blocks in a measurement system. In the literature, the PIs can be classified in different ways. For example, the PIs is classified according to its characteristics into hard versus soft PIs. Hard PIs are pure facts that are possible to measure directly whereas soft PIs are intangible metrics that have to be measured indirectly like for instance attitudes (Rolstadas, 1995).

Also, the PIs can be grouped into three groups according to its purposes and time horizons such as achievement, diagnostics and competence PIs. Achievement PIs are direct metrics for actual business achievement such as net profit, return on investment, market share, export share etc. as well as diagnostics PIs are indirect metrics for business achievement. These PIs are critical success factors such as delivery precision, delivery flexibility, product quality, product reliability, lead time on customer request, customer satisfaction, outstanding claims etc. Competence PIs is used to describe how well the company is prepared for the future or to meet new requirements (Rolstadas, 1995).

In the other framework, there are two types of performance measures such as process performance measures and output performance measures. While process performance measures monitor the activities of a process, output performance measures report the results of a process. Process performance measures are used to motivate people within the process as well as output performance measures are used to control resources (Hronec, 1993).

Optimal performance measurement systems would be developed to serve different purposes and provide different time horizons by balancing of various PIs. The best performance measures give balance to the company's operations and are deployed throughout the organization in a way that links strategy to processes and processes to one another. Therefore, developing an objective measurement system and determining accurate performance indicators are a comprehensive and difficult task for any kind of enterprise. There are a number of different performance measurement and analysis systems available for companies. The Balanced Scorecard, the Performance Pyramid System and the Performance Prism are globally known. There are also numerous different implementation processes and practice examples for companies presented in the literature and scientific articles (Tehhumen et.al, 2002).

Using recognized objective indicators and evaluation systems is necessary for a rational justification of higher education institutions. European University Association (EUA) supports and executes the special studies to develop a shared reference system for indicators and evaluation procedures for higher education institutions in Europe. It reported a number of principles that are fundamental to define and use PIs of higher education (Tavenas, 2003):

- HE performance indicators will differ depending on the level of analysis envisaged.
- The statistical indicators of any university activity have to be regarded as elements that support a particular judgment rather than objective facts.
- Indicators have to be used in complementary clusters so as to give a very precise and thorough picture of the activity concerned;
- Indicators should preferably be concerned with the distinctive features of a particular institution or a university sector and enable it to monitor its strategic orientations.
- Analysis of performance indicators at any level (institutional, regional or national) must therefore take information on the variety of academic disciplines in terms of their nature and relative representation fully into account.
- Performance indicators too firmly rooted in the diversity of disciplines may no necessarily do this. By using indicators applicable to the major branches of learning such as natural sciences applied sciences, life sciences, the social sciences and arts, this potential pitfall is largely averted.

- The use of uniform performance indicators in a university system is only justified if all the institutions in this system have similar fundamental goals and responsibilities. If not, the adoption of such indicators carries with it the considerable risk that the system will eventually become uniform and sacrifice its diversity. They should therefore only be used discriminatingly and with the agreement of all concerned.

An establishing a measurement system and determining performance indicators for the higher education institutions is getting difficult because of their inherent complexity. EUA also declined these difficulties in the following points (Tavenas, 2003):

1. An availability, representativeness, and reliability of raw statistical data,
2. A relation between the level at which data are aggregated and their meaning,
3. A diversity of academic disciplines,
4. Possible dangers inherent in using performance indictors to evaluate and finance institutions.

Conceptual Model of Institutional Performance Evaluation of HEIs

There are various studies about measuring the performance of higher education institutions as well as determining the performance criteria. Most of the studies try to answer what performance criteria should be and how performance criteria can be measured. For example, Centra (1997) determined the university evaluation criteria as classroom teaching, number of publications, quality of publications, research and/or creative activity. Martin (2003) evaluates the performance of 52 departments of Saragossa universities by using the collective model of envelopment analysis with three input variables: human resources, financial resources and equipment (material resources) and two outcome variables: educational and research in a coordinate way. In the other study, Azma (2010) described key performance indicators and presented a conceptual framework for the evaluation of the performance of the universities according to the key performance indicators. According to this study there are ten factors such as area and facilities (cultural area, research area, lab area, office area, education area, sport area), research and scientific journals, processes, education and technology, cultural and social services, faculty members, employees, students and graduates (Azma, 2010). In the other study, Wu et al. (2011) developed a set of appropriate performance evaluation indices mainly based on balanced scorecard for extension education centers in universities by utilizing multiple criteria decision making.

On the other hand, some studies focus on special dimension of the higher education institutions and use the different techniques for selection of the performance indicators. Lee (2010) focused on especially an intellectual capital (IC) and developed IC evaluation model to facilitate the understanding of their contribution to the university performance. He also applied Analytic Hierarchy Process (AHP) to formulate and prioritize the IC measurement indicators for constructing the IC evaluation model. In this study; university evaluation criteria were defined as administration, curriculum, technology transfer, research, teaching and service (Lee, 2010). Ahmadi (2012) aimed that cognition of performance appraisal system of this university and also introduced AHP technique in performance appraisal (Ahmadi, 2012). Kiakojoori et al. (2011) evaluated the performance of each branch of the Azad Islamic University (IAU) in Mazandaran province, determining the role model and reference branches to define the inefficient branches by applying envelopment analysis and ranking the efficient branches of AIU in Mazandaran province by applying Anderson Peterson Method.

After all, the beginning of any study about performance measuring of higher education institutions should be started by designing a reference model. Therefore, this study aims to provide the performance evaluation model for higher education institutions by considering the findings of above mentioned studies and EUS's principles. The proposed model consists of ***indicators sub-model*** and ***measurement process*** which are described in detail in the following sections.

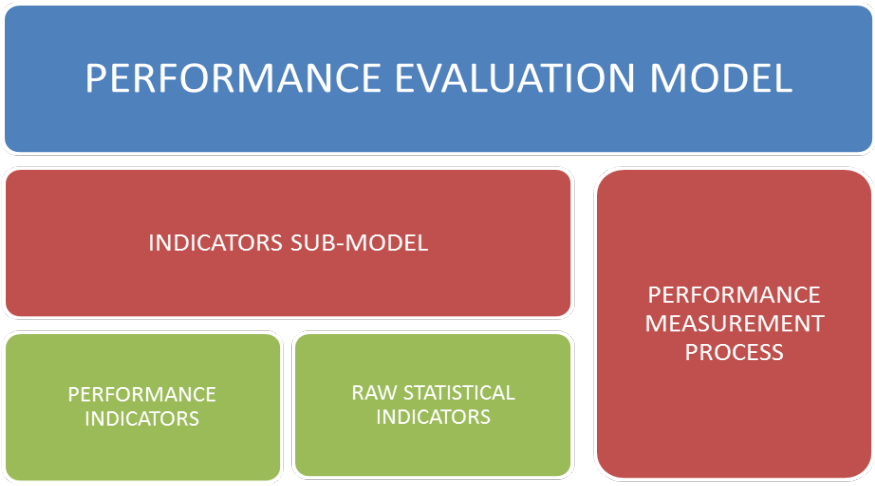

Figure 1: Performance evaluation model for higher education institutions

1. Indicators Sub-Model:

The indicators are classified into Performance Indicators and Raw Statistical Indicators in the indicators sub-model. ***Raw Statistical Indicators*** are the statistical numbers which are not processed and do not give any judgment about the situation. For example, "the numbers of the students of any departments" don't give any meaning for the situation and performance of this department. Therefore, we need to calculate some data to assess a performance of process or department. Raw Statistical Indicators could be Student Data, Academic Staff Data, Administrative Staff Data, Degree Programs Data, Course Data, Facility Data and Financial Data.

On the other hand, ***Performance Indicators*** are the calculated numbers about the process or the units in the higher education and can be used directly to evaluate this process or departments. The performance indicators consist of Strategic Performance Indicators and Process Performance Indicators:

- The Strategic Performance Indicators (SPI) are used for measuring the achievement of the institutional targets and they are output PI. Strategic Performance Indicators are grouped into following clusters for higher education institutions:
  - ✓ Education and Training PI
  - ✓ Research and Development PI
  - ✓ Community Services PI
  - ✓ Administrative and Management PI
- The Process Performance Indicators (PPI) can be used to monitor the processes which are executed in the institution, and these processes support the strategies of the HEI by determining the process targets in line with the strategic targets. Process Performance Indicators (PPI) are grouped into following clusters for higher education institutions:
  - ✓ Education and Training Processes PI
  - ✓ Research and Development Processes PI
  - ✓ Services Processes PI
  - ✓ Administrative Processes PI
  - ✓ Management Processes PI

As a consequent, the indicator has two dimensions in the proposed performance indicators sub-model such as:

1. Statistical versus Performance dimensions
2. Strategic versus Process dimensions

This classification also provides that the performance indicators can be differed depending on the level of strategic (institutional) or process analysis. The SPI can be used for strategic analysis, and derived from raw statistical indicators and the PPI which is used for process analysis. For example, "number of published paper" is the

indicator of knowledge creation process of higher education institution, and "number of published paper per academicians" is the institutional performance indicators of the higher education from the same dimension.

Figure 2: Relationship between indicators

Following table was constituted by using the Sakarya University's performance indicators based on the proposed model.

Table 1: Examples of Sakarya University's based on the model.

INDICATOR EXAMPLES OF SAKARYA UNIVERSITY			
Evaluation Focus	**Process Performance Indicators**	**Raw Statistical Indicators**	**Strategic Performance Indicators**
Education and Training	Number of revised courses according to the student surveys	Total number of courses	Ratio of revised courses (Number of revised courses/Total number of courses)
	Number of courses whose materials shared on web		Ratio of courses material sharing
	Number of enrolled students	Number of expected students	Ratio of fulfillment of programs
Research and Development	Number of published papers in SCI, SCI-expanded, SSCI and AHCI indexed journal	Total number of faculties	Number of published paper per faculty
	Number of national projects		Number of national project per faculty
	Number of international projects		Number of international project per faculty
Community Services	Number of supported projects for community	Number of appealed projects for community	Supporting percentage for community services
	Number of activity carried with the non-governmental organizations (NGOs)	Number of total NGOs	Effectiveness of collaboration with NGOs (Number of activity carried with the NGOs/ Number of total NGOs)
	Number of activities carried for social benefit	Number of departments	Number of activities carried for social benefit per departments

2. Performance Measurement Process:

The other component of the proposed PI model is the performance measurement process shown in the following figure. This component is to formalize the relationships of PIs and to describe the performance measuring procedure through the higher education institutions. The performance measurement process also links strategies to processes and processes to another.

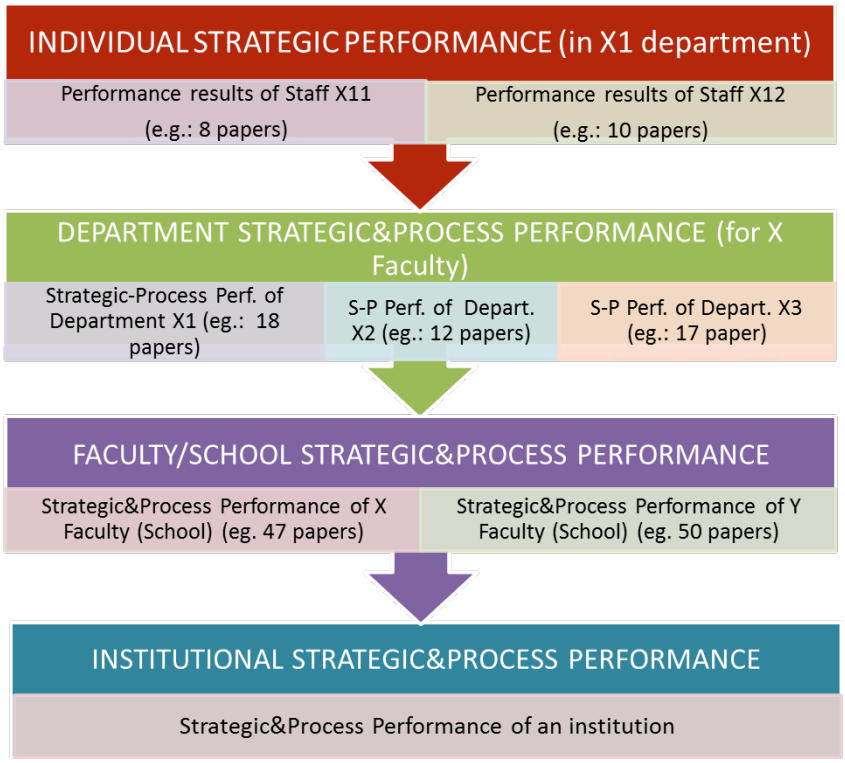

Figure 3: Performance evaluation process of higher education institutions

The performance evaluation process starts with determination the results at the individual level. After that, the department's performance values are calculated from individual results. The faculty's performance results are determined by aggregating performance results of all departments in the faculty and so on, the institution performance is calculated by similar ways from faculty to institution.

Conclusions

Todays, the performance evaluation is essential for any kind of institutions as well as higher education institutions. There are numerous different implementation practices for companies and for higher education institutions in the literature and scientific articles. Especially, EUA's studies about performance indicators and performance evaluation of higher educations are considerable. The aim of this study is to provide the performance evaluation model for higher education institutions by clarifying the required knowledge for performance measuring, formalizing and integrating the concept of performance indicators. This model also provides the knowledge basis for the implementation of information technology in a performance measuring system. The performance evaluation model consists of indicators sub-model which is classified into performance indicators and raw statistical indicators, and performance measurement process.

References

Ahmadi S.A.A. (2012). *Performance evaluation of Tehran province payame noor university staffs (open university) by AHP technique,* Interdisciplinary Journal of Contemporary Research in Business, 4, 226-235.

Azma F. (2010). *Qualitative indicators for the evaluation of universities performance,* Procedia Social and Behavioral Sciences, 2, 5408-5411, Elsevier.

Centra J.A. (1997). *How universities evaluate faculty performance: a survey of department heads,* GRE Board Research Report, Graduate Record Examinations Board.

Hronec S.M. (1993). *Vital Signs: using quality, time and cost performance measurements to chart your company's future*, Arthur Andersen &Co., American Management Association.

Martin E. (2003). *An application of data envelopment analysis methodology in the performance assessment of the Zaragoza University departments,*Documento de Trabajo 2003-06. Facultad de Ciencias Economicas y Empresariales, University de Zaragoza.

Kanji G.K.(2007). *Performance Measurement: A System Approach for Excellence*, 51st European Organization for Quality, 22-23 May, Prague.

Kiakojoori D., Aghajani H., Roudgarnezhad F., Alipour H.& Kojoori K.K. (2011). *Performance Appraisal of Islamic Azad University Branches of Mazandaran Provinceusing data envelopment analysis,* Australian Journal of Basic and Applied Sciences, 5, 840-848.

Lee S.H. (2010). *Using fuzzy AHP to develop intellectual capital evaluation model for assessing their performance contribution in a university,* Expert Systems with Applications, 37, 4941-4947, Elsevier.

Rolstadas A. (1995). *Performance Management: A business process benchmarking approach*, Chapman&Hall, London.

Tavenas F.(2003). *Quality Assurance: A Reference System for Indicators and Evaluation Procedures,* Report published by European University Association, Brussels Belgium.

Tehhumen J., Ukko J., Markus T.& Rantanen H. (2002). *Designing a performance measurement system: a case study in the telecom business*, Frontiers of e-business research.

Wu H.Y., Lin Y.K.& Chang C.H. (2011), *Performance evaluation of extension education centers in universities based on the balanced scorecard*, Evaluation and Program Planning, 34, 37-50, Elsevier.

Different treatment trains for rainwater purification for human consumption in México City

M. N. Rojas-Valencia[1]
A. Cordero Ibarra[1]
R. Gallardo Bolaños[1]
M. Vaca Mier[2].

[1]National Autonomous University of Mexico, Institute of Engineering, Coordination of Environmental Engineering, Post Box 70-472, Coyoacán 04510, Mexico, D.F. Mexico

[2] Departamento de Energía. Ciencias Básicas e Ingeniería, Universidad Autónoma Metropolitana- Azcapotzalco, Av. San Pablo 180, México. D. F. 02200

E-mail: nrov@pumas.iingen.unam.mx

Abstract: This work offers options for harvesting and reusing rainwater. In order to know the quality of the various rainwaters, microbiological and physical-chemical analyses are conducted based on the Mexican standards. The microbiological results showed various types of bacteria such as bacilli, cocci, coliforms, among them *Escherichia coli and Enterobacter aerogenes*, while the physical-chemical analyses reported low concentrations of total suspended solids (8.9 mg/L), biochemical oxygen demand in five days (2.7 mg/L), chemical oxygen demand (6.7 mg/L) and total organic carbon (1.9 mg/L). This work also relates to the adaptation of a catchment system in an already build construction with a treatment train supplying appropriate water quality. The analyzed parameters are mostly within NOM-041 limits; however, treatment is needed to ensure optimum water quality. The results obtained in the instant research show that rainwater purity should not be taken for granted. Before alleging that rainwater is drinkable it is important to conduct microbiological analysis in order to determine the most appropriate treatment.

Key words: Catchment system, rain, treatment, reuse, quality.

Introduction

In Mexico, water management has traditionally been poor, each family wasting on average 150 L/day due to bad habits, increasing thus the average consumption per person to 200 or even 300 L/day, when 100 L/day per head should be more than enough for urban domestic use.

In most urban areas, the appropriate supply of water to meet the growing needs of the population and ensure water access equity is an important and urgent challenge for the decision makers. Two solutions are available for ensuring water sustainable management. The first one is to find new alternative water resources, while the second is to use efficiently the limited water resources on hand. Up to now, the efforts have been focused on the first option and only limited attention has been given to the second (Ahmed et al; 2009).

An example of alternative resource is rainwater. Since only a catchment system is needed, it has some advantages such as energy savings because there is no need of extraction process and piping for the distribution system or pumping for transportation to the consumption areas. Besides, the treatment conditions for ensuring a quality appropriate for human consumption are relatively economical (Amin and Han, 2009). A disadvantage is that water availability is limited to high rainfall season and varies depending on the region of the country. Moreover, it depends on the size of the catchment area and on the size of the cistern in the building. Another obstacle is that there are no reports regarding rainwater quality and thus it should be used carefully for human consumption.

Taking into account the advantages and disadvantages of rainwater, as well as data shortages, the objective of this research was to determine the quality of rainwater from the southern area of the Federal District. It was also to establish an alternative rainwater catchment and treatment process through a system permitting to harvest as much water as possible and, after treating it, use it for cleaning, in sanitary buildings and even for personal use and drinking purposes.

Materials and Method

The methodology comprised two phases: the first phase focused on the design and catchment of rainwater and the second phase focused on the physical-chemical and microbiological characterization of rainwater.

Rainwater samples were taken and stored in two harvesting systems currently working located in Tlalpan delegation in the medium height Ajusco in the southern zone of Mexico City. The two systems were called house 1 and house 2. It is marginalized zones were access to water through the supply network is not reliable and thus rainwater harvesting could solve the needs of this community. A study was conducted regarding the main contaminants present in rainwater. Moreover, five treatment trains were installed and used in order to identify the treatments stages leading to rainwater that fulfills the Mexican norm and thus appropriate for human consumption.

The in site pretreatment, catchment system and storage system for each sample source was different. In Table 1, the various characteristics of the sample site are listed.

Table 1: Characteristics of the catchment and storage systems

Data	**House 1**	**House 2**
Address	Becal Mz. 13 Lote 22.	Izamal Mz. 22 Lote 17.
Material of the catchment area	Ferrocement.	Cistern rotoplas 600 L.
Exposition to sun light	Buried in the ground.	Cistern exposed to the sun.
Chlorination	Cloralex 0.5 mL/L.	Trichloroisocyanuric acid, 10 g per 10,000 L.
Filters	None.	50 μm filter.
Use	For plant watering, bathrooms and cloth washing.	For all domestic activities.

In both cases, the catchment system had an interceptor.

The harvested rainwater was submitted to five treatment trains consisting of several stages in order to test which was the most appropriate for obtaining drinkable water fulfilling the norm in force and meeting the needs of the people.

Five different trains were designed with different stages for both houses and were assigned a letter for reference purposes:

A) Original sample

B) Pump + 50 µm cellulose paper filter

C) Pump + 50 µm cellulose paper filter + granular activated carbon filter

D) Pump + granular activated carbon filter

E) Pump + 50 µm cellulose paper filter + granular activated carbon filter + 50 µm polypropylene filter + 50 µm activated carbon filter

F) Pump + 50 µm cellulose paper filter + granular activated carbon filter + 50 µm polypropylene filter + 50 µm activated carbon + UV

A 1-L sample was taken in each case, and thus globally twelve samples were obtained that were kept in 0.5-L sterile bags for further analysis.

The samples taken were analyzed on the sampling day in the laboratories. Water quality evaluation was determined using three indicators, BOD_5, COD and TSS. Moreover, in the case of each sample, total Kjeldhal nitrogen and pH analyses were performed.

Figure 1, shows a summary of the second part of the methodology.

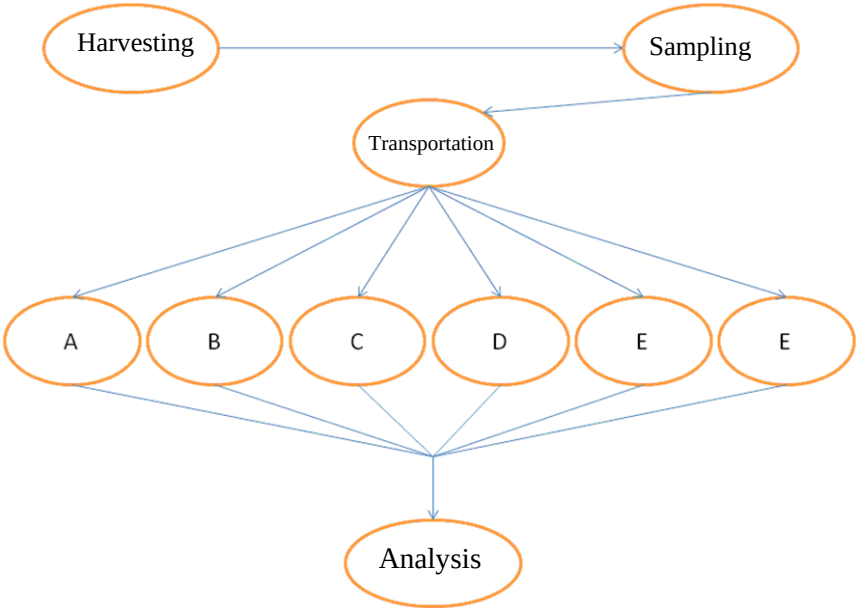

Figure 1: Flow chart of the second part of the methodology

The analytical methods used for each parameter are shown in Table 2.

Table 2: Analytical methods used

Parameter	Analytical Method	Units
Total coliforms	NMX AA-042-1987	NMP/100 ML
Total BOD_5	NMX AA-028-SCFI-2001	mg/L
Total COD	NMX AA-030-SCFI-2001	mg/L
Total solids	NMX AA-034-SCFI-2001	mg/L
Total Kjeldhal nitrogen	NMX AA-026-SCFI-2001/EPA 351.2-1978	mg/L
pH	Meter Orion 210A	---

Results and discussion

Microbiological results

The microbiological results showed various types of bacteria such as bacilli, cocci, coliforms, among them the genera *Bacillaceae, Leuconostoc* and *Aerococcus,* which were reportedly widely distributed in the air, soil and water.

Other species identified in this research was *Escherichia coli (E. coli)* isolated from the selective medium for total coliforms. This is the most commonly bacteria species found in clinical laboratories and its presence has been reported in infectious diseases involving human tissues. Transmission is through contaminated foods, water and personal contact, the main habitat of this bacterium being the intestinal flora. In the same selective medium, *Enterobacter aerogenes* was found which is widely distributed in the respiratory apparatus, and is known for affecting skin wounds and occasionally may cause septicemia (blood poisoning) and meningitis (Lee et al; 2009).

In countries such as Korea, Nigeria, Australia, New Zealand and others, researchers have been interested in rainwater quality, and all the studies conducted, based on their own sampling methodology, coincide in the presence of biological indicators such as *E. coli* and total coliforms from rainwater. For example, in Korea, total coliforms (TC) and *Escherichia* (EC), were found in 91.6% and 72%, respectively, of the samples of harvested rainwater, at the upper levels of the guidelines for drinkable water (Lee et. al., 2009). In Australia, 65% of the samples taken from rainwater harvested from a roof were positive for *E. coli, showing* the following concentrations: 20% between 1 and 10 CFU/100 mL, 18% between 11 and 100 CFU/100 mL, 19% between 101 and 1000 CFU/100 mL and 7% >1001 CFU/100 mL, while 82% of the samples analyzed were positive for *enterococci* with the following concentrations: 18% between 1 and 10 CFU/100 mL, 31% between 11 and 100 CFU/100 mL, 23% between 10 and 1000 CFU/100 mL and 10% >1001 CFU/100 mL (Ahmed et. al., 2009). Other bacteria genus found in catchment cisterns in India is Streptococci with a total of 43 colony forming units (CFU) in non-treated water (Cochran and Ray, 2008). On the other hand, in two different sampling zones in Korea, the *E. coli* indicator was present in 96 and 72% of the samples harvested from the rainwater storage system (Amin et al., 2009).

Australia has reports of pathogen agents contained in harvested rainwater in which bacteria such as *Salmonella, G. lamblia and L. pneumophila* were found, besides *E. coli* strains (Ryan et al., 2009), while in New Zealand, *E. coli* was present in 12 from 18 samples.

In Nigeria, various levels of microbiological contamination were found in various samples. All the samples contained high concentrations of heterotrophic bacteria (from $5.8X10^1$ to $7.6X10^3$ UFC/mL) while *Pseudomonas* spp ranged from 1.0X10 to $4.0X10^2$ UFC/mL (Nnene, 2000).

Physical-chemical parameters results

The physical-chemical analyses reported low concentrations of total suspended solids (8.9 mg/L), biochemical oxygen demand in five days (2.7 mg/L), chemical oxygen demand (6.7 mg/L) and total organic carbon (1.9 mg/L). The pH varying from 5.5 to neutral according to the progress of the rainy season reaching a pH 7 and maintaining this level till the end of the rainy season.

In the case of total BOD_5, the typical value reported for rain drainage is 100 mg/L, however water is considered drinkable if its total BOD_5 value is below 5 mg/L. Figure 4 shows that BOD_5 values obtained do not fulfill the standard except in some cases. When more stages are used in the treatment train, BOD_5 increases considerably and it can thus be concluded that the filtration train could have been contaminated with organic material leading to an increase of total BOD_5 when stages were added to the treatment train. However, all the samples are below the typical value observed in most waters for human consumption insuring thus that rainwater has a low organic concentration.

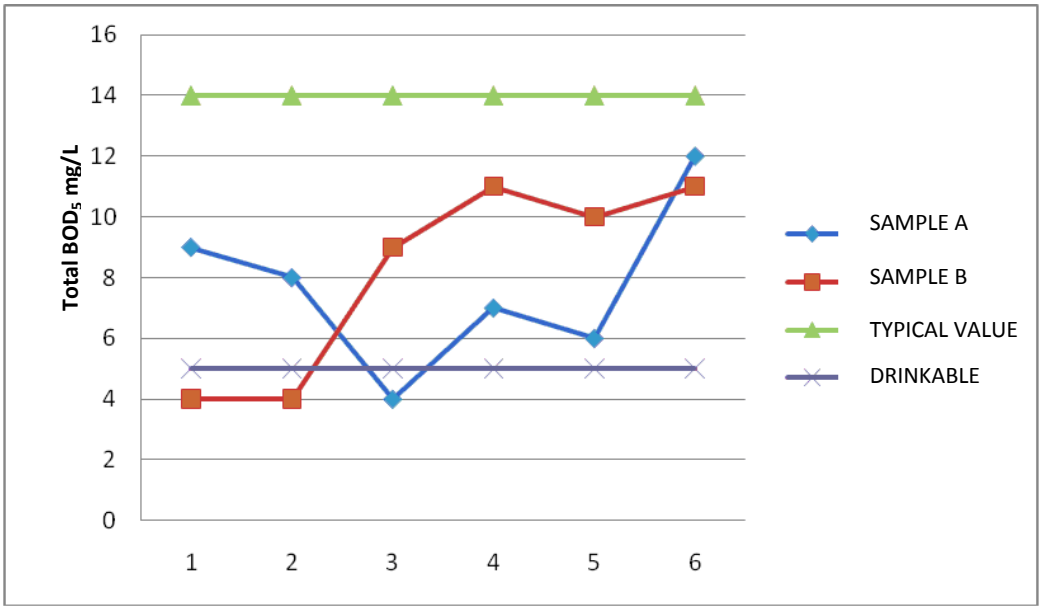

Figure 2: BOD_5 variation

In the case of total COD sample, the test was only conducted on the control samples i.e., the samples without treatment because the presence of this parameter is considered little probable and this was confirmed since it was undetectable in the studied samples.

With regard to the total solids analysis, the permissible limit according to Mexican Official Standard NOM-041-SSA1-1994 is 500 mg/L. The results obtained from both samples are not above the limit established by the standard. The values average 120 mg/L. However, there is no reduction in the total solids and it can thus be concluded that the treatment train is not appropriate for reducing the total solids contents in rainwater.

Non-treated rainwater is within the permissible limits according to Mexican Official Standard NOM-041-SSA1-1994, but the same case occurs as with regard to the BOD_5 parameter. Nitrogen quantity increases with the increase of the stages in the treatment train and thus at some stage of the filtration there must have been a large quantity of organic material. Despite the above, in the case of house 1, the treatment train in stages 5 and 6 is appropriate since the total nitrogen quantity is not detectable.

In the case of house 2, the first treatment trains are the ones that best fulfill the limits indicated in Mexican Official Standard NOM-041-SSA1-1994. i.e., only the physical treatment reduces considerably the total nitrogen quantity present in the sample.

The permissible limits reported are not over the limits indicated in Mexican Official Standard NOM-041-SSA1-1994 with regard to pH ranging from 6.5 to 8.5.

Currently, all over the world, large-scale efforts are made to harvest rainwater and use it in houses in urban zones for various purposes depending on its quality. Some examples are: the Ringdansen Project in Sweden, the multipurpose stadiums in Nagoya, and Fukoka Tokyo, Japan, the Millenium Dome Stadium in London, the Technological University of Nanyang in Singapore and the group of buildings Daimler Chrysler Potzdamer Platz in Berlin, Germany, to mention only a few of them.

In Ringdansen, a residential zone located in the southeastern part of Norrköping, Sweden, harvested rainwater has been destined to the following uses: WCs, water for cleaning clothing and washing cars as well as watering plants.

In Japan, there are several examples of large-scale rainwater catchment systems. The harvested water is used for WCs, and for watering plants. Rainwater catchment areas are 16.000, 25.900 and 35.000 m^2, respectively. The tank volumes are 1000, 1800 and 1500 m^3, respectively.

The Millenium Dome in London is another example of a large-scale rainwater catchment system. The roof of the cupola has a surface of about 100.000 m^2, from which water is harvested through hoppers unloading into a series of main rings around the entire circumference of the dome. A study of the functioning of the system showed that rainwater meets about 10% of the water demand although harvesting is limited because of the site storage.

The residential area located in the central part of Fornebu, in Oslo, Norway, includes the building of 6 000 houses. There is an interest for using water as a revitalizing element within the structure of the park vegetation. This objective is reached substituting conventional urban drain piping through filters, storage and treatment systems designed for natural processes. All this is possible if some hydraulic and water quality criteria are met.

Conclusions

The best rainwater purification option is the sequence: filtration, activated carbon, ionic exchange, UV radiation and ozonization. Various microorganisms that could represent a health hazard are bacteria *E. coli* and *Enterobacter aerogenes* that, despite their very low concentration, make it necessary to install a treatment system before reusing rainwater. According to NOM-003-SEMARNAT-1997, harvested rainwater fulfills the parameters established for direct contact with humans.

References

Ahmed, W., Goonetilleke, A., Gardner, T., 2009. Quantitative detection of pathogens in roof harvested rainwater, Microbiology Australia 30(1), 35-37.

Amin, M.T., Han, M.Y., 2009. Probable sources of microbial contamination of stored rainwater and its remediation. College of Engineering, Seoul, 1-10

Cochran, J., Ray, I., 2009. Equity Reexamined: A Study of Community-Based Rainwater Harvesting in Rajasthan, India. *World Development* **37-2**, 435–444.

Lee, J.Y., Yang, J.-S., Han, M. Choi, J., 2009. Comparison of the microbiological and chemical characterization of harvested rainwater and reservoir water as alternative water resources, Korea, Science of Total Environment 408-4, 896-905.

Nnene, U., Aghogho, O., 2000. Rainwater quality from different roof catchments in the Port Harcourt district, Rivers State, Nigeria. *AQUA* **49,** 281-288.

Effect of Wave Impeding Barrier Depth on Buried Pipeline

Fatih Göktepe[1], H. Serdar Küyük[2] ve Erkan Çelebi[1]

[1]Sakarya University, Engineering Faculty, Department of Civil Engineering, Sakarya-Turkey
[2]UC Berkeley, Berkeley Seismological Laboratory, Berkeley, U.S.A.
e-mail: fgoktepe@sakarya.edu.tr

Abstract: Pipelines are one of most important component of lifeline engineering. For instance, the Southern Caucasus- Eastern Turkey energy corridors are formed by several key pipelines carrying crude oil and natural gas from Azerbaijan, via Georgia, to world markets through Mediterranean Sea. Many project accomplished recently and construction of new corridors are still going on. They should be protected from earthquake disaster especially when they pass through high seismicity zones. The wave impeding barrier (WIB) based on the cut-off frequency of a soil layer over bedrock can be used to reduce the earthquake excitation of this vulnerable the infrastructures. In this paper, efficiency of WIB with the application of various depths underneath of pipeline is investigated. The proposed model is analyzed as numerical simulation using 2D finite element analysis. A parametric study carried out for various depths of embankment of WIB. The soil is defined as semi-infinite medium by using absorbent boundaries and Mohr-Coulomb material model is chosen in the analysis. Results showed that artificial bedrock can be very promising as an isolator to protect pipelines when they buried for a certain depth.

Key words: Wave impeding barrier, Dynamic FE analysis, infrastructures, earthquake motion, passive isolation, absorbent boundaries

Introduction

Excessive dynamic loading during strong ground motion causes in enormous stress and deformation on underground structures in active tectonic regions. Last decade, shallowly buried pipelines are utilized for a wide range of key applications, such as natural gas/oil transmission, telecommunication and water supply. Damages to small pipelines were observed in some earthquakes such as 1964 Niigata and Alaska earthquakes however fewer damages were generally reported to large underground structures compared to surface structures. On the other hand, real performance of recent project of new energy corridors such as Southern Caucasus- Eastern Turkey natural gas pipelines still unknown under strong ground motion. These vital underground structures will affect the environment extensively and the countries that depend on them. Sustainability, durability and security of these pipelines are very critical for all earth habitants. Thus, recently, earthquake induced damages followed by severe earthquakes and earthquake corresponding resistance design have received considerable attention by the authors (Hall and O'Rourke, 1991, Liu and Song, 2005) in many countries.

There can be two way for reducing the response of pipeline as: I) by modifying the wave dissipation characteristics of the soil deposit underneath of pipeline, and b) by partially interrupting the spreading of waves into the understructure or by providing the structure more damping by means of installation certain devices such as additional base isolation systems which can be very costly. It is also possible to modify the dynamic transmitting behavior of local sub-soil through a complex mechanism of wave reflection and mode alteration around the vibration source by constructing a suitable wave barrier at the bottom of pipeline (Göktepe et al., 2010). Various numerical techniques for analyzing the influences of soil heterogeneity and layering on the vibration screening by means of trench and wave impeding barriers are investigated by the authors (Beskos et al., 1986, Leung et al., 1991, Klein et al., 1997, Takemiya, 1998a,b, Chouw and Schmid, 1999, Adam and Chouw, 2001, Pflanz et al., 2002, Adam and Estorff, 2005, Çelebi et al., 2006, Çelebi and Göktepe, 2012) to compare with the few experimental studies which are carried

out full scale tests on site and laboratory model investigations only for particular cases (Woods, 1968, Haupt, 1981, Ahmad and Al-Hussaini, 1991, Forchap and Verbic, 1994).

In this paper a WIB, which behaves as artificial bedrock (concrete in this study), is tested as an isolator to reduce responses of buried pipelines under earthquake strong ground motion. 2D numerical finite element method is used for investigations. It is buried horizontally underneath of trench below the pipelines to be protected in various depths as seen in Fig. 1. A parametric study carried out for optimum depth.

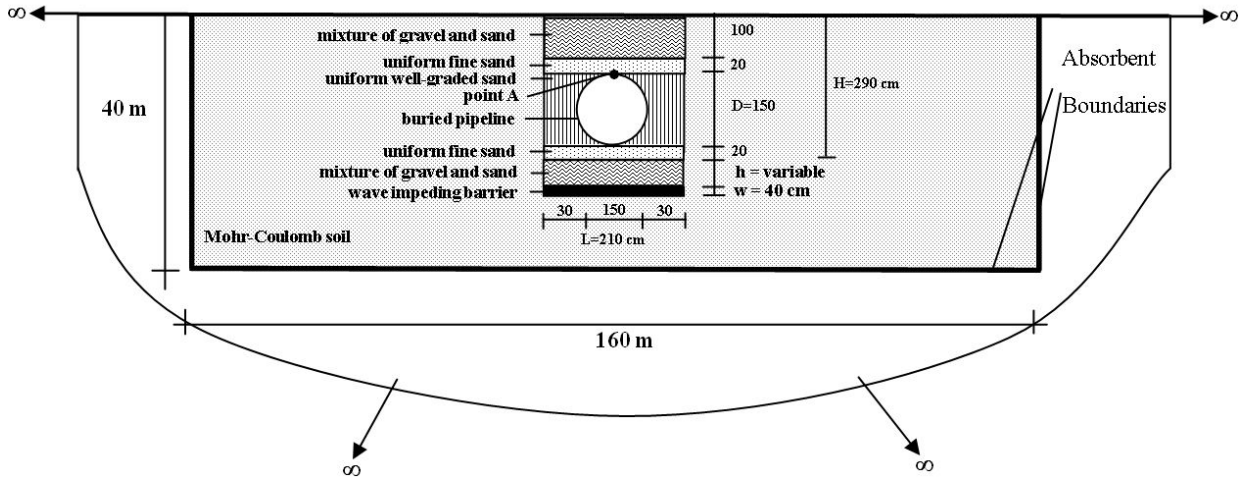

Figure 1: Schematic diagram of the considered soil-structure model with wave impeding barrier

Numerical Model

Soil-structure interaction, wave propagation, defining realistic material properties of the local soil condition and adequate software for the numerical analysis have fundamental influence on soil related finite element analysis.

In order to analyze the wave propagation of surface vibrations in the soil, and to predict the mitigation of buried pipelines responses produced by an earthquake excitation the proposed model and its computational work as numerical simulation with wave propagation in the soil are performed using finite element analysis by the computer program (Brinkgreve et al., 2002).

Special boundary conditions named as absorbent boundaries, which can absorb the energy waves, were specified to both the vertical and horizontal model boundaries to avoid spurious reflection of waves back into the soil medium. The mechanical behavior of the underlying soil medium considered in the model is simulated by an elasto-plastic Mohr Coulomb model under plane-strain conditions. 1990 Upland Earthquake acceleration record is considered as input motion.

Wave-impeding barrier buried in various depth are considered as reduction measure to reveal the optimal geometrical properties. The FE discretization of the soil-structure system with a WIB is shown in Fig. 1. The observation point (A) chosen for investigation is on the top of the buried pipeline as shown in the same figure. The essential material parameters considered in FE model for the underlying and filling soil together with steel pipeline are summarized in Tables 1-3.

Table 1: Properties of soil for undrained FE Mohr-Coulomb model (Gamber, 2004)

Parameter	Symbol	Unit	Magnitude
Total unit weight	γ	(kN/m^3)	16.67
Mass density	ρ	(Mg/m^3)	1.70
Young's modulus	E	(kPa)	34500.00
Shear modulus	G	(kPa)	13270.00
Poisson's ratio	ν	-	0.30
Constrained modulus	M	(kPa)	46440.00
Compression wave velocity	V_p	m/s	165.200
Shear wave velocity	V_s	m/s	88.300
Rayleigh damping with alpha coefficient	α	-	0.001
Rayleigh damping with beta coefficient	β	-	0.01
Void ratio	e	-	0.50
Cohesion	c	(kPa)	0.00
Friction angle	ø	(º)	33.00
Dilatancy angle	ψ	(º)	3.00
Interface strength reduction factor	R_{inter}	-	0.67

Table 2: Properties of filling soil of buried pipeline for undrained FE Mohr-Coulomb model (Zaneta, 2006)

Soil type	Mixture of gravel and sand	Uniform fine sand	Uniform well-graded sand
Mass Density (Mg/m^3)	2.00	1.60	1.80
Young's Modulus(kPa)	15000	15000	20000
Poisson's Ratio (-)	0.25	0.25	0.25
Friction Angle (º)	38.00	32.00	33.00
Cohesion (kPa)	3.00	0.00	0.00

Table 3: Properties of steel pipeline for FE elastic plate-element

Parameter	Symbol	Unit	Magnitude
Total unit weight	γ	(kN/m^3)	77.00
Mass density	ρ	(Mg/m^3)	7.85
Young's modulus	E	(kPa)	$2x10^8$
Damping factors	α, β	-	0.05
Poisson's ratio	ν	-	0.30

Results

In order to obtain the influence of a wave impeding block as an isolator when constructed underneath of pipeline in various depths, a parametric investigation has been performed for reducing adverse effects of earthquake vibrations. Göktepe et al. (2011) proposed a WIB, investigated various thicknesses from 10 cm to 100 cm and a 40 cm thickness was chosen for given best performance. In the current study depths of embankment 20, 40, 80, 160 and 200 cm are examined. Selected material properties of the concrete block are given in Table 4.

Table 4: Properties of concrete wave impeding block (WIB) for FE elastic model

Parameter	Symbol	Unit	Magnitude
Total unit weight	γ	(kN/m3)	22.00
Mass density	ρ	(Mg/m3)	2.24
Young's modulus	E	(kPa)	$3.7x10^7$
Damping factors	α, β	-	0.01
Poisson's ratio	ν	-	0.25

Mixture of gravel and sand filling soil is used for the depth of embankment. A dimensionless parameter which is obtained from the ratio of depth of embankment (h) to height of trench (H) is derived and proposed for the optimum thickness. The height of trench which is equal to 290 cm is assumed as summation of the radius of pipeline and filling upside down of the pipeline as 20 cm uniform fine sand and 100 cm mixture of gravel and sand is shown Fig. 1. Therefore h/H ratios for 20, 40, 80, 160 and 200 cm depth of embankment are 0.07, 0.14, 0.28, 0.55 and 0.69 respectively.

Vertical displacements recorded after dynamic analysis without WIB and for various h/H ratios are shown in Fig. 2. The ratio with 0.14 results in the best attenuation considering peak ground displacement (PGD). Any depth of embankment seems effective compared without WIB. It is seen that 40 cm is the most effective depth where 92% reduction is achieved on the pipeline.

On the other hand, there is no change at all on horizontal displacements. Displacements are plotted and showed as one centimeter shifted for better visualization (Fig. 3). About 5 cm total displacements are seen in each case which means, the WIB has no effect in horizontal displacement.

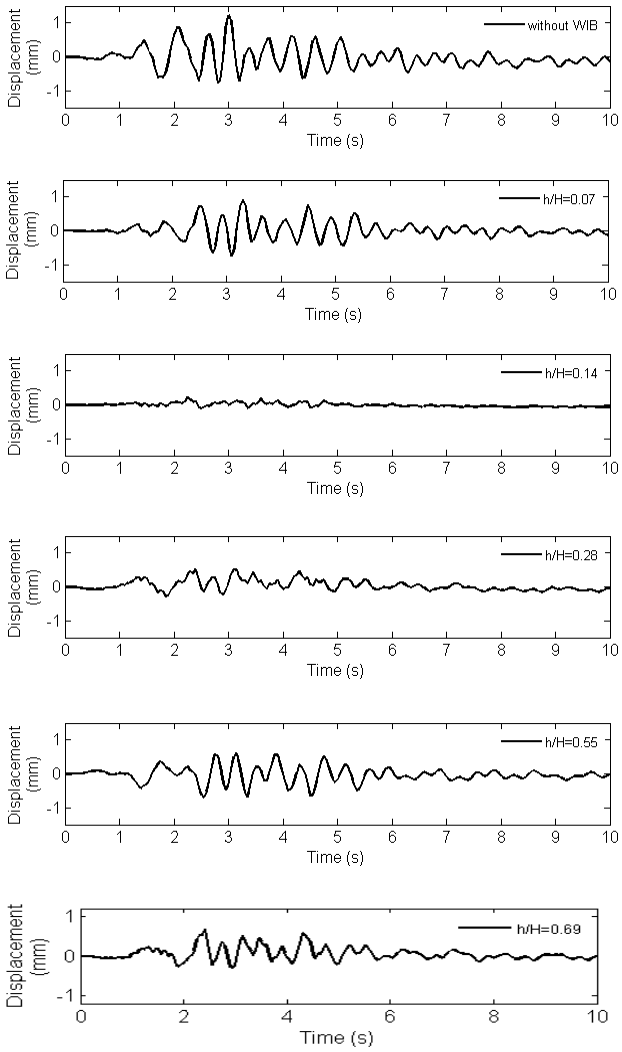

Figure 2: Records of vertical displacements depending on various h/H ratios at point A

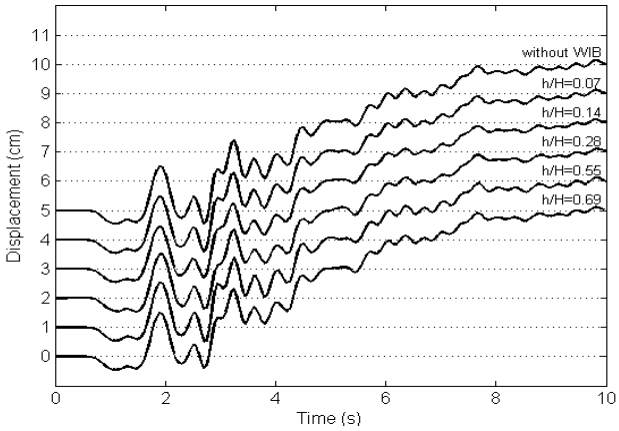

Figure 3: Records of horizontal displacements depending on various h/H ratios at point A (records are shifted 1 cm)

The horizontal acceleration records are plotted in Fig. 4a. Similar tendency is seen for all ratios. The vertical accelerations are also shown in Fig. 4b. Top waveform shows acceleration without WIB where the waveforms underneath demonstrates with different depth of embankment. According to peak ground acceleration (PGA), best result is acquired from the WIB for 0.14 of h/H ratio.

a

b

Figure 4: Records of horizontal acceleration (a) and of vertical acceleration (b) depending on various h/H ratios at point A (records are shifted 150 cm/s2 and 40 cm/s2 respectively)

We introduce a reduction factor which is defined with following equation;

$$RF_{Displacement} = \frac{PGD_t}{PGD_c}, \quad RF_{Acceleration} = \frac{PGA_t}{PGA_c} \tag{1}$$

where indexes t is for various h/H ratios and c is stands for without WIB. Relations of reduction factors (RF) with h/H ratios for acceleration and displacement results are shown in Fig. 5a,b.

Ratio of 0.14 gave the smallest RF for PGD and PGA in the analyses. For the former, a very promising reduction is achieved with 92% and the latter is succeeded 64% reduction in vertical acceleration. Interestingly, only h/H=0.55 is bigger than 1.00 in horizontal acceleration which means wave barrier is amplified around 1% for this depth of embankment as seen Fig. 5.

As for horizontal acceleration, 40 cm embankment made best isolation with 32%. Göktepe et al. (2011) previously found that 20 cm WIB is better than the 40 cm according to horizontal and vertical PGA (not in PGD). We showed that if the 40 cm WIB applied to 40 cm depth, the reduction is better compared with the performance of 20 cm WIB.

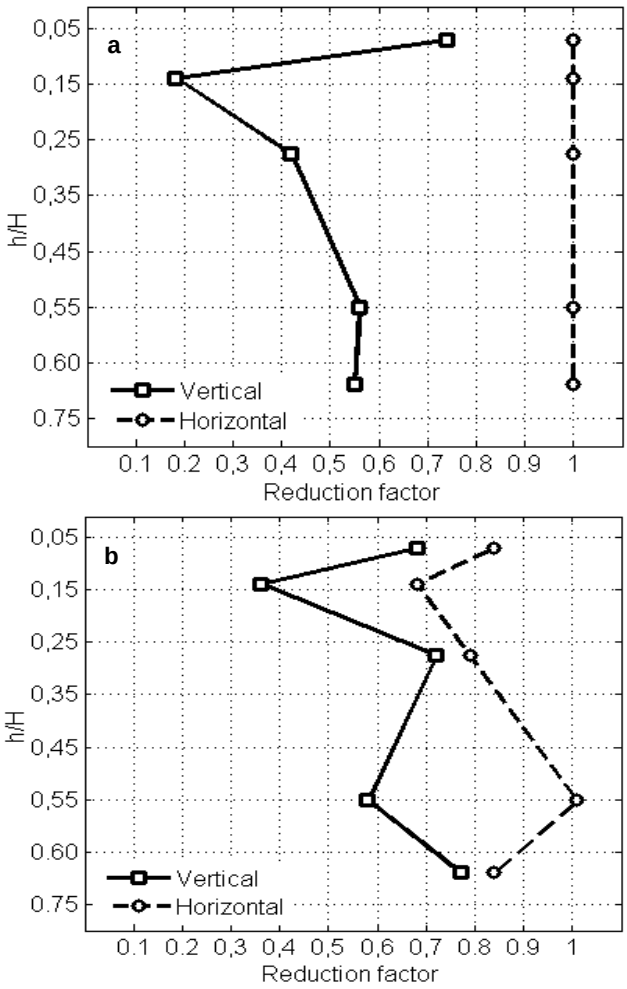

Figure 5: Reduction factors depending on various h/H ratios at the point A. Vertical and horizontal (a) displacements (b) acceleration (RF are dimensionless)

Analyzing the all cases, a general tendency is inferred that employment of wave impending barrier for buried pipelines is a very effective application to reduce the vibration. However a special care should be taken for amplification cases before application.

Conclusion

Earthquakes have caused colossal casualties and severe damages to engineering structures and especially leading to substantial economic loss to the underground structures and/or infrastructures. Security, sustainability, and durability of these pipelines are very vital for many reasons The response of lifeline engineering under earthquake excitation which present a risk for population and environment is influenced by deformability of the buried pipelines such as used in natural gas transmission, especially in case of very soft ground conditions. A parametric investigation has been executed to obtain the influence of a wave impeding block as an isolator when constructed below pipeline for reducing adverse effects of earthquake vibrations. Various depth of embankment for the artificial bedrock (concrete block) are investigated by using 2D finite element method. It is found that even 40 cm depth of embankment with 40 cm thickness of the block can reduce the peak ground acceleration and displacement. It is concluded that wave impending barrier can be used in practice in the field.

References

Adam, M. & Chouw, N. (2001). Reduction of footing response to man-made excitations by using a wave impeding barrier. *Journal of Applied Mechanics* 4 (pp. 423-431).

Adam, M. & Estorff, O.Von. (2005). Reduction of train-induced building vibrations by using open and filled trenches. *Computers and Structures* 83 (pp.11–24).

Ahmad, S. & Al-Hussaini, T.M. (1991). Simplified design for vibration screening by open and infilled trenches. *Journal of Geotechnical Engineering* 117 (1) (pp.67-88).

Beskos, D.E., Dasgupta, G. & Vardoulakis, I.G. (1986). Vibration isolation using open or filled trenches part 1: 2-D homogeneous soil. *Comput. Mech* 1 (1) (pp. 43–63).

Brinkgreve, R.B.J., Al-Khoury, R., Bakker, K.J., Bonnier, P.G., Brand, P.J.W., Broere, W., Burd, H.J., Soltys, G., Vermeer, P.A. & Haag, D.D. (2002). *Plaxis finite element code for soil and rock analyses*. Published and distributed by A.A. Balkema Publisher, The Netherlands.

Celebi, E., Fırat, S. & Cankaya, I. (2006). The effectiveness of wave barriers on the dynamic stiffness coefficients of foundations using boundary element method. *Applied Mathematics and Computation* 180 (pp.683–699).

Chouw, N. & Schmid, G. (1999). Numerical and experimental investigation on wave impediment in soil, *Structural dynamics EURODYN'99* (pp.977-982). Fryba & Naprstek, Balkema, Roterdam,

Çelebi, E. & Göktepe, F. (2012). Non-linear 2-D FE analysis for the assessment of isolation performance of wave impeding barrier in reduction of railway-induced surface waves. *Construction and Building Materials* 36 (pp.1-13).

Forchap, E. & Verbic, B. (1994). Wave propagation and reduction of foundation vibrations, *Berg-Verlag GmbH* (pp. 165-178). Bochum.

Gamber, N.K. (2004). *Shallow foundation systems response to blast loading.* A Thesis Presented to The Faculty of the Fritz J. and Dolores H. Russ College of Engineering and Technology, Ohio University, In Partial Fulfillment Of the Requirement for the Degree Master of Science, Athens.

Goktepe, F., Kirtel, O. & Celebi, E. (2010). Wave impeding block for mitigation of structural responses to train induced vibrations, *9th International Congress on Advances in Civil Engineering.* Karadeniz Technical University, Trabzon, Turkey.

Goktepe, F., Kuyuk, H.S., & Celebi, E. (2011). Efficiency of wave impeding barrier in pipeline construction under earthquake excitation using finite element analysis, *International Conference on Earthquake Engineering and Seismology (ICEES 2011*). NUST, Islamabad, Pakistan.

Hall, WJ. & O'Rourke, T.D. (1991). Seismic behavior and vulnerability of pipelines. *Lifeline earthquake engineering, M. A. Cassaro, ed., American Society of Civil Engineers* (pp. 761–773). New York.

Haupt, W.A. (1981). Model tests on screening of surface waves, *In: Proceedings of the 10th International Conference on Soil Mech* (pp. 215–222). Found. Eng., Stockholm, Sweden, Vol. 3.

Klein, R., Antes, H. & Houedec, D.Le. (1997). Efficient 3D modelling of vibration isolation by open trenches. *Computers & Structures* 64 (1-4) (pp.809-817).

Leung, K.L., Vardoulakis, I.G., Beskos, D.E. & Tassoulas, J.L. (1991). Vibration isolation by trenches in continuously non-homogenous soil by the BEM. *Soil Dynamics and Earthquake Engineering* 10 (3), (pp.172-179).

Liu, H. & Song, E. (2005). Seismic response of large underground structures in liquefiable soils subjected to horizontal and vertical earthquake excitations. *Computers and Geotechnics* 32(4) (pp. 223-244).

Pflanz, G., Hashimoto, K. & Chouw, N. (2002). Reduction of structural vibrations induced by a moving load. *J. Appl. Mech* 5 (pp.555–563).

Takemiya, H. (1998a). Lineside ground vibrations induced by high-speed train passage, *Workshop on Effect of High-Speed Vibration on Structures and Equipment* (pp.43-49). Dept. Civil Eng., Nat. Cheng Kung Univ., Tainan, Taiwan, R.O.C.

Takemiya, H. (1998b). Paraseismic behavior of wave impeding block measured for ground vibration reduction, *Workshop on Effect of High-Speed Vibration on Structures and Equipment* (pp.51-56). Dept. Civil Eng., Nat. Cheng Kung Univ., Tainan, Taiwan, R.O.C.

Woods, R.D. (1968). Screening of surface waves in soils. *J. Soil Mech. Found. Eng. Div., American Society of Civil Engineers* 94 (4) (pp.951–979).

Zaneta, G.Adme. (2006). Analysis NATM tunnel responses due to earthquake loading in various soils. *Mining Technology Bulletin-Institute of Mining Science and Technology* ISSN 1859-0063 No. 2-3/2006 (pp.9-17).

Evaluation of zinc-rich epoxy paint performance by electrochemical impedance spectroscopy

Nadia HAMMOUDA[a], H. Chadli [b], G. Guillemot[c], K. Belmokre [a]

[a] Laboratoire de Corrosion et Traitements de Surface, Dép. Sci. De la Matière, Université du 20 août 1955, Route d'El-Hadaiek, B.P.26, Skikda, Algérie.
[b] Laboratoire de Métallurgie et Génie des Matériaux, Université de Badji Mokhtar, B.P 12-Sidi Ammar, Annaba, 23.000-Algérie
[c] Laboratoire de Métallurgie Physique et Génie des Matériaux, école Nationale Supérieure d'Arts et Métiers de Lille, 8, boulevard Louis XIV 59046 Lille Cedex – France.
e-mail: hammoudanad@yahoo.fr

Abstract: To improve understanding of Zn-rich coatings for use in the storage reservoirs of oil, such coatings are being examined in the laboratory by the suite of testing techniques: Open Circuit Potential (OCP) (E_{cor}) measurements , exposure time to verify electrochemical cathodic protection, electrochemical Impedance Spectroscopy (EIS), Optical Microscopy, local SEM and RAMAN for Zn reaction product ID. These testing techniques are being used in conjunction with a modeling and characterization effort focused on improve understanding of the effects of the metal pigment volume concentration (PVC), particle shape and aspect ratio, particle size and size distribution, as well and particle orientation on coating performance.
The single frequency electrochemical impedance spectroscopy (EIS) measurements of impedance as a function of time for Zn-rich primers, or other active systems, gives insights into the evolution of the electrical properties .These primer coatings are usually top-coated to function optimally and have a long field lifetime. When used properly,
these primers provide almost as much protection to steel as galvanizing. The coatings system of a Zn-rich primer and an exterior durable topcoat provides both barrier and damage (sacrificial/cathodic) protection to steel substrates.

Keywords: zinc-rich primer, cathodic protection, electrochemical impedance spectroscopy, corrosion mechanisms.

Introduction

The application of zinc-rich primers on ferrous substrates is a very efficient method of anticorrosion protection. They are used in many aggressive media: sea water, marine and industrial environments. It is a common fact that in order to achieve a long-life coating system, a zinc primer needs to be applied as the first coat. For solvent-based zinc-rich paints (ZRPs), it seems to be established that, at least at the beginning of immersion, zinc particles provide a cathodic protection of the steel substrate (Hare, 1998, Abreu, 1996). Then, a long term protection develops due to the formation of zinc corrosion products, reinforcing the barrier effect of the paint (Hare, 1998, Morcillo, 1990, p. 2441).
The metallic zinc content in the dry film is a very important parameter to be emphasized in the technical specifications of zinc-rich paints. However, as observed by Lindquist *et al*., (Lindquist, 1985) this parameter is not the only factor determining the performance of this kind of paint. For exemple, Fragata (Fragata, 1987) Del Amo (Del Amo, 1990, p. 347) and Pereira (Pereira, 1990, p.1135) verified that the chemical nature of the binder and the zinc particle size are also very important.
The zinc dust (spherical or lamellar shape, or a combination of both) is dispersed in an inorganic (usually orthosilicates) or organic binder (usually epoxies) (Wicks, 1994, p.185). These particles must be in electrical contact between themselves and the metallic substrate in order to ensure a well-established electrical conduction within the coating. In such conditions of percolation, a galvanic coupling is created between zinc and the substrate (steel) which is nobler than the zinc. Then, zinc can preferentially dissolve, acting as a sacrificial pigment, and allowing a cathodic protection of the substrate. Many studies (Feliu, 1989, p.71, Pereira, 1990, p.30, Armas, 1992, p.379, Fragata, 1993, p.103, Feliu, 1993, p.438, Real, 1993, p.2029, Gervasi, 1994, Abreu, 1999, p.1173, Feliu, 2001, p.591, Vilche, 2002, p.1287) exist in literature and relate the protection mechanisms and degradation processes of such coatings.

Physico-chemical properties and corrosion resistance of solvent-based zinc-rich paints ZRPs strongly depend on pigment volume concentration (PVC), shape and size of zinc dust (Vilche, 2002, p.1287, Abreu, 1997, p.23). In common liquid ZRP, zinc is usually introduced as spherical pigments with a mean diameter ranging from 5 to 10 µm. To ensure good electrical contacts between zinc pigments and the steel substrate, a high pigment concentration is required (usually above 60 % by volume in solvent-based zinc-rich paints ZRPs) (Vilche, 2002, p.1287). A major drawback of classic solvent-based paint is the emission of volatile organic compounds (VOC), which contribute to atmospheric pollution. Since the 1970s, powder coatings are often preferred, because they are composed of dry thermosetting powders (without organic solvent) and more environmental abiding.
The aim of this work was to study the protective mechanisms of a single coat solvent-based zinc-rich paints ZRPs. Primer coating panels were applied on sandblasting steel and were studied when immersed in artificial 3% NaCl solution. Open circuit potential and electrochemical impedance spectroscopy measurements were recorded to study changes in the coating properties with the exposure time. The distribution of the zinc particles in the epoxy binder – which controls the porosity – is considered as the main factor affecting the electrolyte penetration within the coating. Moreover, Raman spectroscopy was used to analyze zinc corrosion products. This study reveals that the behavior of solvent-based zinc-rich paints ZRPs is different from powder coating. This is mainly attributed to the high porosity of solvent-based zinc-rich paints ZRPs, due to their low wetting ability, which insulates some of the zinc particles. However, cathodic protection is active and provides the sealing of the coating pores. Finally, it is found that the barrier effect is lower than the one usually observed with powder coating. S.E.M. observations have also been employed to illustrate the non-homogeneity of our paints. The main objective is to propose a model of EIS results accounting for the zinc particles distribution and mechanisms of water entrance within the coating.

Experimental part

Sample material and preparation

The metallic substrate was A283C steel (according to NF10027 standard) in conformity with the norm API (American Petroleum Industry), used in the storage reservoirs of the Algerian crude oil, the chemical composition of the tested steel is given in Table 1 . Before coating application, the metallic substrate was sandblasted to Sa 2.5 (Swedish Standard SIS 05 59 00/67) (roughness Ra 6.2 µm) or polished with emery paper up to G 400. Commercial epoxy-ZRPs were immediately applied onto steel panels using a brush or a roller (Fig. 1). Once cured, the samples were stocked in a desiccator until the moment of testing. The coating thickness was measured using an Elcometer gauge and was found around 80 µm for all panels, the composition of the coating is proprietary information.

Coated panels were cut out (100 cm×60 cm×4 cm) and an electrical wire was added in order to allow electrochemical measurements. With the aim to achieve the electrochemical measures in the best conditions it has been suited that the areas of about 15 cm^2 exposed to the electrolytic solution were sufficient. It seemed necessary to use a surface of paint relatively big in contact with electrolytic solution in order to compensate the insulating role of the sample as the thickness of the film grows. Mansfeld reports in a technical document (Mansfeld, 1981, p.237) a study of Kendig and Scully suggesting the use of samples covered with a ratio area / thickness of the coating of at least 10^4 to assure satisfactory electrochemical measurement. Samples were exposed under open circuit potential conditions in NaCl aqueous solution normally aired and none agitated whose concentration is 30 g/l for electrochemical impedance.

Electrochemical impedance spectroscopy measurements

The Electrochemical Impedance Spectroscopy (EIS) measurement is carried out in a 3% NaCl solution, using a potentiostat/galvanostat EG&G A273. A frequency response analyser Solartron FRA 1260 connected to an electrochemical interface Solartron SI 1287 was used to perform EIS measurements. A filter (Kemo VBF 8) was also employed to improve the signal to noise ratio. The frequency domain covered was 100 kHz to 10 mHz with the frequency values spaced logarithmically (five per decade). The width of the sinusoidal voltage signal applied to the system was 10 mV. All the measurements were performed at the open circuit potential and at different immersion times. The electrolyte was confined in a glass tube which was fixed to the painted surface by an O-shaped ring. The total tested area was 15 cm^2. Platinum gauze of large area was used as a counter electrode. All the potentials in the current article are referred to saturated calomel electrode (SCE). During the intervals between EIS measurements, the painted specimen was kept in the electrolyte cell without reference electrode. The cell design for EIS measurement was described in detail in a previous work (Novoa, 1989, p.223).

Characterization of wash primer coatings

FTIR analysis

The FTIR spectra of zinc rich epoxy paint were taken with SHIMATZU 8000 *série* + FTIR Spectrometer using ATR attachment in the range 4000–450 cm^{-1}.

Micro-Raman spectroscopy

Cross sections of the zinc-rich epoxy paint were polished and analyzed ex situ by micro-Raman spectroscopy after immersion. Fresh polishing with 1 µm diamond paste was performed just before Raman analysis. Fig.2 shows cross-section obtained by scanning electron microscopy of the ZRP. Only zinc particles (spherical) are observable. This figure shows that the distribution of the spherical pigments is quite inhomogeneous while zinc plates are uniformly distributed. Raman spectrophotometer (Labram from Jobin Yvon with an optical microscope from Horiba) was equipped with a HeNe laser (632.81 nm); the output power was 0.97 mW at the sample. A confocal hole set at 200 µm allowed an analyzed depth lower than 10 µm on transparent products. A 80 ULWD objective from Olympus was used to select the analyzed area. Raman spectra were only acquired on spherical zinc particle frontier.

Results and discussion

Electrochemical properties of sandblasted steel ($Sa\,2\frac{1}{2}$)

To the analysis of the curves (Fig 3), we note a continuous deterioration of the sandblasted steel to Sa 2.5 provoking a change in the state of the metallic surface. It can for example, to cover of corrosion products, weakly adhesive which provoke a stability of the free corrosion potential, the value was around -0.684 V/SCE. The diagrams of Nyquist determined to different time of immersion, in the 3% NaCl solution normally aired and non agitated are represented on the Fig. 3, the values of the different parameters are gathered in the table 2.
The values of the electrolyte resistance R_e are very weak, of the order of *14 Ωcm²*, what shows that the middle is very conductive.

To the analysis of the impedance diagrams, since the first hours of immersion of the metallic substrate, we register a rapid evolution of the charge transfer resistance R_{ct} of the sandblasted steel, we note that at the beginning of the immersion the value of the charge transfer resistance R_{ct} only makes increase until to the fourth days of immersion (96 hours), it means that the process governing the kinetics is under control of load transfer. According to the Fig. 4 we notes that the charge transfer resistance R_{ct} evolves cyclically with time of immersion (growth then decrease) this state of fact to been signalled already by certain author (Belmokre, 1998, p.113, Kruger, p.294, Genin, 1986, p.490).

The tracing of the double layer capacitance C_{dl} curve as a function of exposure time from the values arranged in the Fig.4, show an increase of the capacity of double layer C_{dl} since the first hours of exposure. This growth is more or less important (3.810 to 4.505 $mF.cm^{-2}$) translating the deterioration of steel thus, but beyond the seventh day (168 hours) of immersion it decreases suddenly (2.892 $mF.cm^{-2}$), we think that the slowing of the decrease of the double layer capacitance C_{dl} would be due to the formation of corrosion products (Fig.4) forming a film more or less adhesive to the substrat playing the role of a gate, beyond 216 hours the capacity of double layer fluctuates weakly that we can consider like steady.

This situation has already been met, at the time of our survey with the different states of naked surface. This phenomenon observed by Duprat (Breur, 1998), has been assigned to the porous nature of corrosion products formed at the free corrosion potential and present at the metallic interface (Fig.5).
The model of equivalent circuit proposed and presented in Fig.6 could be used to represent the electrochemical behaviour of our samples after immersion in 3% NaCl solution, in this circuit R_e is the resistance of electrolyte ($\Omega.cm^2$), R_{ct} the charge transfer resistance ($\Omega.cm^2$) C_{dl} the double layer capacitance ($F.cm^{-2}$).

EIS behavior of zinc rich epoxy paint

Zinc-rich primers can only protect the steel cathodically when the zinc particles in the primer have electric contact to the steel substrate. Only the zinc particles in direct contact with the steel substrate, or connected through other zinc particles, will contribute to the cathodic protection. It is therefore necessary to have a large amount of zinc dust in the coating. The potential of ZRP is approximately −1.160 V/SCE, while the steel substrate used here has a potential of approximately −0.65 V/SCE. The measured potentials are mixed potentials between the steel substrate and the “active” zinc-pigments, and will depend on the area ratio between the two. If

only few zinc-pigments are active, the anode area will be small, and the potential will be close to that of the steel. On the other hand, if the area of active zinc particles is large, the potential will be close to that of zinc.
The Nyquist impedance diagrams for the ZRP coated panels obtained in the aerated 3% NaCl solution as a function of immersion time are shown in Fig. 7a. Two time constants (two loops) were clearly defined at the beginning of the exposure, that become more and more distinct as the immersion time increases, which corresponds well with the model shown in Fig.10 one in the high frequency range (Fig. 7b) which is related to the coating properties followed by a second one at lower frequencies which is related to the corrosion process (Deflorian, 1993, Nguyen, 1992). At high frequencies, the impedance reduces to one or two semicircles with diameters of charge transfer resistance and pore resistance. At lower frequencies, a Warburg impedance develops on the Nyquist plot by a straight line superimposed at 45° to both axes, which shows a shielding effect on mass transport of reactants and products. The shape of the impedance plot suggests that the ZRP corrosion changes from charge transfer control process to diffusion control process during time of immersion. By considering the morphology and the EIS of the ZRP, the impedance first decreased for few days showing the zinc particles activation before an increase related to the zinc corrosion products formation.

The fitting of EIS data was performed by Zview software (Scribners Associates, USA) using different electrical equivalent circuits which include two time constants (Marchebois, 2004, p.2945, Grundmeier, 2000, p.2515). Another difference with previous studies on ZRPs was found in the visual observation of panels during immersion. Usually, zinc corrosion products are clearly observed as white scale at the ZRP panel surfaces (Merowe, 2007, p.197) (Fig.8a). These new products would be maintained within the coating at the neighbourhood of the corroded zinc particles. Moreover, they could also contribute to the isolation of zinc particles as a protective barrier which reduces the corrosion rate of zinc and the coating porosity. Fig. 8b shows the visual appearance of zinc rich epoxy paint coated panel after 180 days (six months) of immersion where the whiteness related to the zinc corrosion products was not observed. It means that after zinc corroded, zinc corrosion products were not able to reach the coating/electrolyte interface, the surface appears damaged with the presence of the red rust due to a progressive attack informing on the state of steel substrat, at this stage of deterioration, the coating lost all its protective properties.

E_{cor} evolution

According to Abreu *et al.* (Abreu, 1996, p.2405), the evolution of the free corrosion potential E_{cor} allows to follow the electrochemical activity of the ZRP. It is believed that the electrochemical processes occurring in such systems are the oxidation of zinc particles fig.9 ($Zn \rightarrow Zn^{2+} + 2\grave{e}$) and the reduction of dissolved oxygen ($O_2 + 2H_2O + 4\acute{e} \rightarrow 4OH^-$). The authors reported that the E_{cor} evolution for liquid ZRP coated samples is in close relationship with the ratio of active areas (zinc/steel) and allows to define the cathodic protection (CP) duration which is the period where E_{cor} remains lower than −0.86 V/SCE, a value corresponding to the commonly accepted criterion of a maximum Fe^{2+} concentration of 10^{-6} M. In other words, the increase in this potential corresponds to the decrease of the electroactive zinc area which means the decrease of the cathodic protection intensity. This is generally attributed to the isolation of the zinc particles by the zinc corrosion products in the coating. Fig.10 shows the E_{cor} evolution with time of coated steel substrates with Zinc rich epoxy paint. It can be seen that E_{cor} was cathodic between −1.0 and −0.8 V_{SCE} during the six months of entire immersion, this result could be due to a high zinc particles amount. This shows that the zinc particles in the primers were electrochemically active with a high number of electrical contacts between zinc particles. This high percolation means that zinc pigments improve a good electrical contact which implies that the steel substrate was under a good CP. That means that a higher part of the zinc particles was involved in a percolation process.
However, as the CP duration is due to the activation of zinc particles by the electrolyte penetration, it also means that the zinc dissolution is reduced or that galvanic contact was lost after six months of immersion in 3% NaCl solution, some small spots of iron rust are detected on the film surface, indicating that the iron corrosion process started some days before. For our zinc-rich primers, it has been observed that zinc corrosion products precipitate inside the coating, around the zinc particles that originated them, blocking the pores of the coating and therefore increasing its barrier resistance (Abreu, 1996, p. 2405). After the test the latter sample was covered with red rust in a limited area. Probably the primer was very thin there, so that the zinc particles were consumed and the steel started to corrode.

Equivalent circuit for the EIS simulation

A general model of an equivalent electrical circuit from which a large number of other models can be derived (Fig. 11). This circuit is composed of the electrolyte resistance, followed by a capacitance (coating

capacitance C_c,) in parallel with a resistance (the coating or pore resistance Rp) and finally an element Z which represents the electrochemical process at the metal interface (Feliu, 1993, p.449, Miskovic-Stankovic, 1999, p.4269). It is the definition of Z which mainly distinguishes the circuits proposed in the literature. However, the model in Fig. 10 contains an important assumption: the ion flow and the corrosion process are localized under the coating and they are not homogeneous on the surface. This is because the corrosion process is presumed to be at the base of the defects in the coating, and not involving all the testing area (in this case the faradic reaction would be in series with the coating capacitance).
The diffusion process is suggested as being the controlling step and, with regard to impedance, the electrical behaviour of the interface is dominated by the Warburg element. For other authors the Warburg element does not substitute the double layer capacitance and the charge transfer resistance, but is added in series with the charge transfer resistance.

Micro-Raman spectroscopy

In order to understand the behavior of our organic coating, complementary analyzes were carried out. Raman spectroscopy analyzes were performed at the complete system. This technique allows to identify locally zinc corrosion products inside the coatings. Representative spectra obtained for the complete system sample are shown in Fig. 13. The main Raman band related to the Magnetite (Fe_3O_4) is found around 667 cm^{-1} (Tzolov, 2000). The band centered at 543 cm^{-1} was attributed to a non-stoichiometric oxide $Zn_{1+x}O$ (Cachet, 2002, p.3409, Ligier, 1999, p. 1164).

For all formulations, three kinds of zinc corrosion products were found depending on immersion duration and depth probed: zinc oxide ($Zn_{1+x}O$), simonkolleïte ($4Zn(OH)_2 \cdot ZnCl_2 \cdot H_2O$) . The oxidized forms were first observed at the solution/ coating interface and progressed towards the steel substrate as the immersion duration increased. Since $Zn_{1+x}O$ forms when zinc particles are in contact with electrolytic solution, one can then assume that the formation of $Zn_{1+x}O$ inside the coating allows to follow the progression of the solution through the paint.

FTIR spectral characterization

The FTIR spectrum of the zinc rich epoxy paint is shown in Fig. 13. The peaks around 850 cm^{-1}, 1250 cm^{-1}, 1510 cm^{-1}, 1600 cm^{-1} and 1460 cm^{-1} are due to the resin epoxy. The film is found to be hydrated by the presence of peak at 3400 cm^{-1} due to O–H absorption band. From FTIR spectra result, it can be concluded that the synthesised zinc rich epoxy paint was under a conductive form, which is represented in the Fig.14.

SEM analysis

Cross section S.E.M. micrographs of several ZRP samples exposed to the electrolyte for different time are shown in Fig.15. It was clearly observed that the coating presented zones which did not contain zinc particles. Moreover, it can be seen that the zinc particle shape varied significantly from spherical to elongated forms. Most of the zinc particles were not in direct contact with the substrate. These observations about the zinc particles distribution were considered to analyse EIS spectra.
Fig .15a and b represents a testing panel covered with the oxidation products after exposure to 3% NaCl solution. The oxidation of zinc in the coating creates the so-called “white corrosion”; the shapes of damage were under Cracks and scaling damage. Sealing of pores in a spherical zinc-pigmented coating. Which is necessary to secure the barrier protection of the substrate. The scheme outlines the possible reactions at the appearance of oxidation zinc products; these products are of alkaline nature and can manifest themselves in the neutralization protection mechanism (Kalendová, 2000, p.199, Kalenda, 1993, p.173).

Conclusion

- There is no doubt that zinc-rich primers offer a very efficient method of anticorrosion protection .Zinc offers threefold protection since it seals the underlying metal from contact with its corrosive environment, provides galvanic protection and “repairs” minor damage in a coating forming a barrier to further electrochemical action .
- Corrosion protection properties of zinc-rich epoxy primer coated carbon steel was studied and characterised in 3% NaCl solution. The EIS diagrams showed clearly two capacitive loops, however, classical equivalent circuits used to monitor coating degradation were unable to provide satisfying fitting results. It was found that the

cathodic protection was maintained for six months, due to a low percolation process combined to a low porosity, the reason is high zinc content and poor weldability.

- The good performance of ZRP coatings during immersion can also be explained by the retention of zinc corrosion products into the coating which allow improving barrier properties. However, it is important to remember that the zinc-rich paint effectiveness does not depend solely on electrochemical factors. There are other factors such as mechanical properties (cohesion, adhesion to Sa 2.5, flexibility, etc) that are very important. So, the addition of auxiliary pigments should be controlled carefully in order not to impair the film's physical and chemical characteristics.

Table 1. Chemical composition of A283C steel (% in weight)

C	Mn	S	P	Cu	Si
0.24	0.9	0.04	0.035	0.2	0.4

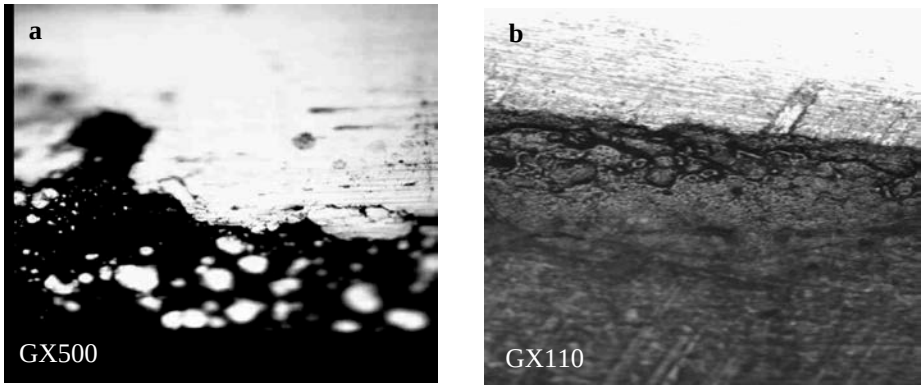

Figure 1: Cross-section of the studied ZRP. (a) Prior to exposition. The observed white particles are due to the spherical zinc particles. (b) After 360 days of immersion in NaCl 3%. Substrate steel is seen as the white region at the top of micrography.

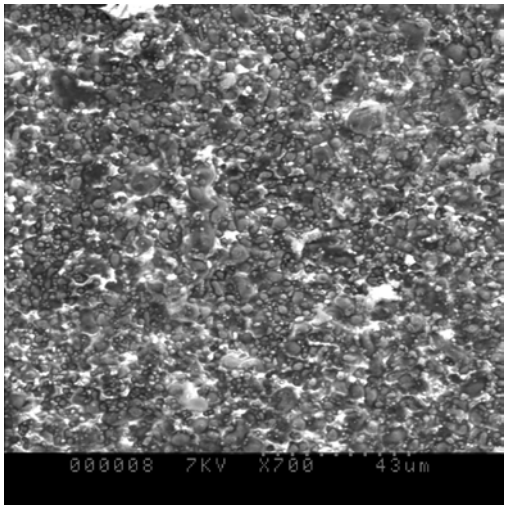

Figure 2 : Cross section SEM micrography of the coating where spherical zinc particle are visible.

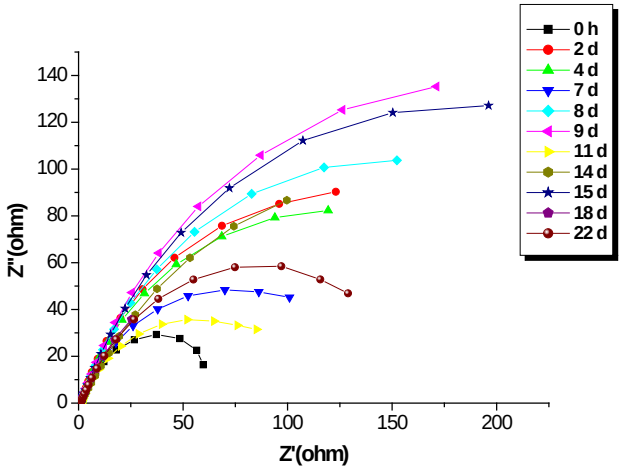

Figure 3: Evolution of Nyquist diagrams as a function of immersion time in 3% NaCl solution for the sandblasted steel (Sa 2.5).

Table 2. Parameters values extracted from the fitting procedure.

Time (days)	R_e ($\Omega.cm^2$)	R_{ct} ($K\Omega.cm^2$)	C_{dl} (mF/cm^2)
0 h	17.97	1.044	3.810
2	13.53	3.804	4.183
4	13.14	3.532	4.505
7	13.77	2.201	2.892
8	14.53	4.460	3.568
9	14.51	5.877	2.707
11	13.65	1.706	2.331
14	14.67	2.991	2.218
15	14.95	5.532	2.876
18	14.28	2.597	2.450
22	16.02	2.546	2.500

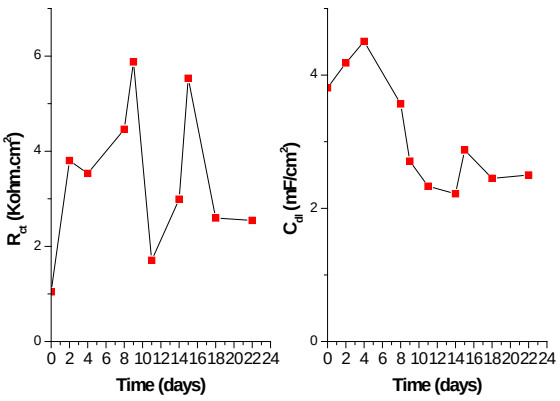

Figure 4: Variation of R_{ct} and C_{dl} with time of exposure.

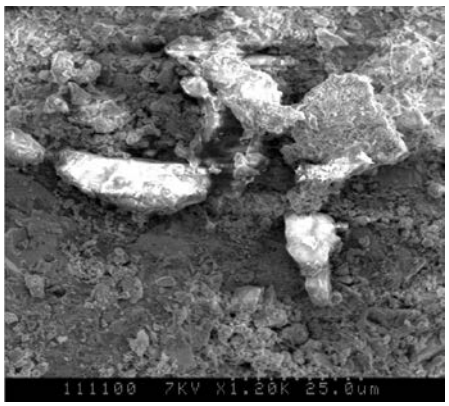

Figure 5: Cross section SEM micrograph on sandblasted steel (Sa2.5).

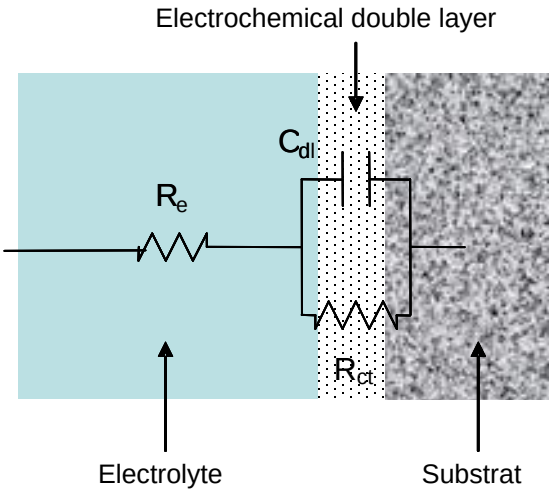

Figure 6: Equivalent circuit used to model sandblasted steel (Sa 2.5) during immersion in 3% NaCl solution.

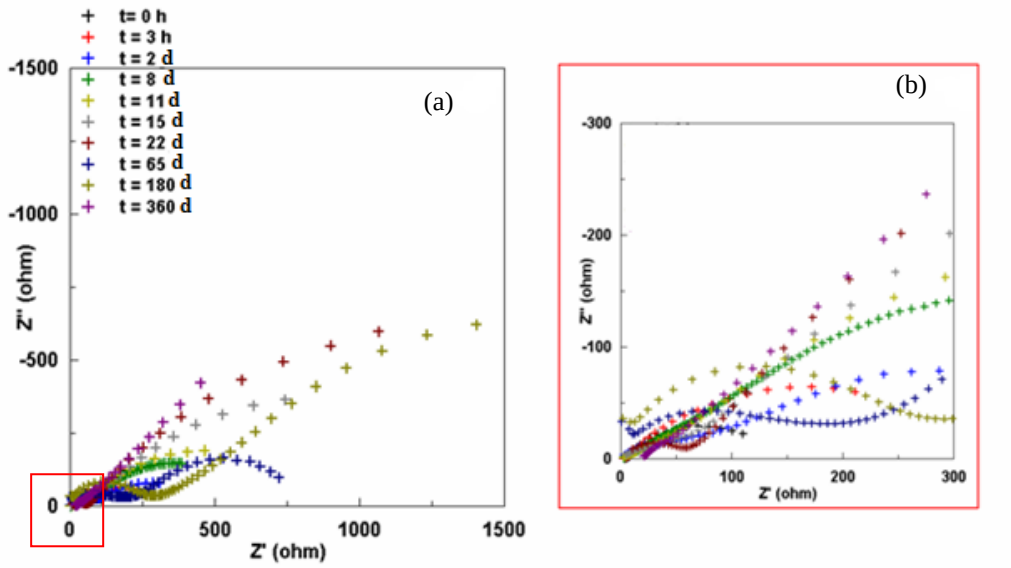

Figure 7: Electrochemical impedance spectroscopy diagrams for ZRP as a function of immersion time in aerated 3% NaCl solution.

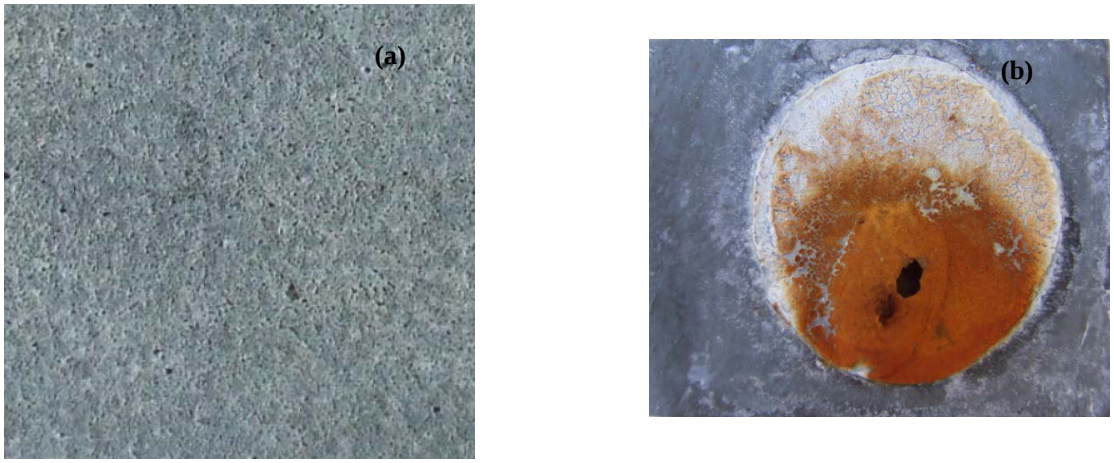

Figure 8: Visual aspect of zinc rich epoxy paint after six months of immersion in 3% NaCl solution.

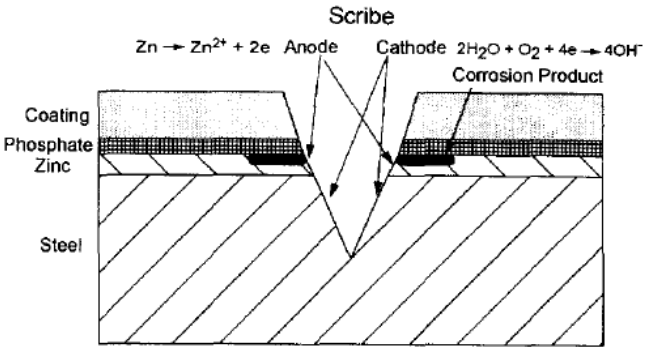

Figure 9: Corrosion process in EIS test.

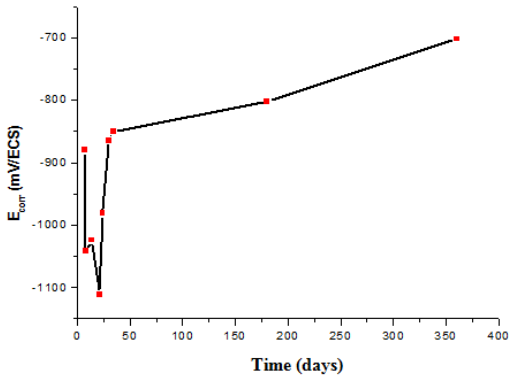

Figure 10: Variations in corrosion potential with time for ZRP exposed in 3% NaCl solution at ambient temperature.

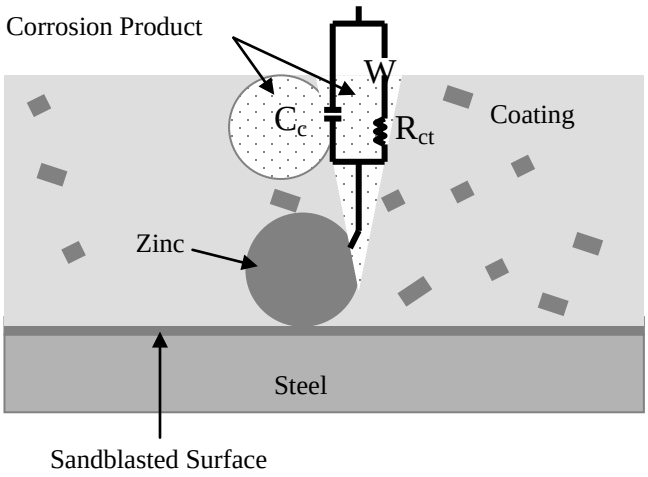

Figure 11: Electrical circuits used to simulate the EIS results.

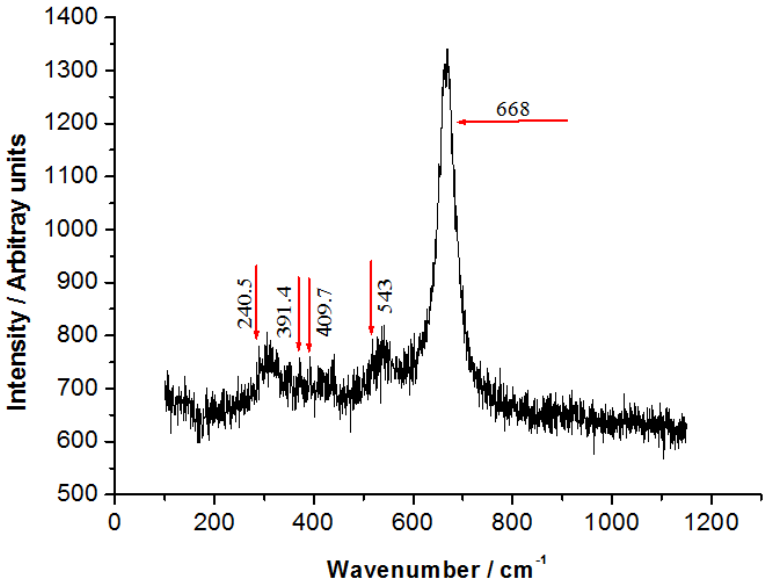

Figure 12: Raman spectrum of zinc particles near the interface film/electrolyte after six months of immersion in 3% NaCl solution.

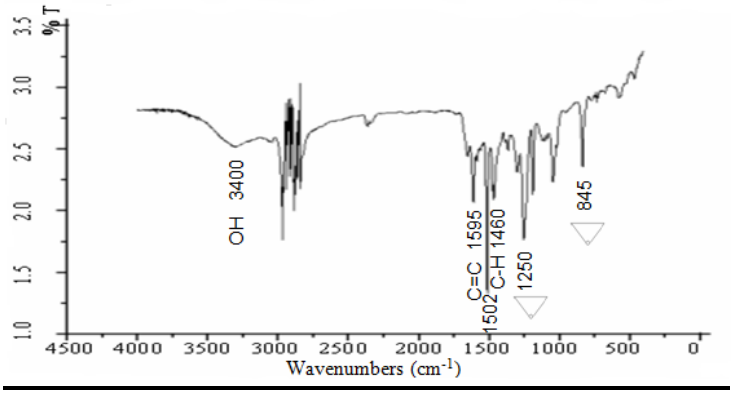

Figure 13: FTIR spectra of zinc rich epoxy paint (ZRP).

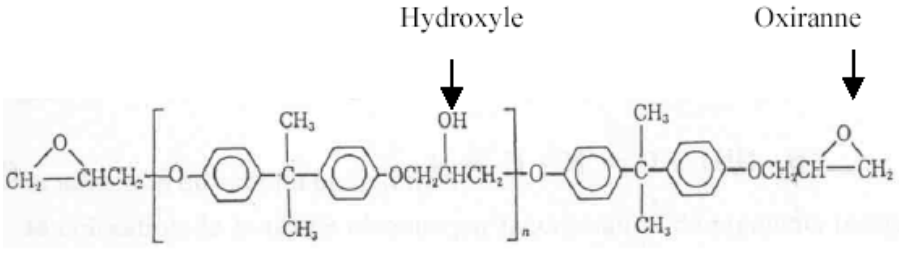

Figure 14: Structural formula of the zinc rich epoxy paint.

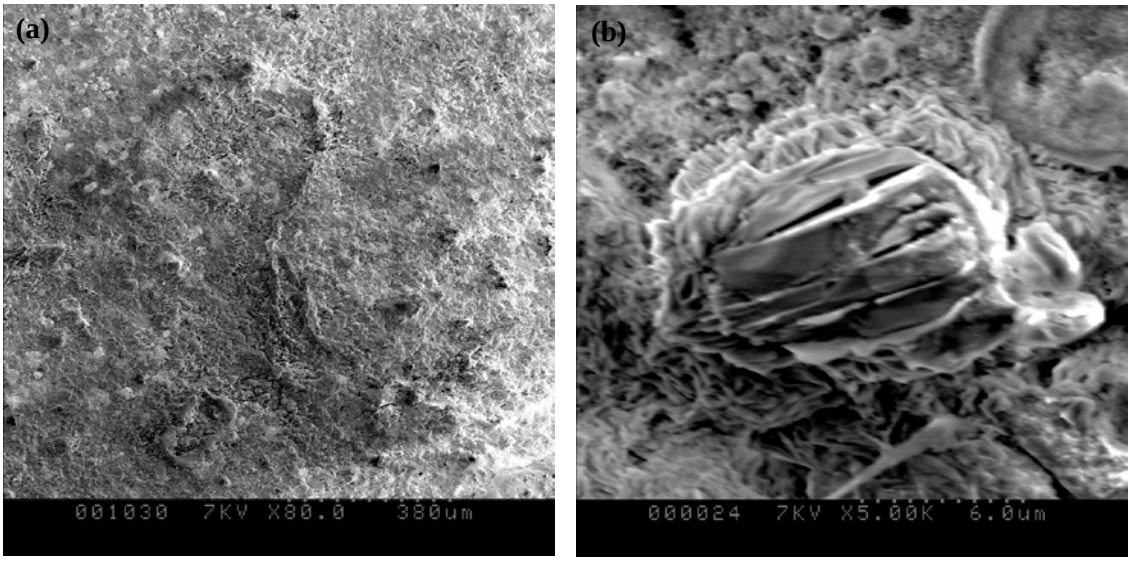

Figure 15: SEM pictures of zinc rich epoxy paint in 3% NaCl solution.

References

Hare, C.H. (July 1998). J. Protect. *Coat. Linnings* ,15, p. 17.

Abreu, C.M. & Izquierdo, M. & Keddam, M. & Novoa, X.R. & Takenouti, H. (1996). *Electrochim.Acta*, 41 pp .2405.

Morcillo, M. & Barajas, R. & Feliu, S. & Bastidas, J.M. (1990). *J. Mater*. Sci. 25, pp .2441.

Lindquist, S.A., Méssaros, L., and Svenson, L. (1985). "Aspects oh Galvanic Action of Zinc-Rich Paints. Electrochemical Investigation of Eight Commercial Primers," *J.Oil & Colour Chemists Assoc.*, 68, No1, pp .10.

Fragata, F.L, Sebrão, M., and Serra, E.T.(1987). "The influence of particle Size and Metallic Zinc Content in the Behaviour of Zinc - Rich Paints," *Cor.e Prot. De Materials*, 6, pp .12
.
Del Amo, B. and Giùdice, C.A. (1990). "Influence of Some Variables on Behaviour of Zinc-Rich Paints Based on Ethyl Silicate and Epoxy Binders," XI Int. *Corros. Congress*, "Italy, Proc. Vol. 2, pp .347.

Pereira, D., Scantlebury, J.D., Ferreira, M.G.S., & Almeida, M.C.(1990)."The Application of Electrochemical Measurements to the Study and Behaviour of Zinc – Rich Coatings, "*Corrosion Sci.*, 30, No. 11, pp .1135.

Wicks Jr, Z.W., Jones, F.N. & Pappas, S.P. (1994).Organic Coatings: *Science and Technology*, vol. II, Wiley, New York, pp . 185.

Feliu, S. , Barajas, R. , Bastidas, J.M. &Morcillo, M. J. (1989). *Coat. Technol*. 61, pp .63.

Feliu, S. , Barajas, R. ,. Bastidas, J.M & M. Morcillo.(1989). *J. Coat. Technol*. 61, pp . 71.

Pereira, D. , Scantlebury, J.D. , Ferreira, M.G.S. & Almeida, M.E. (1990). *Corros. Sci*. 30 , pp .1135.

Armas, R.A. , Gervasi, C.A. , Di Sarli, A. , Real, S.G. , Vilche, J.R. (1992). *Corrosion* , 48, pp .379.

Fragata, F.L. , Mussoi, C.R.S. , Moulin, C.F. , Margarit, I.C.P. & Mattos, O.R. (1993) . *J. Coat. Technol*. 65, pp.103.

Feliu, S. , Barajas, R. , Bastidas, J.M., Morcillo, M. & Feliu, S. (1993). in: J.R. Scully, D.C. Silverman, M.W. Kendig (Eds.), Electrochemical Impedance; Analysis and Interpretation, ASTM STP 1188, *American Society for Testing and Materials*, Philadelphia, pp. 438.

Real, S.G. , Elias, A.C. , Vilche, J.R. , Gervasi, C.A. & Di Sarli, A.R. (1993). *Electrochim. Acta*, 38 , pp .2029.

Gervasi, C.A. , Di Sarli, A.R. , Cavalcanti, E. , Ferraz, O. &Bucharsky, E.C. (1994). S.G. Real, J.R. Vilche, *Corros. Sci*. 36, pp .1963.

Abreu, C.M. , Izquierdo, M. , Merino, P. , Novoa, X.R. &Perez, C. (1999). *Corrosion 55*, pp .1173.

Feliu Jr., S. , Morcillo, M. & Feliu, S. (2001). *Corrosion*, 57, pp .591.

Vilche, J.R. , Bucharsky, E.C. & Giudice, C.A. (2002). *Corros. Sci*. 44, pp .1287.

Abreu, C.M. , Espada, L. , Izquierdo, M. , Merino, P. & Novoa, X.R. (1997). in: *Eurocorr'96, Fedrizzi and Bonora Ed*., vol. 20, pp . 23.

Mansfeld, F. , Lumsden, J. B. , Jeanjaquet, S. L. & Tsaï, S. (1981). Evaluation of surface pretreatment methods for application of organic coatings, Corrosion Control by Organic Coatings, H. Leidheiser, Jr. - Editor, *NACE*, pp. 227-237.

Novoa, X .R. , Izquierdo, M. , Merino, P. & Espada, L. (1989). *Mater. Sci.* Forum 44 & 45, pp.223.

Belmokre, K. , Azzouz, N. , Kermiche, F. & Pagetti, M.J. (1998). *Materials and Corrosion*, 49(2), pp.108-113.

Kruger, J. &Volken, H. T. *Corrosion*, pp. 294.

Genin, J. MR. , Rezel, PH. Bauer, D. , Olowea. A. (1986). Electroch. Methods in corrosion Research, pp . 477-490.

Breur, H. J. A. , Ferrari, G. M. , Turnhout, J. Van & de Wit, J. H. W. (July 1998) . Modern experimental techniques for the assessment of the water sensivity of organic coatings, Symposium "New trends in Organic Coatings for Marine Environments", *Euromat '98*: Lisbon Portugal, pp.22-24.

Deflorian, F. , Fedrizzi, L. , Lenti, D. & Bonora, P. L. (1993). *Prog.Org. Coat.* 22, pp .39.

Lin, C. , Nguyen, T. & McKnight, M. (1992) . *Prog. Org. Coat. 20*, pp. 169.

Marchebois, H. , Savall, C. , Bernard, J. & Touzain, S. (2004). *Electrochim. Acta* ,49, pp . 2945.

Grundmeier, G. , Schmidt, W. & Stratmann, M. (2000). *Electrochim. Acta* , 45, pp .2515.

Merowe, A. & Touzain, S. (2007). Prog. *Org. Coat*. 59, pp .197.

Abreu, C.M. , Izquierdo, M. , Keddam, M. , Novoa, X.R. & Takenouti, H. (1996). *Electrochim. Acta* , 41, pp . 2405.

Feliu Jr., S. , Barajas, R. , Bastidas, J.M. , Morcillo, M. & Feliu, S. (1993) .Study of protection Mechanisms of zinc rich paint by electrochemical impedance spectroscopy, in: J.R. Scully, D.C. Silverman, M.W. Kendig (Eds.), Electrochemical Impedance: Analysis and Interpretation, ASTM STP 1188, *American Society for Testing and Materials, Philadelphia*, pp. 438–449.

Miskovic-Stankovic, V.B. ,Zotovic, J.B. ,Kacarevic-Popovic, Z. & Maksimovic, M.D.(1999). *Electrochim. Acta* 44, pp .4269.

Le Thu, Q. , Takenouti, H. & Touzain, S. (2006). *Electrochim. Acta* ,51, pp .2491.

Tzolov, M. , Tzenov, N. , Dimova-Malinovska, D. , Kalitzova, M. , Pizzuto, C. , Vitali, G. , Zollo, G. & Ivanov, I. (2000). *Thin Solid Films* , 379, pp .28.

Cachet, C. , Ganne, F. , Joiret, S. , Maurin, G. , Petit jean, J. , Vivier, V. & Wiart, R. (2002). *Electrochim. Acta* 47, pp . 3409.

Ligier, V. , Wéry, M. , Hihn, J. Y. , Faucheu, J. & Tachez, M. (1999) .Formation of main atmospheric zinc end products: $NaZn_4Cl(OH)_6SO_4.6H_2O$, $Zn_4SO_4(OH)_6.nH_2O$ and $Zn_4Cl_2(OH)_4SO_4.5H_2O$ in [Cl^-] [SO_4^{2-}] [HCO_3^-] [H_2O_2] electrolytes, *Corrosion Science*, Vol. 41, pp. 1139-1164.

Kalendová, A. (2000). Prog. *Org. Coat*. 38, pp .199.

Kalenda, P. (1993) .in: Proceedings of the International Conference on the Production and Application of Special Inorganic Pigments, *Pardubice*, pp . 169–173.

Integrating Malay Tangible Cultural Heritage into Furniture Design: An Approach to Enhance Product through Emotional and Spiritual Contents

Ab. Aziz Shuaib, Olalere Folasayo Enoch

Faculty of creative Technology and Heritage, University Malaysia Kelantan (UMK)
Locked Bag 01, 16300 Bachok, Kelantan. Malaysia

e-mail: folasayoidd@yahoo.com

Abstract: Product demand has been transformed from quantitative consumption to perceptual consumption along with the arrival of an era that revolves around concept development. Therefore, functionality of a product now lies between two entities; technical and emotional function. Technical function is how product works, while emotional function is how product makes user feels. Choosing a product is now largely an emotional process; hence, engaging emotion as a partner to technology will deliver the next market place products that will captivate customers. However, it's only when the formal attributes (colour, shape, form, etc.) of an object come together to act as a medium for an emotion does an object become expressive. The tangible heritage of Malay is not only known for uniqueness, but also the realistic traditional concept of art in Malay. It is a reflection of the splendour and beauty of aesthetical elements or ornamentations adorning them that carry deeper philosophical and sacred meanings. Thus, integrating elements of Malay tangible cultural heritage into contemporary home furniture is seen as an approach towards creating products that has emotional and spiritual contents coupled with aesthetic appeal. Therefore, this paper seeks the knowledge regarding the global trend in home furniture design, the Malay cultural heritage and also practically illustrates by example how the elements of Malay tangible heritage can be integrated into contemporary home furniture.

Key words: Conceptual age, Emotion, Furniture, Malay tangible heritage

Introduction

Oxford English Dictionary (1999) defines emotion as an intense feeling contrasted with reason. According to Carson (1997), emotions differ from moods in term of time and physiological effects; emotions elicit a sharp change with a physiological change while moods are longer and less intense. Emotions tend to be closed to probabilities and likelihoods and to be absolute in their judgments and have control over the action system. They are elicited by events appraised as real, and their intensity varies according to the level of reality attributed. However, a sincere emotion is involuntary (Mark Twain, 1835-1910), it's only when the formal attributes (colour, shapes, etc.) of an object come together to act as a medium for an emotion does an object become expressive.

The tangible heritage of Malay is known to be a reflection of the splendor and beauty of aesthetical elements or ornamentations adorning them that carry deeper philosophical and sacred meanings. This is because the Malay craftsmen are highly artistic and skillful, endured with strength and inspiration to transform the traditional design elements into unique and aesthetically pleasing pieces that carries a wide variety of messages. Thus, integrating elements of Malay tangible cultural heritage into contemporary home furniture is seen as an approach towards creating products that has emotional and spiritual contents coupled with aesthetic appeal. Therefore, this paper seeks the knowledge regarding the global trend in home furniture design, the Malay cultural heritage and also

practically illustrates by example how the elements of Malay tangible heritage can be integrated into contemporary home furniture.

Trends in Furniture Design

Furniture is the mass noun for the movable objects intended to support various human activities such as seating and sleeping. Furniture is also used to hold objects at a convenient height for work (as horizontal surfaces above the ground), or to store things. Furniture can be a product of design and is considered a form of decorative art. In addition to furniture's functional role, it can serve a symbolic or religious purpose. Furniture can be made using a variety of woodworking joints which often reflect the local culture.

Furniture industry has a tremendous market potential locally and internationally considering the world population reaching over 7 billion people (7,065,514,277) according to February 2013 estimate by US Census bureau (2013). However, the past decade has been known for some trends in furniture design. The trends are seen as the undercurrents that drive what we see. Abe (2013) analyzed top ten (10) furniture trends for the decade; these include

i. *Furniture going Green*: Technology has been an integral part of our lives, the globe seems to be shrinking and there is a rising concern for the environment. Therefore, green furniture now seems to be going mainstream (Abe, 2013). The environmental concerns such as awareness of how deforestation affects climate change and the effects of toxic finishes on the air inside homes have led furniture buyers to demand green furniture.

ii. *Furniture with a smaller Profile*: Since our living spaces are shrinking, this decade preferred furniture with a smaller profile. Large furniture piece now seems out of place in today's shrinking homes.

iii. *Multifunctional Furniture*: Although multifunctional furniture is not a new concept by any means, but it has really come into its own as there is a rising demand for it. This, according to Abe (2013) could also be as a result of the smaller space living. Space at a premium needs furniture that can perform multiple tasks.

iv. *Technology Driven Furniture Design*: Furniture design has been greatly influenced by the use of modern technology during the last decade.

v. *Popularity of Vintage Furniture*: Buying vintage furniture has been a feasible choice in the last decade; this is as a result of the hard economic times. However, by buying or using inherited vintage furniture, we rescue it from going to landfills thereby encouraging sustainability.

vi. *Globally Inspired Furniture*: According to Abe (2013), the idea of bringing the world to our homes is catching on. This is because the globe seems to be shrinking and other cultures no longer seem as distant or foreign. Therefore, people are search for exotic and romantic furniture from other parts of the world and gone-by eras.

vii. *The Growing Importance Outdoor Furniture*: Casual furniture or outdoor furniture has made leaps and bounds in the last decade (Abe, 2013). This is as a result of consumers discovering they could significantly add to their existing spaces by using outdoor areas as well.

viii. *Custom-made Furniture*: Customization of furniture seems to be a trend that is catching on where customer provides specifications for fabric, colour, patterns or leg and arm style.

ix. *Specialty Sleep Surfaces*: Specialty sleep surfaces began with waterbeds and has grown and developed over the years so that specialty sleep products now make up a sizable share of the sleep market (Abe, 2013).

x. *Leather Furniture*: Leather known as an old favorite now has a new face. There are now colours and designs that were never seen before in leather. Some other advantages of leather is that it is easy to maintain and clean and retains its appeal much longer than fabric (Abe, 2013).

Malay Tangible Cultural Heritage

Cultural heritage is the legacy of physical artefacts and intangible attributes of a group or society that are inherited from past generations, maintained in the present and bestowed for the benefit of future generations (UNESCO, 2012). Tangible heritage includes buildings and historic places, monuments, artifacts, etc., which are considered worthy of preservation for the future. These include objects significant to the archaeology, architecture, science or technology of a specific culture. The Malay tangible cultural heritages are explained below based on the forms, patterns/motifs used.

Malay Tangible Heritage Forms

Forms are specific shape or quality an artistic expression takes. It can also be explained as the three-dimensional composition or object within a three-dimensional composition. Form can either be geometric (man-made) or organic (natural). It may be created by combining two or more shapes and can be enhanced by tone, texture and colour. It can be illustrated or constructed. The Malay tangible heritage forms are combination of lines, curves and geometrical shapes. Some of them are illustrated below;

i. *Bendul*: *Bendul* is a Malay word for a specially designed wooden beam (Fig. 1). This beam (bendul) is one of the elements of the Malay traditional house that serve to secure the structural framework of the house. Without it, the pillars of the house would not be stable. In Kelantan, bendul is the frame at the outer end of the floor. It is made to encircle the house, and served to separate the different portions of the house such as the veranda, the main house, the passage way and the kitchen (Wan & Abdul, 2011).

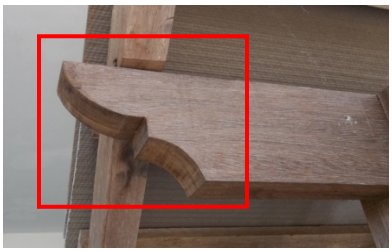

Fig. 1: Image of *bendul* wooden frame

ii. *Sulur Bayung: Sulur* means the branch of a locally found creeping plant, the root that grows from the main trunk of a tree or a piece of metal wire. According to Abdullah (1990), *sulur bayung* refers to a decorative element on the roof. Has explained by Abdul Rahman (2000), *sulur* means the shoots of ivy like plant while *bayoung* is termed as a kind of decoration representing the long beans type of plant. The carvings are found on the four corners of a hip roof; they are either made of ceramic or cement plaster (Fig. 2). Has described by Abdullah (1978), this type of decoration in traditional Malay architecture looks like an image of a dragon, but according to craftsman in Kelantan the protruding element at the hip roof is called *ekor itek*..

Fig. 2. Images of *ekor itek* and *sulur bayung* crept at the hip roof

iii. *Gunungan: Gunungan* is one of the ancient legacies in Malaysia. Similar to the Balis, ancient Malays held on to religious and cultural traditions of Hinduism. Therefore, the tops of their doors are design with *gunungan* (having motifs of their god's image), which is similar to the Bali. However, in line with the development of

Islam, the concept of *gunungan* was still maintained but the gods shaped image motifs were removed and replaced with flora elements (Fig. 3).

Fig. 3: *Gunungan* with flora motif

iv. *Tunjuk Langit:* In terms of functionality, *tunjuk langit* has no role except for establishing identity. It is widely available in Terengganu and Kelantan. There are two significant forms of *tunjuk langit* ; straight vertical shape (*Jenis batang*) and pumpkin-shaped (*jenis bulat*). *Jenis Batang* is a type of *tunjuk langit* are formed using a piece of timber in an upright position at the tip of the gable end (Fig. 4a), while *Jenis Bulat* is commonly used on hip or pyramid type of roofing. They are positioned at the middle and top of the roof and most are made of carved timber or cement (Fig 4b).

(a)  (b) 

Fig. 4: (a) *Tunjuk Langit .Jenis* batang; (b) T*unjuk Langit.Jenis bulat.*

v. *Tiang Gantung:* According to Rashid & Amat (2008), other names for *tiang gantung* are *buah butung*, *saka bentung*, *tiag bunting*. Yaakub (1996) defines *tiang gantung* as hanging column while Halim (1985) describes it as hanging column constructed on the bottom of the gable end of the roof (Fig. 5). It has a round shape looking very similar to bees' nest (Rashid & Amat, 2008). Also Utaberta et al, (2012) described it as a wood measuring about 60cm to 100cm mounted on the roof. It is a badge or symbol of a construction formwork, just like a gravestone on the tomb. Halim (1985) refers to it as a symbol of power and might of the house and its owner. It is commonly believed that if this form of decoration falls, it indicates bad omen to the occupant of the house (Rashid & Amat, 2008). Therefore, to avert the bad omen, a gathering or a special ceremony must be held to reposition the fallen *tiang gantung* to its original place.

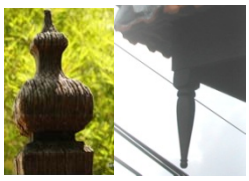

Fig. 5: Picture of *Tiang Gantung*

Malay Tangible Heritage Patterns/Motifs

A pattern in general can be defined as a discernible regularity in the world or in a manmade design. As such, the elements of a pattern repeat in a predictable manner. In art and architecture, a pattern can be achieved by combining and repeating decorations or visual motifs to form patterns designed to have a chosen effect on the viewer. The inspiration for motif compositions in art of Malay is from five plant sources which include leaf, stalk, flower, fruit and tendrils. According to Haziyah et al (2012), leaf compositions are usually composed from the odd numbers of one, three, five, and so on depending on the surface of the carving. The patterns usually comprise leaves splits into two, three and five. The motifs used are usually from plants which are vital in Malay society; having

aesthetic, medicinal and nutritional values. Examples are *sesayap leaf, telinga kera, telipot, kerak nasi*, etc. These motifs are commonly used in Metalwork (Fig. 6a), Pottery (Fig. 6b), but mostly used in wood carving (Fig. 6c).

(a)  (b)  (c) 

Fig. 6. (a) metal work; (b) pottery ware; (c) woodcarving

Motif carving technique is usually based on two forms; two dimensional or three dimensional. Two dimensional motifs are usually associated with flat surface which can only be seen from one angle. This type of motifs is commonly used as wall decorations, door-leaf, and louvered screens in traditional Malay buildings. An example of this is *tebuk tembus* wood carvings and is usually found above the entrance between two different functional spaces. It is also available in the wall for ventilation and natural lighting. The carving often have floral motif of scented flowers (Fig. 7).

Fig. 7. *Tebuk tembus to facilitate ventilation.*

However, three-dimensional motif form emphasizes the forms that can be appreciated from all angles (Fig. 8). These motifs are usually found in ceremonial items, agricultural implements, household equipments and row of post (*tiang larik*) in traditional Malay house.

Fig. 8. Three dimensional motifs form

Apart from carvings motifs, some patterns are also created by arranging pieces of wood in a regular or irregular repeated manner to create a design pattern. An example of this is *dinding janda berhias* (Fig. 9). *Dinding janda berhias* is a wall panel, usually made with wooden material. These walls are usually found in the house of high social status in ancient Malay.

Fig. 9. *Dinding janda berhias*

The New Direction for Furniture in the 21st Century

With the emergence of cross domain disciplines like outsourcing, we are witnessing a trend towards creative knowledge, rational application and innovation. We are now progressing from an era that was information-dependent towards the era (21st century) that revolves around concept development which will be dominated by new senses (design, story, symphony, empathy, play and meaning) thereby creating a need to diverge from the current reliance on linear and sequential algorithmic practices in outsourcing and to adopt cognition based approaches (Patki, T., Patki, & Kulkarni, 2009).

We are now moving from an economy and a society built on logical linear, computer like capabilities of "the information age" to an economy and a society built on the inventive, empathic, big-picture capabilities called "The Conceptual Age" (Pink, 2005). Therefore, the future belongs to a very different kind of person with a very different kind of mind; that is, creators and empathizers, pattern recognizers and meaning makers. These people (artists, inventors, designers, storytellers, caregivers, consolers, big picture thinkers) will now reap society's richest rewards and its greatest joys (Pink, 2005). With the great transformation taking place this present time, consumers are now shifting from materialistic needs to emotional needs. Therefore, people will get richer, wealthier and smarter but will seek more on spiritual products (Rolf, 2009).

However, Rolf Jensen's theory has raised the question if the upcoming 21st century will be the end of mass marketing era; because, focussing on small brand and individualism, producer would become smaller in quantity but still uphold their unique traditional way. With these added values, price will be high, but notwithstanding, the money is believed to be paid willingly and happily by future consumers who want to consume not just product but the story. Research by Boatright & Cagan (2010) revealed that people pay for products that address their emotional needs in all types of business; that means product emotion is critical to the long-term success of any product that consumers interact with directly or indirectly.

Malay tangible cultural heritage is known to be a reflection of splendour and beauty, emotionally and spiritually engaging and also rich in story and meanings that have emotional impacts. Therefore, integrating Malay tangible heritage into furniture design is seen as an attempt towards creating products with emotional and spiritual contents that will meet the 21st century demand.

The Fusion of Malay Tangible Heritage into Furniture Design

Based on some of the Malay tangible heritages explained earlier, this section illustrates by examples how these tangible heritages can be integrated into furniture design.

Figure 10 below is an illustrative diagram of a ceremonial chair with Malay tangible heritage features. Some of these tangible heritage features are the *gunungan* shape integrated at the top and lower part of the chair, *tebuk tembus* decorative design and the flora motifs (Fig. 10). *Tebuk tembus* design and the flora motifs are produced by woodcarvers (Fig. 11).Malay woodcarvers are highly artistic and skillful, endured with strength and inspiration to transform the traditional design elements into unique and aesthetically pleasing pieces. Therefore, the structure of work carries a wide variety of messages and meanings.

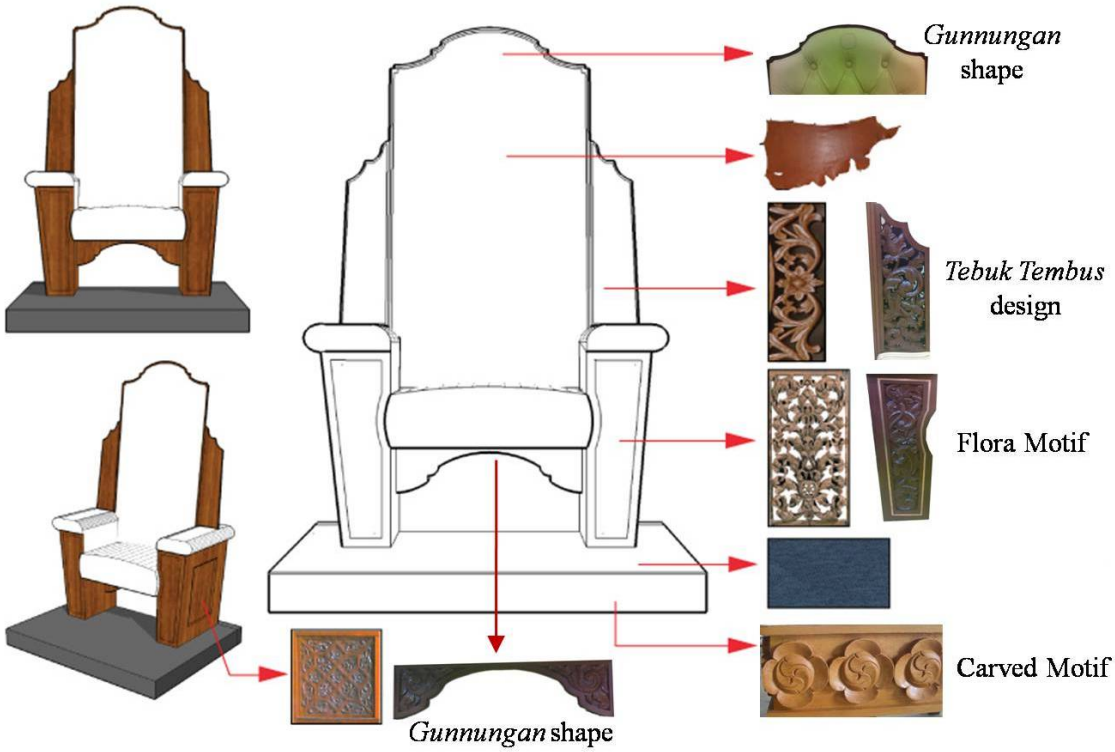

Figure 10: A Diagram of a chair with tangible heritage features

Figure 11: Malay wood carver

According to Haziyah et al. (2012), Malay wood carving is a reflection of the beauty of the soul and culture of Malay society which can be discerned from the arrangement and composition of the leaf, stalk, flower, fruit, and tendrils in a particular carving. The ornaments found in Malay carvings are also connected with particular meanings and stories associated with the carvings themselves (Haziyah et al, 2012). Also, the beauty in wood carving represents what can be appreciated in the art of wood carving in the past and the expression shown through wood carvings represent character and culture of the Malays in Malaysia. Therefore, integrating such tangible heritage in home furniture design (Fig. 12) is an approach towards creating products with emotional and spiritual contents.

Figure 12: Image of the completed ceremonial chairs

Figure 13 is an illustrative diagram and an image of a stand for ceremonial staff (mace). The design also features some tangible heritage of Malay culture. These include the *gunungan* shape at the two ends and the *tebuk tembus* motifs used to decorate the surface of the furniture.

Figure 13: A stand for ceremonial staff (mace)

Conclusion

In order to produce best quality furniture, manufacturers needs to adopt a design with universal values that will cater for the global market; also invest on skill workers and state of the art production technology. With the artistic and talented designers; rich tangible cultural artefacts and the availability of varieties of timber species that can be exploited, Malaysia is believed to have the potential to be a competitive edge in furniture design. Most works of old in Malaysia have spiritual contents and craftsmen in those days made things spiritually involved; therefore, all products were passionately crafted with strong attachment to belief system. Hence, since choosing a product is largely an emotional process, contemporary product that has emotional and spiritual contents coupled with aesthetic appeal will indeed be a boutique quality for the upcoming ere (conceptual age).

References

Abdul, R. A. (2000). Petua Membina Rumah Melayu dari sudut etnis antropologi. *Perpustakaan Negara Malaysia: Kuala Lumpur*.

Abdullah, M. (1990). Batik kita: Falsafah motif-motif dan sejarahuya. *Warisan Kelantan IX, Perbadanan Muzium Negeri. Kelantan: Kota Bharu.*

Abdullah b. Mohamed (1978), Bentuk-Bentuk Bangunan Masjid ; Kunci Memahami Kebudayaan Melayu. *Kementerian Kebudayaan, Belia dan Sukan, Malaysia : Kuala Lumpur*.

Abe, A. (2013). Top 10 Furniture Trends of the Decade: New Directions for Furniture in the 21st Century. Retrieved February 11, 2013, from http://furniture.about.com/od/buyingfurniture/ tp/dec_trends.htm

Boatwright, P., & Cagan, J. (2010). *Product emotion: The way to captive customers*.

Carlson, R. (1997). *Experienced cognition*. Mahwah, NJ: Lawrence Erlbaum.

Halim, N. (1985). Pengenalan rumah tradisional Melayu semananjung Malaysia. *Darul Fikir: Kuala Lumpur*.

Haziyah, H., Zawiyah, B., Aminuddin, H., Aishah@Eshah, H. M. (2012). The philosophy in the creation of traditional Malay carving motifs in Peninsula Malaysia. *Malaysia Journal of Society and Space*, 8(7), pg 88-95, ISSN 2180-2491

Lucinda, C., & Martin, N. (1999). *Oxford English Dictionary* (4th ed.). Oxford, UK: Oxford University Press.

Patki, A. B., Patki, T., & Kulkarni, M. (2009). *Transformation from the information age to the conceptual age: Impact on outsourcing*. Retrieved September 30, 2012 from http://ssrn.com/abstract=1350536

Pink, D. H. (2005). *A whole new mind*. Riverhead Books: Penguin Group (USA) Inc. New York.

Rashid, S. & Amat, C. S. (2008). The traditional Malay architecture: Between aesthetics and symbolism. *Proceeding Seminar on Intellectual Property and Heritage Issues in Built Environment*, Renaissance Hotel Kuala Lumpur. 20-21st July 2008.

Rolf, J. (2009). *Dream society* (2nd ed.). Mcgraw Hill Prof (Business), ISBN-10-0071486496

UNESCO (2012). Tangible cultural heritage. http://www.unesco.org/new/en/cairo/culture/ tangible-cultural-heritage/

U.S. Census Bureau (2013). World POPClock Projection. http://www.census.gov/population/ popclockworld.html

Utaberta, N., Sojak, S. D. M., Surat, M., et al, (2012). Typological study of traditional mosque ornamentation in Malaysia: Prospect of traditional ornament in urban mosque. *World Academy of Science, Engineering and Technology*; (67) pg 624-631

Wan, H. & Abdul, H. N. (2011). *The traditional Malay house*. ITNM Berhad

Yaakub, I. (1996). Rumah tradisional Negeri Sembilan: Satu analsis bina Melayu. *Penerbit Fajar Bakti* Sdn. Bhd. Shah Alam.

Levels of Schools in Terms of Having Effective School Qualities According to the Opinions of Education Shares

Celal GÜLŞEN, Aysel ATEŞ, Emine Gürer BAHADIR

Fatih University, Department of Education Management, Inspection, Planning and Economy -İstanbul /Turkey
e-mail: celalgulsen@gmail.com

Abstract : The aim of this research is to study primary and secondary schools have the indicators of effective school and its level from the point of view of managers, teachers, students and parents. Additionally, this research has been done because school effectiveness is measured if or not school reaches its goal and how successfully school responds the needs of shareholders. Some illations are made according to the result of the research. The pattern of the research is cross-hatching model. A questionnaire, which is developed by researcher in 2012 and named "questionnaire of effective school features" ,is used to collect datum from managers, teachers, students and parents. The questionnaire is based on Peter Mortimore's (1995) effective school indicators. In the research four dimensions of effective school are evaluated. The dimensions are manager, parents and school environment, student and teacher. According to the results of research, the most effective dimension is "teacher" by mean $(\overline{X})$ "2.53" and the least effective dimension is school environment and parents by mean $(\overline{X})$ "2.35". From the light of research results it can be mentioned that the relationship between school, parents and school environment are need to be improved.

Keywords: Effective school, manager, teacher, parent, education, shareholder.

Introduction

It is seen that favorable change efforts that are conducted or considered to be conducted are in service for better, more qualified and more effective education corporations. Education corporations especially basic level schools are wanted to be 'effective' at the end of these favorable efforts. In this effectiveness, schools are expected to have qualities in terms of 'school management', 'student', 'teacher', 'environment of school' and 'parent' dimensions. (Kaplan, 2008).

School that is expected to be effective is defined as a system 'preparing and offering lives that brings in new behaviors or removing unwanted behaviors for students it wants to educate' and it is also defined as a means of 'making the young accept the role he would bear as an adult, keeping him busy, preparing him for job and acquiring the values of society'. (Özdemir, 2000). From this point of view it cannot be denied that corporations that are called schools play an important role in enriching culture of individuals and preparing them for life. Thus we are confronted with an inevitable reality that corporations that are called schools' being effective schools.

According to the transfer of Orhan (2011) and Balcı (2011), in 1930's Bamard defined effectiveness as the level of an organization in terms of achieving its goals and he defined efficiency as level of and organization in terms of meeting its sharers' needs. On the other hand Schreens defined efficiency as the level of achieving best with minimum most. There are many definitions of effectiveness but no straight definition that adapts academic frames could be made. But it is agreed that effectiveness is a multi-dimensional concept. Lack of definition of effectiveness that adapts academic frames made it hard to define effective school. According to Klopf and others (1982) effective school is defined as the school that has the optimum learning environment that

is designed to provide development for students in cognition, affective, psychomotor and esthetic fields. Brookover (1985), based on the view that equal opportunities underlie effective school, defined effective school as not only the place only selected students gain basic abilities but also the place all students gain these abilities. (Balcı, 2011; Orhan, 2011).

There must be some qualities and variances that separate effective schools from other schools. According to Özdemir (2000) effective schools must have following qualities.

- It has clear and apparent goals and school mission which focuses on these goals.
- Managers get into act as education leaders.
- All sides have high expectations.
- Opportunities that improve learning are offered.
- Development of student is followed and plentiful academic programs are available.
- School-family relationship bears importance.
- They interiorize strong managerial leadership type.
- Appropriate school environment is available.
- Development of basic abilities bears importance.
- Directing system is effective.
- The usage of school resources are devoted to the improvement of the success of student.

According to the transfer of Kaptan (2008) and Celep (2000) Purkey and Smith explains the important practice indication qualities and variances of effective schools as following:

1. Management dimension of school: In most of the studies it is determined that in solving the problems of education managers and education servers there is a need for autonomy.
2. Teaching leadership: Leadership is needed to commence and maintaining of school improving.
3. Server determination: Maintaining the success of a school which has achieved success for a length of time can be provided via education.
4. Clarity and organizing of the program: In secondary education level, a planned curriculum can be more beneficial than a program that involves elective courses.
5. Improvement of servers about issues that are related to school: It compromises the change of attitudes and behaviors of people.
6. Family attention and support: Informing families about the aims and problems of school is regarded beneficial.
7. Acceptance of academic success in school field: It is seen in the customs of school culture, symbols and its success that is accepted officially.
8. Top-tier learning time: By increasing scientific activities in school there will be more time for academic issues.
9. Local support: Support of local government bears importance for change.

Efforts to make schools effective schools are continuing day by day increasingly. These restoration attempts in schools show their face in schools of our country as well as all around the world. One of the school improvement approaches that prescribe a change in system dimension directed to restoration attempts in Turkish Education system is school based management. School based management confronts us as an important innovation in being student based in education, democratization, transferring of authority, realizing the goals and functions of schools and restoration of culture. School based management provides us and opportunity to control education process more by giving authority and responsibility to education society members in budget, personnel and program fields. Increasing autonomy by giving deciding authority and responsibility to schools and as a result making ‘this is our school’ perception dominant are indicators of being an effective school. In such proper environments of school, teachers love students, school, sharers that have relation with school, and themselves; they behave more willing, diligent and careful in their jobs (Güçlü, 2000; Keleş 2011; Özdemir, 2002). This attitude gives leadership qualities of managers, teachers and servers in effective schools prominence.

Mortimore (1995) when explaining professional leadership concept which is one of the factors of effective school: remarks that professional leadership requires managers to determine apparent and straight aims and when defining these aims taking education sharers' ideas into account and adding them to managing partially. (Çelik 2012). This reminds us of the term governance. Governance is formed by the combination of management, communication and interaction. Due to the fact that open contact of manager with the personnel in school will bring about interaction: a natural environment which governance needs will form. Common goals come into existence thanks to the natural environment governance provide; and these goals form a frame for a vision around which all sharers will be united (Şişman, 2011). Mission is defined and started according to determined frame. The effort achieve the mission that is accepted by sharers create a positive school environment. Thus positive school environment brings about colleague relationship and collective working. Such an environment will start a process in which not only the students but also all the personnel will learn and constantly improve themselves. Because all education sharers will focus on learning in this inceptive process, the maximization of learning time will be provided automatically. This will bring about a school culture that focuses on success. Because goals will be clear in created success focused culture, thanks to well-structured interclass processes, goals will be achieved. (Çelik 2012). In schools in which success culture exist, education sharers' having more expectation than each other to achieve determined goals is the basic indicator. Sharers are aware of this expectation correlatively.(Aydoğan and Helvacı, 2011). This awareness is reinforced with clear, fair discipline and feedback. Because the direction of reinforcement is positive, it is possible to define it as positive reinforcement. While performance of the student is increased via positive reinforcement, on the other hand improvement performance of the student in process is managed. Assessments of student performance are feedback to school performance. Management of student performance requires student to take responsibility (Şişman, 2011). According to improvement management, responsibilities given to student provide student self-control by increasing his self-confidence. When factors that are mentioned above are realized, school will be a learning organization with all its personnel. Effectiveness as a learning organization of education organizations that are called school will be possible with school sharers' realizing the goals of school in an upmost level and creating the most appropriate learning environments. This will lead up development of personnel based on school. (Aslan, Beycioğlu, 2010; Gülşen ve Gökyer, 2012; Kaplan, 2008).

In the settling process of school based management approach in a school, taking sharers opinions, making them join management with governance understanding bears great importance. In virtue of this importance, in this research levels of having effective school qualities of primary and secondary schools are tried to be determined with Yakuplu Kemal Arıkan primary and seconday school sample, in accordance with views of education sharers (manager, teacher, student and parent) according to 'school dimension', 'school environment and parent dimension', 'school management dimension' and 'teacher dimension'. In determining process of these dimensions, factors that are determined by Mortimore(1995) are accepted as criterion; views of Yakuplu Kemal Arıkan primary and seconday school sharers are tried to be defined in consideration of findings in studies of this field. (Başar, 2006; Füsun, 2008; Mortimore, 1995; Orhan, 2011; Şahin, 2011).

Method

This research is carried out with general scanning model. 'Effective School Qualities Survey' is used in order to determine views.

Managers, teachers, students and parents of Istanbul Yakuplu Kemal Arıkan Primary and Secondary School are chosen as research universe. A judgment is tried to be made by looking at the assessments of education sharers (manager, teacher, student and parent) about student dimension, school environment and parent dimension, school management dimension and teacher dimension.

All teachers and managers of Yakuplu Kemal Arıkan primary and secondary school are incorporated into workgroup. A school manager, two assistant managers and a total of thirty five teachers constitute workgroup. Seventeen of these teachers are at primary school and eighteen of them are at secondary school.

Also in order to determine students in workgroup, name list was taken by school management and each ninth student from this list was determined and added to workgroup. The number of total students in primary

school is five hundred eighteen and the number of total students from secondary school is three hundred nine. Twenty students from primary school and thirty three students from secondary school were added to workgroup. In order research data to be neutral, election was made this way from the list.

In order parents that will be involved in research not to be parents of the students that were added to the workgroup, parents of each tenth student from the list were added to workgroup. Total number of parents in primary school is five hundred eighteen and total number of parents in secondary school is three hundred nine. Twenty parents from primary school and thirty three parents from secondary school were added to workgroup. . In order research data to be neutral, election was made this way from the list.

In research in which personal factors are not allowed, the survey which consists of five sections and each of these sections have five questions were carried out with managers, teachers, students and parents. In this survey, research sharers are wanted to assess school in five category. These are student dimension, school environment, parent dimension, school management dimension and teacher dimension.

Average that is calculated according to each item in explication of data is accepted as that item's realization level. Survey that is carried out in order to gather information is formed of four dimensions of school as student, school environment and parent, school management and teacher. There are five items for each dimension. In these statements, participants are wanted to express their opinions according to triplet likert typed options. While this evaluation is carried out, the idea that the gaps in survey are equal is the departure point. Options about the views in the survey, bounds of options and weight levels are determined in Table 1.

Table 1. Weights and Bounds of These Weights Given To Participation Degrees to Statements

WEIGHT	OPTION	BOUNDS
1	Don't agree	1,00-1,67
2	Slightly Agree	1,68–2,34
3	Totally agree	2,35–3,00

Findings

Findings that are gained through research are tried to be interpreted by being placed on table. In assessment, opinions of managers, teachers, students and parents that participated and expressed their opinions in the survey were interpreted by being averaged arithmetically and interpreted according to general arithmetic average and frequency numbers.

Table 2- Assessments of education sharers about 'school management' dimension of effective school

Managers of these school generally		**Manager** $\overline{X}$	**Teacher** $\overline{X}$	**Student** $\overline{X}$	**Parent** $\overline{X}$	**N**	**General average** $\overline{X}$
1	Visit classes and guides teachers	2,50	1,76	2,25	2,00	144	2,05
2	Success is important and worth being awarded	3,00	2,61	2,65	2,80	144	2,76
3	Try to create an integrating culture by making personnel loyal to school	2,50	2,15	2,45	2,40	144	2,40
4	Are in touch with students and parents as well as teachers	3,00	2,38	2,65	2,35	144	2,54
5	Have great expectations from teachers and students in education and teaching	3,00	2,46	2,65	2,80	144	2,72
General							2,49

When table 2 is analyzed, it is seen that there is a general participation to these statements with $\overline{X}$=2,49 degree as general average.When analyzed of group basis, except from teachers, all other sharers subscribed the point that managers visit classes frequently and guide teachers. Arithmetic average is either two or above two. However, it is seen that teachers subscribed this item with the option of slightly agree with a degree of $\overline{X}$=1,76. The statement with lowest participation according to general arithmetic averages is 'slightly agree' statement with a degree of $\overline{X}$=2,05.

Except from this statement, both as general arithmetic average and all groups (manager, teacher, student and parent) expressed their opinions as 'totally agree' about all other statements.

Table 3- Assessment of education sharers about 'teacher' dimension of effective school

Teachers of this school generally		**Manager** $\overline{X}$	**teacher** $\overline{X}$	**student** $\overline{X}$	**parent** $\overline{X}$	**N**	**General average** $\overline{X}$
1	Give importance to collective working about issues related to education-teaching	2,50	2,61	2,75	2,25	144	2,68
2	Believe all students can learn basic abilities	3,00	2,23	2,60	2,60	144	2,58
3	Have high expectations from students	2,50	2,07	2,55	2,60	144	2,49
4	Gives importance to professional development	3,00	2,23	2,60	2,60	144	2,58
5	Techniques they use are appropriate for learning goals	2,00	2,46	2,85	2,46	144	2,59
General arithmetic average							2,58

When table 3 is analyzed, it is seen that there is a general participation to 'totally agree' option to these groups' statements with $\overline{X}$=2,58 degree as general arithmetic average.According to general arithmetic averages, all of managers, teachers, students and parents expressed their opinions as 'totally agree. While top level subscribe is to 'Give importance to collective working about issues related to education-teaching' item with a degree of $\overline{X}$ =2,68, lowest level subscribe is to the 'Have high expectations from students' item among statements of this group. When evaluation is carried out on the basis of each group, lowest-level subscribe is to the item 'Techniques they use are appropriate for learning goals' to which managers subscribed 'slightly agree' with a degree of $\overline{X}$ =2,00. The statements which are subscribed top-level as 'totally agree' with a degree of $\overline{X}$=3,00 , again subscribed by managers, are 'Believe all students can learn basic abilities' and 'Gives importance to professional development' items.

Table 4- Assessment of education sharers about 'school environment and parent' dimension of effective school

The environment and parents of this school generally		**manager** $\overline{X}$	**Teacher** $\overline{X}$	**student** $\overline{X}$	**parent** $\overline{X}$	**N**	**General average** $\overline{X}$
1	Parents know what school expects from them and they try to support school in this direction	2,50	1,92	2,65	2,30	144	2,39
2	There is an open communication between parents and school	3,00	2,46	2,45	2,60	144	2,58
3	Parents are conscious and responsible.	1,50	1,84	2,75	2,25	144	2,33
4	School and family are supportive to each other about student discipline issue	2,50	1,76	2,60	2,40	144	2,37
5	They visit school and teacher frequently	3,00	1,84	2,35	2,35	144	2,30
General arithmetic average							2,39

When views about 'school environment and parent' dimension in table 4 is analyzed, it is seen that even if in the least there is a general participation to 'totally agree' option to these groups' statements with $\overline{X}$=2,39 degree as general arithmetic average.Top-level subscribe is to the statement 'There is an open communication between parents and school' which is subscribed fully with a degree of $\overline{X}$=2,58. All groups stated that they subscribed this statement with the option of 'totally agree' according to arithmetic averages. It is seen that among the statements in this to group to which they subscribed 'slightly agree' are 'They visit school and teacher frequently' statement with $\overline{X}$=2,30 and 'Parents are conscious and responsible' statement with $\overline{X}$=2,33 .

When evaluation is carried out on the basis of each group, lowest-level subscribe is to the item 'Parents are conscious and responsible.' to which managers subscribed 'don't agree' with a degree of $\overline{X}$=2,00. This statement is the only statement that is subscribed with 'don't agree' option. The statements which are subscribed top-level as 'totally agree' with a degree of $\overline{X}$=3,00 , again subscribed by managers, are 'There is an open communication between parents and school' and 'They visit school and teacher frequently' statements.

Table 5- Assessment of education sharers about 'student' dimension of effective school

	Students of this school generally	**manager** $\overline{X}$	**teacher** $\overline{X}$	**student** $\overline{X}$	**parent** $\overline{X}$	**N**	**General average** $\overline{X}$
1	Their expectations about being successful is high	2,50	2,15	2,45	2,50	144	2,44
2	They have the right to speak when decisions about them are made	2,50	2,15	2,55	2,55	144	2,49
3	They know that is expected from them	1,50	2,07	2,45	2,45	144	2,35
4	They spare most of their time at school to learning activities	2,00	2,23	2,50	2,20	144	2,39
5	They are eager to work collaboratively and to take responsibility	2,50	2,07	2,35	2,65	144	2,44
General arithmetic average							2,42

When views about 'student' dimension in table 5 is analyzed, it is seen that there is a general participation to 'totally agree' option to these groups' statements with $\overline{X}$=2,42 degree as general arithmetic average.Top-level subscribe is to the statement 'They have the right to speak when decisions about them are made' which is subscribed fully with a degree of $\overline{X}$=2,58. All groups stated that they subscribed all statement with the option of 'totally agree' according to arithmetic averages. It is seen that among the statements in this group to which they subscribed at the lowest-level is 'They know that is expected from them' statement.

When evaluation is carried out on the basis of each group, lowest-level subscribe is to the item 'They know that is expected from them.' to which managers subscribed 'don't agree' with a degree of $\overline{X}$=1,50. This statement is the only statement that is subscribed with 'don't agree' option. The statement which is subscribed top-level as 'totally agree' with a degree of $\overline{X}$=3,00 , again subscribed by managers, is 'They are eager to work collaboratively and to take responsibility' statement.

Results and Discussion

When findings gained through research are interpreted and an assessment is made as a whole, it is seen that 'totally agree' option is used as an average with a degree of $\overline{X}$=2,47in four different dimensions.

When general arithmetic averages are analyzed as sub-dimensions;

It is seen that education sharers subscribed assessment about 'school management' dimension in general with the option of 'totally agree' with a degree of $\overline{X}$=2,49.

It is seen that education sharers subscribed assessment about 'teacher' dimension with the option of 'totally agree' with a degree of $\overline{X}$=2,58 as general arithmetic average.

It is seen that education sharers, even if it is a low-level subscription, subscribed assessment about 'school environment and parent' dimension with the option of 'totally agree' with a degree of $\overline{X}$=2,39 as general arithmetic average.

It is seen that education sharers subscribed assessment about 'student' dimension with the option of 'totally agree' with a degree of $\overline{X}$=2,42 as general arithmetic average.

It is seen in general that in group level only two statements were subscribed with 'don't agree' option. According to the results of assessment that is carried out in group basis, managers don't subscribe assessment of effective school about 'parents are conscious and responsible' statement of 'school environment and parent' dimension with a degree of $\overline{X}$=1,50 and assessment of effective school about 'they know what is expected from them' statement of 'student' dimension with a degree of $\overline{X}$=1,50. Managers believe that parents are not responsible about issues related to the effectiveness of school. Managers also believe that students don't know what is expected from them.

When results are analyzed as a whole, education sharers (managers, teachers, students and parents) who subscribed in this research either subscribed 'limited participation) or subscribed 'full participation'.

It is seen that manager-environment and manager-student relationships are not at expected level. Besides this, confidence level about all students can learn basic abilities and all students give importance to professional development are not at expected level.

It is seen that school managements have goals in terms of professional leadership. It can be said that these goals increase motivation of both teachers and students. On the other hand teachers don't find visits and guidance of school management sufficient. When analyzed from this point of view there is a motivation decreasing effect.

Managers, students and parents stated that teachers are qualified in terms of profession and are open to development. Vision and goals of school that is part of research are accepted by education sharers. This shows that goal congruence is provided in school.

If we analyze schools that are part of research in terms of learning environment, it can be said that there is a positive school environment in these schools and it effectscolleague relationship positively. If we analyze school environment in terms of teaching and focusing on teaching, both schools work collaboratively.

The following results are attained based on findings in research:

- Managers, teachers, students and parents subscribe to statements about effective school according to arithmetic averages.
- Top level subscribe is to the statements related to 'teacher' dimension of effective school.
- The lowest-level subscribe is to the 'School environment and parent' dimension.
- 'School management' and 'student' dimension of effective school are subscribed totally and are close to each other.
- In general, only two statements were subscribed with 'don't agree' option in group (manager, teacher, student and parent) level. Managers from education sharers stated that they don't subscribe 'parents are conscious and responsible' and 'students know what is expected from them' statements.
- School managers don't find parents conscious and responsible enough. This situation shows that school management-environment relationships are not at expected level.

Conclusions

The following suggestions are made according to results attained in research:

- More responsibility should be given to parents and students to improve relationships between school management with student and parent.
- Opinions of other sharers should be taken in order school to show all qualities of effective schools.
- School sharers should be educated about effective school issue periodically.

Acknowledgement

Thanks to Yakuplu Kemal Arıkan Primary and Secondary School education sharers (managers, teachers, students and parents) who participated in the research with their opinions.

References

Aslan, Mahire ve Beycioğlu, Kadir (2010). *Okul Gelişiminde Temel Dinamik Olarak Değişim ve Yenileşme: Okul Yöneticileri ve Öğretmenlerin Rolleri*. Yüzüncü Yıl Üniversitesi Eğitim Fakültesi Dergisi. Haziran 2010.Cilt:VII, Sayı:I, 153-173.

Aydın, İnayet.(2002). *Alternatif Okullar*. Pegem Akademi Yayınları, Ankara.

Aydoğan, İsmail ve Helvacı, M.Akif.(2011). *Etkili Okul ve Etkili Okul Müdürüne İlişkin Öğretmen Görüşleri*. Uşak Üniversitesi Sosyal Bilimler Dergisi. (2011) 4/2: 41-60.

Balcı, Ali (2011). *Etkili Okul ve Okul Geliştirme Kuram Uygulama ve Araştırma*. Pegem Akademi Yayınları. Ankara.

Celep, Cevat. (2000). *Eğitimde Örgütsel Adanma ve Öğretmenler*. Ankara: AnıYayıncılık.

Çelik, Vehbi (2012). *Okul Kültürü ve Yönetimi*. Pegem Akademi Yayınları. Ankara.

Çelik, Vehbi (2012). *Eğitimsel Liderlik*. Pegem Akademi Yayınları. Ankara.

Güçlü, Nezahat. (2000). *Okula Dayalı Yönetim*. Gazi Üniversitesi Kastamonu Eğitim Fakültesi Dergisi Cilt:8, Sayı:1,s: 65-78.

Gülşen, Celal ve Necmi Gökyer. (2012). Türk Eğitim ve Okul Yönetimi. Anı Yayıncılık. Ankara.

Kaplan, Füsun. (2008). *Anadolu Liselerinin Etkili Okul Olma Özelliklerini Karşılama Düzeyi: Ankara İl Örneği.*Gazi Üniversitesi: YayımlanmamışYüksek Lisans Tezi. Ankara.

Keleş, Başar. (2006). *İlköğretim Okullarının Etkili Okul Özelliklerine Sahip Olma Dereceleri Hakkında Öğretmen Görüşleri* (Çorum İlÖrneği). Gazi Üniversitesi Yayımlanmamış Yüksek Lisans Tezi. Ankara.

Mortimore, Peter & at All. (1995). *Key Characteristics of Effective Schools: A review of School Effectiveness Research*. London (www.highreliability.co.uk), pp: 17-47.

Orhan, Mustafa (2011). *Etkili Okul Karakteristikleri Çerçevesinde Okul Yöneticilerinin Davranışsal Özellikleri* (Erzurum İl Örneği). Atatürk Üniversitesi: Yayımlanmamış Yüksek Lisans Tezi. Erzurum.

Özdemir, S. (2000).*Eğitimde Örgütsel Yenileşme*. Ankara: Pegem A Yayıncılık.

Özdemir, Asım. (2002). *Sağlıklı Okul İkliminin Çeşiti Görünümleri ve Öğrenci Başarısı*. Gazi Üniversitesi Kastamonu Eğitim Fakültesi Dergisi. Cilt:10, sayı: 1, s:39-46.

Şahin, Muhsin.(2011).*Etkili Okul Ve Aile İlişkisine Dair Öğretmen Algıları* (İstanbul İli Anadolu Yakası Örneği).Maltepe Üniversitesi: Yayımlanmamış Yüksek Lisans Tezi. İstanbul.

Şişman, Mehmet.(2011). *Eğitimde Mükemmellik Arayışı* –Etkili Okullar, Pegem Akademi Yayınları, Ankara.

Şişman, Mehmet.(2011). *Öğretim Liderliği*, Pegem Akademi Yayınları, Ankara.

Multiuser detection in CDMA — A comparison of minimum mean square error and simulating annealing heuristic algorithm

Nacera Larbi[1], F. Debbat[2], A. Boudghen Stambouli[3]

[1]Space Techniques Centre - CTS, 01 Avenue de la Palestine, PB 13, Arzew 31200, Algeria
[2]Computer Science Department - Faculty of Sciences and technology - University of Mascara- Algeria
[3]Electronics Department - Faculty of Electrical and Electronic - USTO University of Oran - Algeria
e-mail: nacera73@hotmail.com

Abstract: In the conventional single user detector in Direct Sequence-Code Division Multiple Access (DS-CDMA) systems, multiple access interference and near-far effect cause limitation of capacity. On the other hand, the optimal multiuser detector (OMUD) suffers from computational complexity that grows exponentially with the number of active users. During the last two decades, there has been a lot of interest in development of suboptimal multiuser detectors, which are low in complexity but deliver reasonable performance. In this paper, we present a novel multiuser detector based on the heuristic algorithm known as simulating annealing algorithm (SA). We evaluate performances of the proposed algorithm and compare it to the performances of Minimum Mean Square Error (MMSE) multiuser detectors. We show that the new algorithm outperforms the other one.

Key words: Direct Sequence-Code Division Multiple Access (DS-CDMA), Multiuser Detection (MUD), Simulating Annealing (SA), Minimum Mean Square Error (MMSE), Bit-Error Rate (BER).

Introduction

In Direct-Sequence Code Division Multiple Access (DS-CDMA) systems, Multiple Access Interference (MAI) is regarded as the main source limiting the system capacity. Multiuser Detection (MUD) is a well-known technique dealing with MAI (Hsieh & Wub, 2011). Different from the architecture of conventional single-user receivers, MUD conducts detections for all users simultaneously and can achieve much better performance. In (Verdu, 1986) a maximum-likelihood multiuser receiver was first proposed. Although significant performance enhancement can be obtained, the required computational complexity is very high, growing exponentially with the user number. This adversely affects its real world applications. As a consequence, many suboptimum alternatives were then proposed (Moshavi, 1996; Duel-Hallen et al., 1995; Verdu, 1998).

Recently, there has been considerable interest in linear multi-user detection based on MMSE criterion (Moshavi, 1996). It is shown that MMSE detector, relative to other detection schemes has the advantage that explicit knowledge of interference parameters is not required, since filter parameters can be adapted to achieve the MMSE solution. Although it does not achieve minimum Bit-Error Rate (BER), MMSE detector has been proved to achieve the optimal near-far resistance.

Recently, methods based on heuristic algorithms are being applied to improve the performance of suboptimal multiuser detectors. They view the MUD problem from a combinatorial optimization form and try to approximate the optimal solution iteratively. Genetic algorithms were the first heuristic algorithms applied to the MUD problem(Ergun & Hacioglu, 2000; Yen & Hanzo, 2000; Yen & Hanzo, 2001; Yen & Hanzo, 2004; Wu et al., 2003). In (Tan & Rasmussen, 2002) a tabu search algorithm is proposed. In (Morra et al., 2009) a particle swarm algorithm is tested and in (Ciriaco et al., 2006) evolutionary algorithm is proposed. In this work a MUD detector based on Simulating Annealing (SA) is proposed.

The rest of the article is organized as follows: Section II gives a system model description. Section III describes the proposed simulating annealing multiuser detection algorithm. Section IV gives the simulation results and section V draws the conclusion.

System model

In this paper, we consider the vector channel mode of a simple K users symbol synchronous CDMA system with a common single path additive white Gaussian noise (AWGN) channel, in order to clearly demonstrate the characteristics of each of the detection strategies. For synchronous system with a common single-path AWGN channel, it is sufficient to consider the signal received in one signal interval. Hence, the continuous time received waveform may be expressed as

(1)

Where is the signature waveform of the user, is the information bit transmitted by user k, and is the WGN process with two-sided power spectral density.

Each signature waveform is zero outside the bit interval, and the information bits of the users are assumed to be independent and equiprobable.

The sampled output of the matched filter (MF) of the kth user is

(2)

Letting the vector of MF output samples be defined as, the data vector, then the vector of the matched filter outputs can be expressed as

(3)

Where the amplitudes of the K users are collected into a diagonal matrix

And R is the correlation matrix with elements

(4)

The Gaussian noise vector z has zero mean and autocorrelation matrix

(5)

Note that y constitutes a set of sufficient statics for estimating the transmitted data vector d.

The optimum ML detector selects the most likely (maximum likelihood) hypothesis given the matched filter output

(6)

Since we are considering an AWGN channel, the negative log-likelihood function based on the is proportional to. The binary constrained ML problem is then described as

(7)

The solution to (7) requires a search over all the possible combinations of the components of the vector d. it is thus clear that the computational complexity increases exponentially with the number of users (Tan & Rasmussen, 2004).

Simulating annealing multiuser detection

Figure1 shows a flowchart of the Simulating Annealing Multi-user detection.

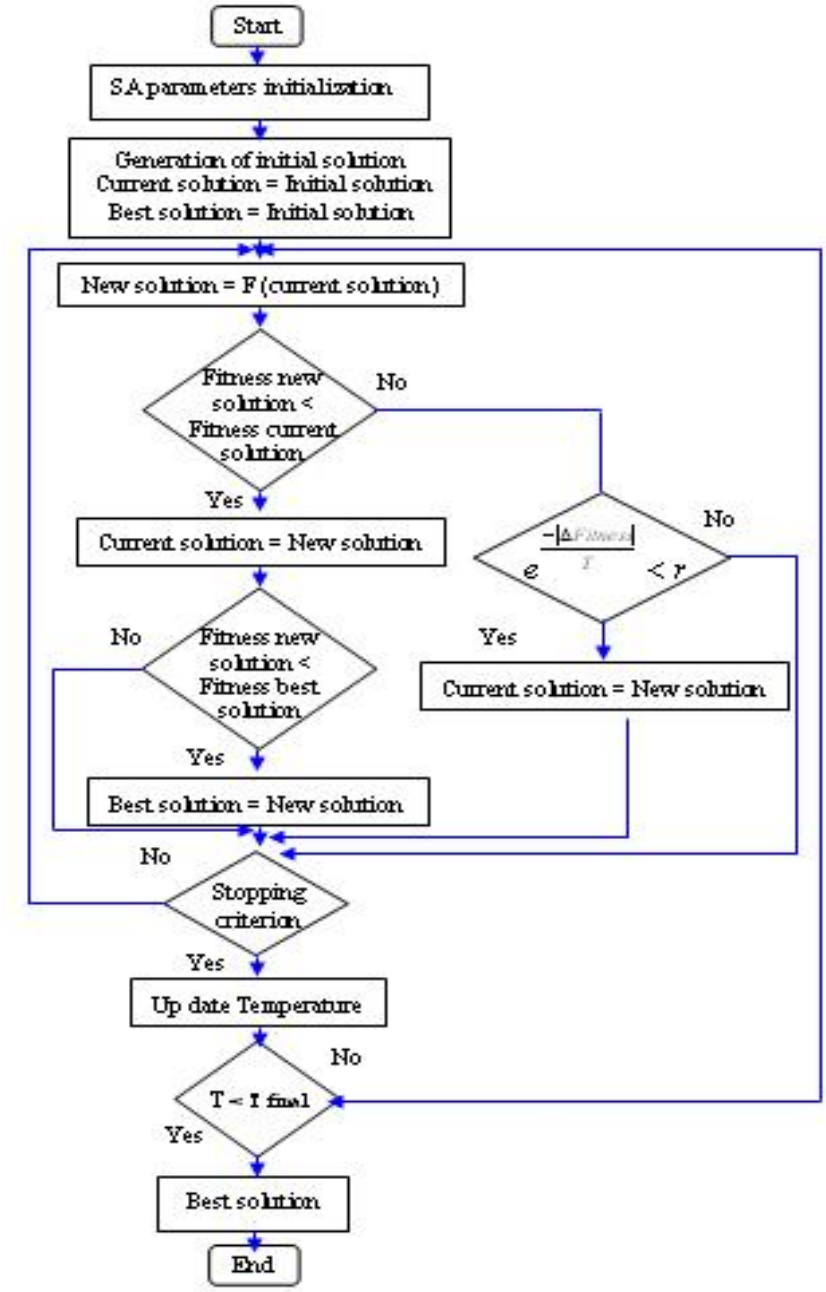

Figure 1: Flow chart of the SA-MUD

The basic algorithm is shown bellow

1. 1. Definition of the input data: initial temperature $T_{initial}$, final temperature T_{final}, temperature reduction factor , number of iterations at fixed temperature *itr*. As well as, the DS-CDMA MUD parameters: such as the number of users k and the length of spreading sequence N.

1. 2. Initialization of the best solution of the SA algorithm by the initial solution. The output of the matched filter (MF) is included as the first initial trial vector of the generation of the population.

1. 3. Generation of a neighboring solution (new solution) from the current solution. The generation is performed by which is a random transformation function of the solution, in our case; it is based on a single mutation between elements selected randomly of the current solutions vector. If the fitness value of the new solution is less than the fitness value of the current solution, the current solution becomes the new solution. If not this current solution will become the new solution according to the Boltzmann probability.

1. 4. The fitness of this new solution is also compared with the fitness of the best solution, if the fitness of this new solution is less than the fitness of best solution, best solution will be the new solution.

1. 5. This process is repeated for a number of iterations fixed in advance.

1. 6. After the updated temperature, we test the algorithm stopping criterion.

1. 7. End

Simulations, results and analysis

In this section the performance of the above described systems will be analyzed by simulations. After the specification of the system parameters the simulation results of the synchronous DS-CDMA system with simulated annealing (SA) multi user detection over an AWGN channel with Gold spreading code N=31 will be presented. All the users are transmitting with the same power. Figure 2 shows BER versus Es/No of the MMSE and SA-MUD.

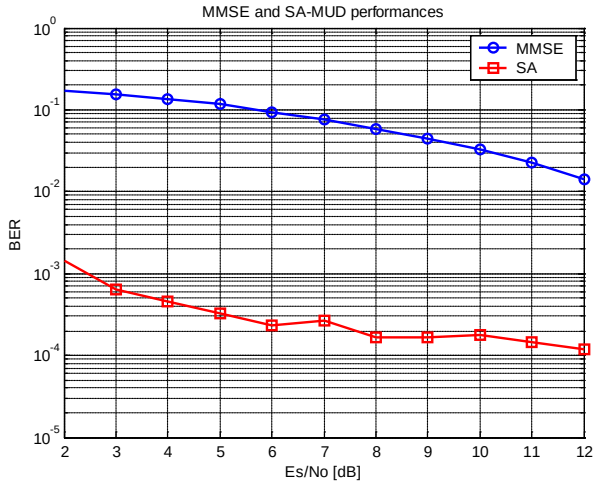

Figure 2: The BER vs. Es/No of SA-MUD (N=31, K= 20, *itr*=300)

In Figure 2 it can be seen that the proposed SA-MUD performs best, since it shows the least BER in comparison of the MMSE detector (in this simulation the number of users is K=20 and the number of iteration *itr*=300). This algorithm proved its efficiency and power since its BER=10^{-4} on the other hand the BER of the MMSE is about BER=10^{-2}.

Figure 3 shows the SA and MMSE algorithms performances evolution according to the total iteration numbers (*itr*). The SA algorithm gives the best performances for a high iteration numbers.

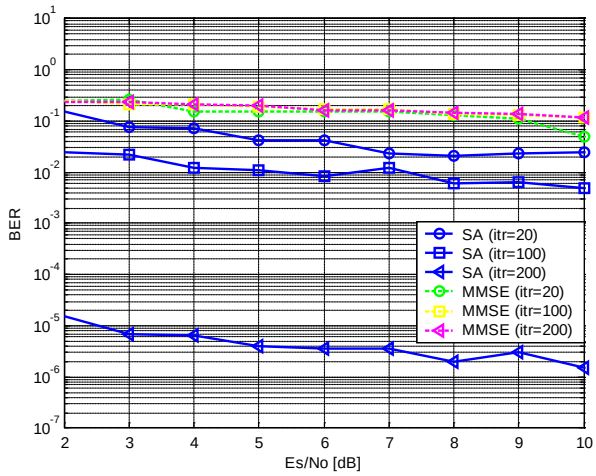

Figure 3: The BER vs. Es/No of SA-MUD (N=31, K= 10)

For the same iteration number (*itr*=100) and with different number of users (K=4 & 14), the SA detector performance is better if the number of users is smaller as seen in Figure 4.

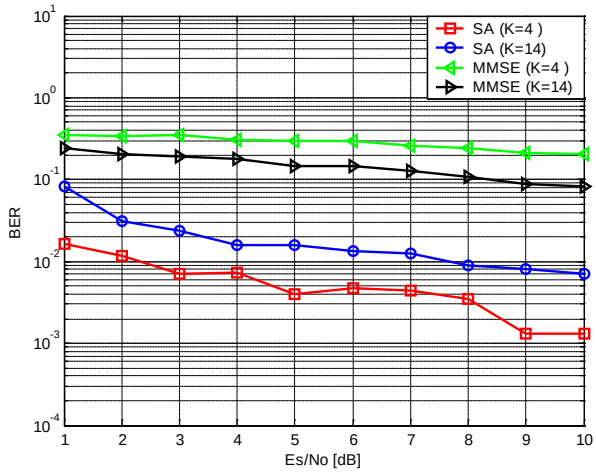

Figure 4: The BER vs. Es/No (N=31, *itr*= 100)

A common form in order to compare algorithms complexity can be done through the O notation, which means the order of magnitude of the algorithm complexity. But comparing algorithms only with O can be insufficient, mainly when they are similar or have the same order of magnitude [Ciriaco et al., 2006]. This work presents the algorithms complexity using only the mean computational time required for a specific optimization as illustrated in Figure 5, rather than the O notation and the number of computed instructions

The CPU time is obtained in the MATLAB environment on a 1,66 GHz; Pentium Intel(R) Core (TM)2 CPU T5500; personal computer with 1,00 Go of RAM.

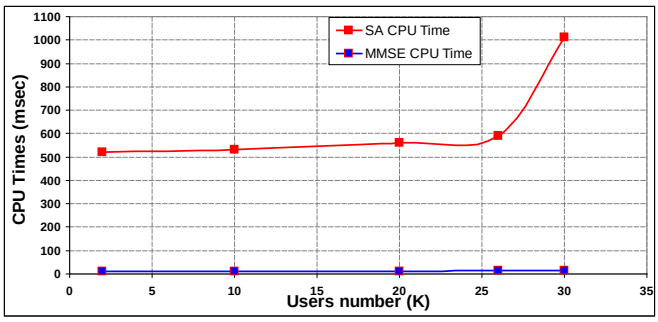

Figure 5: CPU Times comparison of various user numbers (N=31, itr=200)

The execution time is not affected by increasing the number of users and it does not progress exponentially as shown in Figure 5.

Conclusions

A novel simulating annealing algorithm with an extremely low complexity has been proposed for DS-CDMA multiuser detection. From the investigations conducted, it is observed that the BER performance of the proposed receiver is much better in comparison with conventional MMSE receiver. Thus, it is shown that the SA detection algorithm is a very promising multi-users detection especially for the future mobile radio systems. In future work, we plan to widen our investigations to the new meta-heuristic algorithms.

References

Ciriaco, F., Abrao, T., Jeszensky P. J. E. (2006). DS/CDMA Multiuser Detection with Evolutionary Algorithms. Journal of Universal Computer Science, vol. 12, pp. 450-480.

Duel-Hallen, A., Holtzman, J., Zvonar, Z. (1995). Multiuser detection for CDMA systems. IEEE Personal Commun. Vol. 2, pp. 46–58.

Ergun, C., Hacioglu, K. (2000). Multiuser detection using a Genetic-algorithm in cdma communication systems. IEEE Trans. on Commun. Vol. 48, , pp. 1374–1383.

Hsieh, Y. T., Wub, W. R. (2011). Adaptive parallel interference cancellation for CDMA systems—A weight selection and filtering scheme. Signal Processing, vol. 91, pp. 1–14.

Morra, H., El Sheikh, A. U., Zerguine, A. (2009). Optimum multiuser detection in cdma using particle swarm algorithm. The Arabian journal for science and engineering, vol. 34, pp.197–202.

Moshavi, S. (1996). Multi-user detection for DS-CDMA communications. IEEE Commun. Mag. Vol. 34, pp. 124–136.

Moshavi, S. (1996). Multiuser detection for DS-CDMA communications. IEEE Commun. Mag., vol. 34, pp. 132–136.

Tan, P. H., Rasmussen, L. K. (2002). A reactive tabu search heuristic for multiuser detection in CDMA. IEEE International symposium on information theory, pp.472.

Tan, P. H., Rasmussen, L. K. (2004). Multi-user detection in CDMA-A Comparison of Relaxations, Exacts, and Heuristic Search Methodes. IEEE Transactions on wireless Communications, Vol. 3, pp. 1802–1809.

Verdu, S. (1986). Minimum probability of error for asynchronous Gaussian multiple-access channels. IEEE Trans. Inf. Theory vol. 32, pp. 85–96.

Verdu, S. (1998). Multiuser Detection. Cambridge University Press, Cambridge, UK.

Wu, X., Chuah, T. C., Sharif, B. S., Hinton, O. R. (2003). Adaptive robust detection for cdma using genetic algorithm. IEE Proceedings Communications, vol. 150, pp. 437–444.

Yen, K., Hanzo, L. (2000). Hybrid genetic algorithm based multiuser detection schemes for synchronous CDMA systems. In Procceding of 51th IEEE Vehicular Technology Conference. Tokyo, Japan, pp. 1400–1404.

Yen, K., Hanzo, L. (2001). Genetic algorithm assisted joint multiuser symbol detection and fading channel estimation for synchronous cdma systems. IEEE Journal on Selected Areas in Communic., vol. 19, pp.985–997.

Yen, K., Hanzo, L. (2004). Genetic-algorithm-assisted multiuser detection in asynchronous CDMA communications. IEEE Trans. On Vehicular Technology, vol.53, pp.1413–1422.

Performance improvement of road embankment on Algeria Sabkha soils by geosynthetics

Naima Benmebarek*, Sadok Benmebarek and Lamine Belounar

Numerical Modelling and Instrumentation Laboratory, Biskra University, Algeria
e-mail:benmebarekn@yahoo.fr

Abstract: Road engineers in Algeria like Tunisia, Arabi Saoudit, USA, India and Australia often face the challenge to design a solid road foundation on top of very soft soils which are characterized by Sabkha soils. These soils are very sensitive to moisture whereby complete collapse and large reduction in the bearing capacity are anticipated when these soils are in contact with water. With the help of geosynthetics innovative, economic and durable solutions can be offered to several situations where standard soil improvement techniques are still extensively used. This paper is interested by the construction technique of the road with reinforced embankment crossing the Sebkha flat of Chott El Hodna on 11 km length in the north middle of Algeria. The visual site observation and the analysis of the characteristics of the geotechnical investigation show that the surface layer is very weak bearing capacity, made up of deposit of mud with traces of silt, rests on a layer of thick muddy marl. The weak bearing capacity of the ground and the presence of water table make serious difficulties of construction. The design of this road was carried out using the FLAC -2D software specialized in geotechnics. The need for a reinforcement by geogrid associated with separation geotextile was well highlighted by the numerical simulations and confirmed by the difficulty reencountered in the placement of the two first embankment lift.

Key words: *Reinforced embankment, numerical simulation, geosynthetics, weak bearing capacity, road.*

Introduction

Sabkha is originally an Arabic name for saline flats that are characterised by very low bearing capacities and underlain by sand, silt and clay, and often encrusted with salt. Sabkha soils are very sensitive to moisture whereby complete collapse and large reduction in the bearing capacity are anticipated when these soils are in contact with water (Al-Amoudi et al. 1992). Such behaviour is attributed to the fact that some of the cementing materials that bond the mineral grains of sabkha together, such as halite, are highly soluble in water, while others, such as gypsum, aragonite, and calcite are less soluble. The work done by Aiban et al. (1998) on different sabkha soils confirms the acute water sensitivity and chemical aggressiveness of sabkhas.

Road engineers in Algeria like Tunisia, Arabi Saoudit, USA, India and Australia often face the challenge to design a solid road foundation on top of very soft soils which are characterized by sabkha soils. Several field stabilization techniques have been implemented to improve the inferior sabkha properties, with various degrees of success (Juillie and Sherwood, 1983). However, it has generally been found that the use of geosynthetics as reinforcement has the advantages of being practical, economical, and easy to apply.

Sabkha soil is extensively distributed along the inland regions of the Algeria. The susceptibility of these soils to strength loss and collapse upon wetting makes their use in construction very risky, particularly if proper treatment has not been undertaken.

In the present paper, the site investigated is the road embankment about 11 km constructed on sabkha of Chott El Hodna located in the M'Sila department in the north middle of Algeria (Figure 1). This road reduces the current distance from two towns by 140 km and improves considerably the commercial and agriculture activities The in situ observations show that in summer surface soil is partially dry and soft enough where only a very small weight vehicles can cross the Sabkha. However, in winter the sabkha is inundated where water table may arise up to

60 cm over ground surface. Figure 2 presents photograph showing the sabkha surface state taken in July 2005.

After the description of the project and soil investigation, the need of reinforced embankment by geosynthetic was well highlighted by numerical modelling using an explicit finite difference code and confirmed by the difficulty reencountered in the placement of the first embankment lift and the compaction performance.

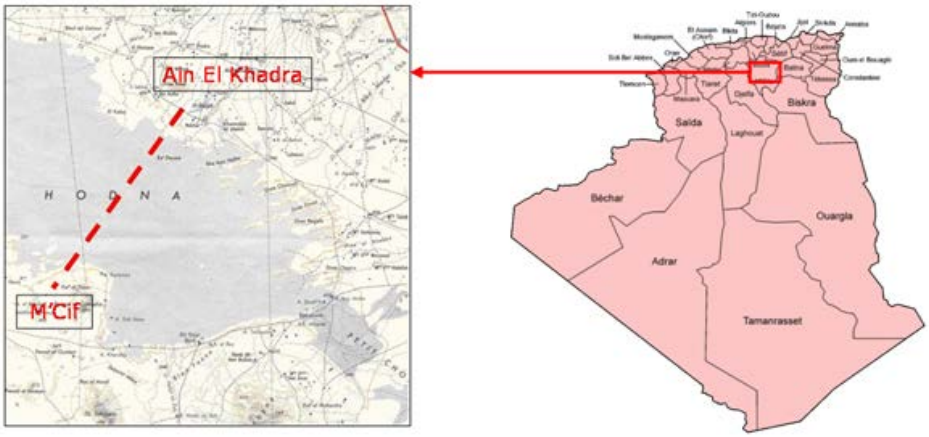

Figure 1: Site project

Figure 2: Subsurface state of the project road

Hydrological and subsurface soil investigations

The sabkha of Chott El-hodna in the middle north of Algeria is a large closed flat of 26000 km^2 developed where surface runoff converges from the Saharian Atlas in the South and the Tellien Atlas in the North and also by soil infiltration. In summer, the surface is encrusted with salt. The embankment road devises the sabkha in two parts. The hydrological study shows the maximum water level which may reach 1.40 m over ground surface for a one period of thousand-year-old return. The program of sabkha subsurface investigations contains boring hole, cone penetration test and vane shear test every 300 m of the embankment length.

Due to the poor bearing capacity sabkha surface and the arising water table over the ground surface serious difficulties were faced during the investigation of the subsurface soil. Therefore, the subsurface investigations were accomplished with the advancement of the two first lifts reinforced by geosynthetic of the embankment.

Subsurface state conditions at the middle of the Sabkha consists of a brown muddy clay layer with thickness

varying from 3m to 5m, underlain by grey muddy marl and gypsum concretions with traces fine sand with thickness varying from 5m to 7m (Figure 3). Near the edges of the sabkha the thickness of the soft layers decreases.

The partially laboratory testing results show that the compression index C_c varying from 0.31 to 0.56, the plasticity index I_p varying from 27.5 to 48.5 and the dry density varying between 1.38 and 1.64 indicating high soil compressibility. The undrained shear strength of the layers brown muddy clay and grey muddy marl reaches 9 kPa.

In the sabkha centre, the thickness of the very soft layers may reach 10 m. These results are in good agreement with the static cone penetration test results showing no point resistance for this depth (Figure 4).

Figure 3: Bore hole soil samples

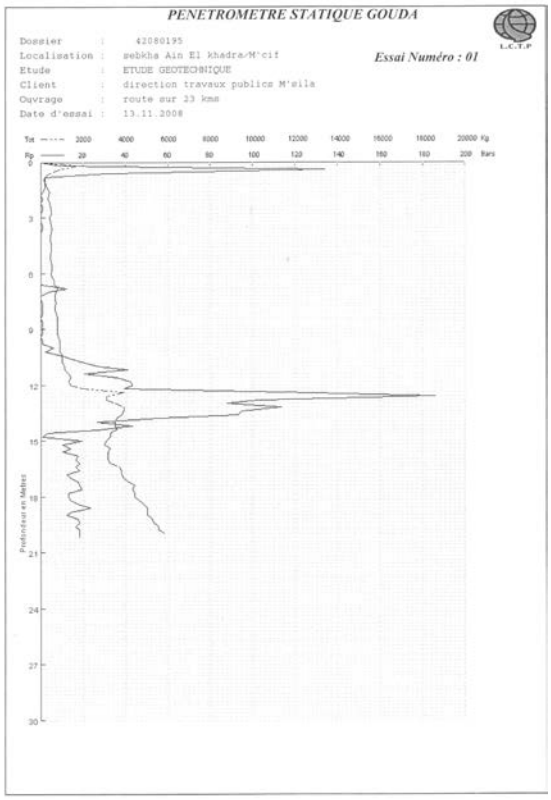

Figure 4: Typical cone penetration test results

Reinforced embankment and slope protection

Due to the poor bearing capacity sabkha surface (Figure 5) and the arising water table over the ground surface for a section road of 11 Km, the improvement of the road embankment by geosynthetic is preferred. Tthe geotextile is used to separate the subsoil and the embankment aggregate, while the reinforcement by geogrid layer is used to increase the stiffness of the foundation and to increase the compaction quality. For the embankment, a sandy gravel material was chosen to allow free drainage of the foundation soils and reducing the pore pressure build-up below the embankment;

The construction steps used as showing in Figure 6 can be summarised as following:

- Laying directly over sabkha surface corresponding to embankment base a nonwoven geotextile layer as separator/filter to prevent contamination of embankment material (Figure 7).

- Construction of the first lift of 30 cm thickness compacted to obtain plane surface;
- Laying the geogrid over the surface to uplift the tensile strength to the embankment base (Figure 8);
- Construction the embankment layer by sub-layers with compaction control by static plate load test;
- After reaching the embankment height 1.70m, the hydraulic PEHD reinforced tubes were installed (Figures 9-10). These tubes are flexible and inert to sabkha soil aggressively;
- Protection of embankment slopes from erosion (Figure 11) with separate geotextile GT 2 placed under rock ripraps (Figure 12).

Figure 5: Difficult to construct the first layer embankment

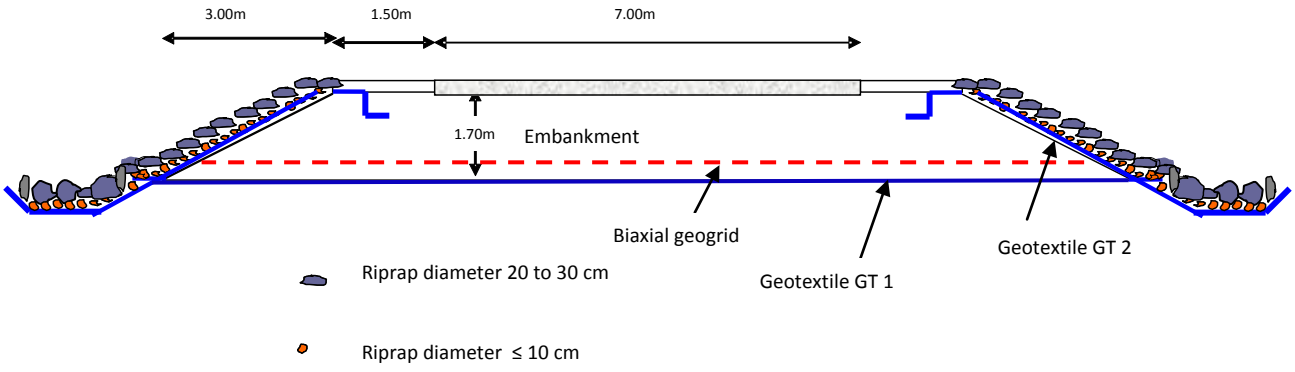

Figure 6: Reinforcement and protection of the embankment

Figure 7: Laying directly over sabkha surface a nonwoven geotextile GT 1

Figure 8: Laying the biaxial geogrid over the first lift of the embankment

Figure 9: PEHD reinforced tubes installation.

Figure 10: PEHD tubes extremity protection.

Figure 11: Risk of slope erosion

Figure 12: Protection of embankment slopes

Numerical analysis of the embankment reinforcement

For reinforcement applications, solutions have been proposed for situations where the tensioned-membrane reinforcement function will be realized and for situations where the lateral base course restraint mechanism is appropriate. Since separation is typically an integral part of the tensioned-membrane reinforcement function, design solutions for this geosynthetic function generally lump these two functions together.

Designs incorporating the tensioned-membrane reinforcement function are applicable for unpaved roads and situations where relatively large rut depths in the roadway can be tolerated and where the traffic is mainly canalized. This approach was recommended by Holtz et al. (1995) for temporary unpaved roads. However, incorporation of the lateral base course restraint mechanism is applicable for roadways where rut depth needs to be limited to 25 mm. The performance of the road and embankment base reinforcement over soft subsurface depends on several factors particularly the geogrid stiffness, characteristic of the subsurface and parameters of the interface ground-reinforcement (Rowe and Ho 1997, Alfaro and Al 1997). This area of research is very favourable to numerical computations. The present work interests with the numerical simulation of reinforced embankment base over soft subsurface in order to improve the bearing capacity. The improvement of the bearing capacity is evaluated by comparing the wheel load-displacement response corresponding. The analysis was carried out using the computer code FLAC^{-2D} (Fast Lagrangian Analysis of Continua) (Itasca 2005) which is a commercially available finite difference explicit program.

The embankment material and the soil behavior were modeled by the elastic-perfectly plastic Mohr-Coulomb model encoded in this code. The embankment fill from river was assumed to be purely frictional granular soil with a unit weight γ=20 kN/m^3 and a friction angle φ=35°. The sabkha soil was characterized by the undrained cohesion C_u =9kPa.

The geogrid, modelled by beam element without flexural strength, is connected to embankment material via interface elements obeying the criterion of Mohr-Coulomb and characterized by a null cohesion and a friction angle δ representing the angle of friction of the contact geogrid-embankment material. For the reason of the lack of the laboratory tests, the friction angle δ was taken equal to the 2/3 of the friction angle of the embankment (φ=35°).
The wheel load-displacement response was determined by this study in large strain analysis for embankment first layers with and without reinforcement. Using a FISH function, the bearing capacity can be calculated as the integral of stress components for all soil zones in contact with the footing area or by the reaction force resultant in the vertical direction at footing nodes. From these simulations it was deduced the improvement made by the reinforcement. A cross section of the embankment was modelled in two dimensions assuming plane strain conditions. The procedure of simulation used in the present analysis was based on the two following steps:

- A mechanical calculation of the geostatic stresses : These were computed assuming the material to be elastic;
- A mechanical calculation of the improvement of the bearing capacity: the bearing capacity was modeled by a downward velocity applied to the area representing the wheel load until obtaining tolerable rut for construction embankment. The value of the velocity applied to the footing area was 2.5×10^{-6} m/step for this analysis. This value was sufficiently small to minimize any inertial effects in the present conditions.

Figure 13 visualizes the vectors of displacement (yellow vectors) and tensile effort (red curve) mobilized in the biaxial geogrid with tensile strength 58 KN/m in the two directions for a lengthening of 12% for the simulation of the bearing capacity for the two first lifts of the embankment by indenting the tires of an axle.

A typical plot of the load-displacement curve is shown in Figure 14 for the both cases: without reinforcement and with reinforcement by geogrid. The asymptotic limiting value corresponds to the ultimate bearing capacity for the first case. However the bearing capacity increases with displacement for the second case. These simulations show an improvement of the bearing capacity about 60% for a tolerable rut limited to 10 cm. This improvement of the bearing capacity has been very beneficial for the progress and compaction control.

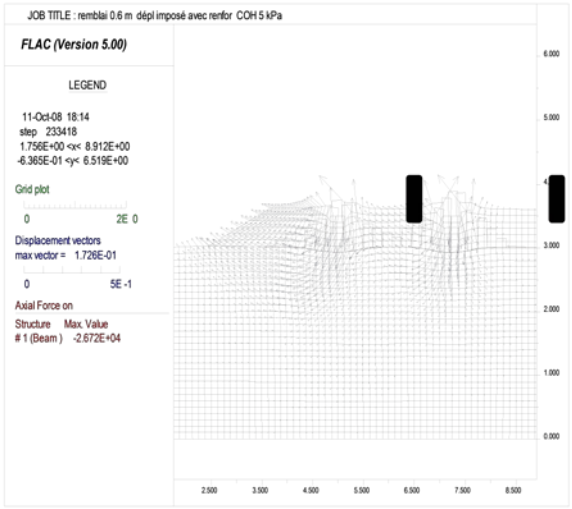

Figure 13: Visualisation of the field displacement and the geogrid tensile due to wheel indentation

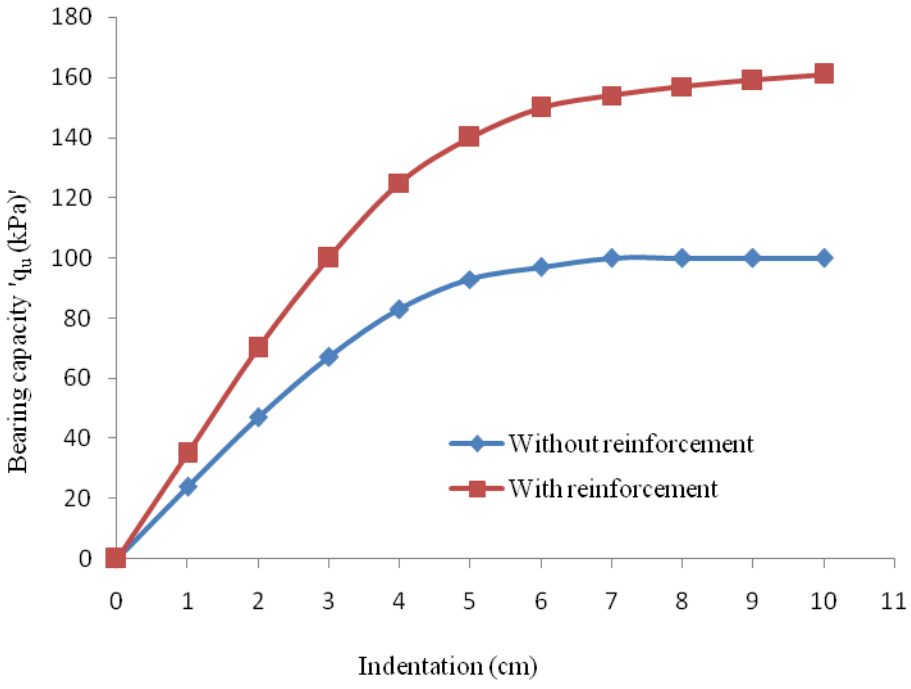

Figure 14: Reinforcement Influence on soft subsurface bearing capacity

Conclusions

In light of the work observations and the numerical computation results, the following conclusions may be drawn:

- From soil investigation the present sabkha subsurface is dominated by a muddy clay very sensitive in wet conditions;
- In the present project, without separating geotextile it was not possible to prevent the mixing of the first aggregate lift and the soft subgrade;
- The need of reinforced embankment by geotextile separation and geogrid was well highlighted by numerical computation and confirmed by the difficulty reencountered in the placement of the first embankment lift and the amelioration of the compaction performance;
- Numerical computations of the present project show an improvement about 60% of the bearing capacity of reinforced embankment. This improvement has been very beneficial for the progress and compaction quality.

References

Al-Amoudi, O.S.B., Abduljauwad, S.N., El-Naggar, Z.R. and Rasheeduzzafar, M. (1992). Response of Sabkha to Laboratory Tests: A Case Study. *Engineering Geology*, Vol. 33 (pp 111-125).

Aiban, S.A., Al-Amoudi, O.S.B., Ahmed, I.S. and Al-Abdul Wahhab, H.I. (1998). Reinforcement of a Saudi Sabkha Soil Using Geotextiles. *Proceedings of the Sixth International Conference on Geosynthetics*, IFAI, Vol. 1 (pp 805-810). Atlanta, Georgia, USA, March.

Holtz, R.D., Christopher, B.R. and Berg, R.R. (1995). Geosynthetic Design and Construction Guidelines: Participant Notebook, *FHWA Publication No. FHWA-HI*-95-038 (p 417). Federal Highway administration.

Rowe R.K. and Ho, S.K. (1997). Continuous panel reinforced soil walls on rigid foundation. *Journal of Geotechnical and Geoenviromental Engineering* (pp 912-920). ASCE, 123(10).

Alfaro, M.C. Hayashi, S. Miura, N. and Bergado, D.T. (1997). Deformation of reinforced soil wall- embankment system on soft clay foundation (pp 33-46). Soils and Foundations 37(4).

Itasca Consulting Group (2005). *FLAC - Fast Lagrangian Analysis of Continua*, v 5.00, Itasca Consulting Group Inc., Minneapolis, MN, USA.

Role of construction industry wastes on the properties of mortars

Niyazi Ugur Kockal

Department of Civil Engineering, Akdeniz University, Turkey

e-mail:ukockal@yahoo.com

Abstract : This study investigated the performance of cement mortars prepared by substituting 30% and 60% of crushed calcareous fine aggregate (CNA) with waste fine aggregates namely, crushed brick aggregate (CBA), crushed marble aggregate (CMA) and crushed ceramic aggregate (CCA). For this purpose, absorption, unit weight, compressive strength, flexural strength, resistance to high temperature up to 400 ^{o}C and resistance to freeze-thaw cycles were determined for these mortars. In addition, XRF analysis was performed on cement and waste aggregates. From the experimental results, it is found that CBA mortars exhibited the lowest strength values and worst durability properties. However, CBA and especially CCA mortars were more effective in relative strength gain at 56 days.

Key words: Strength, high temperature, freeze-thaw, morphology.

Introduction

More than 25 billion tons of concrete are produced each year all around the world. Aggregates, usually provided from natural resources, occupy up to 80% of volume of concrete. Unfortunately, the available natural aggregate used in concrete and mortar production will soon remain insufficient to supply all the demands of the construction industry. Therefore, construction industry is seeking for other alternatives in order to meet the needs in concrete manufacturing.

Using construction based waste materials in cementitious mixtures have been seen revived interest in recent years. Many researchers (Böke, Akkurt, İpekoğlu, & Uğurlu, 2006; Bektas, Wang, & Ceylan, 2009; Gonçalves, Tavares, Toledo Filho, & Fairbairn, 2009; O'Farrell, Sabir, & Wild, 2006) analyzed some properties mainly strength and durability of mortars containing different types of ground brick (calcined clays) subjected to various treatments. The properties of mortars and/or concretes containing ceramic waste aggregates were examined in some investigations (Higashiyama, Sappakittipakorn, Sano, & Yagishita, 2012; Medina, Sánchez de Rojas, & Frías, 2012; Pacheco-Torgal, & Jalali, 2010; Senthamarai, Devadas Manoharan, & Gobinath, 2011). Mortars and concretes containing marble waste were also studied by evaluating their fresh and hardened state properties (Aruntas, Guru, Dayı, & Tekin, 2010; Belaidi, Azzouz, Kadri, & Kenai, 2012; Hebhoub, Aoun, Belachia, Houari, & Ghorbel, 2011).

The main aim of this work is to compare the mortars manufactured with common construction wastes and evaluate the effects of wastes on performance employing mortar specimens. Knowing these effects will aid in assessing the physical–mechanical performance and the resistance of mortars to different treatments and also their compatibility with other building materials.

Materials and Method

Cement used in the mixtures was CEM II/A-M (P-L) 42,5N complying with TS EN 197-1 with a specific gravity of 3.05. All wastes (brick, marble and ceramic) were collected from construction sites [Figure 1] and ground until a similar grading as of natural crushed sand was obtained. Natural crushed fine aggregate utilized in the study was calcareous sand provided from Dirmil, Burdur. Chemical admixture used for providing consistency of mortars constant was a modified lignin sulphonate based water reducing/plasticizer admixture consistent with TS EN 934-2.

Figure 1: Wastes disposed in the construction site

As fundamental physical material characteristics, water absorption, specific gravity, rodded and loose bulk density of crushed aggregates were determined by following the test procedures in the relevant standards [Table 1].

Table 1: Physical characteristics of waste materials.

Materials	Water absorption (%)	Specific gravity (Dry)	Rodded bulk density (Dry)	Loose bulk density (Dry)	Void content (%)
Sand	2.24	2.71	1741	1589	35.63
Brick	14.08	2.57	1093	1210	57.39
Marble	2.96	2.63	1571	1399	40.15
Ceramic	2.57	2.49	1196	1305	51.87

Specific gravity and water absorption of fine aggregates were determined according to ASTM C 128. Aggregates were tested in oven-dry condition utilizing the shoveling and rodding procedure to determine the unit weight (loose and rodded) and void content according to ASTM C 29-97. Chemical compositions of cement and waste aggregates are given in Table 2.

Table 2: Chemical compositions of materials used in mortar preparation by weight (%).

Materials	Na_2O	MgO	Al_2O_3	SiO_2	K_2O	CaO	Fe_2O_3
Cement	1.25	2.33	6.38	21.77	1.06	56.66	2.68
Brick	2.00	6.51	14.92	54.24	2.27	8.79	5.82
Marble	0.58	1.10	0.35	1.62	0.06	52.94	0.15
Ceramic	2.73	5.07	15.14	63.99	1.68	4.88	2.33

Cement: water: aggregate proportions in mixes were 1: 0.50: 3, respectively. Natural crushed sand was replaced with waste aggregates in a ratio of 30 % and 60 %. All substitutions were made in volume. The flow diameter values of fresh mortar mixtures were remained constant as 210±14 mm by adjusting the percentage of plasticizer used. All sample preparations were processed in a similar manner, according to European Standard EN 196-1. The mortars were cast into 40x40x160 mm prismatic moulds and kept for 24 h. The hardened mortar specimens were then demoulded and maintained under lime-saturated water at 20 ± 2 ^{o}C until the age of testing.

40x40x160 mm prismatic specimens were subjected to temperature of up to 400 ^{o}C at an incremental rate of 10 ^{o}C per minute from room temperature, using an electrically-heated furnace and exposed to a treatment involving freeze in air and thaw in water in a cabinet from -20 C to +20 C for 10 cycles completed in 2 days.

The consistency test involves placing the mould in the center of the flow table and filling it in two layers each layer being tamped 20 times with the tamper according to ASTM C 270. The table was then jolted 25 times, and the diameter of the spread mortar was measured in two directions at right angles to each other using callipers.

The bulk density, water absorption and porosity values were obtained by testing 100 mm cube specimens according to ASTM C 642. The flexural and compressive strength of hardened mortar specimens were determined in accordance with EN 1015-11. The flexural strength of a hardened mortar was evaluated by three point loading of a 160x40x40 mm prism specimen, subsequent to the failure and breakage of this specimen the compressive strength was determined on each half of the prism specimen. Three specimens of each formulation were prepared for each test.

Results and Discussion

The bulk density, water absorption and porosity test results are shown in Table 3. In contrast to CNA mortars, CBA mortars had the highest porosity and thus water absorption. However, the lowest apparent bulk density and dry bulk density were obtained by CCA and CBA mortars, respectively. The corresponding values dropped while the replacement ratios increased due to the high porosity of brick and ceramic aggregates.

Table 3: Bulk density, absorption and porosity of mortars.

Age	Specimen	Dry bulk density	Water absorp. (% wt.)	Apparent bulk density	Apparent porosity (%)
28 Days	CNA	2.09	5.72	2.37	11.93
	CBA30	1.96	7.98	2.32	15.61
	CMA30	2.03	6.28	2.32	12.73
	CCA30	2.02	5.96	2.30	12.07
	CBA60	1.88	10.50	2.34	19.76
	CMA60	2.05	6.08	2.34	12.47
	CCA60	2.01	5.26	2.24	10.56
56 Days	CNA	2.08	5.48	2.35	11.42
	CBA30	1.94	7.96	2.29	15.41
	CMA30	2.10	6.04	2.40	12.66
	CCA30	2.04	5.61	2.30	11.42
	CBA60	1.94	8.78	2.34	17.03
	CMA60	2.07	5.71	2.34	11.79
	CCA60	2.01	4.09	2.19	8.24

Table 4 gives the mechanical properties of 28 and 56-day mortars with and without treatments. The strength loss ratios due to the various treatments were higher for flexural strength than those for compressive strength. Generally, for all situations, CBA mortars exhibited the lowest mechanical properties and these properties

worsened with the substitution level owing to the high water absorption and open porosity percentages of brick aggregates. Although other mortars prepared with CNA, CCA and CMA showed close values, the best performance was observed by CCA mortars when considering reduction in strength values at overall situations. The resistance to high temperature was high for the CCA mortars when analyzing the relative residual compressive strength values. Besides, analyzing the relatively residual flexural strength values presented the superiority of CBA mortars. This fact can be attributed to the higher temperatures experienced by the bricks and ceramics previously in the manufacturing process. In addition, generally one face of ceramic aggregates was glazed, thus the proper adherence could not be achieved leading to lower flexural strength compared to CBA mortars. Exposing the freeze-thaw cycles to mortars weakened CBA mortars mostly rather than the other mortars. Despite similar behavior could be expected for CCA mortars, CCA mortars deteriorated less than CBA mortars. The reason of this result could be the structure of voids in the aggregates.

In contrast to CBA, CCA had mostly closed porosity seen also in SEM images (not presented in this study). The strength gain was more pronounced in the case of CBA and especially CCA mortars as relevant to the pozzolanic behavior of these mentioned aggregates containing amorphous silica and alumina phases. As compared to test results of specimens subjected to high temperature, the strength loss ratios of specimens exposed to freeze-thaw cycles were lower. The reason of this result could be the less number of cycles applied on specimens.

Table 4: Flexural and compressive strength values of mortars with and without treatments.

Age	Specimen	Flexural Strength (MPa)			Compressive Strength (MPa)		
		No treatment	High Temperature	Freeze-Thaw	No treatment	High Temperature	Freeze-Thaw
28 Days	CNA	8.6	5.8	8.0	43.8	36.2	42.3
	CBA30	7.7	6.2	6.7	39.0	33.1	34.2
	CMA30	8.1	5.6	7.4	42.1	34.2	40.4
	CCA30	8.5	6.3	7.8	43.0	38.1	41.2
	CBA60	6.8	5.7	5.8	37.4	32.4	32.5
	CMA60	7.8	5.1	7.2	40.2	34.7	37.4
	CCA60	7.9	5.6	7.5	42.8	38.9	41.7
56 Days	CNA	8.8	6.3	8.2	46.4	38.6	44.9
	CBA30	8.1	6.6	7.0	44.1	37.6	39.0
	CMA30	8.3	6.1	7.6	42.9	35.5	41.5
	CCA30	8.6	6.7	8.3	45.1	40.4	43.4
	CBA60	7.6	6.4	6.8	41.1	37.9	37.6
	CMA60	8.1	5.5	7.4	41.4	37.2	39.1
	CCA60	8.3	6.3	8.0	44.2	42.1	42.9

Conclusions

Following conclusions can be drawn from the experimental results:

Strength loss ratios after high temperature exposure tests of CCA and CBA mortars were lower than those of CMA and CNA mortars. However, particularly CBA had highest strength loss in the case of freeze-thaw cycle exposure due to the open void structure allowing high penetrability of water. Strength development was higher for CCA and CBA mortars at later age probably owing to the pozzolanic reactions resulting from high glassy phase content produced by sintering during manufacturing process.

Acknowledgements

This work was supported by Akdeniz University Scientific Research Center with Project number 2011.01.0102.009.

References

Aruntas, H. Y., Guru, M., Dayı, M., & Tekin, I. (2010). Utilization of waste marble dust as an additive in cement production. *Materials and Design*, *31*, 4039–4042.

Bektas, F., Wang, K., & Ceylan, H. (2009). Effects of crushed clay brick aggregate on mortar durability. *Construction and Building Materials*, *23*, 1909–1914.

Belaidi, A. S. E., Azzouz, L., Kadri, E., & Kenai, S. (2012). Effect of natural pozzolana and marble powder on the properties of self-compacting concrete. *Construction and Building Materials*, *31*, 251–257.

Böke, H., Akkurt, S., İpekoğlu, B., & Uğurlu, E. (2006). Characteristics of brick used as aggregate in historic brick-lime mortars and plasters. *Cement and Concrete Research*, *36*, 1115–1122.

Gonçalves, J. P., Tavares, L. M., Toledo Filho, R. D., & Fairbairn, E. M. R. (2009). Performance evaluation of cement mortars modified with metakaolin or ground brick. *Construction and Building Materials*, *23*, 1971–1979.

Hebhoub, H., Aoun, H., Belachia, M., Houari, H., & Ghorbel E. (2011). Use of waste marble aggregates in concrete. *Construction and Building Materials*, *25*, 1167–1171.

Higashiyama, H., Sappakittipakorn, M., Sano, M., & Yagishita F. (2012). Chloride ion penetration into mortar containing ceramic waste aggregate. *Construction and Building Materials*, *33*, 48–54.

Medina, C., Sánchez de Rojas, M. I., & Frías, M. (2012). Reuse of sanitary ceramic wastes as coarse aggregate in eco-efficient concretes. *Cement & Concrete Composites*, *34*, 48–54.

O'Farrell, M., Sabir, B. B., & Wild, S. (2006). Strength and chemical resistance of mortars containing brick manufacturing clays subjected to different treatments. *Cement & Concrete Composites*, *28*, 790–799.

Pacheco-Torgal, F., & Jalali, S. (2010). Reusing ceramic wastes in concrete. *Construction and Building Materials*, *24*, 832–838.

Senthamarai, R. M., Devadas Manoharan, P., & Gobinath, D. (2011). Concrete made from ceramic industry waste: durability properties. *Construction and Building Materials*, *25*, 2413–2419.

Study of the effect of pesticides on some physico-chemicals and microbiologicals parameters of soil and water in north-eastern Algeria

Ouahiba Bordjiba and Abdelhakim Belaze

BADJI Mokhtar Annaba University, P.O.Box 12, 23000 Annaba Algeria.
Faculty of Sciences, Department of Biology
Plant Biology and environmental Laboratory

E-mail: ouahiba_bordjiba@yahoo.fr

Abstract : Among the chemicals most commonly used currently in our environment, Those are undoubtedly pesticides and related products. If pesticides are at first appeared beneficial, harmful side effects have been gradually revealed. Their toxicity, due to the molecular structure is not limited indeed to only species that we wish to eliminate. They are particularly toxic to the various components of the environment.
Our study aims to assess the degree of pollution of soil and surface water in farming areas situated in the North-Est of Algeria and subject to the effect of pesticides for several years. To do this, the physico - chemical characteristics of water and soil were determined. The analyzes have focused on pH, BOD5,COD, electrical conductivity, organic matter, nitrites and nitrates. The total microflora samples of water and soil was also evaluated. The physico-chemical parameters studied were analyzed by standard methods according to the general guidelines for storage and manipulation. The fungal microflora was determined using identification keys. The identification of isolated and purified bacteria was instead performed by a scan apiweb software (Api web Biomerieux France).
The results show that there is a pollution of water and soil. The values of some parameters often exceed the prescribed standards and especially those of nitrite and electrical conductivity. The isolated microflora consists of 97% whose most frequent are Bacillus and Micrococcus and 3% of fungi with a predominance of Aspergillus.

Keywords: pesticides, physico-chemical parameters, water, soil, microflora, bacteria, fungi.

Introduction

Most pesticides used in developing countries are highly toxic chemicals. Approximately 73% of imports of pesticides belong to categories 1a (extremely toxic) and 1b (highly toxic) according to World Health Organization. Although the application of these pesticides ensures a certain quality of crop production (in particular the performance and phytosanitary quality), it contributes to contaminate the different compartments of the environment, especially soil and water resources.

Pesticides affect soil quality by reducing fertility (loss of nutriments and organic matter, reducing the total microbial biomass). Herbicides such as sulfonylureas, bensulfuron methyl (B) and metsulfuron methyl generate a considerable reduction of the soil microbial biomass (Taiwo and Oso, 1997; Boldt and Jacobsen, 2006; Baxter and al., 2008). Also Agricultural pesticides also pollute surface water and groundwater. This contamination is seasonal, the highest concentrations being measured during and after application of rainfall period (up to a few µg / l can then be measured in the samples analyzed). In recent years, various studies realized in Algeria have demonstrated the presence of many pesticides in water (Annaba, Algiers, Sétif) and also in our food: more than 50% of fruit and vegetables produced by intensive agriculture contain various molecules of pesticides. All these toxic compounds eventually end up in our organism, brought by the soil, water and food.

So ahead this situation, the main objective of our study was to check the quality of soils and waters surface in regions of north-eastern Algeria subject to the effect of several pesticides.

Material and methods

Collect of samples

Samples are taken from farming areas located in the north-eastern part of Algeria intended to the vegetable crops (tomato, potato, pepper and wheat) and subject to the effects of many pesticides. The main pesticides used are: bromuconazol, fluazifop- p butyl, cimoxanil, propineb, mancozeb, deltamethrine, pendimethaline and tebuconazol. Soil samples were collected in sterile tubes closed. They are then placed in the same conditions in which they are mixed to obtain a representative microflora, and then kept at 4 ° C until analysis. Water are collected in bottles designed

for water samples. These are stored at 4 ° C and transported to the laboratory on the same day with a view to analysis.

Analysis of physico-chemicals parameters

Regarding water, the analyzes focused on pH, electrical conductivity, BOD5, COD, nitrates and nitrites. The techniques used are those described by Rodier (1996). Regarding the soil, only the following parameters: organic matter, electrical conductivity, pH were evaluated by standard methods and compared with the scales reported in soltner (1981), Gaucher (1981) and durand et al., (1992) .

Evaluation of the total soil microflora

The suspension is prepared by the dilution method described in the standard DIN 54379 for the total count of colonies.

1 g of soil from each sample was stirred in 100 ml of sterile Ringer's solution (cassagne, 1966). The resulting suspension is diluted to 1/10th and 1/100th and 1/1000th from which 1 ml is taken that spread in a Petri dish and empty 10 ml of sterile culture medium. The dishes are incubated at 30 ° C temperature for 5 to 7 days.

Isolation of fungal species is made on PDA and Muller-hinton method of Warcup (Parkinson and Waid., 1960) by seeding depth. Aliquots of soil are distributed in Petri dishes (90 mm diameter) and covered with sterile nutrient medium. The petri dishes in triplicate for each case were incubated at 30°C

Identification of the microflora isolated

Bacterial isolates were purified by subculturing on Muller-Hinton. After studying the morphology, Gram staining and study of physico-chemical characteristics galleries with API 20 E and API 20 NE, identification is then performed by a scanning software API Web (Web API Biomerieux France) .
Regarding fungal strains after purification on Sabouraud medium, they are determined using identification keys de Botton et al., 1980 (Tome1 and 2)

Results and discussion

Analysis of water physico-chemicals parameters

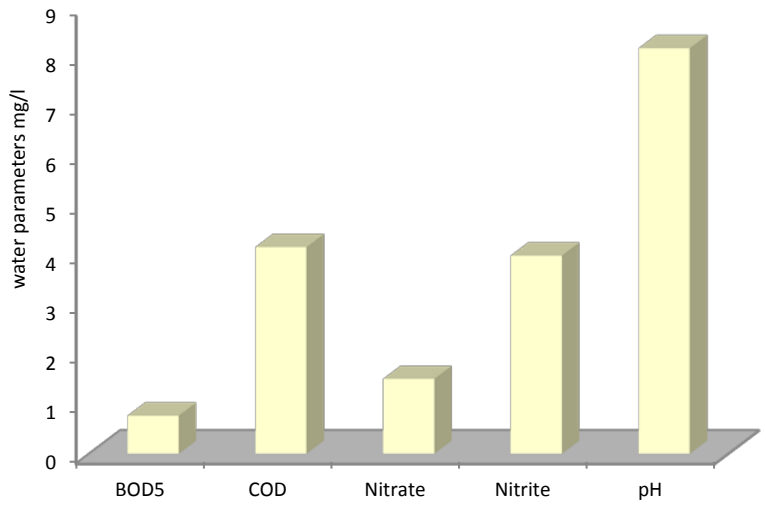

Figure 1 : mean values of physico-chemicals parameters of waters analyzed

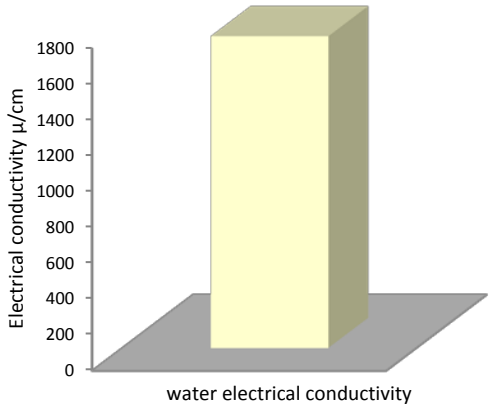

Figure 2 : Mean values of the electrical conductivity of waters analyzed

The physico-chemicals analyzes performed on water samples show firstly a high concentrations of nitrite (4 mg/l) above the allowable values which are between 1 and 3 mg/l, indicating the presence of toxic substances. Nitrites are toxic to organisms. It seems that the situation is very critical when a concentration is more than 3 mg/l of nitrite (Lisec, 2004). On the other hand, the values obtained for the electrical conductivity are also very high above international standards eligible with an average of 1745µ/cm. These high values show the presence of salts dissolved in water (MSPE, 1987). Other analyzed parameters appear below the standards values.

Analysis of physico-chemicals soil parameters

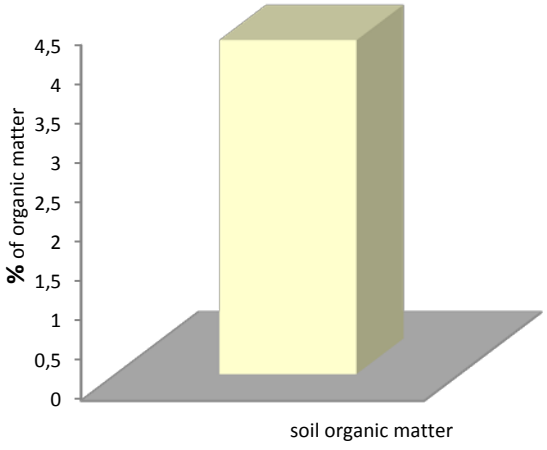

Figure 3 : Mean values of organic matter soils

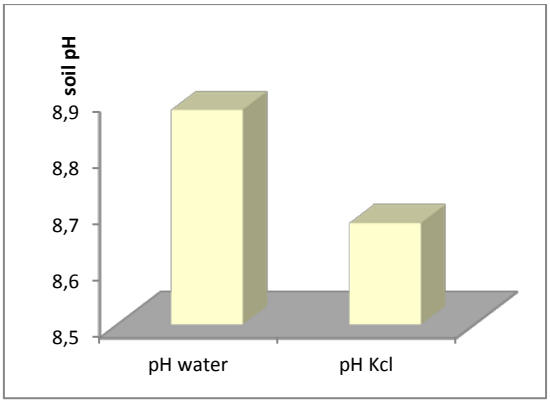

Figure 4 : mean values of pH soils

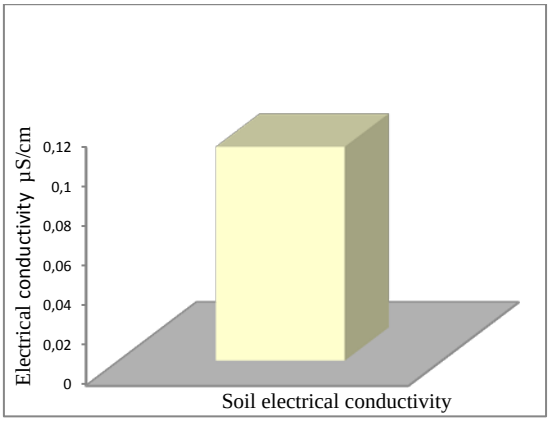

Figure 5 : Mean values of the electrical conductivity soils

The values of the parameters determined and compared with those of several authors scales indicated that the soil is rich in organic matter, with basic pH and unsalted poor in minerals with a very low conductivity probably due to the presence of pesticides.

Evaluation of the total soil microflora

Table 1: Evaluation of fungal and bacterial microflora of different analyzed soils

number of bacteria /gramme of soil	number of fungi / gramme of soil	Total
51407	1088	52495

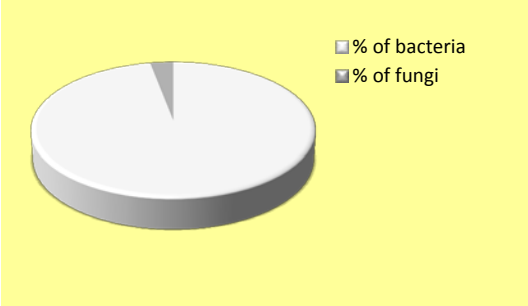

Figure 6 : percentage of bacteria and fungi/ gramme of soil analyzed

Table 2 : Identification of isolated soil microflora

bacterial strains	fungal strains
Aeromonas *Bacillus* *Chryseobacterium* *Micrococcus* *Pasteurella* *Pneumotropica* *Serratia* *Vibrio*	*Absidia* *Aspergillus* *Fusarium* *Penicillium* *Trichoderma*

The total microbial microflora isolated is composed of 52495colonies / g soil, most of which consists of bacteria (97%). The bacteria appear to be more tolerant to the effects of pesticides sprayed on the ground. The fungal microflora appears to be more sensitive because it is less abundant with a much smaller number (3%). In addition, we find that there is not much difference from a sample to another, the same genera are present in almost all samples with higher or lower frequencies.The most common bacteria are mainly *Micrococcus*, *Bacillus*, *Aeromonas*, *Chryseobacterium* and *Serratia*. *Aspergillus*, *Penicillium* and *Trichoderma* are the most predominant among fungal microflora.

Conclusion

This study allowed us to obtain a fairly rich microflora distributed almost uniformly throughout all sites. It is composed of several microbial species which may survive in the conditions of a highly polluted soil by the action of several herbicides, fungicides and insecticides. However, the growth of fungal species is sometimes inhibited in most samples. We think that this inhibition is probably due to the presence of pesticides in the treated soil.
The accumulated doses following repeated treatments for several years, become toxic to the fungal strains.
Micrococcus, *Bacillus* and *Aspergillus* particular are the most predominant microorganisms of the microflora. They are resistant to various pollutants and endure high concentrations of herbicides (Domsch and al., 1980; Sage and al., 1997 ; Steiman and al., 1992).

The distribution of the soil microflora is influenced by the characteristics of the habitat, such as, pH, organic matter content, humidity, soil texture and electrical conductivity.

References

Baxter, J & Lumming, S.P. (2008). The degradation of the herbicide bromoxynil and its impacts on bacterial diversity in a top soil. *Journal of Applied Microbiology*. 104 (6) : 1605-1616

Blieffert, C & Perraud, R. (2001). Chimie de l'environnement : air, eau sol, dechets. *Ed.Deboeck université* .

Boldt, TS., & Jacobsen, CS. (2006). Different toxic effect of the sulfonylurea herbicides metsulfuron methyl, chlorsulfuron and thifensulfuron methyl on fluorescent Pseudomonas isolated from an agricultural soil. *FEMS. Microbiology Letters*. 161 (1) : 29-35.

Botton, B. (1990). Moisissures utiles et nuisibles .Importance industrielle. *2eme Ed. Paris Masson*. 210-220.

Cassagne, H. (1996). Milieux de culture et leur application. *Ed. La tourelle. Saint-Mandé (Seine).* 2eme.ed. 379 p.

Domsch, K.H., Gams, W., & Anderson, T.H. (198). Compendium of soil fungi. Vol 1 et 2. *Academic. Press*. London.

Durand, P**.,** Neal, C., & Lelong., F. (1992). Effects of land-use and atmospheric input on stream and soil chemistry: field results and long term simulation at Mont-Lozere (Cevennes National Park, Southern France). *Sci. Tot. Environ*., 119, 191-209. (1.455).

Lisec. (2004). Contrôle van de fysicochemische kwalit eit van de viswaters van het brussels hoofdstedelijk Gewest. R*apport effectué pour le compte de l'IBGE*.
Parkinson, D & Waid, J. S. (1960). The ecology of soil fungi. Liverpool University Press.

Ministère de la santé publique et de l'environnement (MSPE). (1987). Arrêté royal du 4 novembre 1987 fixant les normes de qualité de base pour les eaux du réseau hysdrographique public relative aux déversement des eaux usées, dans les eaux de surface ordinaires. *MB du 21-11-87.*

Organisation mondiale de la santé (OMS). (2002). Directives de la qualité de l'eau de boisson. Genève 2002.

Rodier, J., Bazin, C.,B routin, J.P., Chambon, P., Champsaur H., & Rodi, L.(1996). L'analyse de l'eau. Eaux naturelles, eaux résiduaires, eaux de mer, 8ème edition. *Dunod (ed), Paris*.France.

Sage, L., Bennasser, L., Steiman, R., & Seigle-Murandi, F. (1997). Fungal microflora diversity as a function of pollution in oued Sebou (Morroco). *Chemosphere* 35(4): 751-759.

Steiman, R., Benoit-Guyod, J. L., Seigle-Murandi, F., & Muntalif, B**. (**1992). Degradation of pentachloronitrobenzene by micromycetes isolated from soil. *Sci. Tot. Environ*. 123/124 : 299-308.

Taiwo, L.B., & Oso, B. O. **(**1997). The influence of some pesticides on soil microbial flora in relation to changes in nutrient level roch phosphate solubilization and release under laboratory conditions. *Agric. Ecosyst. Environ*. 65 (1) : 59-68.

Study on Supercritical Fluid Extraction of Aromatic Compound from Roasted Cocoa Beans Using Multilevel Factorial Design

Azila A.K and Nur Aida, W.A.W.

Cocoa Innovation & Technology Centre, Malaysian Cocoa Board, PT12621, Nilai Industrial Area, 71800 Nilai, Negeri Sembilan, Malaysia
e-mail: aziela@koko.gov.my

Abstract: Extraction of aromatic compound from cocoa beans was carried out using Supercritical Fluid Extraction (SFE) in order to obtain natural cocoa extract for perfume formulation. The experiment was carried out by multilevel factorial design to investigate which factors; pressure (100, 125, 150 & 200 bar) and time (30, 45, 60 and 75 minutes), influence the extraction condition of cocoa aromatic (5-methyl-2-phenyl-2-hexenal), fatty acid (hexadecanoic acid) and alkaloid (caffeine) compounds. It was found out that the factors influence, significantly, yield of extract and extraction of fatty acid compound, while only pressure significantly affected amount of aromatic compound extracted. Extraction with high amount of aromatic compound (24.5mg/g extract) was obtained at 200 bar and 45 minutes. This result is used as a based to investigate further on the optimum condition to obtain high yield of aromatic compound in order to formulate the natural cocoa-scented perfume.

Keywords: Roasted Cocoa Bean, Supercritical Fluid Extraction, Aromatic Compound

Introduction

Cocoa aroma is contributed by at least by eleven groups of compounds (Table1), including pyrazines, esters, carbonyls, phenols and hydrocarbons (Jinap, et al. 1998; Jinap, et al. 2004). Acidic compounds such as acetic, isobutyric, isovaleric, hexanoic and pentanoic acids were reduced during roasting (Krysiak, et al. 2007). Van Praag, et al. (1968) suggested that cocoa aroma was contributed by aldehydes and pyrazines by extraction using steam distillation in three portions (acidic, neutral and basic). The basic fraction consists of compounds with nutlike smelling components such as alkyl substituted pyrazines, while the acidic fraction gave the slight phenolic odor. Among these three fractions, the neutral fraction was the most important as it contains 5-methyl-2-phenyl-2-hexanal which possess deep and bitter persistent cocoa note together with isovaleraldehyde and methyl disulfide. Furthermore, Bonvehi, et al. (2005) identified that 5-methyl-2-phenyl-2-hexenal gave the intense bitter taste to cocoa, as well as 4-methyl-2-phenyl-2-pentenal. In addition, chocolate aroma comes from 2,3,5,6-tetramethylpyrazine, while cocoa and roasted nuts aroma comes from 2,5-dimethylpyrazine. Caramelizing of sucrose during roasting increases furans compound in roasted cocoa beans.

Table 1: Examples of compounds contributes to cocoa aroma in roasted cocoa beans

Group	*Compounds (examples)*	*Aroma attributes*	***References***
Pyrazines	2,3,5,6-tetramethylpyrazine 2,5-dimethylpyrazine	Chocolate, cocoa, coffee cocoa and roasted nuts	Jinap, et al (1998) Bonvehi, et al (2002), Ducki, et al (2008)
Esters	Butyl acetate Ethyl benzoate	Fruity taste and aroma Fatty, fruity	 Bonvehi, et al (2005)
Carbonyls; aldehydes	5-methyl-2-phenyl-2-hexanal 4-methyl-2-phenyl-2-pentanal	deep and bitter persistent cocoa note	Bonvehi, et al (2005)
Phenols	Vanillin (phenolic aldehyde)	vanilla	Bonhevi, et al (2005)
Alcohols	2- heptanol Linalool [3,7-dimethylocta-1,6-dien-3-ol] Phenyl ethyl alcohol [2-phenylethanol]	fruity, herbal, sharp flowery aromatic chocolate note	 Frauendorfer, et al (2008)
Monoterpene hydrocarbons	Pinene Dimethyl-octane	Lemon like	Ducki, et al (2008)
Alkaloids	Caffeine Theobromine	coffee	Ducki, et al (2008)
Furans	2-methylfuran, tetrahydro-2-methylfuran	Sweet and caramel-like aroma of burnt sugar	Krings, et al (2006) Frauendorfer, et al (2008)
Acids	Acetic acid, Valeric acid, Butyric acid, Hexanoic acid, Pentanoic acid	Vinegar	Krysiak, et al (2007) Krings, et al (2006), Ducki, et al (2008)

Voight, et al. (1994) reported that the cocoa-specific aroma precursors were derived from the fermented cocoa seeds. The characteristic aroma of cocoa is a result of crude fermentation of fresh seeds, followed by drying and roasting (Bixler, et al. 1999). During the fermentation, fresh cocoa beans go through complex transformations: (1) the sugars from the mucilaginous pulp of the seeds are rapidly metabolized, producing volatile and nonvolatile organic acids; (2) the degradation of proteins to form peptides and free amino acids; (3) oxidation of polyphenols to form insoluble compounds, mainly *o*-quinones; and (4) hydrolysis of glycosides (mainly anthocyanins). In order for the aroma precursors to develop the cocoa aroma, the cocoa beans must undergo roasting processes. Alkalization during roasting process diminishes the heterocyclic compounds of pyrones and furaneol in cocoa beans (Ziegleder et al., 1991).

Supercritical fluid extraction (SFE) method has been widely used for the extraction of volatile components from plants due to its rapid, effective and solvent-free sample pre-treatment technique (Pourmortazavi, et al. 2007). SFE is highly recommended as an extraction method because it does not leave chemical residue, provide solvent-free product and the CO_2 gas can be recycled and used again as part of the unit operation (Otles, et al. 2009). Determination of optimal condition in SFE is influenced, greatly, by operating temperature and pressure especially in critical region (Gomes, 2007), although other parameters such as sample particle size, flow rate of SFE solvent, extraction time and operation mode have some affects. The two former parameters change the density and viscosity of the SFE solvent mimicking the properties of various conventional solvent as in phase diagram of CO_2 (Figure 1). It was shown that by maintaining certain temperature of extraction and varying the pressure, or vice versa, several density of extracting solvent (CO_2) can be achieved resulting various compounds can be expelled out of the samples, including fat, aromatic compound and alkaloids. Most aromatic and flavor compounds have molecular weight below 250, which are soluble in SF CO_2 (Gomes, 2007) and normally can be extracted at low pressure where SF CO_2 has low density (Reverchon, 1997).

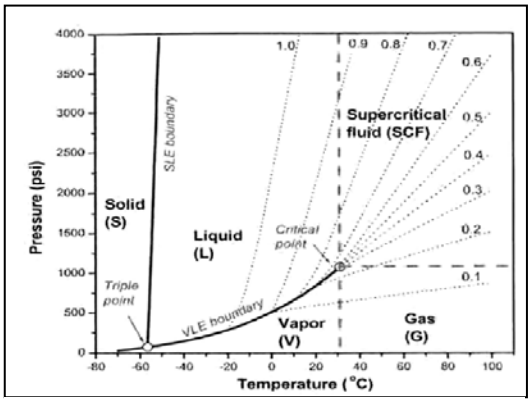

Figure 1: Density of SF CO2 by Temperature & Pressure (Anonymous, 2012)

This method had successfully extracted sesame seed oil (Corso, et al. 2010) and palm kernel oil (Zaidul, et al. 2007). Nevertheless, cocoa butter, polyphenols and pyrazines from cocoa were also successfully extracted *via* this method as reported by Saldana, et al. (2002); Sarmento, et al. (2008) and Sanagi, et al. (1997), respectively. Moreover, Sanagi et al (1997) conducted SFE at 200bar 60^{o}C with modifier to completely extract the pyrazines compounds. Meanwhile, Mohamed, et al. (2002) used high pressure of CO_2 and ethane at more than 152 bar resulting high recovery of cocoa butter, caffeine and theobromine compounds from cocoa beans. In addition, research on SFE cocoa butter was in depth as carried out by Asep, et al. (2008) and as mentioned. Ducki, et al (2008) conducted a research on using solid-phase micro-extraction (SPME) for headspace analysis in cocoa products for identification of cocoa aromatic compounds. SPME coupled with GC-FID was also used by Hasny (2012) in his research work on detection of aromatic compound from roasted cocoa beans. Despite all, most of cocoa aromatic compounds were reported based on study using conventional extraction. Research reports focusing on extraction of cocoa aromatic compound using SFE for perfumery application was also not in extensive. Fragrance application of cocoa extracted using SFE was also scarcely documented (King and Bott, 1993). Therefore this research was carried out to extract the aromatic compound from roasted cocoa beans using SFE in order to develop natural cocoa-scented perfume.

Materials and Procedure

Sample preparation

Fermented cocoa beans were collected from Cocoa Research and Development Centre at Jengka, Malaysia. A latest clone of MCB, namely MCB C1, was selected in this preliminary study, whereas other clones will be

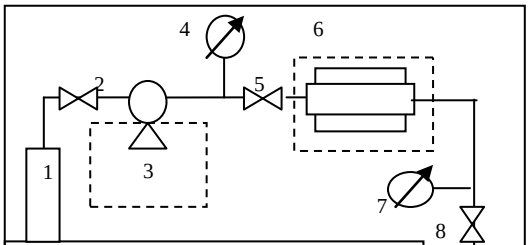

Figure 2: SFE Unit
1. Liquid CO_2 tank 2. Valve
3. Pump with chiller 4 .Flow rate indicator
5. Valve 6. Extraction vessel with insulator
7. Pressure indicator 8. Valve
9. Collection vessel

subjected to the next phase of extraction. The beans were then roasted in the oven at 135°C for 15 minutes. After shell removal, the beans were ground using warring blender and sieved to 1.0-0.5mm mesh size. Ground roasted beans were kept in tight container until extraction using SFE.

Supercritical Fluid Extraction

Extraction was carried out using SFE unit comprise of Intelligent HPLC Pump Model PU980 (Jasco Corporation, Tokyo, Japan) attached to cooling unit (Haake Fison DC 3). To achieve low temperature (-20°C), the cooling unit was operated with mixture of ethylene glycol-water (50:50 v/v). Ground cocoa beans at 10.15±0.16 grams were poured into sew white cloth and loaded into 25ml stainless steel tube (Thar Design, Inc., CL1043). To maintain temperature required, the column was inserted into Column Oven Model CO-960 (Jasco Corporation, Tokyo, Japan). Extraction pressure was controlled using Back Pressure Regulator (BPR) Model BP 880-81. Extraction was carried out using purified liquid carbon dioxide (CO_2) obtained from Linde Malaysia Sdn. Bhd. The used gas was dispersed into the air and the liquid sample was collected in a vials. Figure 2 is the illustration of SFE Unit.

Experimental Design

Multilevel factorial design was chosen for this study prior to optimization. At this stage, two factors were considered, namely pressure (bar) and time of extraction (min). There are four levels for each factor, resulting multilevel factorial design as in Table 2. Sixteen runs of experiments were carried out according to the standard order. Constant temperature at 35±2°C was selected in this study, where the density of SF CO_2 was manipulated (Figure 1). Responses measured were the amount of aromatic, fatty acid and alkaloid compound which represented by 5-methyl-2-phenyl-2-hexenal (cocoa hexenal), hexadecanoic acid and caffeine, respectively. In addition, yield of the extract was also considered.

Table 2: Parameters & Responses

	Parameters		*Responses*				*Total compounds detected*
Run Order	*Pressure (bar)*	*Time (min)*	*Yield (%)*	*Aromatic (mg/g)*	*Fatty acid (mg/g)*	*Alkaloids (mg/g)*	
1	125	45	0.70	5.25	85.05	7.70	19
2	200	75	1.46	8.01	307.28	13.38	16
3	100	75	0.57	5.41	78.63	14.53	17
4	125	75	0.79	9.97	339.38	531.21	8
5	200	45	1.20	24.50	396.22	467.93	15
6	150	75	1.29	18.76	288.46	254.83	18
7	100	60	0.19	2.56	15.96	24.33	18
8	100	45	0.19	2.25	22.65	36.27	14
9	125	60	0.39	6.19	77.12	68.33	19
10	200	60	1.34	14.81	344.62	208.65	18
11	125	30	0.30	4.35	21.75	21.15	19
12	200	30	0.89	10.6	62.19	111.94	16
13	150	60	1.19	14.87	197.42	122.50	13
14	150	45	0.80	11.18	163.27	94.61	16
15	100	30	0.20	0.88	7.32	3.51	14
16	150	30	0.69	6.18	55.3	51.86	21

Determination of compound in the extract

Absolute extract was transferred into gas chromatography (GC) vials by rinsing using 2.5ml n-hexane (Merck) followed by 2.5ml ethanol (HmbG). The calculation for amount of compound was based on the percentage area of each compound from the total yield of extract multiplying by the dilution factor (1:5) based on the solvent used to rinse the extract. Higher amount of compound extract indicated potential pressure and time to be used in further experimental works. Prior to GC-Mass Spectrophotometric (GC-MS) identification, the crude extract was filtered using C18-SepPak column (Supelco) with acetonitrile as the carrier to obtain clean extract. One µl sample was injected into the GC-MS system (Agilent Tech 7890A GC system). The GC-MS system has split-splitless column injector with mass spectrum detector (Agilent Tech System 5975C). Column of HP5MS (Agilent J&W) with dimension 30m x 0.25m i.d x 0.25µm was used in detection of compound. The condition was set at 220°C, 6.544 bar with helium as gas carrier. Library of National Institute of Standards & Technology (NIST 08) was used.

Statistical analysis

Minitab software Release 14 was used for statistical design and data analysis in this study. For this study, all the results were categorized as significant when the p-value is less than 0.05. The values were reported by mean.

Results and Discussion

From the statistical analysis, the pressure and time of extraction were significantly affecting the yield, at p=0.000 and p=0.001, respectively. However, no interaction between the parameters was obtained. The linear model equation obtained, using linear regression analysis, for yield is, YIELD =-1.16+0.00954*PRESSURE+0.0105*TIME (R^2=0.8700). It was indicated from this equation that yield was proportional to the increasing of pressure at nearly ten times in ratio with the time of extraction. The main effect plot for yield was plotted in Figure 3. In addition, pressure at 200 and 150bar has higher effect to the yield in comparison with the lower pressures, which however affecting at longer extraction time.

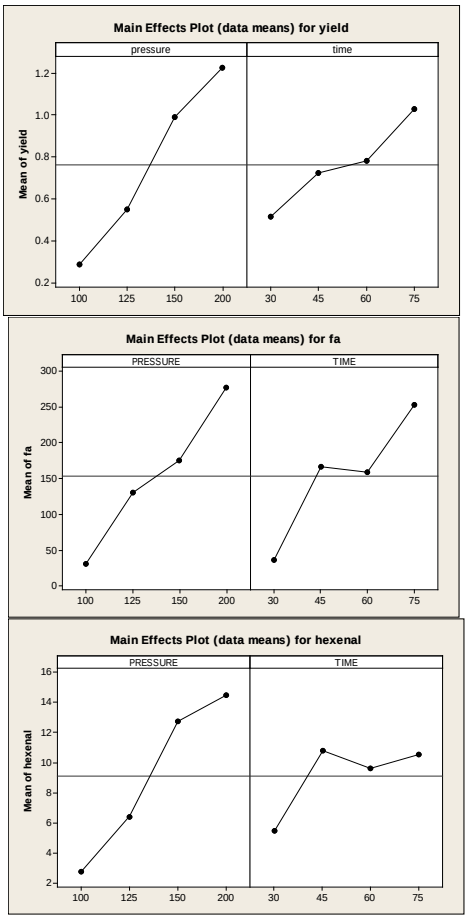

Figure 3: Plots for yield, fatty acid (fa) and aromatic (hexenal) compounds

Pressure and time of extraction was significantly affecting the amount of fatty acid compound extracted in this study at p-value of 0.015 and 0.032, respectively. The main effects were plotted separately in Figure 3 as there is no interaction between the two factors. Among these factors, only pressure has significant effect to the amount of aromatic compound extracted (p=0.022), whereas alkaloids compound was not significantly affected. By referring to Figure 1, the density of SF CO_2 was identified according to operation pressure and temperature. As the temperature was constant, the density was proportional with the pressure. Density of SF CO_2 in this study was 700, 725, 815 and 900kg/m^3, which significantly affected the yield and amount of aromatic compounds at p=0.001 and 0.015, respectively (at 35±2°C).

The amount of fatty acid compounds extracted by this method was significantly higher than the aromatic compounds. Reverchon (1997) reported that this is due to the SF CO_2 behavior of lipophilic solvent, but with adjustable selectivity, which extract lipid compound easily. It is also regarding to the position of paraffin and waxes substances on the surface and surrounding the vacuoles in plant materials which make its easily extracted using SFE. In addition, fat content in cocoa beans is more than 50% of the total weight of dry beans. Therefore, it was not surprising that extraction at any pressure point will result certain amount of fatty acid in the extract. There are two possible solutions worth trying at to overcome this condition, first, is by additionally using serial separators at different temperature and pressure are recommended to be applied to fractionate paraffin and waxes from aromatic compound extracted using SFE. Secondly, the extraction can be carried out at low pressure with high temperature to obtain low SF CO_2 density, where low molecular weight compounds, especially the aromatic compounds, can be extracted (Gomes, 2007).

Although the responses in this study was focusing on three compounds representing the

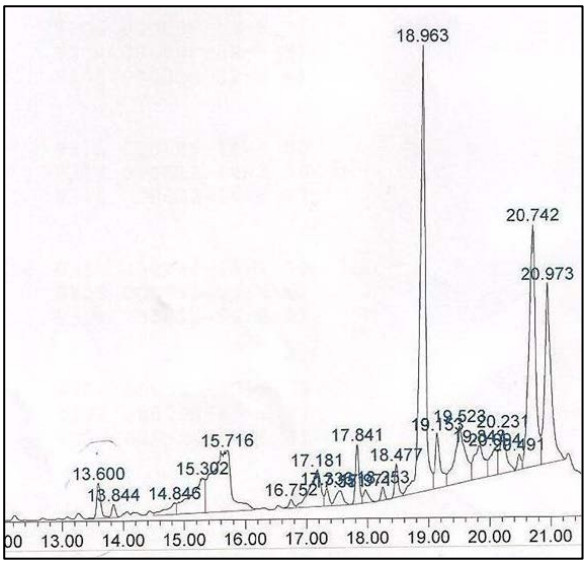

Figure 4: GC-Chromatogram for run 5

numbers of compounds that being identified using GC-MS, there are few aromatic compounds mentioned in Table 1 were not detected in the extract. For example, Ziegleder (1997) mentioned that high amount of linalool, contributed to the flowery and tea-like fragrance in flavor grade cocoa beans, which however absent in extract of cocoa bean in this study. Another key compound, 2,3,5-trimethyl-6-butylpyrazine was only detected at run 5 (pressure 200 bar, time of extraction 45 minutes). Low pyrazines compound was expected as alkalization process was omitted in sample preparation. Alkalization process is an essential step in cocoa processing to develop various color of cocoa powder and enhance the sensorial properties of final cocoa products. Figure 4 was the example of chromatogram for run 5. Other compounds listed in Table 1 were detected in each run (not discussed here). Total numbers of compounds detected for each run was listed in Table 2.

Conclusion

Cocoa aromatic compound can be extracted at 200bar with time of extraction for 45minutes, which however resulting higher amount of fatty acid compounds which is interference in this study. To use this condition, the SFE unit has to be modified with the addition of serial separators to fractionate the extract. On the other hand, lower pressure can be implemented coupled with higher temperature to create $SFCO_2$ with low density that can expel out the aromatic compound that has low molecular weight. The progress on this research is underway to perform these methods in order to obtain high yield of cocoa aromatic compound for formulation of natural cocoa-scented perfume.

Acknowledgement

This project was funded by Ministry of Science Technology and Innovation of Malaysia Government under project number 06-03-13-SF0067. This research was also supported by Malaysian Cocoa Board in providing the facilities and laboratories to carry out this study. The authors would like to express their appreciation to those who involve in data collection in this study.

References

Anonymous (2012). Microweighing in supercritical Carbon Dioxide Part 1 (Nanotechnology). *what-when-how.com/nanoscience-and-nanotechnology*. Date access: 22/10/2012.

Asep, E.K., Jinap, S., Tan, T.J., Russly, A.R., Harcharan, S., Nazimah, S.A.H. (2008). The effects of particle size, fermentation and roasting of cocoa nibs on supercritical fluid extraction of cocoa butter. *Journal of Food Engineering*, 85; 450-458.

Bachu, S. (2002). Sequestration of CO_2 in geological media in response to climate change: road map for site selection using the transform of geological space into the CO2 phase space. *Energy Conversion & Management*, 43; 87-102.

Bixler, R. G. and Morgan, J. N. (1999). Cocoa bean and chocolate processing. In *Chocolate and Cocoa*; Knight, J.,pg 43-60.

Bonhevi, J.S. (2005). Investigation of aromatic compounds in roasted cocoa powder. *Eur Food Res Technol*, 221; 19-29.

Bonhevi, J.S.; Coll, F.V. (2002). Factors affecting the formation of alkylprazines during roasting treatment in natural and alkalinized cocoa powder. *J. Agric. Food Chem.*, 50; 3743-3750.

Corso, P.M., Fagundes-Klen, M.R., Silva, E.A., Filho, L.C., Santos, J.N., Freitas, L.S. and Dariva, C. (2010). Extraction of sesame seed (*sesamun indicum* L.) oil using compressed propane and supercritical carbon dioxide. *J. Supercritical Fluids*. 52:56-61.

Ducki, S., Garcia, J.M., Zumbe, A., Tornero, A., Storey, D.M. (2008). Evaluation of solid-phase micro-extraction coupled to gas chromatography-mass spectrometry for the headspace analysis volatile compounds in cocoa products. *Talanta*, 74; 1166-1174.

Frauendorfer, F., Shieberle, P. (2008). Changes in key aroma compounds of Criollo cocoa beans during roasting. *J.Agric. Food Chem.* 56(21); 10244-10251.

Gomes, P.B., Matta, V.G., Rodrigues, A.E. (2007). Production of rose geranium oil using supercritical fluid extraction. *J. of Supercritical Fluids*, 41; 50-60.

Hasny, M.S. (2012). Optimisation of cocoa bean roasting conditions based on the development of flavour compound. *Thesis*, Universiti Teknologi MARA

Jinap, S. (2004). Cocoa – Wonders for Chocolate Lovers. *Inaugural Speech*. UPM.

Jinap, S., Wan Rosli, W.I., Russly, A.R., Nordin, L. (1998). Effect of temperature and time on sensory quality of cocoa beans during nib roasting. *Journal of The Science of Food and Agriculture*, 77, 441-448.

King, M.B., Bott, T.R. (1993). Extraction of natural products using near-critical solvents. Chapmann & Hall. Pp.1-31.

Krings, U., Zelena, K., Wu, S., Berger, R.G. (2006). Thin-layer high-vacuum distillation to isolate volatile flavour compounds of cocoa powder. *Eur Food Res Technol*, 223; 675-681.

Krysiak, W., Majda, T., Nebesny, E. (2007). An effect of relative air humidity on the content of volatile compounds in roasting cocoa beans. In *Focus on Food Engineering Research and Development.* Vivian, N.P. (Eds). Pp. 467-482. Publisher: Nova Science, Inc.

Mohamed, R.S., Saldana, M.D.A., Mazzafera, P. (2002). Extraction of caffeine, theobromine, and cocoa butter from Brazilian cocoa beans using supercritical CO2 and ethane. *Ind. Eng. Chem. Res.* 41; 6751-6758.

Moyler, D.A. (1993). Extraction of flavours & fragrances with compressed CO_2. In *Extraction of natural products using near critical solvents.* King, M.B., Bott, T.R. (Editors). U.K.: Blackie Academic & Professional. pp.165-166.

Otles, S. (2009). Handbook of Food Analysis Instruments. pg. 35.

Pourmortazi, S.M., Hajimirsadeghi, S.S. (2007). Supercritical fluid extraction in plant essential and volatile oil analysis. *J. Chromatogr. A.*, 1163; 2-24.

Reverchon, E. (1997). Supercritical fluid extraction and fractionation of essential oils and related products. *J. of Supercritical Fluids.* 10; 1-37.

Sahena, F., Zaidul, I.S.M., Jinap. S., Karim, A.A., Abbas, K.A., Norulaini, N.A.N., Omar, A.K.M. (2009). Application of supercritical CO2 in lipid extraction – A review. *Journal of Food Engineering,* 95; 240 – 253.

Saldana, M.D.A., Mohamed, R.S., Mazzafera, P. (2002). Extraction of cocoa butter from Brazilian cocoa beans using supercritical CO2 and ethane. *Fluid Phase Equilibria,* 194-197; 885-894.

Sanagi, M.M., Hung, W.P., Yasir, S.M. (1997). Supercritical fluid extraction of pyrazines in roasted cocoa beans: Effects of pod storage period. *J. Chromatogr. A.*, 785; 361-367.

Sarmento, L.A.V., Machado, R.A.F., Petrus, J.C.C., Tamanini, T.R. and Bolzan, A. (2008). Extraction of polyhenols from cocoa seeds and concentration through polymeric membranes. *J. Supercritical Fluids*. 45:64-69.

Van Praag, M.; Stein, H. S. and Tibbetts, M. S. (1968). Steam volatile aroma constituents of roasted cocoa beans. *J. Agric. Food Chem.* 16:1005-1008.

Voigt, J., Heinrichs, H., Voigt, G., Beihl, B. (1994). Cocoa-specific aroma precursors are generated by proteolytic digestion of the vicilin-like globulin of cocoa seeds. *Food Chem.*, 50; 177-184.

Zaidul, I.S.M., Nik Norulaini, N.A., Mohd Omar, A.K. and Smith, Jr. R.L. (2007). Supercritical carbon dioxide extraction of palm kernel oil from palm kernel. *J. Food Eng*. 79:1007-1014.

Ziegleder, G. (1990). Linalool contents as characteristic of some flavor grade cocoas. *Zeitschrift für Lebensmittel-Untersuchung und -Forschung,* 191(4-5); 306-309.

Ziegleder, G. (1991). Composition of flavor extracts of raw and roasted cocoas. *Z Lebensm Unters Forsch,* 192; 521-525.

Supplier Selection for Automotive Industry Using Multi-Criteria Decision Making Techniques

Özer Uygun[1], Hasan Kaçamak[1], Gizem Ayşim[2], Fuat Şimşir[3]
[1] Department of Industrial Engineering, Sakarya University, Serdivan, Turkey
[2]Undergraduate Student, Department of Industrial Engineering, Sakarya University, Serdivan, Turkey
[3] Department of Industrial Engineering, Karabük University, Karabük, Turkey
e-mail:ouygun@sakarya.edu.tr

Abstract: This paper is aimed to suggest an approach for evaluating and selecting suppliers for an automotive manufacturing company, based on multi-criteria decision making methods. As an initial step, main criteria and sub-criteria which affect the evaluation and selection process of a supplier are identified. Secondly, DEMATEL approach is implemented to the main criteria in order to expose cause and affect interrelationship among them which is required by Analytic Network Process (ANP) method. At the third step, ANP methodology is applied for calculating the weights of each sub-criterion. After obtaining the weights of the sub-criteria, alternative suppliers are evaluated and ranked using TOPSIS method. At the end, the supplier with the highest performance indices is selected as the best supplier.

Key words: Supplier selection, multi-criteria decision making, DEMATEL, ANP, TOPSIS.

Introduction

An automotive manufacturing corporation is a global organization. It requires various technologies to produce a vehicle such as electronics, mechanics, engine technology, tire technology and so on. Each of these technologies is an industry in itself which needs special expertise. It is almost impossible for a main manufacturer to own all the technologies needed to produce such vehicle. Thus, as Razmi et al. (2009) indicated, these organizations must concentrate on their main operations and organizational goals, and outsource all non-strategic operations. To be competitive in a global marketplace, especially in automotive industry, supplier evaluation and selection is a vital process. Proper purchasing strategies, and especially proper suppliers, can play a key role in management of successful organizations and it is worthwhile to invest on making appropriate decision on supplier selection (Razmi et al., 2009).

The studies on supplier selection have begun in 1960s. Dickson (1966) has made an analysis of vendor selection and identified 23 different factors such as quality, delivery, price, performance history, warranties, technical capability, etc. His study showed that quality is the most important criteria and it is followed by delivery and then performance history.

There are several approaches for supplier evaluation and selection. Some of these approaches are data envelopment analysis (Wu et al., 2007; Saen, 2007; Ross et al., 2006), mathematical programming (Ng, 2008; Karpak et al., 2001; Wadhwa and Ravindran, 2007) such as linear programming, goal programming, multi-objective programming, analytic hierarchy process (Hou and Su, 2007), analytic network process (Gencer and Gürpinar, 2007), case-based reasoning (Choy and Lee, 2002) and genetic algorithms (Ding et al., 2005). Ho et al. (2010) mentions that there are several articles reviewing the literature about supplier evaluation and selection models up to 2000 and they have extended them by surveying the multi-criteria supplier evaluation and selection approaches from 2000 to 2008.

The selection process mainly involves evaluation of different alternative suppliers based on different criteria. This process is essentially considered as a multiple criteria decision-making (MCDM) problem which is affected by different tangible and intangible criteria (Önüt et al., 2009).

In this study, hybrid multi-criteria decision making approach is proposed and implemented for evaluating and selecting the most suitable supplier in automotive industry. This approach includes DEMATEL technique for revealing cause and effect interaction among criteria, analytic network process for obtaining the weights of the

sub-criteria based on the result of the DEMATEL method, and TOPSIS method for evaluating and ranking the alternative suppliers according to the sub-criteria and the weights. Main criteria and their related sub-criteria are investigated and determined as given in Fig. 1.

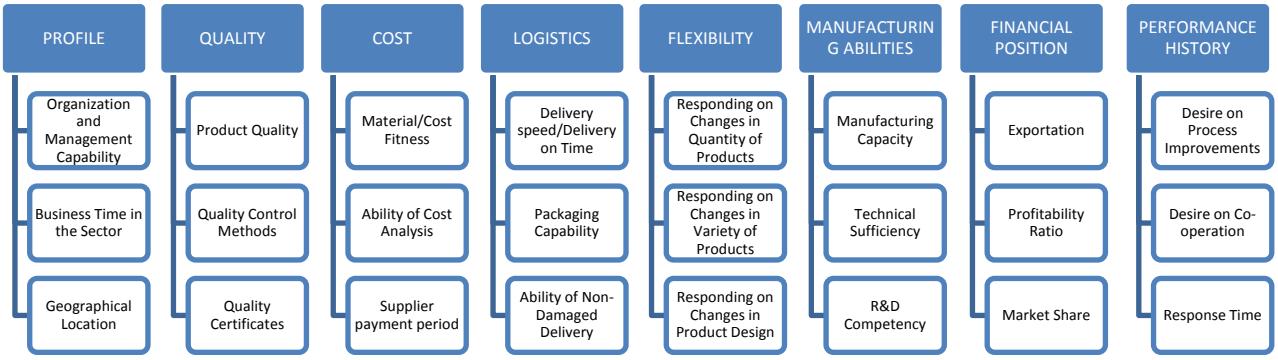

Fig. 1. Main criteria and related sub-criteria for supplier selection model.

Literature Review

A number of alternative approaches have been proposed for supplier evaluation and selection, called mathematical programming models, multiple attribute decision aid methods, cost-based methods, statistical and probabilistic methods, combined methodologies and other methods (Önüt et al., 2009). However, supplier selection process mainly involves evaluation of several alternatives based on different criteria. For that reason, multi-criteria decision-making (MCDM) approaches are used to deal with the selection process.

Extensive multi-criteria decision making approaches have been proposed for supplier selection, such as the analytic hierarchy process (AHP), analytic network process (ANP), case-based reasoning (CBR), data envelopment analysis (DEA), fuzzy set theory, genetic algorithm (GA), mathematical programming, simple multi-attribute rating technique (SMART), and their hybrids (Ho et al., 2010).

Gencer and Gürpinar (2007) developed a model aiming the usage of ANP in supplier selection owning to the evaluation of the relations between supplier selection criteria in a feedback systematic. The proposed model was implemented in an electronic company. Demirtas and Üstün (2008) proposed an integrated approach of ANP and multi-objective mixed integer linear programming for considering both quantitative and qualitative factors in choosing the best suppliers and defining the optimum quantities among selected suppliers to maximize the total value of purchasing and minimize the budget and defect rate. They evaluated four different plastic molding firms working with a refrigerator plant according to fourteen criteria that are involved in the four clusters: benefits, opportunities, costs and risks (BOCR).

Ming-Lang et al. (2009) proposed a novel hierarchical evaluation framework to assist the expert group to select the optimum supplier with ANP and choquet integral with reference to multiple conflicting criteria in supply chain management system (SCMS).

Dalalah et al. (2011) proposed a hybrid fuzzy model for group multi-criteria decision making. A modified fuzzy DEMATEL model was presented to deal with the influential relationship between the evaluation criteria. In addition, a modified TOPSIS model was proposed to evaluate the alternatives according to each criterion. Hsu and Hu (2009) presented an ANP approach to incorporate the issue of hazardous substance management (HSM) into supplier selection. In their study they proposed a multi-criteria decision model in which identification of criteria of HSM competence is categorized into four dimensions.

There are also studies concerning fuzzy set theory integrated with multi-criteria decision making methods. Some of the literature review about fuzzy multi-criteria decision making applications is given in the following part of this section.

Kilincci and Onal (2011), investigated the supplier selection problem of a washing machine company in Turkey, and a fuzzy AHP based methodology was used to select the best supplier firm providing the most customer satisfaction for the criteria determined. Lee (2009) also proposed fuzzy AHP to evaluate various aspects of suppliers

and selecting them under fuzzy environment which incorporates the BOCR concept. A case study of backlight unit supplier selection was presented for a TFT-LCD manufacturer in Taiwan. Vinodh et al. (2011) used fuzzy ANP approach for the supplier selection process and the case study has been carried out in an Indian electronics switches manufacturing company. Razmi et al. (2009) aimed to develop a fuzzy ANP model to evaluate the potential suppliers and select the best one(s) with respect to the vendor important factors. They have augmented the model with a non linear programming model to elicit eigenvectors from fuzzy comparison matrices.

Chang et al., (2011) claims that their study pioneers in using the fuzzy decision-making trial and evaluation laboratory (DEMATEL) method to find influential factors in selecting suppliers. They designed a fuzzy DEMATEL questionnaire which is sent to seventeen professional purchasing personnel in the electronic industry.

Önüt et al, (2009) developed a supplier evaluation approach based on the ANP and TOPSIS methods to help a telecommunication company in the GSM sector in Turkey under the fuzzy environment. Boran et al. (2009) proposed TOPSIS method combined with intuitionistic fuzzy set to select appropriate supplier in group decision making environment. Intuitionistic fuzzy weighted averaging (IFWA) operator is utilized to aggregate individual opinions of decision makers for rating the importance of criteria and alternatives. They have given a numerical example for supplier selection to illustrate application of intuitionistic fuzzy TOPSIS method. Wang et al. (2009) simplified the complicated metric distance method which was introduced by Chen and Chang (2005) and they proposed an algorithm to modify Chen's (2000) Fuzzy TOPSIS. From experimental verification, Chen directly assigned the fuzzy numbers $\tilde{1}$and $\tilde{0}$ as fuzzy positive ideal solution (PIS) and negative ideal solution (NIS). They claimed that Chen's method sometimes violates the basic concepts of traditional TOPSIS. Thus their study proposed fuzzy hierarchical TOPSIS, which can provide more objective and accurate criterion weights, while simultaneously avoiding the problem of Chen's Fuzzy TOPSIS.

Methodology

In this study, hybrid DEMATEL, ANP and TOPSIS methods are implemented in a combined way. Thus these methods are explained in this section.

DEMATEL Method

The Battelle Geneva Institute created DEMATEL in order to solve difficult problems that mainly involve interactive man model techniques as well as to measure qualitative and factor linked aspects of societal problems. (Gabus and Fontela, 1972). It analyzes the influential status and strength between the factors and convert them into an explicit structural mode of a system (Lin and Wu, 2008). The mathematical concepts are then evolved and adapted in many academic fields, such as industrial strategy analysis, competence evaluation, solution analysis, selection, and etc. It has been proven as a useful method to solve complicated problems.

The DEMATEL methodology construction process is described below;

Step 1: Generating the direct-relation matrix.

A group of experts is asked to make pairwise comparisons in terms of influence between criteria. An evaluation scale of 0, 1, 2, 3, and 4 is used for comparison, representing "no influence", "low influence", "medium influence", "high influence" and "very high influence", respectively. The results of these evaluations form an $n \times n$ matrix for each respondent expert where the x_{ij}^k is the score given by the *k*th expert indicating the influential level that factor *i* has on factor *j*. To incorporate all opinions from *K* experts, the direct-relation matrix *A* is calculated using Eq. (1) by averaging each expert's scores.

$$a_{ij} = \frac{1}{K}\sum_{k=1}^{K} x_{ij}^k \quad (1)$$

Step 2: Normalizing the direct-relation matrix.

The normalized direct-relation matrix *M* can be obtained by normalizing *A* using Eqs. (2) and (3).

$$M = k.A \quad (2)$$

$$k = Min\left(\frac{1}{\max_{1\le i\le n}\sum_{j=1}^{n} a_{ij}}, \frac{1}{\max_{1\le j\le n}\sum_{i=1}^{n} a_{ij}}\right) \quad (3)$$

Step 3: Obtaining the total-relation matrix.

The total-relation matrix *T* can be obtained by using Eq. (4), where *I* denotes the identity matrix.

$$\mathrm{T} = \mathrm{M} + \mathrm{M}^2 + \mathrm{M}^3 + \ \ldots = \sum_{\mathrm{i}=1}^{\infty} \mathrm{M}^{\mathrm{i}} = \mathrm{M}(\mathrm{I} - \mathrm{M})^{-1} \quad (4)$$

where $T = \left[t_{ij}\right]_{n\times n}, i, j = 1, 2, \ldots, n.$

Step 4: Compute the dispatcher group and receiver group.

The vectors *D* and *R* represent the sum of rows and columns of matrix *T* respectively, as shown in Eqs. (5) and (6). *D* + *R* value indicates the degree of importance that the corresponding criterion plays in the entire system. The factor having greater value of *D* + *R* has more interrelationships with other factors. On the other hand, criteria having positive values of *D* – *R* are on the cause group and dispatches effects to the other criteria. On the contrary, criteria having negative values of *D* – *R* are on the effect group and receive effects from the other criteria.

$$D = \sum_{j=1}^{n} t_{ij} \quad (5)$$

$$R = \sum_{i=1}^{n} t_{ij} \quad (6)$$

Step 5: Set up a threshold value to obtain the causal diagram.

Since the total-relation matrix *T* provides the information on how one criterion affects another, decision maker group should set up a threshold value in order to filter out some negligible relationships. This way enables the decision maker to choose only the relationships greater than the threshold value and to map the cause-effect relationship accordingly. The causal diagram can be acquired by mapping the dataset of the (*D* + *R*, *D* – *R)* where the horizontal axis *D* + *R* and the vertical axis *D* – *R*.

ANP Method

Analytic network process (ANP) is the general form of analytic hierarchy process (AHP) and was proposed by Saaty (1996) to overcome the problem of interrelation among criteria or factors. It provides measurements to derive ratio scale priorities for the distribution of influence between factors and groups of factors in the decision (Saaty, 2001). The feedback structure does not have the top to bottom form of a hierarchy but looks more like a network, with cycles connecting its components of elements, which we can no longer call levels, and with loops that connect a component to itself (Saaty, 2005).

Through a supermatrix, whose entries are themselves matrices of column priorities, the ANP synthesizes the outcome of dependence and feedback within and between clusters of elements (Yang and Chang, 2012). The initial supermatrix must be transformed to a matrix in which each of its columns sums to unity. For this reason, this matrix must be normalized by the cluster's weight to get the column sums to unity. Hence, the weighted supermatrix is obtained (Saaty and Vargas, 1998). The supermatrix representation is given in Fig. 2.

$$W = \begin{array}{c} \\ C_1 \\ \\ \\ C_2 \\ \\ \vdots \\ C_m \\ \\ \end{array} \begin{array}{c} \begin{array}{cccccccccc} C_1 & & & & C_2 & & \ldots & & C_m & \\ e_{11} & \ldots & e_{1n_1} & e_{21} & \ldots & e_{2n_2} & \ldots & e_{m1} & \ldots & e_{mn_m} \end{array} \\ \begin{pmatrix} W_{11} & & W_{12} & \ldots & W_{1m} \\ W_{21} & & W_{22} & \ldots & W_{2m} \\ \vdots & & \vdots & \ddots & \vdots \\ W_{m1} & & W_{m2} & \ldots & W_{mm} \end{pmatrix} \end{array} \begin{array}{l} e_{11} \\ \vdots \\ e_{1n_1} \\ e_{21} \\ \vdots \\ e_{2n_2} \\ \vdots \\ e_{m1} \\ \vdots \\ e_{mn_m} \end{array}$$

Fig. 2. The supermatrix representation

Pairwise comparisons between the criteria can be implemented according to dependency relationships which are obtained from DEMATEL approach in order to generate local weights assessing relative importance value using a scale of 1 (equal importance) to 9 (extreme importance).

TOPSIS Method

The technique for order preference by similarity to an ideal solution (TOPSIS) was proposed by Hwang and Yoon (1981) and expanded by Chen and Hwang (1992). The main principle in TOPSIS method is that, in a graph, any chosen alternative should have the shortest distance from the ideal solution and the farthest distance from the negative-ideal solution (Opricovic and Tzeng, 2004).

The TOPSIS technique is implemented using the following steps (Triantaphyllou, 2000; Opricovic and Tzeng, 2004):

Step 1. Calculate the normalized decision matrix. D is the decision matrix which refers to *n* alternatives that are evaluated in terms of *m* criteria.

$$D = \begin{bmatrix} x_{11} & \cdots & x_{1n} \\ \vdots & \ddots & \vdots \\ x_{m1} & \cdots & x_{mn} \end{bmatrix}$$

R is the normalized decision matrix and r_{ij} is an element of *R*. The normalized value r_{ij} is calculated as:

$$r_{ij} = \frac{x_{ij}}{\sqrt{\sum_{j=1}^{m} {x_{ij}}^2}}, \quad i = 1, \dots, m; \quad j = 1, \dots, n \tag{7}$$

Then the *R* matrix is formed as follows:

$$R = \begin{bmatrix} r_{11} & \cdots & r_{1n} \\ \vdots & \ddots & \vdots \\ r_{m1} & \cdots & r_{mn} \end{bmatrix}$$

Step 2. Calculate the weighted normalized decision matrix. V is the weighted normalized decision matrix and v_{ij} is an element of *V*. The weighted normalized value v_{ij} is calculated as:

$$v_{ij} = w_i r_{ij}, \quad i = 1, \dots, m; \quad j = 1, \dots, n \tag{8}$$

where w_i is the weight of the *i*th criterion and $\sum_{i=1}^{m} w_i = 1$. Then the *V* matrix is formed as follows:

$$V = \begin{bmatrix} v_{11} & \cdots & v_{1n} \\ \vdots & \ddots & \vdots \\ v_{m1} & \cdots & v_{mn} \end{bmatrix}$$

Step 3. Determine the positive-ideal and the negative-ideal solutions. The positive-ideal donated as A^* and the negative-ideal donated as A^- alternatives are defined as:

$$A^* = \{v_1^*, \dots, v_m^*\} = \left\{\left(\max_j v_{ij} | i \in I'\right), \left(\min_j v_{ij} | i \in I''\right)\right\} \tag{9}$$

$$A^- = \{v_1^-, \dots, v_m^-\} = \left\{\left(\min_j v_{ij} | i \in I'\right), \left(\max_j v_{ij} | i \in I''\right)\right\} \tag{10}$$

where I' is associated with benefit criteria, and I'' is associated with cost criteria.

A^* indicates the most preferable solution and similarly A^- indicates the least preferable solution.

Step 4. Calculate the separation measure. The separation of each alternative from the positive-ideal solution and negative-ideal solution are calculated using *n*-dimensional Euclidean distance method. The distances from the positive-ideal solution and negative-ideal solution can be calculated as follows:

$$D_j^* = \sqrt{\sum_{i=1}^{m} \left(v_{ij} - v_i^*\right)^2}, \quad j = 1, \dots, n, \tag{11}$$

$$D_j^- = \sqrt{\sum_{i=1}^{m}\left(v_{ij} - v_i^-\right)^2}, \qquad j = 1, \dots, n. \tag{12}$$

Step 5. Calculate the relative closeness to the ideal solution. The relative closeness of alternative A_j with respect to A^* is calculated as follows:

$$C_j^* = D_j^- / \left(D_j^* + D_j^-\right), \qquad j = 1, \dots, n \tag{13}$$

where $0 \le C_j^* \le 1$.

If $A_j = A^*$ then C_j^* is equal to 1 and if $A_j = A^-$ then C_j^* is equal to 0.

Step 6. Rank the preference order. The best alternative can be now decided according to the preference rank order of C_j^*. Therefore, the best alternative is the one that has the shortest distance to the ideal solution.

Implementation

The case study is implemented in an automotive factory in Bursa, Turkey. First, interactions among the main criteria are obtained asking experts working for the company and using DEMATEL approach. Then ANP method is implemented according to the experts' opinions in order to calculate the local weights of the sub-criteria. After determining the weights, four SMEs are investigated and graded according to each sub-criterion. As a result, each SME is scored implementing TOPSIS method.

The evaluation of one of the experts in terms of the effect between the main criteria is given in Table 1. Similarly, all of the evaluations from the rest of the experts are obtained and then averages of numbers are calculated using Eq. (1). The average values are given in Table 2. The normalized direct-relation matrix is obtained using Eqs. (2 and 3). After calculating the normalized direct-relation matrix, the total-relation matrix is obtained using Eqs. (4, 5, and 6). The total-relation matrix is shown in Table 3. Then (D + R) and (D – R) values are calculated and also shown in Table 3. The threshold value is determined as 0.51 according to the experts' opinions. The values above the threshold are represented in bold in the table which gives the cause and effect relationship among the main criteria.

Table 1. Evaluation of an expert in terms of effect among the criteria

	C1	C2	C3	C4	C5	C6	C7	C8
C1	0	3	2	2	2	3	4	4
C2	3	0	4	2	1	3	3	2
C3	1	4	0	2	2	2	4	1
C4	3	1	3	0	1	1	3	2
C5	2	3	4	2	0	4	2	2
C6	3	3	4	1	4	0	3	2
C7	3	1	1	2	1	4	0	2
C8	3	3	2	4	2	3	2	0

Table 2. The initial direct-relation matrix (average values of the evaluations of the experts)

	C1	C2	C3	C4	C5	C6	C7	C8
C1	0.00	3.33	2.33	2.33	2.33	3.33	3.33	4.00
C2	2.67	0.00	3.00	1.67	1.67	1.67	3.67	2.00
C3	1.33	3.33	0.00	1.33	1.67	1.67	3.67	1.33
C4	2.67	1.33	2.67	0.00	1.00	1.00	3.00	1.67
C5	1.67	2.33	3.00	1.33	0.00	3.33	2.00	1.33
C6	2.33	2.33	4.00	1.33	4.00	0.00	3.00	1.67
C7	2.67	1.33	1.00	2.00	1.00	4.00	0.00	1.67
C8	3.67	2.67	2.67	4.00	2.67	2.67	2.33	0.00

Table 3. The total-relation matrix

	C1	C2	C3	C4	C5	C6	C7	C8	D	D+R	D-R
C1	0.485	**0.613**	**0.620**	0.504	**0.517**	**0.650**	**0.728**	**0.563**	4.679	8.467	0.892
C2	0.489	0.372	**0.527**	0.387	0.394	0.477	**0.615**	0.400	3.660	7.407	-0.086
C3	0.390	0.461	0.351	0.331	0.353	0.426	**0.557**	0.331	3.199	7.294	-0.896
C4	0.426	0.371	0.445	0.262	0.312	0.382	**0.512**	0.336	3.046	6.192	-0.101
C5	0.418	0.446	0.505	0.344	0.304	0.508	**0.517**	0.346	3.388	6.648	0.127
C6	**0.513**	**0.518**	**0.617**	0.403	**0.526**	0.449	**0.641**	0.418	4.086	8.102	0.069
C7	0.446	0.388	0.410	0.362	0.340	**0.518**	0.407	0.351	3.221	7.873	-1.431
C8	**0.620**	**0.576**	**0.620**	**0.555**	**0.515**	**0.607**	**0.677**	0.391	4.559	7.693	1.425
R	3.788	3.746	4.095	3.147	3.260	4.016	4.652	3.134			

Threshold value = 0.51

According to the cause and effect relationship extracted from the DEMATEL method, the weights of the sub-criteria are calculated following ANP approach in order to form the supermatrix. For example, since "C1: Profile" effects "C2: Quality", the evaluation of importance of sub-criteria of C2 (C21, C22 and C23) in terms of C11 is given in Table 4. Then geometric average is taken after obtaining evaluations of the rest of the experts in order to calculate the local weights. The result is shown in Table 5.

The rest of the local weights are calculated in the same way based on the interaction obtained from the DEMATEL. The supermatrix is formed for the sub-criteria and the local weights calculated are placed into the matrix accordingly. The unweighted supermatrix is presented in Table 6. Then, unweighted supermatrix is normalized to transform it to the weighted supermatrix in which each of its columns sums to 1. The power of the weighted supermatrix is taken until the values of each column are stabilized and equal. These calculations are implemented using MATLAB software and the limit supermatrix is obtained which is given in Table 7. Any column of the matrix shows the weights of corresponding sub-criteria.

Table 4. Pairwise comparison matrix of an expert in terms of C11: Organization and Management Capability

	K21	K22	K23
K21	1.00	0.33	0.20
K22	3.00	1.00	0.33
K23	5.00	3.00	1.00

Table 5. Geometric average of all the expert evaluations, and the weights

	K21	K22	K23	**Wi**
K21	1.00	0.26	0.17	**0.089**
K22	3.87	1.00	0.33	**0.272**
K23	5.92	3.00	1.00	**0.639**

Table 6. The unweighted supermatrix

	C11	C12	C13	C21	C22	C23	C31	C32	C33	C41	C42	C43	C51	C52	C53	C61	C62	C63	C71	C72	C73	C81	C82	C83
C11	.000	.000	.000	.000	.000	.000	.000	.000	.000	.000	.000	.000	.000	.000	.000	.705	.677	.534	.000	.000	.000	.694	.509	.516
C12	.000	.000	.000	.000	.000	.000	.000	.000	.000	.000	.000	.000	.000	.000	.000	.145	.180	.341	.000	.000	.000	.219	.307	.325
C13	.000	.000	.000	.000	.000	.000	.000	.000	.000	.000	.000	.000	.000	.000	.000	.150	.143	.125	.000	.000	.000	.088	.185	.158
C21	.089	.686	.623	.000	.000	.000	.000	.000	.000	.000	.000	.000	.000	.000	.000	.333	.443	.534	.000	.000	.000	.106	.724	.633
C22	.272	.079	.147	.000	.000	.000	.000	.000	.000	.000	.000	.000	.000	.000	.000	.333	.443	.341	.000	.000	.000	.260	.083	.106
C23	.639	.235	.230	.000	.000	.000	.000	.000	.000	.000	.000	.000	.000	.000	.000	.333	.114	.125	.000	.000	.000	.633	.193	.260
C31	.114	.357	.720	.680	.443	.659	.000	.000	.000	.000	.000	.000	.000	.000	.000	.680	.452	.150	.000	.000	.000	.552	.443	.235
C32	.364	.149	.088	.225	.443	.170	.000	.000	.000	.000	.000	.000	.000	.000	.000	.094	.458	.705	.000	.000	.000	.332	.114	.407
C33	.522	.493	.192	.094	.114	.170	.000	.000	.000	.000	.000	.000	.000	.000	.000	.225	.089	.145	.000	.000	.000	.116	.443	.358
C41	.000	.000	.000	.000	.000	.000	.000	.000	.000	.000	.000	.000	.000	.000	.000	.000	.000	.000	.000	.000	.000	.659	.623	.652
C42	.000	.000	.000	.000	.000	.000	.000	.000	.000	.000	.000	.000	.000	.000	.000	.000	.000	.000	.000	.000	.000	.170	.147	.097
C43	.000	.000	.000	.000	.000	.000	.000	.000	.000	.000	.000	.000	.000	.000	.000	.000	.000	.000	.000	.000	.000	.170	.230	.252
C51	.092	.111	.623	.000	.000	.000	.000	.000	.000	.000	.000	.000	.000	.000	.000	.671	.114	.073	.000	.000	.000	.623	.089	.698
C52	.341	.328	.230	.000	.000	.000	.000	.000	.000	.000	.000	.000	.000	.000	.000	.130	.299	.228	.000	.000	.000	.147	.272	.216
C53	.567	.561	.147	.000	.000	.000	.000	.000	.000	.000	.000	.000	.000	.000	.000	.198	.587	.699	.000	.000	.000	.230	.639	.086
C61	.116	.213	.292	.000	.000	.000	.000	.000	.000	.000	.000	.000	.000	.000	.000	.000	.000	.000	.333	.125	.680	.213	.105	.633
C62	.332	.418	.511	.000	.000	.000	.000	.000	.000	.000	.000	.000	.000	.000	.000	.000	.000	.000	.333	.534	.094	.418	.540	.260
C63	.552	.369	.197	.000	.000	.000	.000	.000	.000	.000	.000	.000	.000	.000	.000	.000	.000	.000	.333	.341	.225	.369	.355	.106
C71	.193	.213	.333	.321	.690	.680	.097	.098	.300	.434	.677	.659	.225	.252	.341	.106	.448	.190	.000	.000	.000	.213	.341	.330
C72	.178	.369	.333	.104	.134	.094	.652	.413	.427	.106	.143	.170	.094	.097	.125	.260	.282	.449	.000	.000	.000	.418	.125	.168
C73	.629	.418	.333	.575	.176	.225	.252	.489	.272	.459	.180	.170	.680	.652	.534	.633	.270	.361	.000	.000	.000	.369	.534	.502
C81	.199	.199	.106	.000	.000	.000	.000	.000	.000	.000	.000	.000	.000	.000	.000	.000	.000	.000	.000	.000	.000	.000	.000	.000
C82	.312	.489	.260	.000	.000	.000	.000	.000	.000	.000	.000	.000	.000	.000	.000	.000	.000	.000	.000	.000	.000	.000	.000	.000
C83	.489	.312	.633	.000	.000	.000	.000	.000	.000	.000	.000	.000	.000	.000	.000	.000	.000	.000	.000	.000	.000	.000	.000	.000

Table 6. The limit supermatrix

	C11	C12	C13	C21	C22	C23	C31	C32	C33	C41	C42	C43	C51	C52	C53	C61	C62	C63	C71	C72	C73	C81	C82	C83
C11	.043	.043	.043	.043	.043	.043	.043	.043	.043	.043	.043	.043	.043	.043	.043	.043	.043	.043	.043	.043	.043	.043	.043	.043
C12	.014	.014	.014	.014	.014	.014	.014	.014	.014	.014	.014	.014	.014	.014	.014	.014	.014	.014	.014	.014	.014	.014	.014	.014
C13	.009	.009	.009	.009	.009	.009	.009	.009	.009	.009	.009	.009	.009	.009	.009	.009	.009	.009	.009	.009	.009	.009	.009	.009
C21	.032	.032	.032	.032	.032	.032	.032	.032	.032	.032	.032	.032	.032	.032	.032	.032	.032	.032	.032	.032	.032	.032	.032	.032
C22	.027	.027	.027	.027	.027	.027	.027	.027	.027	.027	.027	.027	.027	.027	.027	.027	.027	.027	.027	.027	.027	.027	.027	.027
C23	.020	.020	.020	.020	.020	.020	.020	.020	.020	.020	.020	.020	.020	.020	.020	.020	.020	.020	.020	.020	.020	.020	.020	.020
C31	.057	.057	.057	.057	.057	.057	.057	.057	.057	.057	.057	.057	.057	.057	.057	.057	.057	.057	.057	.057	.057	.057	.057	.057
C32	.040	.040	.040	.040	.040	.040	.040	.040	.040	.040	.040	.040	.040	.040	.040	.040	.040	.040	.040	.040	.040	.040	.040	.040
C33	.021	.021	.021	.021	.021	.021	.021	.021	.021	.021	.021	.021	.021	.021	.021	.021	.021	.021	.021	.021	.021	.021	.021	.021
C41	.001	.001	.001	.001	.001	.001	.001	.001	.001	.001	.001	.001	.001	.001	.001	.001	.001	.001	.001	.001	.001	.001	.001	.001
C42	.000	.000	.000	.000	.000	.000	.000	.000	.000	.000	.000	.000	.000	.000	.000	.000	.000	.000	.000	.000	.000	.000	.000	.000
C43	.000	.000	.000	.000	.000	.000	.000	.000	.000	.000	.000	.000	.000	.000	.000	.000	.000	.000	.000	.000	.000	.000	.000	.000
C51	.024	.024	.024	.024	.024	.024	.024	.024	.024	.024	.024	.024	.024	.024	.024	.024	.024	.024	.024	.024	.024	.024	.024	.024
C52	.018	.018	.018	.018	.018	.018	.018	.018	.018	.018	.018	.018	.018	.018	.018	.018	.018	.018	.018	.018	.018	.018	.018	.018
C53	.036	.036	.036	.036	.036	.036	.036	.036	.036	.036	.036	.036	.036	.036	.036	.036	.036	.036	.036	.036	.036	.036	.036	.036
C61	.135	.135	.135	.135	.135	.135	.135	.135	.135	.135	.135	.135	.135	.135	.135	.135	.135	.135	.135	.135	.135	.135	.135	.135
C62	.097	.097	.097	.097	.097	.097	.097	.097	.097	.097	.097	.097	.097	.097	.097	.097	.097	.097	.097	.097	.097	.097	.097	.097
C63	.097	.097	.097	.097	.097	.097	.097	.097	.097	.097	.097	.097	.097	.097	.097	.097	.097	.097	.097	.097	.097	.097	.097	.097
C71	.078	.078	.078	.078	.078	.078	.078	.078	.078	.078	.078	.078	.078	.078	.078	.078	.078	.078	.078	.078	.078	.078	.078	.078
C72	.100	.100	.100	.100	.100	.100	.100	.100	.100	.100	.100	.100	.100	.100	.100	.100	.100	.100	.100	.100	.100	.100	.100	.100
C73	.138	.138	.138	.138	.138	.138	.138	.138	.138	.138	.138	.138	.138	.138	.138	.138	.138	.138	.138	.138	.138	.138	.138	.138
C81	.002	.002	.002	.002	.002	.002	.002	.002	.002	.002	.002	.002	.002	.002	.002	.002	.002	.002	.002	.002	.002	.002	.002	.002
C82	.004	.004	.004	.004	.004	.004	.004	.004	.004	.004	.004	.004	.004	.004	.004	.004	.004	.004	.004	.004	.004	.004	.004	.004
C83	.005	.005	.005	.005	.005	.005	.005	.005	.005	.005	.005	.005	.005	.005	.005	.005	.005	.005	.005	.005	.005	.005	.005	.005

After calculating the weights of the sub-criteria, TOPSIS method is implemented, which is going to score the suppliers investigated. Four suppliers are investigated and assigned a score to each supplier for each criterion. The scores are given in Table 7.

Tablo 7. Evaluation of the suppliers in terms of the sub-criteria

	A	B	C	D
C11	85	90	75	87
C12	17	21	5	9
C13	350	120	540	40
C21	90	65	83	77
C22	85	72	74	75
C23	5	3	6	4
C31	91	92	79	81
C32	75	57	61	86
C33	60	60	30	45
C41	88	92	83	78
C42	80	88	91	85
C43	83	90	95	87
C51	86	93	67	78
C52	75	87	65	80
C53	55	59	63	68
C61	80	90	65	70
C62	74	85	65	78
C63	52	50	58	65
C71	40	55	70	80
C72	25	37	30	43
C73	17	10	20	15
C81	70	63	88	76
C82	80	90	75	72
C83	5	6	7	9

Table 7 is normalized by using Eq. (7) and multiplied by the weights obtained from ANP calculations, by using Eq. (8). The new table is called as the weighted normalized decision matrix. Then, the positive-ideal A^* and the negative-ideal A^- values are calculated by using Eq. (9 and 10). See Table 8 for the weighted normalized decision matrix, and for the values A^* and A^-. Minimum value of sub-criterion C13: Geographic location is selected as the positive-ideal A^* value and maximum value of related row is selected as the negative-ideal A^- value since the closer supplier location is better for the company.

The separation or distances of each alternative from the positive-ideal solution and negative-ideal solution are calculated using Eq. (11 and 12). Then, the relative closeness of alternative A_j with respect to A^* is calculated as Eq. (13). Table 9 shows the results and the rank of each supplier.

It is found out that, alternative D is the best supplier among the alternative suppliers. The rest of the alternatives are ranked as C, A and B.

Tablo 8. The weighted normalized decision matrix and positive and negative ideal solutions

	A	B	C	D	A^*	A^-
C11	.0218	.0231	.0193	.0223	.0231	.0193
C12	.0085	.0105	.0025	.0045	.0105	.0025
C13	.0051	.0017	.0078	.0006	.0006	.0078
C21	.0182	.0132	.0168	.0156	.0182	.0132
C22	.0148	.0126	.0129	.0131	.0148	.0126
C23	.0106	.0064	.0127	.0085	.0127	.0064
C31	.0301	.0304	.0261	.0268	.0304	.0261
C32	.0212	.0161	.0172	.0243	.0243	.0161
C33	.0126	.0126	.0063	.0095	.0126	.0063
C41	.0005	.0006	.0005	.0005	.0006	.0005
C42	.0001	.0001	.0001	.0001	.0001	.0001
C43	.0002	.0002	.0002	.0002	.0002	.0002
C51	.0129	.0139	.0100	.0117	.0139	.0100
C52	.0086	.0100	.0075	.0092	.0100	.0075
C53	.0163	.0175	.0187	.0202	.0202	.0163
C61	.0701	.0789	.0570	.0614	.0789	.0570
C62	.0475	.0545	.0417	.0500	.0545	.0417
C63	.0445	.0428	.0496	.0556	.0556	.0428
C71	.0248	.0341	.0434	.0496	.0496	.0248
C72	.0363	.0537	.0435	.0624	.0624	.0363
C73	.0735	.0433	.0865	.0649	.0865	.0433
C81	.0010	.0009	.0012	.0011	.0012	.0009
C82	.0019	.0022	.0018	.0017	.0022	.0017
C83	.0019	.0023	.0027	.0034	.0034	.0019

Tablo 9. Final performance indices of supplier alternatives.

	D_j^*	D_j^-	C_j^*	Rank
A	.0422	.0363	.4626	3
B	.0500	.0351	.4125	4
C	.0367	.0488	.5708	2
D	.0298	.0469	.6111	1

Conclusion

The purpose of this paper is to suggest an approach for evaluating and selecting suppliers for an automotive company, based on hybrid multi-criteria decision making methods. First, main and sub-criteria that affect the evaluation and selection process of a supplier are identified. Then, DEMATEL approach is implemented to the main criteria in order to obtain cause and affect interaction among them which is required by ANP method. After deriving cause and effect interrelationship, ANP methodology is applied for calculating the weights of each sub-criterion. And then, as far as obtaining the weights of the sub-criteria, alternative suppliers are evaluated and ranked using TOPSIS method. At the end, the supplier with the highest performance indices is selected as the best supplier. The proposed approach can be implemented in different multi-criteria decision making problems.

References

Boran, F.E., Genç, S., Kurt, M., Akay, D., (2009), A multi-criteria intuitionistic fuzzy group decision making for supplier selection with TOPSIS method, Expert Systems with Applications, 36, 11363–11368.

Chang, B., Chang, C.-W., Wu, C.-H., (2011), Fuzzy DEMATEL method for developing supplier selection criteria, Expert Systems with Applications, 38, 1850-1858.

Chen, S.J., Hwang, C.L. (1992). Fuzzy multiple attribute decision making: Methods and applications. Berlin: Springer-Verlag.

Choy, K.L., Lee, W.B., (2002), A generic tool for the selection and management of supplier relationships in an outsourced manufacturing environment: The application of case based reasoning, Logistics Information Management, 15 (4), 235–253.

Dalalah, D., Hayajneh, M., Batieha, F., (2011), A fuzzy multi-criteria decision making model for supplier selection, Expert Systems with Applications, 38, 8384–8391.

Demirtas, E.A., Üstün, Ö., (2008), An integrated multi-objective decision making process for supplier selection and order allocation, Omega-The International Journal of Management Science, 36, 76-90.

Dickson, G.W., (1966), An analysis of vendor selection systems and decisions, Journal of Purchasing, 2, 5-17.

Ding, H., Benyoucef, L., Xie, X., (2005), A simulation optimization methodology for supplier selection problem, International Journal Computer Integrated Manufacturing, 18 (2–3), 210–224.

Gabus, A., Fontela, E., 1972. World Problems. An Invitation to Further Thought Within TheFramework of DEMATEL. Battelle Geneva Research Centre. Geneva.

Gencer, C., Gürpinar, D., (2007), Analytic network process in supplier selection: A case study in an electronic firm, Applied Mathematical Modeling, 31 (11), 2475–2486.

Ho, W., Xu, X., Dey, P.K., (2010), Multi-criteria decision making approaches for supplier evaluation and selection: A literature review, European Journal of Operational Research, 202, 16–24.

Hsu, C.-W., Hu, A.H., (2009), Applying hazardous substance management to supplier selection using analytic network process, Journal of Cleaner Production, 17, 255–264

Hwang, C.L., Yoon, K.S. (1981). Multiple attribute decision making: Method and applications. NY: Springer.

Karpak, B., Kumcu, E., Kasuganti, R.R., (2001), Purchasing materials in the supply chain: Managing a multi-objective task, European Journal of Purchasing and Supply Management, 7 (3), 209–216.

Lee, A.H.I., (2009), A fuzzy supplier selection model with the consideration of benefits, opportunities, costs and risks, Expert Systems with Applications, 36, 2879–2893.

Lin, C.T., Wu, C.S., 2008. Selecting marketing strategy for private hotels in Taiwan using the analytic hierarchy process. The Service Industries Journal, 28(8), 1077–1091.

Ming-Lang, T., Chiang, J.H., Lan, L.W., (2009), Selection of optimal supplier in supply chain management strategy with analytic network process and choquet integral, Computers and industrial engineering, 57, 330-340.

Ng, W.L., (2008), An efficient and simple model for multiple criteria supplier selection problem, European Journal of Operational Research 186 (3), 1059–1067.

Opricovic, S., Tzeng, G.H. (2004). Compromise solution by MCDM methods: A comparative analysis of VIKOR and TOPSIS. European Journal of Operational Research, 156, 445-455.

Önüt, S., Kara, S.S., Işik, E., (2009), Long term supplier selection using a combined fuzzy MCDM approach: A case study for a telecommunication company, Expert Systems with Applications, 36, 3887–3895.

Razmi, J., Rafiei, H., Hashemi, M. (2009), Designing a decision support system to evaluate and select suppliers using fuzzy analytic network process, Computers and Industrial Engineering, 57, 1282-1290.

Ross, A., Buffa, F.P., Dröge, C., Carrington, D., (2006). Supplier evaluation in a dyadic relationship: An action research approach, Journal of Business Logistics, 27 (2), 75–102.

Saaty, T.L. (1996). Decision Making with Dependence and Feedback: Analytic Network Process, RWS Publications, Pittsburgh.

Saaty, T.L., (2001). Decision making with dependence and feedback: The analytic network process. RWS Publications. Pittsburgh.

Saaty, T.L., (2005). Theory and Applications of the Analytic Network Process. RWS Publications. Pittsburgh.

Saaty, T.L., Vargas, L.G., (1998). Diagnosis with dependent symptoms: Bayes theorem and the analytic network process. Operations Research, 46(4), 491–502.

Saen, R.F., (2007), Suppliers selection in the presence of both cardinal and ordinal data. European Journal of Operational Research, 183 (2), 741–747.

Triantaphyllou, E. (2000). Multiple-criteria decision making methods: A comparative study. Kluwer Academic Publishers, Dordrecht.

Vinodh, S., Ramiya, R.A., Gautham, S.G., (2011), Application of fuzzy analytic network process for supplier selection in a manufacturing organization, Expert Systems with Applications, 38, 272-280.

Wadhwa, V., Ravindran, A.R., (2007), Vendor selection in outsourcing, Computers and Operations Research 34 (12), 3725–3737.

Wang, J.-W., Cheng, C.-H., Kun-Cheng, H., (2009), Fuzzy hierarchical TOPSIS for supplier selection, Applied Soft Computing, 9, 377–386.

Wu, T., Shunk, D., Blackhurst, J., Appalla, R., (2007), AIDEA: A methodology for supplier evaluation and selection in a supplier-based manufacturing environment, International Journal of Manufacturing Technology and Management, 11 (2), 174–192.

Yang, H.W., Chang, K.F., (2012). Combining means-end chain and fuzzy ANP to explore customers' decision process in selecting bundles. International Journal of Information Management, 32, 381– 395.

The Effect of Antioxidant Proteins due to Salt Stress and Wounding in *Vicia Faba* against Bean Yellow Mosaic Virus

Zenab Aly Torky

Department of Microbiology, Faculty of Science, Ain Shams University, Cairo, Egypt

e-mail:zenabaly72@yahoo.com

Abstract: Environmental stresses like salinity and wounding are very harmful to plants and cause major economical losses especially if the plant is a major crop like bean. Exposure of plants to those types of stresses cause the production of reactive oxygen species which in turn damage the plant cellular system. To reverse this lethal effect, plants have developed a counter attack mechanism to adjust the oxygen level in the cells through anti-oxidant enzymes, a process known as oxygen scavenging. In this research, experiments have been conducted to investigate the relation between the type and magnitude of the stress, together with the timeline of bean yellow mosaic virus (BYMV) inoculation and the level of anti-oxidant enzymes if any, and the resistance to the virus infection. Salinity and mechanical wounding were used on the bean plants as types of the stress, three types of salinity concentrations and two types of mechanical wounding were used, and then the leaves of the stressed plants were inoculated with the virus immediately, after 6 hours, 1 and 3 days to study the systemic effect of the stress on signaling any antioxidant enzymes on those time intervals, and in one and two weeks as well to determine the state of the enzyme in the plant. The enzymes assayed were catalase (CAT), glutathione reductase (GR), superoxide dismutase (SOD), and guaiacol-specific peroxidase (POX). Results revealed that there is a correlation between the stress and the level of the enzymes in the plant. These enzymes seem to trigger the induced resistance in the bean plants to the BYMV.

Keywords: Abiotic stress, antioxidant, ROS, oxygen scavenging, antiviral

Introduction

Due to its low cost, and being a very rich source of protein, *V.faba* or broad beans is a very important crop for humans and animals as well. It was also reported that *V.faba* has a big role in biological fixation of aerial nitrogen (Jelenic et al, 2000).

BYMV, on the other hand, is a wide host range virus that infects *V.faba* systemically, and although the virus does not really kill the plant it can spread very fast in the crop leading to a great economical loss (Checng et al, 2002).

Stresses are the negative impacts of pathogens, environment, and other species on plants and they represent major restrictions in crop agriculture. Flowers and Yeo stated that 50% of the crop land in the world is salt stressed (Flowers and Yeo, 1995). A stress can be biotic where fungi, bacteria, virus or an insect can harm a plant in some way. It can also be abiotic**,** where the harm can be caused by unavoidable factors like salinity, heat, mechanical wounding, intense sunlight, heavy rain, drought, and wind. Abiotic stresses can be even more harmful when combined together (Mittler, 2006).

Environmental stresses can however, induce plant resistance against pathogens (Babosha, 2008). Barley has been reported to have an induced resistance against pathogens when stressed abioticaly (Wiese et al., 2004). It had been reported as well that heat shock could help induce cross adaptation to many environmental challenges in maize (Ming et al., 2004).

The Prime_A_Plant Group et al., studied the state of plant priming, which is a state induced in the plant when it gets attacked by insects, pathogens or when it gets subjected to abiotic stress. The group reported that this primed state of the plant activates the defense responses of the plant more quickly and strongly than the usual (Prime-A-Plant Group et al., 2006).

To better understand how stress can induce resistance in the plant against pathogens attacks, the metabolism inside the stressed plant should be understood. Consider salinity as an example of a stress, as the salt increases in the soil the level of water decreases and consequently the ion uptake increases and reactive oxygen species increase. This abnormal generation of reactive oxygen species is the main reason of oxidative

damage to the lipids, proteins and nucleic acids of the plant cells (Noctor and Foyer, 1998, and Mittler, 2002). There are however, a series of enzymatic systems that developed in plants to revert the effect of the reactive oxygen species and conduct an oxygen scavenging process (Sairam and Tyagi, 2004). On the other hand, when a localized injury happens to a plant leaf by a herbivore, an insect or a mechanical wounding, the injury activates local and systemic responses include metabolic changes and a disorder in the damaged tissues cell structure associated with the drastic loss of water, and consequently increasing the level of the ROS in the plant, which activates the defense mechanisms systemically in the whole plant via complex wound signals (Pearce et al., 1991).

The way this oxygen scavenging works is like this: the plant gets exposed to a stress, at some point stress result in an increased level of ROS. The successive reduction of molecular oxygen to H_2O yields the intermediate radicals $O_2^{\cdot-}$, $HO^{\cdot}$ and H_2O_2 which are toxic. Now the elevation in the level of ROS triggers the production of antioxidant enzymes that naturalize the reactive bad radicals to produce more stable harmless compounds. This process is using multiple enzymes including GR, CAT, POX, and SOD.

Now, the question is, “can those detoxification enzymes used in the process of oxygen scavenging, be the reason of enhancing the plant induced resistance against pathogens?”. It was reported that doubling the glutathione in transgenic tobacco plants caused the seedlings to grow faster than the ordinary plants (Roxas et al., 1995), and that mechanical wounding of sunflower plants triggered the accumulation of the S-nitrosothiols which constitutes a signal of the detoxification process in the plant (Mounira et al., 2011). SOD was also names as the first line of antioxidant defense because it can remove the superoxide anion produced during the bio-oxidation process (Bowler et al., 1992).

In this paper, the *vicia faba* plants will be subjected to either salinity or mechanical wounding stress and then the stressed plant will be examined using the bioassay against the BYMV. For those plants showing resistance against the virus further experiments will take place to determine the level of detoxification enzymes developed in those plants and compare it with the corresponding levels in non stressed plants to determine the protective role of antioxidants expressed due to stress and the acquired resistance of the plant against the BYMV.

Materials and Methods

Plant Material

Seeds of *V.faba* (L) were surface disinfected with solution of mercuric chloride (0.1%) for 30 sec, and were washed immediately and germinated in pots containing vermiculite. Plants grown for 30 days under constant environmental conditions (23°C day : 18°C night) and were watered twice a week.

Virus inoculum

BYMV inoculum was obtained from infected *Vicia faba* leaves ground using a pestle and mortar with a little acid washed sand and distilled water (1:2 w/v). The bulk of the leaf debris and sand was removed by squeezing the pulp through three layers of muslin. The extract was centrifuged at 4,000 xg for 15 min, and the supernatant decanted and kept at room temperature over night to precipitate any proteinaceous virus inhibitor presented in the leaf sap. The supernatant was clarified by further centrifugation at 3,000 xg for 15 min. For each one of the abiotic stress treatments an exact replica of the plant was prepared for the viral bioassay after the treatment.

Abiotic stress

Different treatments according to the type of abiotic stress were applied on the bean plants. After each treatment and according to the corresponding time course the control leaves as well as the treated leaves were inoculated with BYMV according to the method below.

Salt stress

Bean plants were subjected to salinity stress by watering the base by 100, 200, and 300 mM NaCl.

Mechanical wounding

Leaves were wounded using a plastic brush having two rows. Some leaves were punctured with around 200 punctures and some were punctured with around 600 punctures.

Plant viral bioassay

Designated primary leaves of fourteen days old bean plants were inoculated with BYMV. Inoculation was done under green house conditions at 25 ± 5 °C, by dusting virus inoculum with Carborandum (600 mesh). Ten replicates were made for each virus inoculation.

The antiviral bioassay was done on the test plants with same height, and age. For each treatment, ten replicates of equal size were used. For controls, test plant leaves were treated directly with the virus inoculum without prior treatment of salinity or mechanical wounding of the adjacent leaves. After 0, 6 hours, 1 and 3 days of the stress, the designated leaves were sprinkled very lightly with 600mesh carborundum powder and inoculated gently and uniformly with virus inoculum. After inoculation, leaves were washed with distilled water. Plants were observed for the development of mosaic symptoms after 15 days. The inhibitory activity of the BYMV symptoms on bean plants due to stress was calculated according to the ratio between obviously infected plants (showing systemic symptoms) to the total inoculated plants.

SDS-polyacrylamide gel electrophoresis

Discontinuous SDS-PAGE was carried out in 12% separating gel with a 5% stacking gel according to Laemmli (1970). The proteins were visualized by staining with 0.1% Coomassie brilliant blue R-250.

Chemicals

All chemicals used in the assay of enzymes were purchased from Sigma Aldrich.

Extraction of enzymes and antioxidants

Bean leaves were homogenized with 100 mM sodium phosphate buffer (pH 7.5) containing 1 mM EDTA, and 5 mM -mercaptoethanol. The homogenate was filtered through four layers of cheese cloth, centrifuged at 45,000Xg for 20 min. The supernatant was used as source of enzymes, antioxidants, and other components. All the steps in the preparation of the enzyme extract were carried out between 0 to 4°C.

Assay of enzymes

CAT activity was determined by measuring the rate of disappearance of H_2O_2 following the procedure of Dhindsa et al, (1981). 0.5g of leaf sample was homogenized in 5mL of 50mM potassium phosphate buffer pH=7 and 1% PVP. Homogenized samples were centrifuged at 4°C for 10mins at 15000g. An aliquot of 1mL of the supernatant of the enzyme extract was added to the reaction mixture containing 1 mL of 1.5 M H_2O_2 and 3mL of 50 mM potassium phosphate buffer pH=7. Decrease in H_2O_2 is followed as decline 240 nm during 30 sec.

The activity of GR, on the other hand was assayed in 2 mL of 100 mM TRIS-HCl buffer (pH=7.2) containing 0.2 mM NADPH, 5mM glutathione disulphide (GSSG) and 100 µL of plant extract (Anderson, 1996). The change in absorbance at 340 nm was recorded at 25°C in a spectrophotometer. Enzyme activity was based on the oxidation rate of NADPH using an extinction coefficient of 6.2 $mM^{-1}cm^{-1}$.

POX activity was measured by monitoring the formation of tetra guaiacol at 470 nm, using H_2O_2 as substrate (Chance and Machly, 1955). One unit of peroxidase is defined as the amount of enzyme that caused the formation of 1 mM of tetra-guaiacol per minute.

Finally, SOD was extracted in 50 mM potassium phosphate buffer (pH 7.8), 0.1 mM EDTA, 0.1% Triton X-100 and 1% (w/v) soluble polyvinylpyrrolidone (PVP-10), and its activity was determined by the ferric cytochrome *c* method.

Statistical analysis

All data in the tables below are the means of at least ten values. Minitab statistics software was used to compare the mean values together. Analysis of variance (ANOVA) was used and the mean values were compared using lowest standard deviation test with $P<0.05$ for significant difference.

Results and Discussion

Induction of resistance as a result of salt stress

The roots of *Vicia faba* plants of about 14 days of age were watered with 100, 200, and 300 mM NaCl and the primary leaves of each of the stressed plants were inoculated with BYMV after 0, 6, 24, and 72 hours of the watering. Results in table 1 and figure 1 below, show that exposing the roots of the Bean plants to the different salt concentrations did not affect the response of the plant to the virus inoculation or induce any kind of

resistance when it is conducted immediately after salinity stress. After six hours though, the plant started to show up a peak of resistance to the virus for all concentrations. This resistance increased with the increase of concentration. This induced resistance decreased from six hours to a day and sort of stabilized afterwards till three days. These results come in accordance with those reported by Lu et al., (2003), stating that salinity treatment increased the resistance of *Suaeda salsa* against heat stress, and that this resistance increases with the salinity concentration up to 400mM NaCl.

Table 1: Percent inhibition of salt stressed *Vicia faba* plants to BYMV varying by time of inoculation after the salinity stress, and concentration of the salt stress

Time of inoculation after the stress in hours	0	6	24	72
% Inhibition at 100mM salt stress	10±0	60±1.1	50±2	50±0.1
% Inhibition at 200mM salt stress	10±0	80±0.7	60±0.7	60±1.3
% Inhibition at 300mM salt stress	10±0	80±0.9	70±0.8	60±0.9

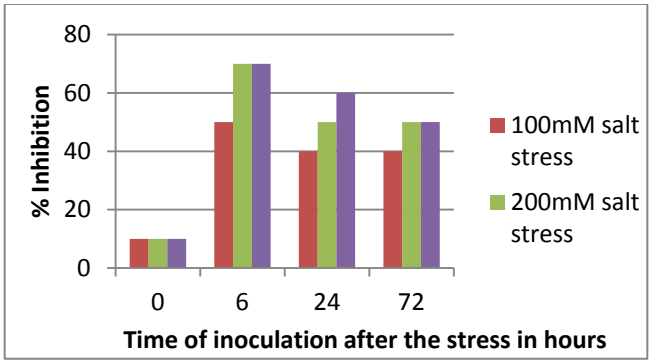

Figure 1: Percent inhibition of salt stressed *Vicia faba* plants to BYMV varying by concentration of the salt stress and timeline of virus inoculation after the stress.

Induction of resistance as a result of leaves mechanical wounding

The designated leaves of bean plants of about 14 days of age were wounded using a plastic brush having two rows. Leaves were punctured with 200, and 600 punctures. After 0, 6, 24, and 72 hours of leaves damage the adjacent leaves were inoculated with BYMV. Results in table 2 and figure 2 below, show that damaging the leaves and inoculating the adjacent ones immediately did not induce any resistance in the plant at all. Some resistance though, started to show up systemically, after 6 hours of leaves damage. This induced resistance persisted after one day of inoculation and started to decay on three days. Those results suggest that, damaging the leaves of the V*icia faba* plants did not induce the resistance until after 6 hours and showing a peak of resistance induction between 6 and 24 hours.

These results agree with those of Francia et al., (2007) who reported that wounding can induce resistance to pathogens with different lifestyles in tomato. Also, Li et al., (2009) discovered a novel Wall-associated protein kinas (WAK) gene induced in rice after mechanical wounding; this gene was proven to play an important role in plant defense. It was also reported by Ito et al., (2002), that cell death and wounding in tobacco plant induced a receptor-like protein kinase gene, which agrees with the results shown here.

Table 2: Percent inhibition of the leaves adjacent to mechanically wounded leaves of *Vicia faba* plants to BYMV varying by time of inoculation after the damage, and the magnitude of the damage

Time of inoculation after the stress in hours	0	6	24	72
% Inhibition at 200 punctures	10±0	30±0.3	25±1.1	10±0.6
% Inhibition at 600 punctures	10±0	35±0.6	30±0.3	20±1.5

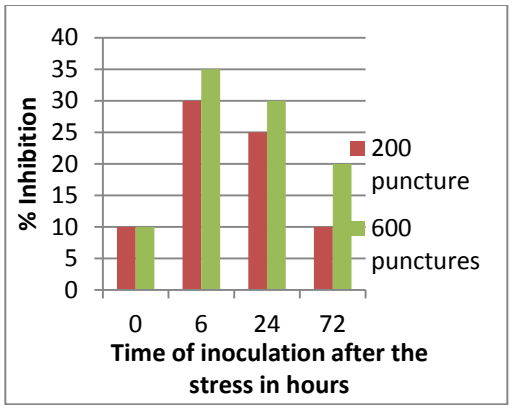

Figure 2: Percent inhibition of the leaves adjacent to mechanically wounded leaves of *Vicia faba* plants to BYMV varying by hours of inoculation after the damage, and the magnitude of the damage

Effect of stress on the total protein in the *V.faba* plants

In order to gain more understanding on what happened inside the *V.faba* plants to induce the resistance to the BYMV as noticed above, SDS-PAGE was carried over to get an insight on the proteins inside the plant and to see if there undergo any change with the different timeline and magnitude of the stress.

Results in figure 3, and figure 4 below and based on the denseometric scanning of protein patterns for the different stress magnitude and timeline (data now shown), show that there was some variation in the number of separated bands and the concentration of protein in each particular band. This variation depends on the type, magnitude of the stress and the timeline.

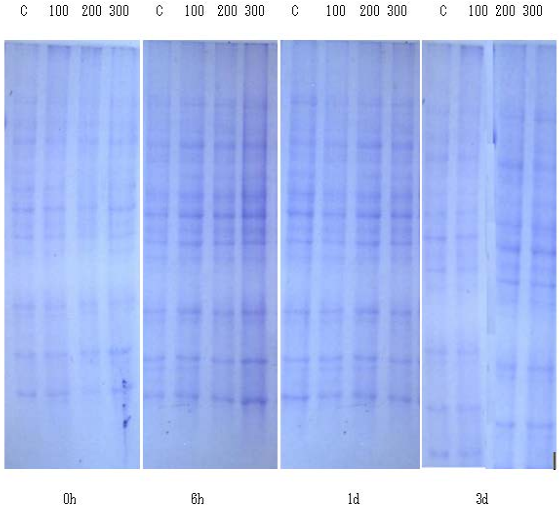

Figure 3: The SDS-PAGE of salt stressed *V.faba* plants varying by concentration of salt and time after the stress

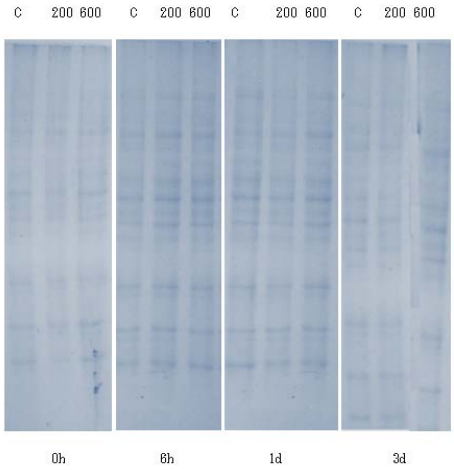

Figure 4: The SDS-PAGE of wounding stressed *V.faba* plants varying by magnitude of the wounding and time after the stress

Assay of antioxidant enzymes

GR, CAT, POX, and SOD were assayed in the leaves of the stressed, non-infected bean plants, at 0h, 6h, 1d, 3d, 1w, and 2w, where h stands for hour, d stands for day, and w stands for week. The reason the assay of the enzymes was conducted on non-infected plants is that the virus itself is a biotic stress to the plant and might as well increase the level of antioxidant enzymes and in this case the assay conducted will not be objective and cannot judge for sure if the environmental stresses used generated any enzymes or not. For every assay in the stressed plant another assay has been done for the same enzyme in the non-stressed plant having exactly the same conditions to serve as a control. Results are shown in tables 3 to10 and figures 5 to 12 below. Results in tables and figures 5 to 8 show that there is almost no change in the enzymes level when measured at the time of the stress, and that there is a very noticeable elevation in the level of the four enzymes for all concentrations, comparing to the control started after six hours of the salt stress, that is in case of 100mM salt stress, 1800 for GR, 1100 for CAT, 1700 for POX, and 530 for SOD (all in IU/g tissue). This elevation was stable till after one day of stress, showing 1650 for GR, 820 for CAT, 1550 for POX, and 500 for SOD, and started to decay suddenly starting at the third day of the stress in case of GR showing 850, and POX showing 800. In case of CAT, and SOD, on the other hand, enzymes levels were 700 for CAT, and 320 for SOD, and there was a steady decay till the second week after the salt stress. Results for the 200mM, and 300mM, were similar to that of 100mM with the exception of the enzyme levels were higher in higher stress concentrations. Comparing with the result of the viral bioassay of the salt stressed plants in table 1, it can be concluded that the enzymes level elevation in the salt stressed plants implied the induced resistance inside the plant till the first day after the stress. At the third day however, the levels of the enzymes showed dramatic decay and this decay was not accompanied with a similar decay in the resistance induced in the plant against the BYMV, which implies that maybe those enzymes elevation in the plant triggered the systemic acquired resistance (SAR) of the plant against the virus and then enzymes started to decay to the normal level, but the resistance persisted in the plant. Those results come in accordance with those reported by Lu et al., (2003)

For mechanical wounding on the other hand, for 200 punctures stress, GR gave a measurement of 900 IU/g tissue after six hours of wounding, while CAT gave 930, 900 for POX, and finally 500 for SOD, showing an elevation in the level of the all enzymes but much less than their corresponding value in the salt stress. These values persisted till the first day after the stress showing 950 for GR, 750 for CAT, 950 for POX and finally 410 for SOD. Those values started to drop after he first day dramatically to almost back to normal level after two weeks of stress.

Results showed that the elevation of the enzymes in the mechanical wounding stress were much smaller than those in the case of salt stressed plants which can be perfectly correlated to the results of the virus resistance which gave better inhibition of the virus in case of salt stress than in the case of mechanical wounding. Results also showed that as the magnitude of the stress increases the enzymes levels increase and the SAR increases. Results agree with those reported by Prime-A-Plant_Group et al., (2006), and Francia et al., (2007). So, it can be concluded from these results that when the *V.faba* plants suffer salt and wounding stress and consequently suffer from an elevation in the level of ROS, the level of antioxidant enzymes increase. This increase triggers the systemic acquired resistance in the plant to fight pathogenic attacks like BYMV.

Table 3: GR enzymatic activity of the leaves of salt stressed *Vicia faba* plants, varying by time after the stress, and the concentrations of the stress

Time	0h	6h	1d	3d	1w	2w
Enzyme activity in 100mM salt stressed plant	100±0.3	1800±2.0	1650±0.4	850±1.5	350±0.3	120±0.5
Enzyme activity in 200mM salt stressed plant	110±0.3	1900±1.4	1600±0.6	870±1.1	400±0.2	100±2
Enzyme activity in 300mM salt stressed plant	100±0.2	1920±0.7	1700±1.5	900±1.2	420±0.2	150±0.5
Enzyme activity in control plant	90±0	90±0	90±0	90±0	90±0	90±0

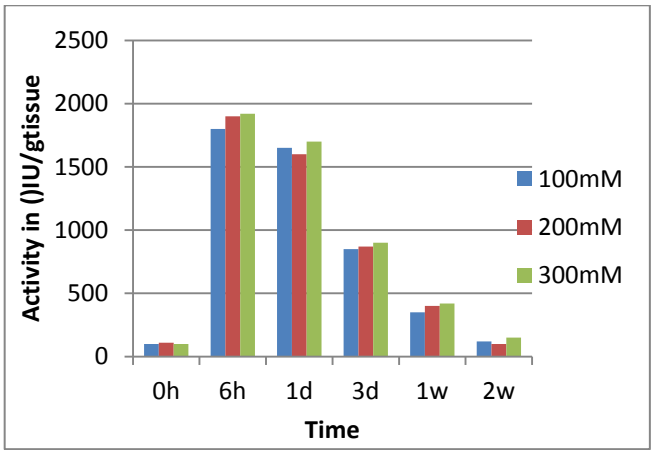

Figure 5: GR enzymatic activity of the leaves of salt stressed *Vicia faba* plants, varying by time after the stress, and the concentrations of the stress

Table 4: CAT enzymatic activity of the leaves of salt stressed *Vicia faba* plants, varying by time after the stress, and the concentrations of the salt stress

Time	0h	6h	1d	3d	1w	2w
Enzyme activity in 100mM salt stressed plant	90±0.1	1100±1.3	820±0.6	700±0.4	230±0.7	115±0.1
Enzyme activity in 200mM salt stressed plant	110±1.1	1300±0.9	900±0.7	750±0.6	300±1.5	210±0.3
Enzyme activity in 300mM salt stressed plant	100±0.3	1500±0.4	1010±0.3	830±0.4	310±0.3	115±0.2
Enzyme activity in control plant	80±0	80±0	80±0	80±0	80±0	80±0

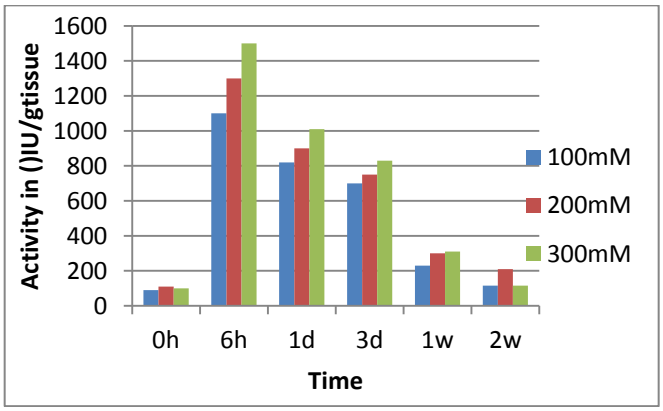

Figure 6: CAT enzymatic activity of the leaves of salt stressed *Vicia faba* plants, varying by time after the stress, and the concentrations of the salt stress

Table 5: POX enzymatic activity of the leaves of salt stressed *Vicia faba* plants, varying by time after the stress, and the concentrations of the stress

Time	0h	6h	1d	3d	1w	2w
Enzyme activity in 100mM salt stressed plant	100±0.1	1700±1.2	1550±0.2	800±0.2	420±0.1	300±0.1
Enzyme activity in 200mM salt stressed plant	110±0.5	1750±0.3	1600±0.5	760±0.4	400±0.3	310±0.3
Enzyme activity in 300mM salt stressed plant	100±0.3	1900±0.3	1600±0.3	850±0.3	515±0.4	370±1.2
Enzyme activity in control plant	95±0	95±0	95±0	95±0	95±0	95±0

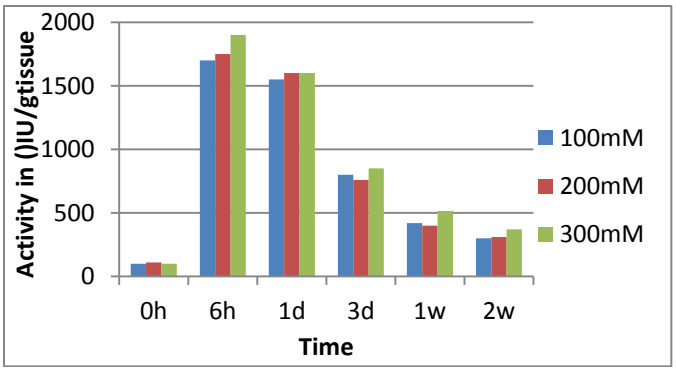

Figure 7: POX enzymatic activity of the leaves of salt stressed *Vicia faba* plants, varying by time after the stress, and the concentrations of the stress

Table 6: SOD enzymatic activity of the leaves of salt stressed *Vicia faba* plants, varying by time after the stress, and the concentrations of the salt stress

Time	0h	6h	1d	3d	1w	2w
Enzyme activity in 100mM salt stressed plant	50±0.1	530±0.1	500±1.2	320±0.1	150±0.1	75±0.1
Enzyme activity in 200mM salt stressed plant	45±0.4	600±0.2	550±0.2	400±1.9	200±0.2	100±0.3
Enzyme activity in 300mM salt stressed plant	75±1.2	730±0.1	700±0.4	600±01.3	230±0.4	80±0.1
Enzyme activity in control plant	30±0	30±0	30±0	30±0	30±0	30±0

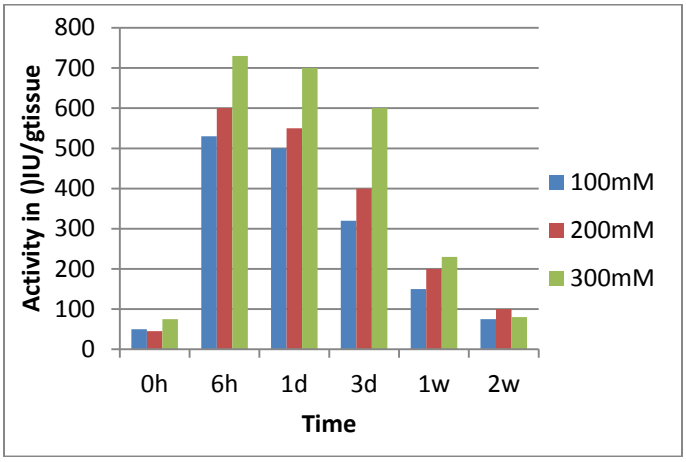

Figure 8: SOD enzymatic activity of the leaves of salt stressed *Vicia faba* plants, varying by time after the stress, and the concentrations of the salt stress

Table 7: GR enzymatic activity of the leaves adjacent to mechanically wounded leaves of *Vicia faba* plants, varying by time after the stress, and the magnitude of mechanical wounding

Time	0h	6h	1d	3d	1w	2w
Enzyme activity in 200 punctured stressed plant	120±0.1	900±0.2	950±0.3	320±0.2	200±0.1	100±0.2
Enzyme activity in 600 punctured stressed plant	100±0.2	950±0.3	970±1.2	250±0.3	260±0.6	130±0.4
Enzyme activity in control plant	90±0	90±0	90±0	90±0	90±0	90±0

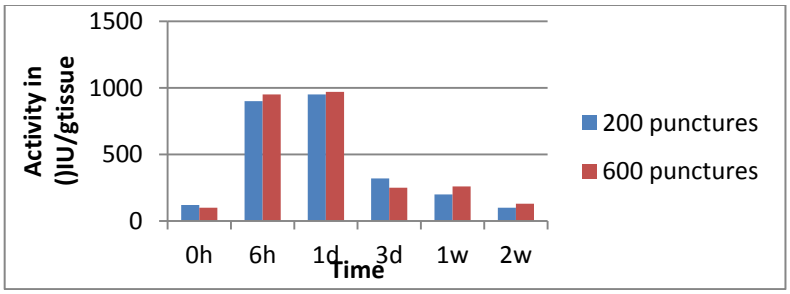

Figure 9: GR enzymatic activity of the leaves adjacent to mechanically wounded leaves of *Vicia faba* plants, varying by time after the stress, and the magnitude of mechanical wounding

Table 8: CAT enzymatic activity of the leaves adjacent to mechanically wounded leaves of *Vicia faba* plants, varying by time after the stress, and the magnitude of mechanical wounding

Time	0h	6h	1d	3d	1w	2w
Enzyme activity in 200 punctured stressed plant	90±0.1	930±0.1	750±0.3	200±0.7	150±0.7	110±0.3
Enzyme activity in 600 punctured stressed plant	75±1.2	800±0.2	710±0.5	310±0.3	170±0.5	130+1.2
Enzyme activity in control plant	80±0	80±0	80±0	80±0	80±0	80±0

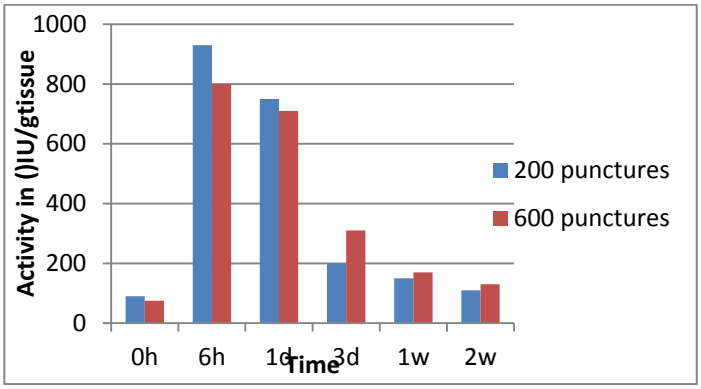

Figure 10: CAT enzymatic activity of the leaves adjacent to mechanically wounded leaves of *Vicia faba* plants, varying by time after the stress, and the magnitude of mechanical wounding

Table 9: POX enzymatic activity of the leaves adjacent to mechanically wounded leaves of *Vicia faba* plants, varying by time after the stress, and the magnitude of mechanical wounding

Time	0h	6h	1d	3d	1w	2w
Enzyme activity in 200 punctured stressed plant	120±0.1	900±0.3	950±0.6	320±0.3	200±0.3	110±0.3
Enzyme activity in 600 punctured stressed plant	100±0.3	950±0.2	970±0.5	250±0.7	220±1.1	120±0.2
Enzyme activity in control plant	95±0	95±0	95±0	95±0	95±0	95±0

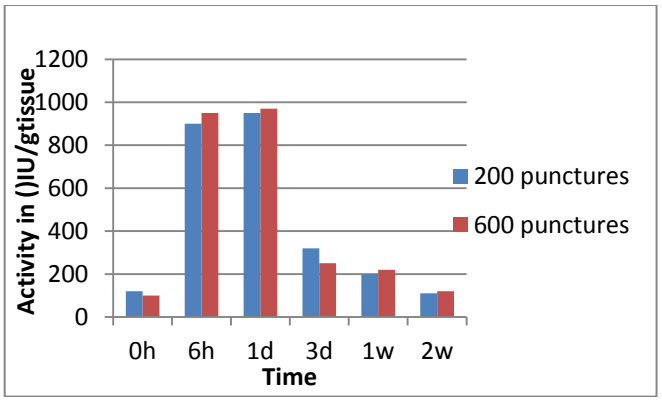

Figure 11: POX enzymatic activity of the leaves adjacent to mechanically wounded leaves of *Vicia faba* plants, varying by time after the stress, and the magnitude of mechanical wounding

Table 10: SOD enzymatic activity of the leaves adjacent to mechanically wounded leaves of *Vicia faba* plants, varying by time after the stress, and the magnitude of mechanical wounding

Time	0h	6h	1d	3d	1w	2w
Enzyme activity in 200 punctured stressed plant	35±0.1	500±0.4	410±0.2	320±03	120±0.5	75±0.6
Enzyme activity in 600 punctured stressed plant	55±0.2	620±0.3	500±1.5	350±0.9	130±0.3	60±0.3
Enzyme activity in control plant	30±0	30±0	30±0	30±0	30±0	30±0

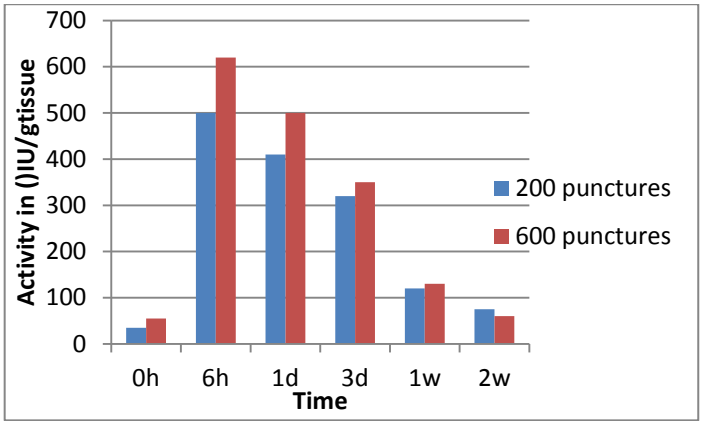

Figure 12: SOD enzymatic activity of the leaves adjacent to mechanically wounded leaves of *Vicia faba* plants, varying by time after the stress, and the magnitude of mechanical wounding

References

Anderson, M.E., (1996). Glutathione. Free Radicals: A practical approach Punchard, N.A. and F.J.Kelly (Eds.), Oxford University Press, pp: 213-226.

Babosha, A.V., (2008). Inducible lectins and plant resistance to pathogens and abiotic stress. Tsitsin Main Botanical Garden, Russian Academy of Sciences.

Beauchamp, C., and Fridovich, I, (1971). Superoxide dismutase: Improved assays and an assay applicable to acrylamide gels. Analytical Biochemistry 44:276-287.

Bowler, C., Van, M., and Inze, D., (1992). Superoxide dismutase and stress tolerance. Ann. Rev. Plant Physiol. Plant Mol.Biol. 43:83-116.

Chance, B, and Machly, A.C., (1955). Assay of catalase and peroxidase. Method Enzymol. 2:764-775.

Cheng, Y., and Jones, R.A.C. (2002). Thackray D. J. Deploying strain specific hypersensitive resistance to diminish temporal virus spread. *Ann Appl Biol*., 140:69 –79.

Davis, K.J., (1995). Oxidative stress: The paradox of aerobic life. Biochemical Society Symposia 61:1-31.

Desbiez, C., Lecoq, H., (1997). Zucchini yellow mosaic virus. Plant Pathology, v.46, p.809-829, 1997.

Dhindsa, R.S.P., and Thorpe, T.A., (1981). Leaf senescence: correlated with increased levels of membrane permeability and lipid peroxidation and decreased levels of superoxide dismutase and catalase. J.Exp.Bot, 32:93-101

Edwards, E.A., Enard, C., Creissen, G.P., Mullineaux, P. M. (1994). Synthesis and properties of glutathione reductase in stressed peas. Planta. 192: 137-143.

Endo, Y., and Tsurugi, K., (1987). RNA N-glycosidase activity of ricine A chain: mechanism of action of the toxic lectine ricine on on eukaryotic ribosomes. J.Bol.Chem.262:8182-8130

Flowers, T.J. and Yeo, A.R. (1995). Breeding for salinity resistance in crop plants: where next? *Aust. J. Plant Physiol.* 22, 875-884.

Francia, D., Demaria, D., Calderini, O., Ferraris, L., Valentino, D., Arcioni, S., Tamietti, G., and Cardinale, F., (2007). Wounding induces resistance to pathogens with different lifestyles in tomato: role of ethylene in cross-protection. Plant Cell Environ; 30(11):1357-65.

Hartley, MR., Chaddock, JA., Bonness, MS., (1996). The structure and function of ribosome inactivating proteins. Trends plant sc., 254-260.

Ito, N., Kim, S.Y., Lim, J.H., Park, M.R., Kim, Y.J., Park, T.I., Seo, Y.W., Choi, K.G., Yun, S.J., (2005). Enhanced antioxidant enzymes are associated with reduced hydrogen peroxide in barley roots under saline stress. J.Biochem Mol.Biol;38(2): 218-24.

Ito, N., Takabatake, R., Seo., S., Hiraqa, S., Mitsuhara, I., and Ohashi, Y., (2002).Induced expression of a temperature-sensitive leucine-rich repeat receptor-like protein kinase gene by hypersensitive cell death and wounding in tobacco plant carrying the N resistance gene. Plant Cell Physiol, 43(3):266-74.

Jelenić, S., Mitrikeski, P.T., Papeš, D., and Jelaska, S., (2000). *Agrobacterium*-mediated transformation of broad bean *Vicia faba* L. Food Technol. Biotechnol. *38*, 167–172.

Kim, S.Y., Lim, J.H., Park, M.R., Kim, Y.J., Park, T.I., Seo, Y.W., Choi, K.G., and Yun, S.J., (2005). Enhanced antioxidant enzymes are associated with reduced hydrogen peroxide in barley roots under saline stress. J.Biochem Mol.Biol;38(2): 218-24.

Laemmli, U.K. (1970). Cleavage of structural proteins during the assembly of the head of T4 bacteriophage. Nature. 227: 680-685.

Li, H., Zhou, S.Y., Zhao, W.S., Su, S.C., Peng, Y.L., (2009). A novel wall-associated receptor-like protein kinase gene, OsWAK1, plays important roles in rice blast disease resistance. Plant Mol Biol., 337-46.

Lowry, O.H., Rosebrough, N.J., Farr, A.R, and Randoll, R.J., (1951). Protein measurement with Folin- Phenol reagent. J. Biol Chem. 193: 265-275.

Lu.C., Qui,N., Wang, B., and Zhang,J.(2003). Salinity treatment shows no effects on photosystem II photochemistry, but increases the resistance of photosystem II to heat stress in halophyte *Suaeda salsa*. J.Exp.Bot. 54(383):851-60.

Ming, G., Checn, B.O., Zhong-Guang, L., and Hong, Guo, (2004). Heat-shock-induced cross adaptation to heat, chilling, drought and salt stress in maize seedlings and involvement of H_2O_2. Department of Life Sciences, Yunnan Normal University, China.

Mittler, R. (2002). Oxidative stress; antioxidants and stress tolerance. Trends Plant Sci. 7:405-410.

Mittler, Ron. (2006). Abiotic stress, the field environment and stress combination. Trends in Plant Science 11(1): 15–19.

Mounira, C., Raquel, V., Ana, M.F., Alfonso, C., Maria, v.G., Jose, R.P., Juan, C.B., Beatriz, S., Francisco, L., Marina, L., Francico, J.C., and Juan, B.B. (2011). Mechanical wounding induces a nitrosative stress by down-regulation of GSNO reductase and in increase in S-nitrosothiols in sunflower (*Helianthus annuus*) seedling.Journal of Experimental Botany, Vol.62, No.6, pp. 1803-1813.

Noctor, G., and Foyer, C.H. (1998). Ascorbate and Glutathione: Keeping active oxygen under control. Annu Rev Plant Physiol Plant Mol Biol, 249-279.

Pearce, G., Strydom, D., Johnson, S., and Ryan, C.A., (1991). A polypeptide from tomato leaves induces wound-inducible proteinase inhibitor proteins. Science 253, 895-898.

Prasad, T.K., Anderson, M.D., and Stewart, C.R., (1995). Changes in isozyme profile of catalase, peroxidase and glutathione reductase during accimilation to chilling in mesocotyls of maize seedlings. Plant Physiol. 109:1247-1257.

Prime-A-Plant Group, Conrath, U., Beckers, GJ., Flors, V., Garcia-Agustin, P., Jakab, G., Mauch, F., Newman, MA., Pieterse, CM., Poissot, B., Pozo, MJ., Pugin, A., Schaffrath, U., Ton, J., Wendehenne, D., Zimmerli, L., and Mauch-Mani, B., (2006). Priming: getting ready for battle. Mol Plant Microbe Interact (10):1062-71

Roxas, V.P., Smith, R.K. Jr, Allen, E.R., Allen, R.D., (1995). Over-expression of glutathione S-transferase/ glutathione peroxidase enhances the growth of transgenic tobacco seedlings during stress. *Nature Biotechnol* 1997, 15:988-991.

Sairam, R.K., and Tyagi, A. (2004). Physiological and molecular biology of salinity stress tolerance in plants. Curr.Sci. (86): 407-420.

Sambrook, J., Fritsch, E.F., and Maniatis, T., (1989). Molecular cloning: A liborartory Manual, 2nd ed. Cold Spring Harbor Laboratory Press, Plainview, NY.

Técsi, L.I., Maule, A.J., Smith, A.M., and Leegood, R.C. (1994).Complex, localized changes in CO2 assimilation and starch content associated with the susceptible interaction between cucumber mosaic virus and a cucurbit host. Plant J. 5, 837–847.

Van Damme, E.J.M., Hao, Q., Charles, D., Barre, A., Rouge, P., Van Leuven, F., and Peumans, W.J., (2000). Characterization and molecular clonning of two different type 2 ribosome inactivating proteins from the monocotyledonous plant Polygonatum multi-florum. Eur, J., Biochem, 267:22746-2759.

Wiese, J., Kranz, S., and Schubert, S., (2004). Induction of pathogen resistance in Barley by abiotic stress. Institute of Plant Nutrition, Interdisciplinary Research Center (IFZ).

The investigation of induction motors under abnormal condition

Benamira Nadir[1], Rachedi Mohamed Faouzi[2], Bouraiou Ahmed[3]
[1,2]Electromechanical department, Badji Mokhtar-Annaba University, P.O box 12, 23000 Annaba, Algeria
[3] Electrical engineering department, 20th August 1955-skikda University, B.P. 26, 21000 Skikda, Algeria

e-mail:nadir-benamira@live.fr

Abstract: This paper aims to present the negative effects of the unbalanced sinusoidal voltage on the operating of induction motors; this voltage quality anomaly could cause serious problems such as highly unbalanced currents on the stator, mechanical oscillations and interference with control electronics. In this research the detection of this unhealthy situation of the motors has been investigated; using firstly, the stator currents data patterns recognition, as a preliminary diagnosis. Secondly, the focus on the second harmonic of the supply frequency in the torque spectrum signal has shown its effectiveness as a complementary indicator of voltage unbalance. The steady-state of the induction motor and the several unbalanced voltage systems presented, were done by a simulation using the well-known Matlab.

Key words: induction motors, Voltage unbalance, Fault detection, Current patterns, THA.

Introduction

The three-phase squirrel cage induction motors are widely used in modern industry because of their Simple construction and ruggedness. However condition monitoring of the induction motor (IM) becomes a necessity to prevent any unplanned stops and breakdowns (Çakır et al, 2009).

Various phenomena can create difficult problems in the performance of IM. The stator unbalanced voltages is one of them, the most of IM is directly connected to the power grid. Hence, it is very important to clarify the effect of voltage unbalance on the characteristics of IM.

The effects of voltage unbalance on the induction motors are stated as reduction on efficiency, mechanical oscillations and highly unbalanced currents on the stator; this last lead to a temperature rise, and decrease the insulation of the electrical conductors in the stator. This thermal stresses lead to the loss of life in induction motors (Çakır et al, 2009).

Voltage unbalance generates negative sequence component in the voltage. The sense of rotation of the field corresponding to the negative sequence is opposed to the one of the field corresponding to the positive sequence. That is why in the case of unbalanced voltage, the resulting magnetic field becomes elliptic rather than circular. This negative sequence flux produces several adverse effects, such as increased copper losses in the stator and in the rotor, power pulsations and torque pulsations. This last is because of a supplementary torque with a double frequency of the applied voltage (Çakır et al, 2009, Donolo et al, 2011).

In this paper the behavior of a simulated IM, under an unbalanced supply voltage have been studied using the well-know MATLAB/Simulink.

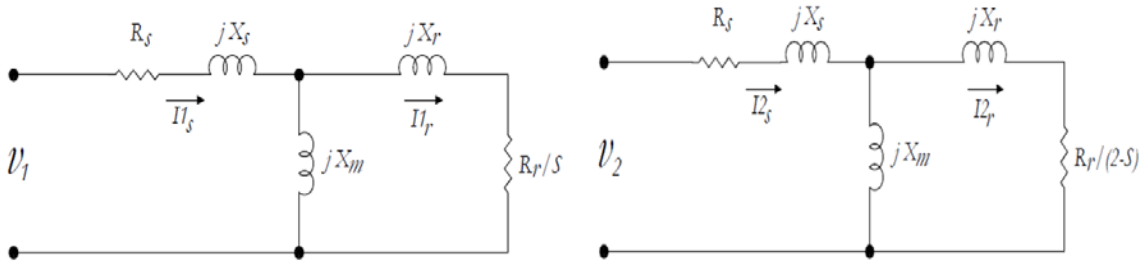

(a) (b)

Figure 1: Single-phase equivalent circuits of the motor: (a) Positive-sequence, (b) negative-sequence. The subscripts s and r denote the stator and rotor, 1 and 2 refers the positive and the negative sequences respectively.

Classification of the voltage unbalances and its different cases

The appearance of some symptoms in the induction motors like vibrations, increased noise levels and the temperature rises in the stator is not necessarily an evidence of an internal fault, like Bearing Faults or stator short-circuit… etc. The stator unbalanced voltage is an external fault, which may cause these symptoms. So, the faults that affect the motor are divided into two parts: internal and external faults, the following figure summarize the various external faults:

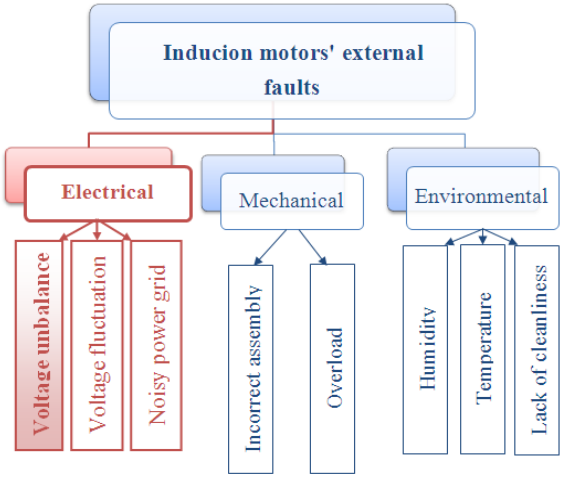

Figure 2: Classification of the external faults

The different unbalanced cases in the three phase systems are (Lee, 1998):
Single phase under-voltage unbalance (1Φ-UV), two phases under-voltage unbalance (2Φ -UV), three phases under-voltage unbalance (3Φ-UV), single phase over-voltage unbalance (1Φ -OV), two phases over-voltage unbalance (2 Φ -OV), three phases over-voltage unbalance (3 Φ -OV), unequal single phase angle displacement (1 Φ -Ang), unequal two phase angles displacement (2 Φ -Ang).

Analysis of balanced and unbalanced condition

Balanced case

The simulated motor (0.75 kW) was supplied by its rated voltage which is 311.12(V) peak for each phase. The simulation of the motor in the steady state and the unbalanced operation is done at no-load condition.

Most of the common methods used to identify faults in induction motor are based on the analysis of the stator currents. The Park's vector and the 3D current pattern approaches, also use the analysis of stator currents. However, in these methodologies, the fault detection will be converted into the pattern and depends on the change on this latter (Samsi et al, 2009). Considering three-phase induction motors without neutral connection, and ideal conditions for the motor and with "unbalanced voltage supply" (Martins et al, 2011), the stator currents are given by:

$$\begin{cases} I_A = I_m \sin(\omega t - \varphi) \\ I_B = I_m \sin(\omega t - \frac{2\pi}{3} - \varphi) \\ I_C = I_m \sin(\omega t - \frac{4\pi}{3} - \varphi) \end{cases} \quad (1)$$

Where I_A, I_B,and I_c :are the three stator currents; I_m : maximum value of the supply phase current; ω : Supply frequency; φ : The phase angle; t: Time variable.

The components of the stator current in a reference system formed by two octagonal shafts which are fixed to the stator are obtained by the following reports:

$$\begin{cases} i_d = \sqrt{\frac{2}{3}} I_A - \frac{1}{\sqrt{6}} I_B - \frac{1}{\sqrt{6}} I_C \\ i_q = \frac{1}{\sqrt{2}} I_B - \frac{1}{\sqrt{2}} I_C \end{cases} \quad (2)$$

Where i_d and i_q are the direct and quadrature axis currents respectively, under ideal operating conditions, when the supply currents constitute a positive sequence system, the three phase currents lead to a Current Park's vector with the components:

$$\begin{cases} i_d = \frac{\sqrt{6}}{2} I_m \sin(\omega t) \\ i_q = \frac{\sqrt{6}}{2} I_m \sin(\omega t - \frac{\pi}{2}) \end{cases} \quad (3)$$

Under this Ideal condition the direct and quadrature axis currents represent a circle centered at the origin of the coordinators. So, this is very simple reference figure that allows the detection and the identification of abnormal conditions by monitoring the deviations of acquired patterns (Cruz et al, 2001).

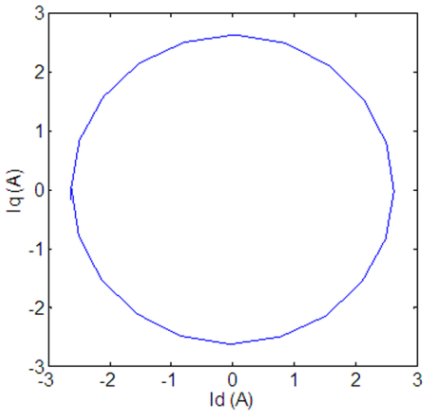

Figure 3: Current Park's vector pattern for ideal operating condition

In the 3D stator current pattern, also we denote a circle centered at the origin of the coordinates, for ideal condition where its radius R is:

$$R^2 = I_A^2 + I_B^2 + I_C^2 \quad (4)$$

Unbalanced cases

The stator asymmetry is a general concept of any stator unbalance, whether stator winding fault or/and voltage unbalance. So under these abnormal conditions, the previous circle pattern no longer appears because the motor supply current will contain negative-sequence component besides the positive-sequence component.

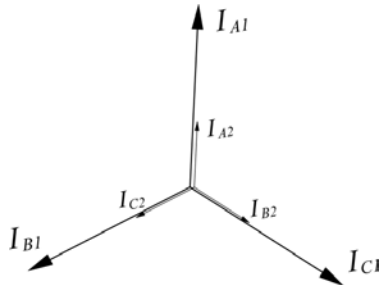

Figure 4: Induction motors' currents under unbalanced voltage

$$\begin{cases} I_A = I_{A1}\sin(\omega t-\varphi)+I_{A2}\sin(\omega t-\varphi) \\ I_B = I_{B1}\sin\left(\omega t-\dfrac{2\pi}{3}-\varphi\right)+I_{C2}\sin\left(\omega t-\dfrac{4\pi}{3}-\varphi\right) \\ I_C = I_{C1}\sin\left(\omega t-\dfrac{4\pi}{3}-\varphi\right)+I_{B2}\sin\left(\omega t-\dfrac{2\pi}{3}-\varphi\right) \end{cases} \quad (5)$$

The motor supply current can be expressed as the sum of a positive and a negative- sequence component. It can also be shown that the length of the major axis is directly proportional to the sum of the amplitudes of the positive and negative-sequence components of the motor supply current, while the difference between the amplitudes of these two components is directly proportional to the length of the minor axis.

$$\begin{cases} i_d = \dfrac{\sqrt{6}}{2}(I_1+I_2)\sin(\omega t) \\ i_q = \dfrac{\sqrt{6}}{2}(I_1-I_2)\sin(\omega t-\dfrac{\pi}{2}) \end{cases} \quad (6)$$

So for an induction motor with a stator asymmetry the current pattern assumes an elliptic pattern whose major axis orientation is associated with the faulty phase (Cruz et al, 2001, Pires et al, 2010, Nejjari, Benbouzid, 2000).

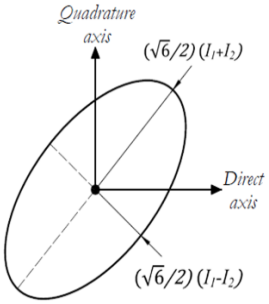

Figure 5: Current Park's vector representation for a stator asymmetry (Cruz et al, 2001)

As the stator currents differ from each other by 120° electrical, it is important to note that the three ellipses' major axis differ from each other by 120 spatial degrees in both park's vector approach and the3-D current referential (Pires et al, 2010, Martins, 2011). The severity of the motor fault must be reported, which is related with the eccentricity of the ellipse. In this way, the new index is proposed, allowing the pattern identification and the fault severity measure.

$$S_{st} = 1 - \frac{\lambda_{low}}{\lambda_{hig}} \qquad (7)$$

The parameters λ_{high} and λ_{low} denote respectively, the highest and lowest length of the ellipse axes. It is important to note that λ_{high} refers to the axis where the fault occurs – principal direction carrying more energy (Morsia, El-hawary , 2011, Martins, 2011). This severity index assumes values between zero and one, being the absence of any fault reported by a zero severity index (S_{st} = 0).

The symmetrical components transformation (Fortescue transformation) is ubiquitous and is used to transform any three-phase system voltages or currents into three single-phase systems using the following symmetrical components transformation matrix in the phasor domain:

$$\begin{bmatrix} V_0 \\ V_1 \\ V_2 \end{bmatrix} = \frac{1}{3}\begin{bmatrix} 1 & 1 & 1 \\ 1 & a & a^2 \\ 1 & a^2 & a \end{bmatrix}\begin{bmatrix} V_A \\ V_B \\ V_C \end{bmatrix}, \begin{bmatrix} I_0 \\ I_1 \\ I_2 \end{bmatrix} = \frac{1}{3}\begin{bmatrix} 1 & 1 & 1 \\ 1 & a & a^2 \\ 1 & a^2 & a \end{bmatrix}\begin{bmatrix} I_A \\ I_B \\ I_C \end{bmatrix} \qquad (8)$$

the subscripts A, B, and C, refer to each one of the components of the phase of the real system, while 0, 1, and 2, are the zero, positive and negative sequence voltages and currents respectively, The operator '*a*' is the Fortescue operator : $a = 1\angle 120°$.

In this paper the obtained elliptic patterns in the following simulation experiments, are resulted from the unbalanced voltage.

Fault detection

Unbalance in the voltages magnitude

- Under voltage in phase A and healthy state for phase B and phase C:

First an unbalance of 10% after this, an unbalance of 20% of the rated voltage is assumed for phase A. The values of the voltage for the three phases in these two cases are:
10% UV-phase A {V_A=280∠0, V_B=311.12∠-120, V_C=311.12∠-240}
20% UV-phase A {V_A=248.89∠0, V_B=311.12∠-120, V_C=311.12∠-240}

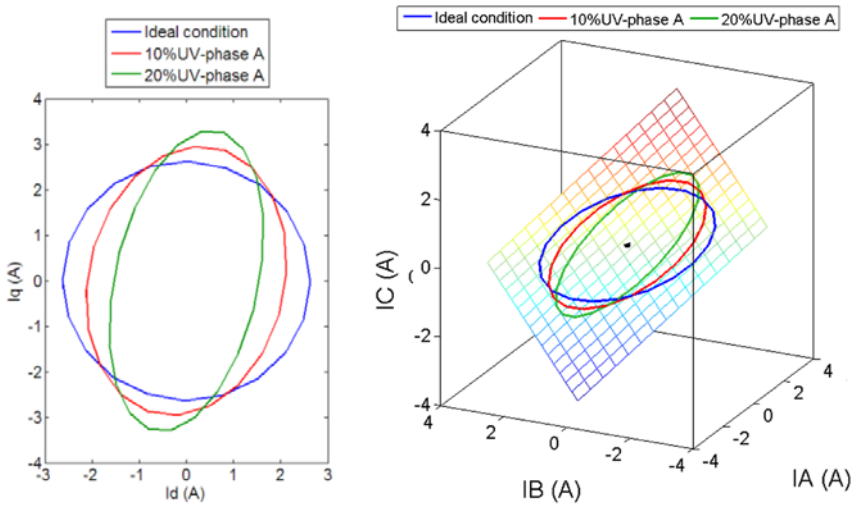

(a) (b)

Figiure 6: (a) Current Park's vector pattern, (b) 3D stator current pattern; for 10% and 20% under voltage in phase A

- Under voltage in phase A, B and C:

An unbalance of 20% of the rated voltage is assumed for phase A, B and C. The values of the voltage for the three phases in these cases are:
20%UV-phase A {V_A=248.89∠0, V_B=311.12∠-120, V_C=311.12∠-240}
20%UV-phase B {V_A=311.12∠0, V_B=248.89∠-120, V_C=311.12∠-240}
20%UV-phase C {V_A=311.12∠0, V_B=311.12∠-120, V_C=248.89∠-240}

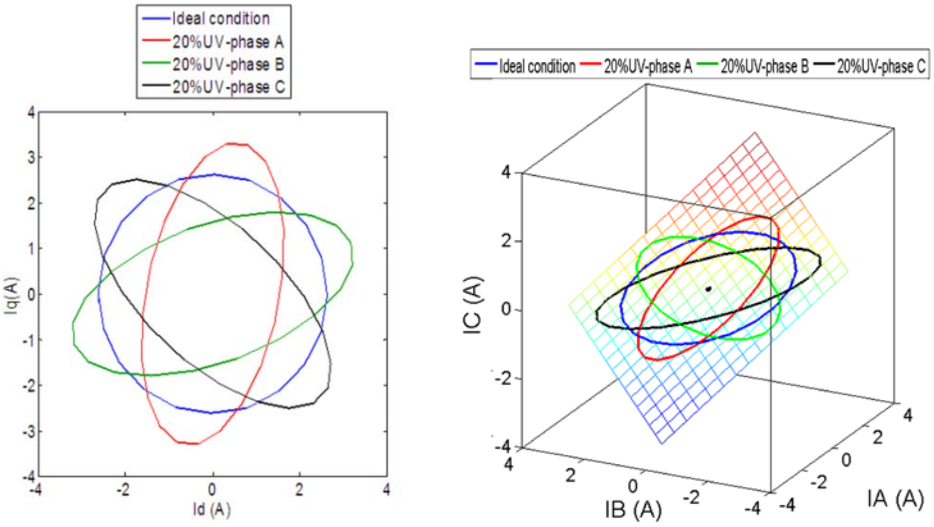

(a) (b)

Figure 7: (a) Current Park's vector pattern, (b) 3D stator current pattern; for 20% under voltage in phase A, B and C

Unbalance in the voltage phase

- (10°) and (20°) angle unbalance displacement of angle's phase B :

First an unbalance of 10° after this, an unbalance of 20° are assumed for the phase A, the values of the voltage for the three phases in these two cases are:
(10°) unbalance -phase B {V_A=311.12∠0, V_B=311.12∠-110, V_C=311.12∠-240}
(20°) unbalance -phase B {V_A=311.12∠0, V_B=311.12∠-100, V_C=311.12∠-240}

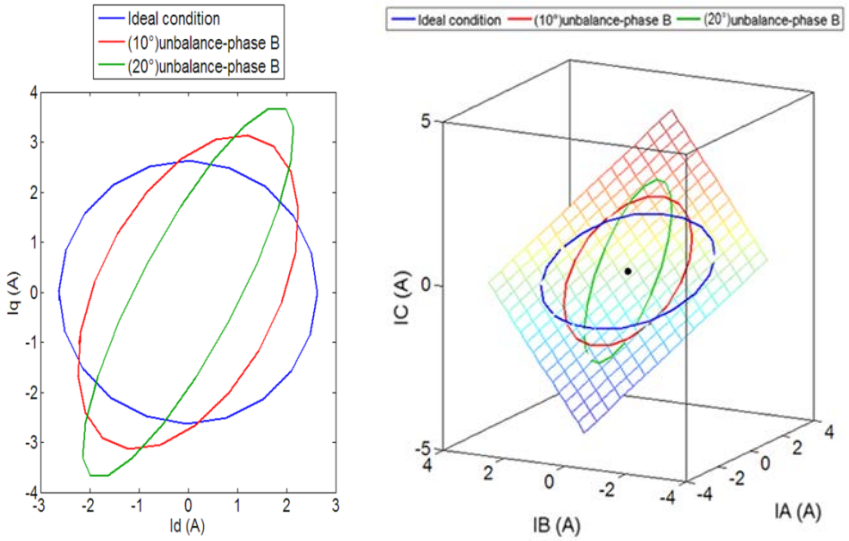

(a) (b)

Figure 8: (a) Current Park's vector pattern, (b) 3D stator current pattern;
for (10°) and (20°) angle displacement in phase B

In certain research the obtained elliptic pattern from the Park's vector approach is considered as direct sign of an unbalanced voltage. Other researches consider the elliptic plot from the 3D currents pattern as sign of a stator winding fault. From a physical point of view, it should be considered as a stator asymmetry in general (stator winding fault and/or voltage unbalance). So, in this work we consider these results as a preliminary diagnosis. And the voltage unbalance must be distinguished from stator winding fault signatures. So using another complementary technique to finalize the investigation is necessary, and that is the content of the next section.

Torque harmonic analysis (THA)

A variety of researches have been done on modeling of unbalanced voltage condition (Phase or Magnitude) in induction motors. To detect this anomaly, has turned to the use of the torque harmonic analysis (THA), in the case of unbalanced voltage, the component spectrum that appears is (100Hz) in the spectrum of the torque, this effective technique will be used in this research. The torque can be written by the following equation (Mirabbasi et al, 2009, Khoobroo et al, 2008):

$$T = \frac{P}{\omega} = \frac{P_0 + P_2}{\omega} = T_0 + T_2 \qquad (9)$$

T_0 is the DC torque; T_2 is the torque component whose frequency is twice the supply frequency.

In order to simplify the survey, we suppose that the induction motor is as an RL load, the torque will be written as follows:

$$T = \left(\frac{1}{\omega}\right) \times \eta \times V \times I \qquad (10)$$

V is the input voltage, I is the current of each phase, η is the motor efficiency.

As we supposed previously, sinusoidal waveforms for voltage and current is applied, so the equation can be rewritten as:

$$T = K\cos(2\pi 50t + \alpha) \times \cos(2\pi 50t + \beta) \qquad (11)$$

So,

$$T = K'\{cos(\alpha - \beta) + cos(2\pi 100t + \alpha + \beta)\} \qquad (12)$$

Based on this equation the resulting torque would include a DC term and a term with twice of the fundamental frequency of the applied voltage ($2.fs$) as expected, this component which is absent in normal operating condition, can detect the fault. So any kind of unbalanced voltage in induction machines is detectable via torque harmonic analysis.

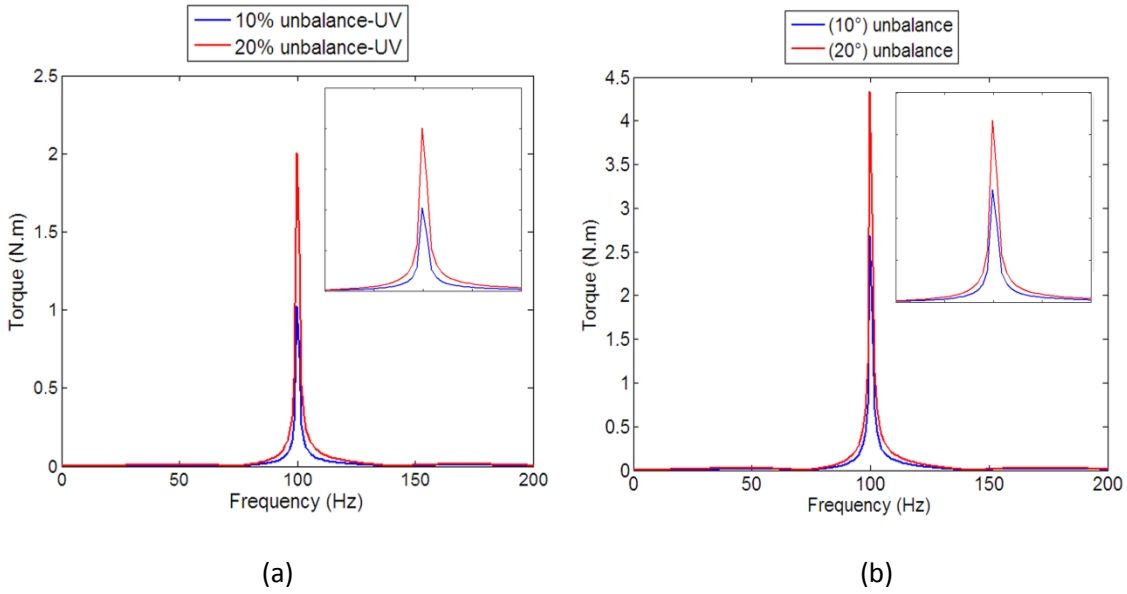

Figure 9: Torque harmonic analysis in case of (a) 10% and 20% under voltage; (b) 10° and 20°angle displacement

Conclusion

It has been reviewed that the stator voltage imbalance has a negative effects on the performance and the efficiency of the induction motors.

In order to detect this anomaly the stator currents data pattern (Park's vector approach or 3D stator currents pattern) is used. Because of the similarity of the obtained signatures between the stator unbalanced voltage and the stator winding fault, these last are considered as an initial diagnosis. To distinguish between these two faults, the torque harmonic analysis is used as a complementary technique in this study. The second frequency component ($2.fs$) that appears in the spectrum of the torque can detect and specify any kind of voltage unbalance in the induction motors.

References

Cakır Abdulkadir, Hakan Calıs, Ecir U. Kucuksille. (2009). Data mining approach for supply unbalance detection in induction motor, Expert Systems with Applications, vol. 36 (pp.11808– 11813).

Cruz Sergio .M. A, A. J. Marques Cardoso. (2001). Stator winding fault diagnosis in three-phase synchronous and asynchronous motors by the extended parks vector approach, IEEE transaction on industrial application, vol. 37 n. 5 (pp. 1227-1233).

Donolo Pablo , Guillermo Bossio, Cristian De Angelo. (2011). analysis of voltage unbalance effects on induction motors with open and closed slots, Energy Conversion and Management, vol. 52 (pp. 2024–2030).

Khoobroo .A, M. Krishnamurthy. M, B. Fahimi, Wei Jen Lee. (2008). Effects of system harmonics and unbalanced voltages on electromagnetic performance of induction motors, the 34th Annual Conference of IEEE Industrial Electronics (pp.1173 – 1178).

Lee Ching-Yin, Bin-Kwie Chen, Wei-Jen Lee, Yen-Feng Hsu. (1998). Effects of various unbalanced voltages on the operation performance of an induction motor under the same voltage unbalance factor condition, Electric Power Systems Research, vol. 47 (pp.153–163).

Martins João .F, Vitor F. Pires, Tito Amaral. (2011). Induction motor fault detection and diagnosis using a current state space pattern recognition, Pattern Recognition Letters, vol. 32 (pp. 321–328).

Mirabbasi .D, G. Seifossadat, M. Heidari.(2009). Effect of unbalanced voltage on operation of induction motors and its detection, IEEE international conference of Electrical and Electronics Engineering Conference Publications (pp.189 – 192).

Morsia .W.G, M.E. El-Hawary. (2011). On the application of wavelet transform for symmetrical components computations in the presence of stationary and non-stationary power quality disturbances, Electric Power Systems Research, vol. 81(pp.1373–1380).

Nejjari Hamid, Mohamed El Hachemi Benbouzid. (2000). Monitoring and Diagnosis of Induction Motors Electrical Faults Using a Current Park's Vector Pattern Learning Approach, IEEE Transactions on industry applications, vol. 36 n. 3 (pp. 730–735).

Pires Fernao .V, J.F. Martins, A.j. Pires. (2010). Eigenvector/eigenvalue analysis of a 3D current referential fault detection and diagnosis of an induction motor, Energy Conversion and Management, vol. 51 (pp. 901–907).

Samsi Rohan, Asok Ray, Jeffrey Mayer. (2009). Early detection of stator voltage imbalance in three-phase induction motors, Electric Power Systems Research, vol. 79 (pp. 239–245).